Influence of E-LDL and Ox-LDL on the Metabolism of ApoE, Cholesterol, Sphingolipids and Glycosphingolipids as well as on the Raft-Composition in Human Macrophages

DISSERTATION ZUR ERLANGUNG DES DOKTORGRADES DER NATURWISSENSCHAFTEN (DR. RER. NAT.) DER FAKULTÄT FÜR CHEMIE UND PHARMAZIE DER UNIVERSITÄT REGENSBURG

vorgelegt von

Margot Grandl aus Regensburg

2005

Promotionsgesuch eingereicht am: 22.12.2005

Die Arbeit wurde angeleitet von: Prof. Dr. Gerd Schmitz

Prüfungsausschuß:

Vorsitz: Prof. Dr. Sigurd Elz

1. Gutachter: Prof. Dr. Armin Buschauer

2. Gutachter: Prof. Dr. Gerd Schmitz

3. Prüfer: Prof. Dr. Jörg Heilmann

This work was performed at the institute of Clinical Chemistry and Laboratory Medicine at the University of Regensburg between September 2001 and December 2005 under the supervision of Prof. Dr. Gerd Schmitz.

Table of contents

Abbreviations

ABC	ATP-binding cassette transporter
ACAT	acyl-coenzyme A:cholesterol acyltransferase
ACEH	acid cholesterol ester hydrolase
Ac-LDL	acetylated low density lipoprotein
AD	alzheimer disease
ALLN	N-acetyl-Leu-Leu-norleucinal
APC	antigen presenting cell
Apo	apolipoprotein
APP	amyloid precursor protein
ATRA	all-trans retinoic acid
CAPK	ceramide-activated protein kinase
CE	cholesterol ester
Cer	ceramide
CETP	cholesteryl ester transfer protein
CNR	cadherin-related neuronal receptors
CR	complement receptor
CRP	C-reactive protein
DAG	diacylglycerol
DC	dendritic cells
DIG	detergent insoluble glycolipid-enriched domain Detergent insoluble glycolipid-enriched domains
DiI	1,1´-Dioctadecyl-3,3,3´,3´-tetramethylindo-carbocyanineperchlorate
DMPE-TMR	1,2-dimyristoyl-sn-glycero-3-phospho-ethanolamine-tetramethyl-rhodamine
D-PDMP	D-threo-1-phenyl-2-decanoylamino-3-morpholino-1-propanol
EBP	enhancer binding protein
EDG	endothelial differentiation gene

EEA	early endosomal antigen
EGF	endothelial growth factor
E-LDL	enzymatically degraded low density lipoprotein
ER	endoplasmatic reticulum
FcγR	Fcγ receptor
FITC	fluorescein-isothiocyanate
GAG	glucosaminoglycan
Gal	galactose
GalCer	galactosylceramide
GalT	UDP-galactose:ceramide:galactosyltransferase
Gb_3Cer	globotriaosylceramide
GGC	galactosyl (α1-2) galactosylceramide
Glc	glucose
GlcCer	glucosylceramide
GlcT-1	UDP-glucose:ceramide:glucosyltransferase
GLTP	glycolipid transfer protein
GM2AP	GM2 activator protein
GPBP	good pasture antigen binding protein
GPI	glycosylphosphatidylinositol
GSL	glycosphingolipid
HDL	high density lipoprotein
HMG-CoA	3-hydroxy-3-methylglutaryl-coenzyme A
HSPG	heparin sulphate proteoglycan
ICAM	intracellular adhesion molecule
IDL	intermediate density lipoprotein
IG	immunoglobuline
IL	interleukin
IFN	interferon

ITAM	immunoreceptor tyrosine-based activation motifs
ITIM	immunoreceptor tyrosine-based inhibition motifs
kDa	kilo Dalton
LacCer	lactosylceramide
LAMP	lysosomal associated membrane protein
LCAT	lecithin:cholesterol acyl transferase
LBP	lipopolysaccharide binding protein
LCB	long chain base gene
LDL	low density lipoprotein
LDLR	low density lipoprotein receptor
LOX	lectin like Ox-LDL receptor
LPC	lysophosphatidylcholine
LPS	lipopolysaccharide
LPL	lipoprotein lipase
LRP	low density lipoprotein receptor-related protein
MARCO	macrophage scavenger with collagenous structure
MAP	mitogen activated protein
MCP	monocyte chemoattractant protein
MCSF	monocyte colony stimulating factor
mDab	mammalian disabled protein
MDM	monocyte derived macrophages
MDR	multi drug resistance
Mena	mammalian ena
MMP	matrix metalloproteinase
MSR	macrophage scavenger receptor
NGF	nerve growth factor
NPC	Niemann-Pick type C
NSAD	non steroidal antiinflammatory drug

Ox-LDL	oxidized LDL
PAI	plasminogen activator inhibitor
PC	phosphatidylcholine
PDGF	platelet derived growth factor
PE	phosphatidylethanolamine
PE	phycoerythrin
PerCP	peridin chlorophyll protein
PH	pleckstrin homology
PI3K	phosphoinositol 3 kinase
PL	phospholipids
PLTP	phospholipid transfer protein
POPC	1-palmitoyl-2-oleyl-sn-glycero-3-phosphocholine
PPAR	peroxisome proliferator-activated receptor
PPRE	peroxisome proliferator response element
PS	phosphatidylserine
RA	retinoic acid
RAR	retinoic acid receptor
RARE	retinoic acid responsive elements
RCT	reverse cholesterol transport
RXR	retinoic X receptor
SAA	serum amyloid A
SAP	serum amyloid P
SAP	sphingolipid activator protein
SF	steroidogenic factor
SIAT	sialyltransferase
SL	sphingolipid
SMC	smooth muscle cell
SR	scavenger receptor

SRCR	scavenger receptor cystein-rich domain
SREBP	sterol regulatory element binding protein
SREC	scavenger receptor expressed by endothelial cells
SM	sphingomyelin
SMase	sphingomyelinase
SMS	sphingomyelin synthase
SPHK	sphingosine kinase
SPT	serine-palmitoyl CoA transferase
SREBP	sterol regulatory element binding protein
S1P	sphingosine-1-phosphate
TD	tangier disease
TG	triglyceride
TNF	tumor necrosis factor
TRL	triglyceride rich lipoprotein
TX	triton-x
TZD	thiazolidone
UC	unesterified cholesterol
UDP	uridinediphosphate
VCAM	vascular cell adhesion molecule
VLDL	very low density lipoprotein
VSMC	vascular smooth muscle cell

I. Introduction

1. Pathogenesis of atherosclerosis

Atherosclerosis is one of the main causes of death in Western societies and may well account for over 50% of the mortalities in the UK and USA which may affect about 500 individuals/day or 170,000 annually.

Atherosclerosis is a multifactorial process which goes along with the formation of atherosclerotic lesions isolated in large and medium-sized arteries, the brain, the heart and the legs. The atherogenic process starts at an early age with the deposition in blood-vessel walls of lipids such as cholesterol, derived from lipoproteins circulating in the bloodstreams, which leads to the formation of the characteristic “fatty streaks”, the earliest lesion in the atherosclerotic process. Over time and with continued irritation these streaks progress into protruding and more complicated lesions containing an accumulation of lipids and necrotic cells (1). Fatty streaks consist mainly of macrophage foam cells that have taken up massive amounts of cholesterol. The formation of fatty streaks is initiated by the adherence of circulating monocytes to activated endothelial cells at lesion-prone sites within large arteries. Adherent monocytes subsequently migrate into the subendothelial space in response to locally produced chemoattractant molecules, where they further differentiate into macrophages and develop into foam cells by lipid uptake (Fig.1). The lipid taken up by macrophages is believed to originate predominantly from oxidized low density lipoproteins (Ox-LDL) (2). Myocardial infarctions occur frequently as a result of plaque rupture, a late-stage complication seen in vulnerable plaques. These plaques are characterized by large, necrotic, highly thrombogenic lipid cores with a high content of lipid and necrotic debris. A thin fibrous cap contains increased numbers of macrophages and T lymphocytes in shoulder regions where plaque rupture clinically occurs (3). Evidence suggests that matrix metalloproteinases (MMPs) contribute to plaque destabilization by degrading the matrix in the fibrous cap, thus contributing to the weakness and ultimate rupture of the plaque (4). Mechanical forces are also thought to be involved. The MMPs are a large, complex, highly regulated family of matrix (collagen)-degrading enzymes produced by vascular smooth muscle cells (VSMCs) and macrophages (1). An alternative mechanism contributing to lesion formation is that of superficial erosion of the endothelium (5).

As a result of atherogenesis, thrombosis, coronary heart disease, myocardial infarct and stroke may occur. Surgical treatment is sometimes effective, but there is no specific cure. A low-cholesterol diet combined with cholesterol synthesis and absorption inhibitors as well as control of predisposing factors, such as hypertension, smoking, diabetes and obesity, are usually recommended.

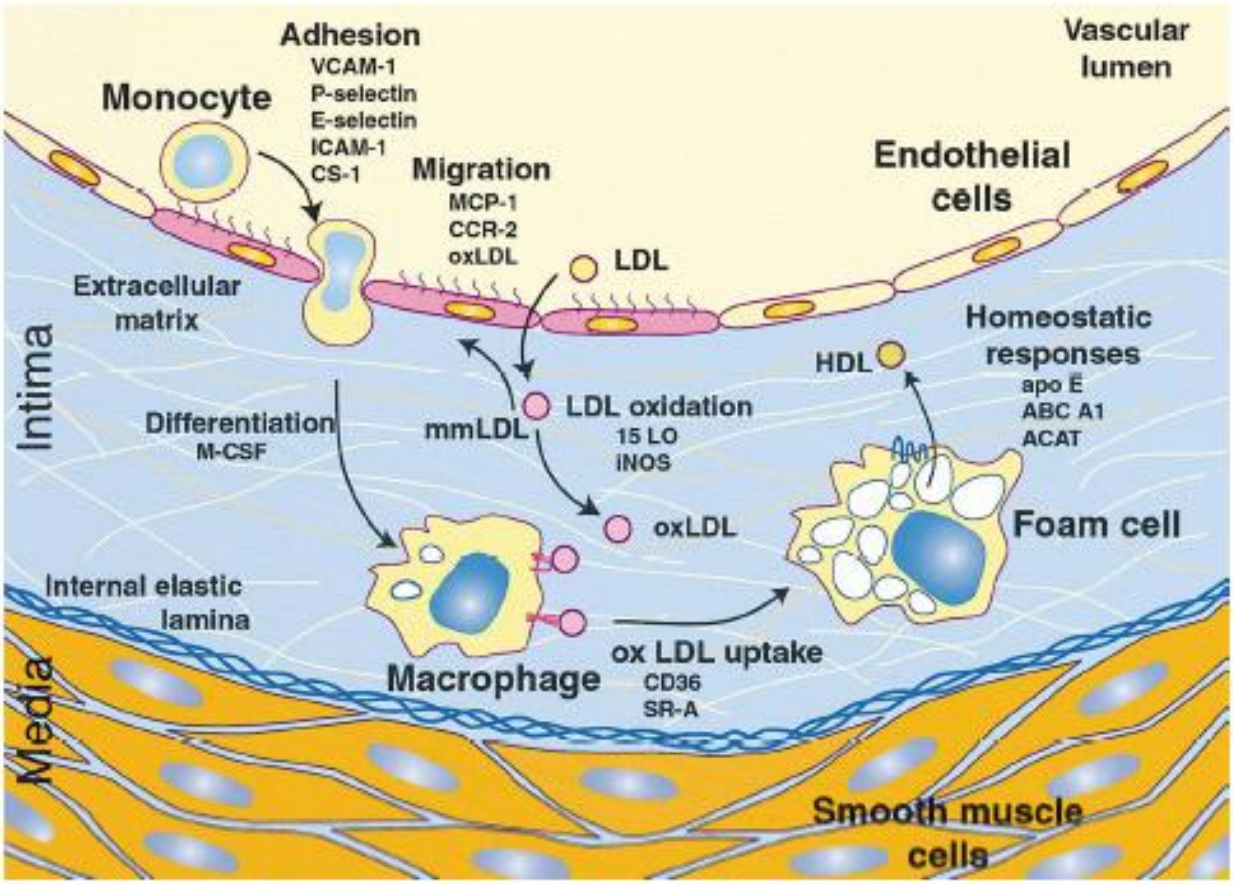

Glass C. and Witztum J. Atherosclerosis: The Road Ahead; Cell, Vol. 104, 503-516, Feb. 23, 2001

Fig. 1: Role of lipoproteins and monocytes/macrophages in lesion formation and progression
Monocytes attach to endothelial cells that have been induced to express cell adhesion molecules by mmLDL and inflammatory cytokines. Adherent monocytes migrate into the subendothelial space and differentiate into macrophages. Uptake of Ox-LDL via scavenger receptors leads to foam cell formation. Ox-LDL cholesterol taken up by scavenger receptors is subject to esterification and storage in lipid droplets, is converted to more soluble forms or is exported to extracellular HDL acceptors via cholesterol transporters, such as ABCA1.

1.1. Response to injury hypothesis

The modified response to injury hypothesis of atherosclerosis emphasizes endothelial dysfunction rather than denudation as the first step in atherosclerosis (2). This hypothesis stated that the endothelium helped to regulate homeostasis of the cardiovascular system. This was supported by the fact that an intact endothelium is capable of releasing antithrombic and fibrinolytic factors in addition to the potent vasodilator nitric oxide. In normal blood vessels, nitric oxide and acetylcholine induce vasodilatation, but with endothelial damage, disruption of cell state negates normal function and the actions of potent vasodilators. The damaged endothelium causes abnormal responses from acetylcholine by increasing the production of vasoconstricting agents such as thromboxane A2 and prostaglandins. In addition to eliciting the development of abnormal intracellular signalling mechanisms which augment an increase of intracellular Ca^{2+} and endothelin-derived vasoconstricting factors. Endothelial damage also triggers platelets to adhere and aggregate

at the site of the damage, this enhances monocytes to enter the tunica intima, and induces SMC-proliferation within the tunica-media junction of the artery. This effect causes the arterial wall to be injured at this site. With increased monocyte invasion into arteries, and continual lesion development and fibrosis the lumen of the artery can become progressively reduced. This combination of biochemical and anatomical alterations contributes to oxidative stress and increased vascular damage; the so-called precursors for atherogenic changes within arteries.

1.2. Response to retention hypothesis

This hypothesis proposes that the retention and modification of atherogenic lipoproteins in the arterial lining is one of the initiating events that triggers the inflammatory response (6).

The atherogenic apolipoprotein B100 (apoB100)-containing lipoproteins enter the subendothelial space and are bound and retained through ionic interactions between positively charged residues on the atherogenic lipoproteins, and negatively charged residues in the extracellular matrix molecules. Of these extracellular matrix components, proteoglycans in particular appear to play an important role. Proteoglycans are macromolecules composed of a core protein and complex, long-side-chain carbohydrates, called glycosaminoglycans (GAGs), which consist of repeating disaccharide units, all bearing negatively charged, usually sulphate or carboxylate, groups (7). The interaction between LDL and proteoglycans involves positively charged amino acids arginine and lysine in apoB100, the protein moiety of LDL, that bind ionically with the negatively charged GAGs of the proteoglycans (8).

The consequence of the retention of atherogenic lipoproteins is not only a net accumulation of lipid, but also prolonged exposure to local oxidants and other non-oxidative enzymes in the vessel wall resulting in a variety of modified lipoproteins and their constituents which trigger an inflammatory reaction that accelerates lesion development (6)

2. Cellular constituents of atherosclerosis

The pathobiology of atherosclerosis may be determined by numerous cellular entities involved in the atherosclerotic process. These cells can be broadly organized into structural elements of the arterial wall, inflammatory cells that enter the arterial wall and circulating elements (e.g., platelets, leukocytes) (3). Vascular cells with important, well-defined roles in atherosclerosis include the endothelial cell and the VSMC (1). Endothelial responses include the induction of adhesion molecules, a decisive step early in atherogenesis and the change in the production of nitric oxide, a critical, short lived molecule that helps to maintain normal endothelial reactivity while limiting thrombosis and inflammation (9).

The VSMCs are integral to many processes implicated in normal vessel function as well as to atherosclerosis and hypertension (10). Atherosclerosis can be characterized by the migration

of VSMCs from the media to the intima and their subsequent proliferation in this location (11). Also, VSMCs provide the main source for the extracellular matrix, which forms the fibrous cap overlying the lipid core atherosclerotic plaques (1). In this role, VSMCs provide an essential function, albeit a reaction to a pathologic state.

Inflammatory cells, including monocytes, macrophages, and lymphocytes (predominantly T cells), are critical to the development of atherosclerosis (2). Circulating monocytes and lymphocytes are attracted to arterial sites of endothelial injury by the stimulation of chemoattractant cytokines (chemokines), a large, complex family of small proteins that signal through specific chemokine receptors on the surface of inflammatory cells (12). Endothelial adhesion molecules-including vascular cell adhesion molecule-1 (VCAM-1), intracellular adhesion molecule-1 (ICAM-1), P-selectin and E-secletin (13-18), have specific roles leading to rolling, firm adhesion, and ultimate entry of these cells into the arterial wall (19) (Fig.1). These adhesion molecules and also monocyte chemoattractant protein (MCP-1), interleukin-1 (IL-1) and tumor necrosis factor-alpha (TNFα) as well as degraded collagens and elastins (2) are highly up-regulated by the elevation of the levels of atherogenic lipoproteins (Ox-LDL and Lp(a)) and cytokines in vitro (5;13).

Among all the mediators reported thus far, MCP-1 and Lysophosphatidylcholine (a component of Ox-LDL) may be the most important and are the best characterized chemoattractants in the lesions (20).

Macrophages appear at a very early stage in the development of atherosclerotic lesions and persist throughout their evolution, indicating a pivotal role for these cells in the disease process. T lymphocytes also provide important signals to the process. For example, T-cell-derived inflammatory cytokines are thought to contribute to monocyte, VSMC, and endothelial cell activation (21-23).

2.1. Differential expression of the monocyte innate immunity receptor complex defining monocyte subpopulations

Following adherence to endothelial cells, defined subpopulations of circulating monocytes that express the lipopolysaccharide (LPS) receptor CD14, the Fcγ-receptor IIa/CD32 and the Fcγ-receptor IIIa/CD16a ($CD14^{bright}$ $CD16^{+}$) might extravasate into the subendothelial space (24-26).

In normal subjects, five different subpopulations of blood monocytes have been discriminated by cell expression densities of various antigens involved in extravasation, uptake of atherogenic lipoproteins, differentiation and inflammation. The Fcγ receptors (FcγRs), in particular CD16a/FcγRIII, together with the LPS receptor CD14, appear to be key players in defining monocyte subpopulations. Their heterogeneous expression suggested a different capacity for IgG-dependent phagocytosis (24). The pool size of $CD14^{dim}$ $CD16^{+}$ monocytes

correlates with plasma lipids and lipoprotein metabolism as well as inflammation and the acute phase reaction stressing a link between peripheral blood monocyte heterogeneity and cardiovascular risk factors (27). Monocytic CD14 expression is reduced in systemic inflammation (28) and an atherogenic lipoprotein profile is associated with an expansion of a more differentiated monocyte subpopulation with a lower expression of CD14 and Fcγ-RIIIa/CD16a (24;26). Moreover, a functional genetic polymorphism of CD14 is associated with myocardial infarction (29), suggesting a role of CD14 in inflammation and atherogenesis. As described by Pfeiffer et. al. (30) results the binding of lipopolysaccharide and ceramide, a constituent of atherogenic lipoproteins in ligand-specific receptor clustering in rafts (detergent resistant membrane microdomains). Lipid rafts on monocytes/macrophages provide a dynamic microenvironment for an integrated CD14-dependent clustering of a set of receptors involved in innate immunity and clearance of atherogenic lipoproteins (31). In resting cells, CD14 was associated with CD55, the Fcγ-receptors FcγRIIA/CD32 and FcγRI/CD64 and the pentaspan CD47. Cer further recruited the complement receptor 3 (CD11b/CD18) and the scavenger receptor CD36 into proximity of CD14. LPS, in addition, induced co-clustering with Toll-like receptor 4, Fcγ-RIIIa/CD16a and the tetraspanin CD81 while CD47 was dissociated (Fig.2). Thus clustering of signalling competent receptors to a common recognition platform in rafts may provide an interesting mechanism by which different ligands induce distinct cellular processes in systemic inflammation (SIRS or sepsis) and cardiovascular disease.

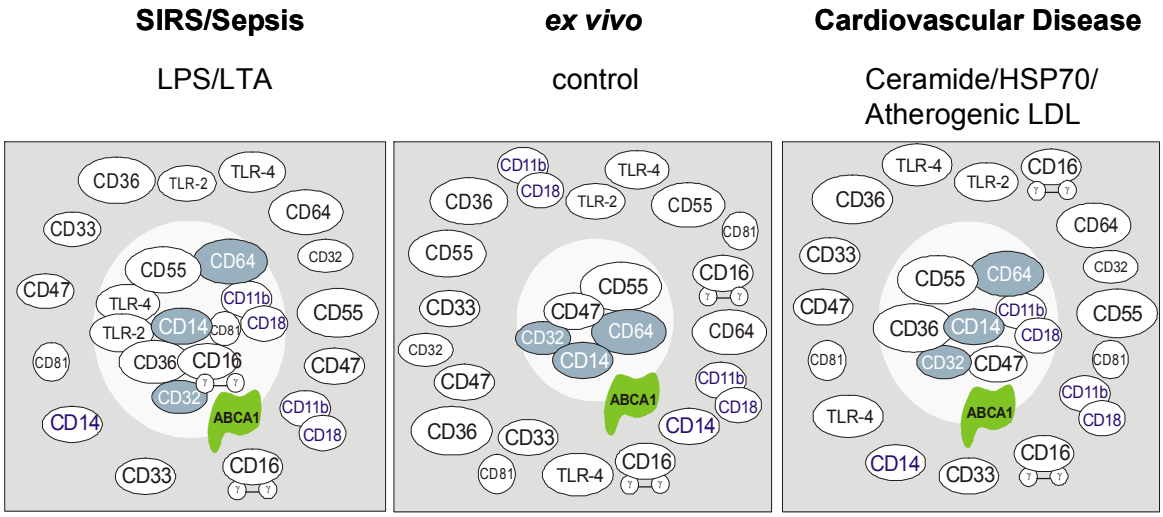

Fig. 2: The innate immunity receptor complexes in inflammation and cardiovascular disease
The basic cluster includes specific and non-specific opsonin recognition sites (ex vivo, control) whereas ligand induced clustering is dependent of ligand surface composition (LPS/LTA or ceramide/HSP70) and atherogenic LDL

2.2. Foam-cell formation

After monocytes bind to the surface of the arterial wall, they migrate into the subendothelial space, where they differentiate to macrophages and are transformed by lipid uptake into foam cells (Fig.1). They are called foam cells because, by light microscopy, the lipid deposits make the cells look foamy. Low density lipoproteins which have become modified are the major source of lipid for foam cell formation. These altered lipoproteins are taken up into the cell via receptor-mediated endocytosis and delivered to lysosomes. The cholesterol accumulating in foam cells is known to be ultimately derived from circulating plasma lipoproteins. However, incubation of neither monocytes and macrophages nor arterial smooth muscle cells with native LDL, even at very high concentrations, increases their cellular cholesterol content substantially (32;33). These cells, like other cells, protect themselves against cholesterol overloading by decreasing the number of LDL receptors on their surface when overloaded with cholesterol (34). Therefore LDL must be somehow modified before it can induce foam-cell formation (33) and the binding and internalization of these modified lipoproteins are mediated by receptors, principally scavenger receptors, on macrophages (35). Unlike the LDL receptor, scavenger receptors are not significantly down-regulated and they potentially can produce large amounts of cholesterol accumulation. Among the possible candidate scavenger receptors involved in atherosclerosis, CD36 is currently a leading candidate (36). Chemical modifications that induce uptake by scavenger receptors and other poorly regulated receptors include acetylation and oxidation of LDL (37). The resulting cholesterol–filled “foam cell” macrophages are a characteristic feature of atherosclerotic lesions and contribute to lesion development in a number of ways. The large cholesterol-rich core of advanced lesions appears to be substantially derived from necrosis and/or apoptosis of foam cells (38) and cholesterol enrichment of macrophages also affects the expression and secretion of several proteins and enzymes (39). Foam cells also contain small but significant amounts of various lipid oxidation products, which are potent mediators of macrophage function.

3. Cholesterol Transport

3.1. Cholesterol efflux from macrophages to prevent foam cell formation

When cholesterol acceptors such as high density lipoprotein (HDL) are present, cholesterol efflux from macrophages is accelerated, which prevents foam cell formation. To produce this efflux, neutral cholesteryl ester hydrolase catalyzes the intracellular hydrolysis of cholesteryl esters (CE) into free cholesterol in the lysosome. The mobilization of cholesterol from late endosomes and lysosomes requires functional Niemann-Pick type C 1 (NPC1) and NPC2 proteins, originally identified as an important secreted protein from human epididymis (HE1)

(40). Excess free cholesterol is esterified by acyl-coenzyme A:cholesterol acyltransferase 1 (ACAT1,SOAT), an enzyme that localizes to the ER to form CE which are stored in cytosolic lipid droplets. Free cholesterol respectively unesterified cholesterol/phospholipids complexes (UC/PL) are transported via the ATP-binding cassette transporters (ABCs) ABCA1 and ABCG1 through cell membranes and are accepted on the membranes by apolipoprotein A-I (apoA-I), which generates preβ (nascent)-HDL particles (Fig.3). In humans and mice, apoA-I is produced primarily in the liver and intestine. Extracellular sources of apoA-I have been shown to increase cholesterol efflux from macrophages in vitro,(41) and the presence of apoA-I in the extracellular space is considered to be necessary for the activation of cholesterol efflux through the ABCA1 pathway (23). The Rho family GTPase Cdc42 directly interacts with ABCA1 to control filopodia formation, actin organization and intracellular lipid transport (Fig.3) (42;43). Also vesicular transport processes involving different interactive proteins like β-2 syntrophin are involved in cellular lipid homeostasis controlled by ABCA1 (44) (Fig.3). It could be shown by Drobnik et al. (45) that ABCA1 and Cdc42 were partially localized in Lubrol- but not in Triton-X (TX) detergent resistant membrane microdomains (rafts) and that apoA-I preferentially depleted UC/PL from Lubrol rafts, whereas HDL_3 additionally decreased the cholesterol content of TX rafts (Fig.3).

Mutations in the ABCA1 transporter gene cause a disorder of cholesterol efflux known as Tangier disease (TD), a familial HDL deficiency syndrome, which leads to the development of either coronary artery disease or splenomegaly dependent on ABCA1 mutations (46).

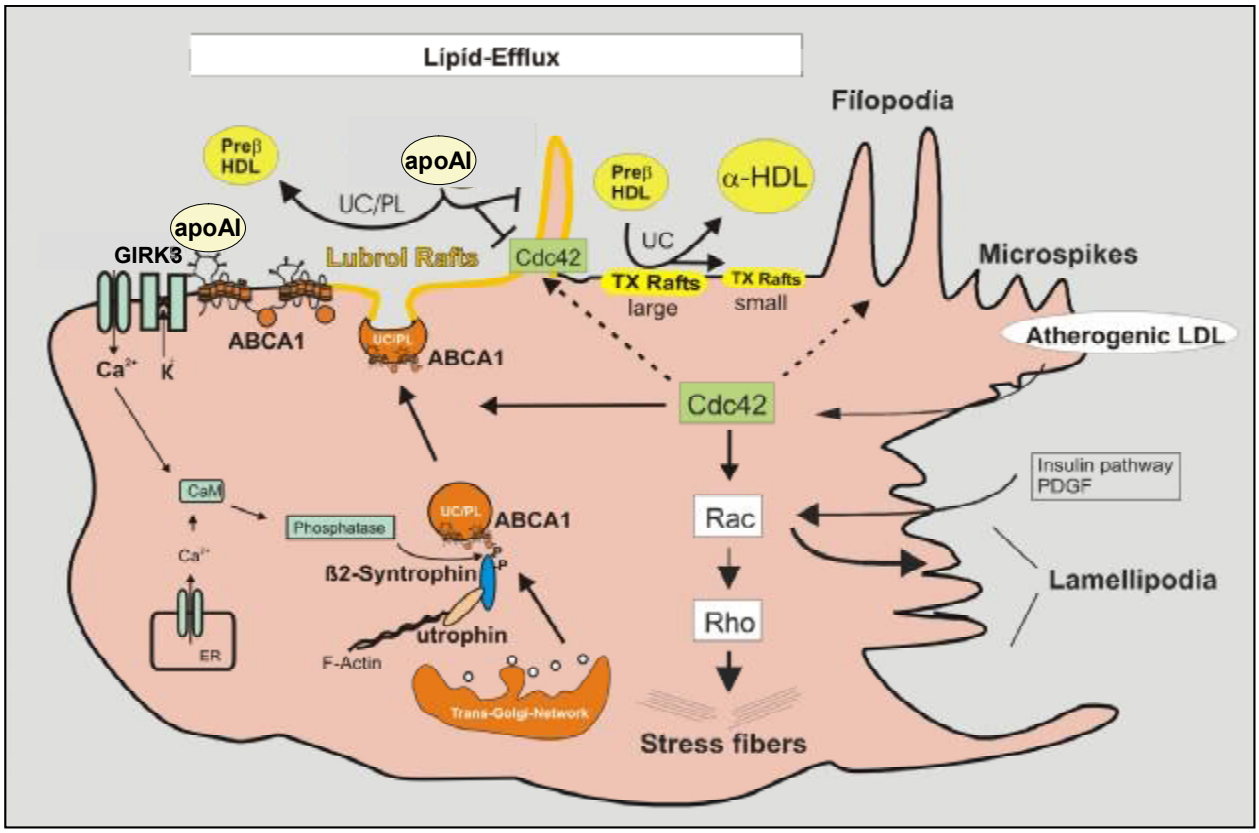

Fig. 3: ABCA1 a regulator of lipid rafts, vesicular transport and filipodia formation

3.2. Further cholesterol transport candidates

NPC1 and 2 are involved in the exit of cholesterol and/or other lipids from the endosomal or lysosomal membranes. NPC1 may function as a permease to allow phospholipids and cholesterol to exit the endosomal system. This activity may depend on NPC2 wich may function as a chaperone for sterol insertion into the endosomal/lysosomal membrane by acting as a bridge to allow free cholesterol, released from its fatty-acid moiety by the action of lysosomal acid lipase, to insert into the inner membrane of the organelle (Fig.4). MLN64, a protein which was initially identified as an upregulated transcript in malignant cells has been colocalized with NPC1 in the membrane of the late endosome, indicating that it might play a role in cholesterol egress together with NPC1. MLN64 however could also act independently of NPC1 to facilitate shuttling of cholesterol between the endosomal membrane and an acceptor (47).

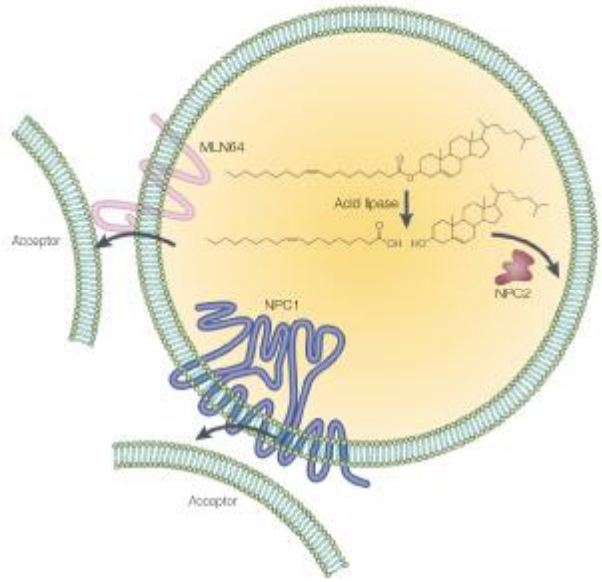

Fig. 4: Cholesterol binding and transport proteins
NPC1, MLN64 and NPC2 reside in the endosomal-ysosomal system.
(MLN64, malignancy antigen 64; NPC1 and 2, Niemann-Pick disease Type C 1 and 2)
(figure from Ioannou 2001(47))

3.3. Niemann-Pick Disease Type C- a cholesterol storage disease

Niemann-Pick Disease Type C (NPC) is caused by mutations in the NPC1 or NPC2 gene. NPC is a rare autosomal-recessive lipidosis, characterized by the accumulation of unesterified cholesterol in late endosomes, lysosomes and the Golgi apparatus (48;49). Further cholesterol relocation to and from the plasma membrane is delayed. Patients show progressive neurodegeneration and hepatosplenomegaly, which leads to death during early childhood. Although it has been assumed that NPC is primarily a cholesterol-storage disorder, sphingolipids like lactosylceramide (LacCer) or globotriaosylceramide (Gb_3Cer) also accumulate to similar degrees in peripheral organs (Fig.5) (50).

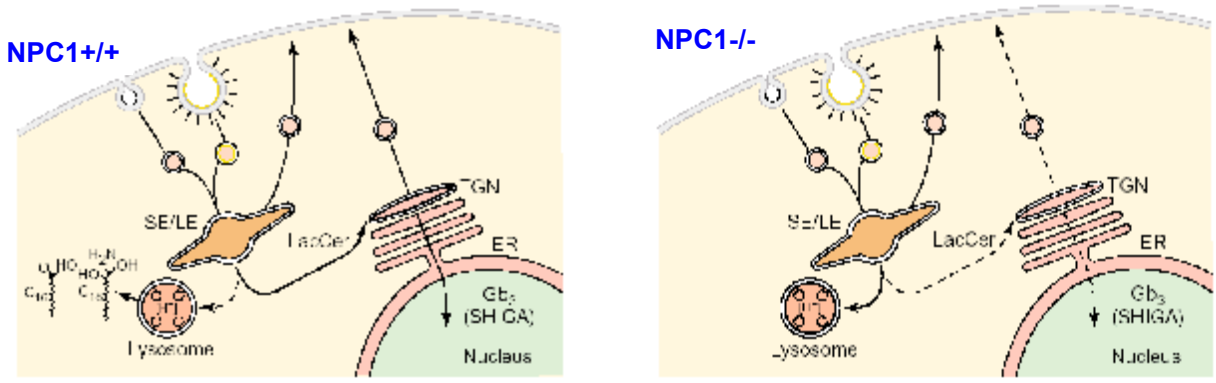

Fig. 5: Model for altered sorting in NPC
In the normal state (left picture) LacCer is transported to the trans-Golgi network (TGN) following by exocytosis to the plasma membrane.
In the diseased state (right picture) LacCer is predominantly transported to the lysosome where it accumulates.
(Abbreviations: ER, endoplasmatic reticulum; LE/SE, late or sorting endosome)
(figure from Sillence, Platt 2003(50))

4. Role of lipoproteins in the development of atherosclerosis

Lipids are transported between the intestine, liver and periphery in soluble complexes defined as lipoproteins. These circulate as spherical lipoprotein particles and comprise a core of neutral lipids, such as cholesteryl esters (CE) and triglycerides, and a surface shell of polar phospholipids, cholesterol, other polar lipids and apolipoproteins (apos). Apos are specific lipid-binding proteins that are integral constituents or attach to the surface of the particle, to stabilize it and to function as ligands for cell membrane receptors or as enzyme activators. Lipoproteins can be separated by density centrifugation and electropheretic mobility. The largest and least dense lipoproteins, those that contain the most lipid relative to protein, are the chylomicrons (d=<0.96g/ml). In order of increasing density because of escalating percent protein composition and smaller particle size, are the other major lipoproteins: very low density lipoprotein (VLDL) (d=0.96-1.006g/ml), low density lipoprotein (LDL) (d=1.019-1.063), and high density lipoprotein (HDL) (d=1.063-1.210). In addition, there are subfractions of these major classes of lipoproteins, for example, intermediate density lipoproteins (IDL), which lie between VLDL and LDL in density (d=1.006-1.019). Chylomicrons and VLDL carry the greatest proportion of their lipid as triacylglycerol, while CE is the lipid in highest concentration in LDL. Relative to other lipoproteins, HDL carry the least percentage of lipid as triacylglycerol, but is rich in CE and phospholipid.

After the uptake of various lipoproteins by macrophages through various routes of endocytosis, most of the lipoproteins are finally transported into lysosomes, digested therein and degraded into amino acids and free cholesterol. Within late endosomes and lysosomes,

CE is hydrolyzed by acid lipase (CE hydrolase) into free cholesterol, which is released into the cytosol and further into the extracellular space.

4.1. Chylomicrons

These are large particles composed mainly of triglyceride, synthesised in the small intestinal mucosa and transported from dietary fat. Chylomicrons contain phospholipid, cholesterol, apos, for example apoB48, apoA-I, apoA-I, C-apolipoproteins (C-I, C-II, C-III) and apoE. The presence of apoC-II surface protein activates the capillary endothelial enzyme lipoprotein lipase that is responsible for the conversion of chylomicrons into chylomicron remnants and VLDL into IDL and to deliver fatty acids and cholesterol to peripheral cells. Both of these products circulate in peripheral tissues to be later absorbed by hepatic apoB and apoE receptors.

4.2. VLDL

VLDLs are the products of endogenous triglyceride synthesis within the liver. A major function of this lipoprotein is to transport endogenously synthesized triacylglycerol from the liver to extrahepatic tissues. They contain the apoB100 and apoE proteins which are catabolised by lipoprotein lipase within peripheral tissues. VLDL upon reaching capillaries of adipose tissue or muscle extract the triglyceride units leaving enriched CE with two apoprotein units. VLDL are broken down with small apos and transferred to HDL which produce smaller fragments or IDL. The VLDL pathway, including its metabolism to IDL and LDL, is the endogenous pathway of triacylglycerol and CE transport.

4.3. IDL

As triacylglycerol molecules are lost from the VLDL particle, apoC-II and apoE are transferred back to HDL. This results in formation of an IDL that contains apoB100 and some remaining apoE. IDL, like HDL and chylomicron remnants can be cleared by the apoE receptor on liver. Genetic defects in the apoE ligand or its receptor elicit Type III hyperlipidemia, in which IDL, as well as chylomicron remnants and HDL, are elevated. Further hydrolysis of triacylglycerol in IDL by lipoprotein lipase and transfer of the remaining apoE to HDL results in formation of LDL.

4.4. LDL

LDL is the major cholesterol carrying lipoprotein in normal plasma. It has been shown that the higher the concentration of LDL, the higher the risk of developing atherosclerosis. (51). LDL is composed of a core of 1500 molecules of cholesterol enclosed in layers of phospholipid and unesterified cholesterol molecules. CE in LDL may originate from

cholesterol directly synthesized by the liver (endogenous pathway), or indirectly from the diet via the clearance of chylomicron remnants by the liver (exogenous pathway). The hydrophilic portions of the molecule are arranged on the outside which allows LDL to dissolve in blood or extracellular fluid. ApoB-100 is embedded in this hydrophilic layer. This protein is recognised and binds to the LDL receptor, a transmembrane glycoprotein, which spans the full thickness of cell's plasma membrane in clusters within specialised regions referred to as "clathrin coated pits". These pits pinch inward to allow LDL to be carried into the cell, a process called receptor mediated endocytosis. Endocytosed vesicles containing LDL rapidly lose clathrin and fuse with a vesicle that has an internal pH of about 5.0, to form a sorting endosome. The acidity induces LDL to dissociate from its receptor. LDL and its CE accumulate inside a transport vesicle, while the LDL receptors recycle to the plasma membrane. When the transport vesicle fuses with a lysosome, apoB100 is degraded to its component amino acids and CE are hydrolyzed by acid cholesterol ester hydrolase (ACEH) to free cholesterol and fatty acids (Fig. 6). After cholesterol leaves the lysosome, it is transported to the endoplasmatic reticulum (ER) and to the plasma membrane by means of an intermediate step through the Golgi apparatus. Excess free cholesterol is esterified by acyl-coenzyme A:cholesterol acyltransferase 1 (ACAT1), an enzyme that localizes to the ER, and is stored as cytosolic droplets of CE. The most important mechanism in order to regulate cholesterol synthesis by the cell is to adjust the number of LDL receptors in order to meet the demands of cholesterol but not the excesses. If the demand exceeds the supply, then an accumulation of receptors will occur and vice versa. Lipoprotein disorders in which LDL receptors, or their capacity to bind the apoB100 ligand, are defective, result in an increased level of cholesterol in LDL remaining in circulation, causing hypercholesterolemia and atherosclerosis. Because of this and its potential to become oxidized to an atherogenic form, LDL is called the "bad" cholesterol carrier.

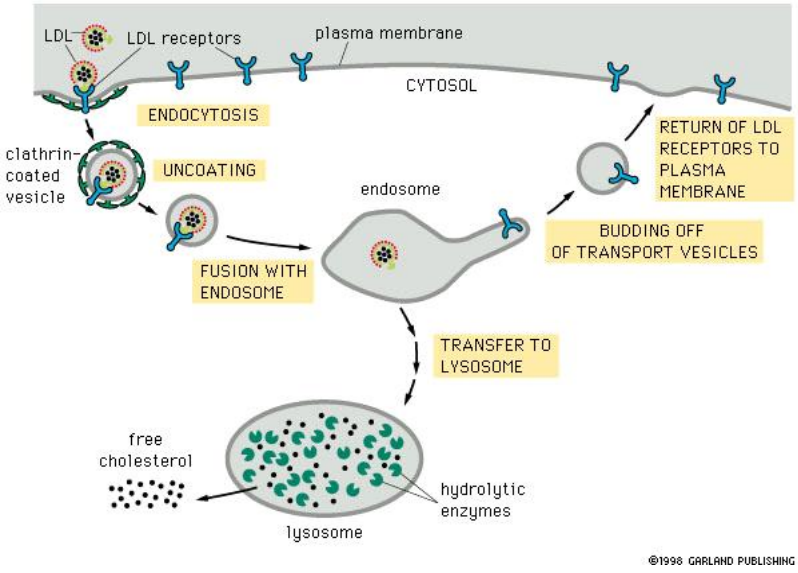

Fig. 6: Receptor mediated endocytosis of LDL (from Garland publishing 1998)

4.5. HDL

HDL has essentially the opposite function of LDL: it takes up cholesterol from peripheral cells. HDL is synthesized in liver and secreted into plasma as nascent HDL, which are discoidal pre-β-migrating complexes of phospholipid and apoA-I. Mature HDL contains lecithin, CE, lecithin:cholesterol acyl transferase (LCAT), and apoA-I, apoC-II, and apoE. Circulating HDL acquires cholesterol by using LCAT to extract cholesterol from the plasma membranes of peripheral cells. This process of cholesterol removal by HDL is facilitated by ABCA1, an ATP-binding cassette protein transporter. ABCA1 is activated by apoA-I and flips unesterified cholesterol and lecithin to the outer layer of cell membranes. ABCA1 delivers free cholesterol and lecithin as substrates for LCAT on HDL. ApoA-I activates LCAT in the nascent HDL, and also functions as a ligand for a cell surface receptor that exists on peripheral cells. CE, the product of LCAT catalysis, move to the core of nascent HDL. The entire process of LCAT extraction of cell cholesterol and incorporation into HDL for liver clearance is called "reverse cholesterol transport." The CE moiety of HDL is taken up selectively by the liver via SR-BI (52). HDL functions as a cholesterol scavenger, facilitating the transport of cholesterol to the liver for conversion to bile acids and secretion into the bile for elimination or recycling in the enterohepatic bile acid cycle. It is this cholesterol-removing property that renders HDL the "good" cholesterol carrier. Of course another major function of HDL is to serve as a depository for apoA-I, apoC-II and apoE. Transfer of apoC-II is required for the metabolism of chylomicrons and VLDL, and apoE is crucial for clearance of chylomicron remnants, IDLs and HDLs. Therefore, HDL contributes to both the exogenous and endogenous pathways of lipid transport. HDL as an anti-atherogenic lipoprotein protects against atherogenesis via reverse cholesterol transport and plays an important role as an antiinflammatory factor. Several beneficial functions of HDL have been documented (table 1) and it is expected that the therapeutic use of HDL elevation may open avenues for the treatment of atherosclerosis in the future (53).

Table 1: Possible anti-atherogenic effects of HDL

Effects	**Possible mechanisms**
Inhibition of lesion formation ↓	Reverse cholesterol transport
Adhesion of monocytes to endothelial cells ↓	Inhibition of adhesion molecules and decreased cytokine production
Thrombosis ↓	Modulation of endothelial antithrombotic and profibrinolytic properties
Antioxidant effects ↑	Modulation of paraoxonase
Cellular death ↓	Inhibiton of apoptosis
Cellular proliferation ↓	Inhibition of SMC proliferation

↓: reduced or inhibited; ↑: enhanced

Table from Jianglin Fan and Teruo Watanabe: inflammatory reactions in the pathogenesis of atherosclerosis, review. J Atheroscler Thromb, 2003; 10: 63-71.

5. Proteins involved in HDL metabolism

5.1. Apolipoproteins

Apolipoproteins are constituents of various lipoproteins. The major apolipoproteins include apoA-I, apoA-II, apoA-IV, apoB, apoC-I, apoC-II, apoC-III and apoE. Specific apolipoproteins function in the regulation of lipoprotein metabolism through their involvement in the transport and redistribution of lipids among various cells and tissues, through their role as cofactors for enzymes of lipid metabolism, or through their maintenance of the structure of the lipoprotein particles. Defects in apolipoprotein structure or synthesis may affect lipid metabolism resulting in progression to coronary artery disease.

5.1.1. ApoA-I

ApoA-I, a single polypeptide of 243 amino acids is synthesized mainly in the liver and to a lower extent in the small intestine. ApoA-I is secreted as a discoidal, nascent HDL particle, having little or no core of cholesteryl ester which is then metabolized in plasma to mature HDL. It is the major protein found in HDL and plays an important role in HDL cholesterol metabolism and regulation of cholesterol transport (54). ApoA-I is the obligatory cofactor of the enzyme lecithin-cholesterol acyltransferase (LCAT) and is known to be the most powerful LCAT activator which results in enhancement of esterification of free cholesterol and cholesteryl ester enrichment of HDL (55;56). Therefore apoA-I is a major participant in the regulation of reverse cholesterol transport from peripheral tissues to the liver (57) which explain the correlation between plasma apoA-I levels, HDL cholesterol levels and reduced risk of atherosclerosis. Further apoA-I may facilitate hepatic cholesterol uptake by serving as a ligand for binding of HDL to hepatic receptors (58). ApoA-I production rates can directly influence plasma concentrations of HDL-cholesterol (59-61). The relationship between apoA-I production and HDL cholesterol levels suggests the possibility that increasing expression of the apoA-I gene could slow or prevent progression of atherosclerosis which has been shown in transgenic mice where overexpression of apoA-I raises HDL cholesterol levels (60) and inhibits the development of early atherosclerotic lesions (61). An apoA-I abnormality has implicated in lipoprotein disorders such as Tangier disease (62-65).

5.1.2. ApoC-I

ApoC-I is a 6.6 kDa protein with 57 amino acids in a single polypeptide chain that belongs to the apoC family of small apolipoproteins that share a similar molecular mass, a similar distribution among lipoprotein classes (constituents of chylomicrons, VLDL, HDL) and coincident purification (66). It has been reported that in the fasting state, apoCs are mainly associated with HDL, whereas in the fed state, they preferentially redistribute to the surface

of chylomicrons and VLDL particles (67). Being predominantly expressed in the liver apoC-I is under control of an array of elements throughout the whole gene cluster on chromosome 19 that also regulates apoC-II, apoC-IV and apoE expression (68;69). The physiological function of apoC-I is not clear yet. Modulation of binding properties to the LDL receptor or LDL receptor related protein of beta-VLDL through displacement of apoE from the lipoprotein particle or conformational changes of apoE in presence of apoC-I has been reported (70-73). Further the binding of lipoproteins to the VLDL receptor was completely inhibited by apoC-I (74). It has also been shown that apoC-I acitvates the enzyme lecithin cholesterol acyltransferase (LCAT) (55;56;75). LCAT is known to catalyze the esterification of free cholesterol in plasma and is further able to esterify lysophosphatidylcholine (LPC) to phosphatidylcholine (PC) (76). This lysolecithin acyltransferase activity was also activated by apoC-I (77). Further apoC-I can inhibit lipoprotein lipase an enzyme which is involved in lipoprotein processing (78) and phospholipase A2 (79) which amplify atherogenic processes by liberating potent pro-inflammatory lipid mediators and by generating pro-atherogenic LDL (80). CETP, which mediates the transfer of cholesterol ester from HDL to apoB-containing lipoprotein particles, is inhibited by apoC-I (81;82) which indicates a role of apoC-I in HDL metabolism. Because of the fact that apoC-I has inhibitory respectively stimulatory effects on a variety of receptors and enzymes involved in the major metabolic pathways of lipoprotein metabolism it can be concluded that apoC-I play a complex role in diseases associated with hyperlipidemias.

Human apoC-I transgenic mice overexpressing apoC-I, exhibited hyperlipidemia with elevated levels of cholesterol and TGs owing to an accumulation of VLDL-size particles in the circulation. The elevated lipid levels in the plasma of apoC-I transgenic mice are primarily due to an enhanced production or disturbed lipolysis of VLDL (68;74;83). Overexpression of human apoC-I in mice inhibits VLDL uptake by the liver, probably due to displacement of apoE or a direct interaction with hepatic receptors (74;83). Surprisingly, apoC-I knockout mice had normal serum lipid levels on a chow diet (84). Only when fed a high-fat and high-cholesterol diet did apoC-I deficient mice develop hyprcholesterolemia. In vitro binding experiments revealed that apoC-I deficient VLDL was a poor competitor for LDL binding to the LDLR, suggesting that total apoC-I deficiency leads to an impaired receptor-mediated clearance of remnant lipoproteins (84). Later, these results were confirmed in a more detailed characterization of these apoC-I knockout mice, demonstrating than an impaired in vivo hepatic uptake of VLDL is the primary metabolic defect in apoC-I deficient mice (85). ApoC-I deficiency in humans does not alter serum lipid levels unless a high fat and cholesterol diet is fed also leading to elevated VLDL levels that are likely to result from VLDL-enrichment with apoA-I and apoA-IV (84;85).

5.1.3. ApoE

ApoE is a member of a 48kb gene cluster on chromosome 19 that also harbours the genes encoding for apoC-I, apoC-II, apoC-IV and the apoC-I´ pseudogene (66). ApoE, a 34-kDa polypeptide composed of 299 amino acids is a major component of several plasma lipoproteins, including VLDL, IDL, chylomicron remnants, and certain subclasses of HDL that facilitates transport and metabolism of lipids. It is composed of two domains: a 22-kDa NH2-terminal domain (residues 1-191) and a 10-kDa COOH-terminal domain (residues 216-299) (86). The 22kDa NH2 terminal domain contains the primary heparan sulfate proteoglycan (HSPG)-binding site (residues 140-10) (87) colocalized with the LDL receptor binding site (88-90). ApoE is mainly synthesized in the liver, but also by cells of the central nervous system, VSMCs and macrophages including those within the atherosclerotic plaque where apoE has a protective effect on atherosclerosis (91). ApoE binds to cell surface HSPG and serves as a ligand for the LDL receptor (LDLR), the LDL receptor related protein-1 (LRP-1) and other members of the LRP-family. For the internalization of apoE three major pathways are illustrated. First, apoE uptake can take place directly by binding and internalization via the LDLR. Another possibility of apoE internalization is the HSPG-LRP pathway in which apoE particles interact with cell-surface HSPG and are either transferred to the LRP for internalization or are taken up directly with the HSPG-LRP complex (92;93) (Fig. 7). The HSPG may serve as a reservoir for apoE, allowing the particles to be enriched in apoE, which facilitates their interaction with the LRP. Further HSPGs alone can mediate the direct uptake by serving as receptors and as alternate pathway (Fig. 7) (94). Interaction of apoE with lipid is necessary for its high affinity binding to the LDLR while lipid association of apoE is not required for binding to the LRP or HSPG. In contrast to binding to the LDLR, the stringency for binding of apoE to the LRP or HSPG appears to be less severe (95). Another molecule, lipoprotein lipase (LPL), binds to HSPG and has also been shown to be a ligand that can enhance cellular binding and uptake of triglyceride-rich particles with or without apoE (96).

Binding of apoE to HSPG affects neurite extension in neurons (97) and localizes secreted apoE to the surface of macrophages (98). The ability of apoE to interact with members of the LDLR family and with HSPG can also be significant for cell signalling events (99). Binding of apoE to LRP activates cAMP-dependent protein kinase A and inhibits platelet-derived growth factor-stimulated migration of SMCs (100). Inhibition of SMC proliferation by apoE is, on the other hand, mediated by its binding to HSPG (99). In addition, the interaction of apoE with HSPG has been implicated in neuronal growth and repair and, consequently, is involved in the progression of late onset familial Alzheimer´s disease (101).

Studies on nonhepatic cell lines revealed that the LRP and HSPG pathway begin to function only after particle concentration increases above levels required to saturate the LDL receptor

(94). The absence of apoE in human subjects or in apoE knockout mice also associated with premature atherosclerosis (102) and in apoE deficiency states, triglyceride rich particle plasma levels are markedly elevated, and these particles almost certainly enter cells largely through nonreceptor pathways. These properties of apoE appear to be involved in what has been termed the “secretion-recapture” role of apoE (103).

Another possibility of apoE and also of apoA-I to induce internalization signals is the binding to ATP-synthase (Fig. 7). Mitochondrial ATP synthase has two main domains, F1 and F0. The β-chain belongs to F1, a peripheral membrane protein complex containing binding sites for ATP and ADP, and the catalytic site for ATP synthesis or hydrolysis. F1 is bound on the membrane by its interaction with F0, an integral membrane protein complex in mammalian mitochondria that contains a transmembrane channel for protons (104). The protons lead to an acidic pH in early endosomes which triggers the dissociation of internalized ligand-receptor complexes and is also required for the activity of degradative enzymes within lysosomes and phagosomes.

The ectopic β-chain of ATP-synthase was identified as an apoA-I receptor with ATP hydrolase activity in hepatic HDL endocytosis (105). Receptor stimulation by apoA-I, binding to the β-chain of ATP-synthase on the cell surface, triggers the endocytosis of HDL particles by a mechanism that depends strictly on the generation of ADP. Thus, membrane-bound ATP-synthase has a role in modulating the concentrations of extracellular ADP and is regulated by apoA-I. In addition, the α- and β-chains of ATP synthase have been identified as a receptor for apoE-enriched HDL (106;107). The presence of ATP synthase at the cell surface of lymphocytes (108) and human endothelial cell has been reported (109). The membrane bound ATP-synthase triggers a cellular response, in particular endocytosis signalling, by generating ADP through ATP hydrolysis with the probable involvement of specific downstream receptors.

Other ligands for apoE are glycosphingolipids (Fig.7), especially ceramide (Cer) because apoE binds more avidly to Cer enriched microdomains on sphingomyelinase (SMase) treated liposomes as compared to the unmodified sphingomyelin (SM) rich particle surface and incorporation of SM into the emulsion surface reduced the binding capacity of apoE (110;111). These observations indicate a function of Cer rafts in apoE dependent lipid metabolism. Further it could be demonstrated that the generation of Cer in lipoproteins by SMase may stimulate HSPG and LRP-mediated uptake by macrophages, which could be intensified by apoE, and play a crucial role in foam cell formation (112).

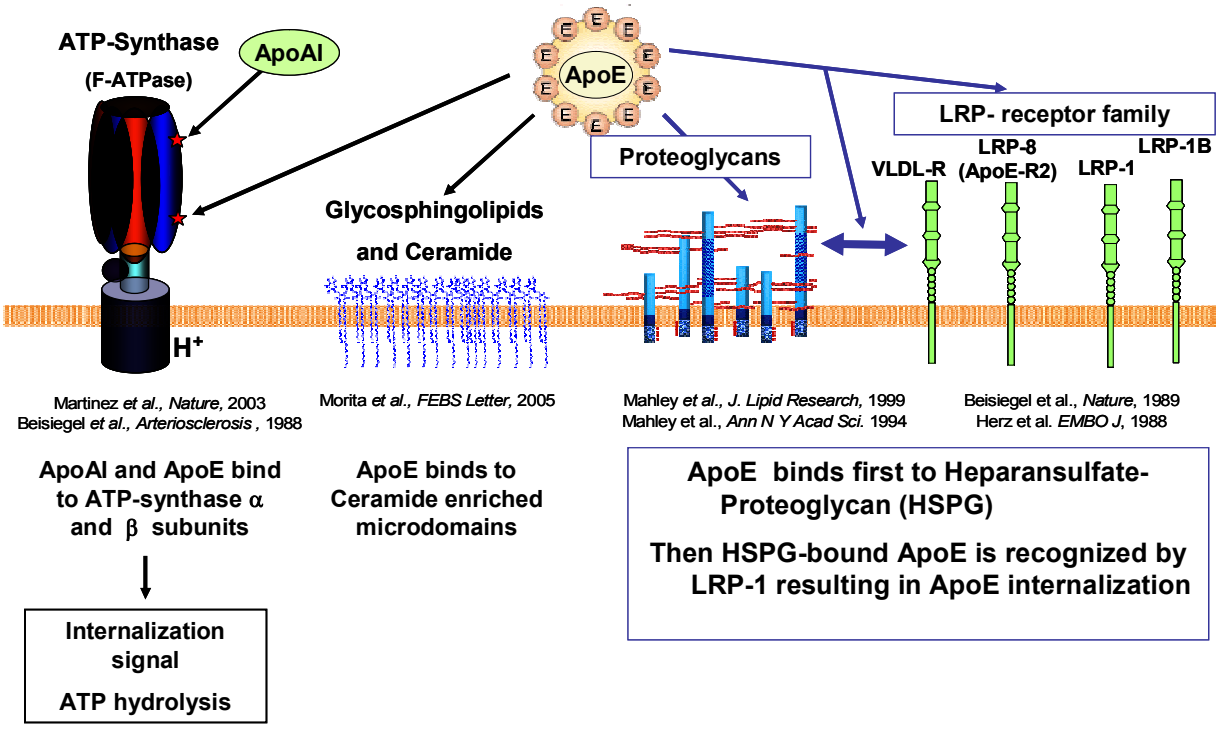

Fig. 7: ApoE is a multireceptor ligand that modulates LRP-receptor family mediated turnover of plasma membrane proteins

ApoE also plays an important role in the process of reverse cholesterol transport by promoting cholesterol efflux from macrophages which is mediated via a mechanism that is not dependent on ABCA1 (113). Extracellular apoE and endogenously synthesized apoE by macrophages facilitate cholesterol efflux through distinct mechanisms (114). Exogenous apoE-mediated cholesterol efflux requires its interaction with the scavenger receptor SR-BI, while in cells that express endogenous apoE, SR-BI does not promote cholesterol efflux (115). Other functions of apoE, unrelated to lipid transport are known, including modulation of cell growth and differentiation as well as immunoregulation (116). Recently it has been reported that apoE binds lipid antigens and delivers them by receptor-mediated uptake into endosomal compartments containing CD1 in antigen-presenting cells (APCs) (117). CD1 molecules survey endocytic compartments and bind lipid antigens that are presented at APC surface to lipid antigen-reactive T cells (118;119). Further ApoE mediates the presentation of serum-borne lipid antigens and can be secreted by APCs as a mechanism to survey the local environment to capture antigens or to transfer microbial lipids from infected cells to bystander APCs (117). Thus, the immune system used a component of lipid metabolism to develop immunological responses to lipid antigens.

The secretion of endogenous apoE by macrophages is modulated by ABCA1 and ABCG1 (120). After receptor-mediated endocytosis of triglyceride rich lipoproteins (TRL) into the liver, TRL particles are immediately disintegrated in peripheral endosomal compartments. Whereas core lipids and apoB are delivered for degradation into lysosomes, TRL-derived

apoE is efficiently recycled back to the plasma membrane. This is followed by apoE re-secretion and association of apoE with HDL (121). Further it could be demonstrated that apoE is linked to HDL_3-dependent and independent cholesterol efflux (121). In the presence of HDL the re-secretion of apoE and cholesterol leads to the formation of apoE/cholesterol-enriched HDL particles. After internalization TRL-derived apoE and cholesterol remain associated in early endosomal antigen 1 (EEA1)-positive endosomes. Most importantly, apoE recycling involves the internalization of HDL_3-derived apoA-I and its targeting to apoE/cholesterol-containing endosomes, indicating that endosomal HDL_3-derived apoA-I can mobilize pre-existing apoE/cholesterol complexes. A number of reports (122) hypothesized an interaction between apoA-I and apoE and concluded that apoA-I concurrently stimulates secretion of endogenous apoE and cholesterol efflux from lipid-loaded macrophages. In addition secretion of apoE from macrophages is at least in part associated with cell-derived cholesterol (123;124).

Degradation of apoE which in turn affects apoE secretion can take place via two pathways: the proteasomal ER-associated degradation (ERAD) pathway and the re-uptake pathway from the cell surface. Before degradation by proteasomes ubiquitination of apoE is necessary. It could be demonstrated that ubiquitinated apoE accumulates in macrophages and hepatocytes treated with specific proteasomal inhibitors indicating that the protein undergoes degradation in proteasomes (125). The re-uptake from the cell surface takes place after binding of nascent apoE containing particles to LDL receptors or HSPGs. After endocytosis of apoE, delivery to lysosomes and proteolytic degradation follows (126). The re-uptake pathway is stimulated by sterol deprivation (127), which induces LDL receptor expression. Until now a third pathway, the post ER presecretion proteolysis (PERPP)-pathway have been shown to be involved in apoB degradation (128) but not in apoE degradation (129). This pathway acts between the ERAD and the re-uptake patway after exit of apolipoproteins from the ER but before export across the PM. The PERPP patway involves the post-ER compartment and phosphoinositol 3 kinase (PI3K) signalling and does not act via microsomal transfer protein inhibition, active proteosomes, cell surface LDL-receptors, cell surface HSPGs or functioning lysosomes. It is regulated by insulin and highly unsaturated fatty acids (Ω-3 fatty acids) such as DHA (docosahexanenoic acid (C22:6)) and EPA (eicosapentaneoic acid (C20:5)) in fish oil.

5.2. Transfer proteins

5.2.1. Cholesteryl esterase transfer protein (CETP)

CETP is a hydrophobic 74 kDa member of the lipid transfer/lipopolysaccharide-binding protein (LBP) gene family, which also includes phospholipid transfer protein (PLTP),

lipopolysaccharide-binding protein (LBP) and bactericidal/permeability-increasing protein (BPI). Although these four proteins possess different physiological functions, they share marked biochemical and structural similarities. CETP which is not expressed in murines is mainly associated with the HDL particle in the circulation and promotes the transfer of CE from HDL to apoB-containing particles (i.e. VLDL and LDL) in exchange for triacylglycerols. CETP can be seen as a facilitator of cholesterol flux through the reverse cholesterol transport system. Through its action CE (derived from HDL) can be taken up by the liver through receptor-mediated uptake of apoB containing lipoproteins. CETP regulates the plasma levels of HDL and the size of HDL particles. The deficiency of CETP causes various abnormalities in the concentration, composition, and function of both HDL and LDL and causes hyperalphalipoproteinemia (HALP) (130). CETP gene is induced by sterols via LXRα/RXRα and LXRβ/RXRα which transactivates the CETP promoter via its DR4 element (131). Human cultured monocyte derived macrophages (MDM) synthesize and secrete CETP (132). Induction of CETP expression occurs during the differentiation of monocytes into macrophages (133). The intracellular accumulation of CE is positively correlated with secretion of CETP, suggesting that CETP may function to maintain intracellular cholesterol homeostasis during differentiation and in response to an excess of cholesterol accumulation. CETP also mediates HDL conversion like PLTP (134). But in contrast to PLTP no release of lipid-poor apoA-I was detected in HDL conversion mediated by CETP (135).

5.2.2. Phospholipid transfer protein (PLTP)

PLTP (previously known as lipid transfer protein II, LTP-II) is like CETP a member of the LBP gene family and was originally characterized in human plasma as a factor capable of transferring phospholipids between the major lipoprotein classes (136). PLTP is present in human atherosclerotic lesions, is expressed by macrophages and induced during foam cell formation (137). The regulatory role of PLTP is achieved via its two main functions, phospholipid transfer activity and the capability to modulate HDL size and composition in a process called HDL conversion (138;139). PLTP promoted preferentially the formation of large HDL particles whereas CETP favoured the occurrence of small HDL (140). Further PLTP also participates in the exchange of phospholipids between HDL particles and plays a critical role in HDL metabolism. Through HDL conversion with a concomitant release of lipid-poor apoA-I, PLTP is capable of generating preβ-HDL which acts as an efficient acceptor in the cholesterol efflux process at the plasma membrane of peripheral cells. On the other hand PLTP has a major role in maintaining the HDL levels in the circulation due to its ability to transport surface remnants after lipolysis of triglyceride-rich lipoproteins. Thus PLTP could play an important role in the prevention of atherosclerosis (141). The activity of PLTP is closely related to HDL levels. Disruption of PLTP in mice dramatically reduces plasma HDL

cholesterol and phospholipid levels (142). PLTP is regulated by liver X receptors in vivo and plays an important role in LXR agonist-mediated increase in HDL cholesterol and size in mice (143).

PLTP also promotes the transfer of α-tocopherol (144), LPS (145) and cholesterol (146).

6. Atherogenic modified lipoproteins

6.1. Enzymatically degraded LDL (E-LDL)

After infiltration into atherosclerotic lesions, LDL particles are degraded in situ by enzymes secreted by a variety of vascular cells, including macrophages. Enzymatic degradation of LDL in vitro is achieved by trypsin which degrades apoB, rendering underlying lipids accessible to cholesterol esterase for the cleavage of CE. This modified LDL particles are in structure, biological properties, and composition similar to lipid particles that accumulate in atherosclerotic lesions (147) and possess an atherogenic moiety (148). E-LDL is rapidly internalized by macrophages by means of a scavenger receptor (SR)-dependent pathway that is mediated partly via CD36 but not macrophage scavenger receptor A (MSR-A). (149). Highest E-LDL binding was observed on CD14 high CD16+ (MNP2) monocytes, suggesting a selective interaction of E-LDL with distinct subpopulations of monocytes (149). In addition it could be demonstrated that FcγRIIA/CD32 has the highest surface expression density on MNP2, proposing an involvement of FcγRII/CD32 in E-LDL binding on peripheral blood monocyte subpopulations (149). Studies have demonstrated the binding of E-LDL to C-reactive protein (CRP) and complement activation (150). CRP is an acute-phase protein in humans which activates the complement system and is probably involved in early atherogenesis. On monocytes, specific CRP binding occurs through FcγRI/CD64 with low affinity as well as FcγRIIA/CD32 with high affinity (151). Immunohistochemical colocalization of E-LDL and activated complement in the extracellular space at the earliest stage of atherosclerotic lesion development (152) could be shown. Further selective adhesion and transmigration of monocytes is induced by E-LDL through endothelial cell monolayers (153). Further E-LDL stimulates MCP-1 production in macrophages (154). Free fatty acids present in E-LDL selectively stimulate IL-8 secretion in endothelial cells which is crucial for firm adherence and transmigration of circulating monocytes into the intima (155). These data show that the extracellular generation of E-LDL by enzymatic degradation is an event occurring during the earliest stage of atherosclerosis and that E-LDL induces monocyte recruitment into atherosclerotic lesions and is internalized by monocyte-derived macrophages, leading to foam cell formation during atherogenesis.

6.2. Oxidized LDL (Ox-LDL)

A prerequisite for macrophage uptake and cellular accumulation of cholesterol is oxidative modification of LDL (156). The initiation of the oxidation process is induced by the intracellular generation of lipoperoxides which are transferred to LDL through the development of O_2 derived free radicals. These species later initiate a series of chemical reactions that are generally referred to as lipid peroxidation. Ox-LDL, generated in vitro by treatment with copper as a catalyst and extensive dialysis, is taken up avidly by macrophages and can cause foamcell formation. Oxidation of LDL leads to a number of changes in the composition of the particle, which vary depending on the type and concentration of oxidant used and the time of exposure (157;158). The rates at which specific components undergo oxidation vary greatly. In general, the unsaturated fatty acyl chains of phospholipids, CE, and triglycerides are oxidized most readily, while cholesterol and saturated fatty acids react more slowly. In addition, a significant proportion of the unsaturated acyl chains of CE and phospholipids is oxidized to hydroperoxides, isoprostanes, and more advanced oxidation products (159). A small proportion of cholesterol is converted to oxysterols, initially 7-hydroperoxycholesterol. ApoB, the sole protein of LDL, is subject to both direct oxidative modification and reaction with products of lipid oxidation. Depending on the degree of oxidation, in 'minimally', lightly or mildly Ox-LDL, apoB is modified only to a minor extent and is still able to bind to the LDL receptor and is taken up via clathrin coated pits while in heavily Ox-LDL, apoB prevent LDL from binding to LDL receptors, and instead Ox-LDL is recognised by receptors such as scavenger receptor A (SR-A) and CD36 (160;161).

Recent studies have indicated that the subsequent metabolism of Ox-LDL differs substantially from non-oxidized lipoproteins (162;163). In particular, Ox-LDL is poorly able to induce cytoplasmic CE accumulation. This appears to be the result of the chemical alterations during oxidation to components of LDL. For mildly oxidized LDL mediated accumulation, it is known that initially lysosomal CE hydrolysis generates free cholesterol accumulation in lysosomes (164). This cholesterol, however, is restricted from exiting the lysosome. This would suggest that certain modifications of lipoproteins, or excess free cholesterol itself, can inhibit trafficking of cholesterol out of the lysosome.

Mildly oxidized LDL also has a number of biological activities that are potentially proatherogenic. These include effects on macrophage viability, migration, and proliferation, and on cholesterol export, signalling, protein expression, and secretion. While modest levels of OxLDL stimulate macrophage survival and proliferation, there is agreement that high doses cause death. The toxic components of Ox-LDL are not well defined, but may include oxysterols (165). Ox-LDL contains lysophosphatidylcholine (LPC) which is a potent chemoattractant for macrophages (13) because it upregulates the expression of vascular cell

adhesion molecule such as ICAM-1 which is present within the endothelium and increases monocyte adhesion.

Ox-LDL itself is directly chemotactic for monocytes and T cells (but not for B cells or neutrophils, neither of which are found in lesions) (20;166). Among other biological effects, Ox-LDL (and its various oxidized lipid components) is cytotoxic for endothelial cells (167), mitogenic for macrophages and smooth muscle cells and stimulate the release of MCP-1 and of monocyte colony-stimulating factor (MCSF) from endothelial cells. Further, Ox-LDL can stimulate the production of many inflammatory mediators (e.g. endothelin-1) from other vascular cells, in turn resulting in diverse inflammatory responses in the arterial wall.

All atherogenic lipoproteins, once deposited in the intima, may exert direct or indirect proinflammatory effects. Table 2 summarizes the potential roles of Ox-LDL in atherogenesis, with special reference to its properties as an inflammatory mediator.

In summary atherogenic lipoproteins exert diverse effects by inducing chronic inflammatory reactions during lesion formation. They can augment the production of cytokines by vascular cells, and through the autocrine and paracrine mechanisms, the inflammatory reaction may lead to a vicious cycle resulting in lesion progression.

Table 2: Possible proatherogenic effects of oxidized LDL

Effects	**Possible mechanisms**
Adhesion of monocytes to endothelial cells ↑	Increased expression of adhesion molecules on endothelial cells
Monocyte and T lymphocyte chemotaxis ↑	Induction of MCP-1 production and direct chemoattractant effect
Scavenger receptor A and CD36 ↑	Activation of AP-1 and its transcription factors
Foam cell formation ↑	Enhanced uptake of Ox-LDL mediated by scavenger receptors
Induction of proinflammatory genes	Activation of NFκB, and AP-1, and increased cAMP
Increased cellular death	Activation of apoptosis and formation of cholesterol crystals
Thrombosis ↑	Induction of tissue factor, increased platelet aggregation
Impaired vascular functions	Dysfunction of ET-1 and NO
Plaque rupture ↑	Increased MMPs production

↑: enhanced

Table from Jianglin Fan and Teruo Watanabe: inflammatory reactions in the pathogenesis of atherosclerosis, review. J Atheroscler Thromb, 2003; 10: 63-71 and see also Atherosclerosis an inflammatory disease, Schmitz G., Torzewski M, Inflammatory and Infectious Basis of Atherosclerosis, 2001, Birkhäuser Verlag, Basel/Switzerland.

7. Uptake of modified lipoproteins by macrophages

7.1. Scavenger receptors (SRs)

SRs are heterogeneous types of receptors which are expressed on macrophages and macrophage derived foam cells in atherosclerotic lesions, and are important for these cells to remove lipoproteins deposited in the lesions.

SRs are defined as receptors binding to chemically modified lipoproteins such as acetylated LDL (AcLDL), Ox-LDL and often many other types of ligands. They have heterogeneous molecular structures, and consist of various types. These receptors are divided into classes A, B, C, D, E, F, and G and different types of receptors are members of each class (23).

7.1.1. SRs: classA

Class A receptors include type I, type II, and type III macrophage scavenger receptor (MSR), and MARCO (macrophage receptor with collagenous structure). These receptors are generally called macrophage scavenger receptor class A (MSR-A). They possess a collagenous domain required for ligand recognition and are expressed on macrophages. (168;169). MSR-A I,II are expressed on the cell membrane of macrophages. Their binding properties are currently considered identical.

The C-terminal type-specific domain in MSR-A I is called the scavenger receptor “cysteine-rich” domain (SRCR) which is not predictive of SR activity; the selective upregulation of this receptor accomplishes the uptake of modified LDL during differentiation of monocytes into macrophages, and its expression is important for foam cell formation (170). MSR-A II is also important for the uptake of modified LDL by macrophages (171). MSR-A III is localized in cytoplasmic vesicles and is not expressed on the cell surface. Thus, this receptor is unable to bind to any extracellular ligands (172). In the trans-Golgi system, MSR-A I,II are packed into secretory vesicles, and the vesicles are transported into the cell periphery of macrophages, thus recycling MSR-A I,II to the cell membrane for reutilization (173).

A number of different biological roles for the SR-A are suggested. These include the endocytosis of modified lipoproteins and its association with vascular disease, the adhesion of macrophages to the substratum and other populations of cells, the binding and ingestion of microbes, the detoxification of pathogen-specific components and the phagocytosis of apoptotic or unwanted host cells (174).

However, the development of atherosclerosis was not completely inhibited by MSR-A I, II deficiency, suggesting that SRs other than MSR-A I,II, such as MARCO, CD36, and macrosialin/CD68, are implicated in the uptake of Ox-LDL by macrophages and in the transformation of the macrophages into foam cells during atherogenesis.

MARCO is a 210-kDa membrane glycoprotein consisting of molecular trimeric structures similar to those of MSR-A I,II, and III. It has an extremely long collagen like domain and a short α-helical coiled coil domain (175). Because of these molecular structures, the MARCO receptor is unable to dissociate from ligands within endosomes, and MARCO-ligand complexes are directly transported into lysosomes without receptor-ligand dissociation.
The SR cystein rich CD163 is a macrophage-restricted endocytic receptor for haemoglobin-haptoglobin complexes.

7.1.2. SRs: class B

CD36 and SR-BI (scavenger receptor type BI) belong to class B of SRs. CD36 is a double spanning SR with a very different structure from SR-A. CD36 is an 88-kDa glycoprotein expressed on monocytes/macrophages, platelets, and endothelial cells, and in adipose tissue; it binds to various ligands such as fatty acids, anionic phospholipids, collagen, thrombospondin, and Ox-LDL (36). CD36 was shown to function as an Ox-LDL receptor in macrophages (160) and a fatty acid transporter in adipocytes (176). In atherosclerotic lesions of human aorta, the expression of CD36 predominates in macrophage-derived foam cells compared to non-loaded macrophages and is distinct from the expression of MSR-A I,II suggesting a different role of these two receptor types (177). CD36 also plays a role in macrophage fatty acid metabolism, adhesion, and phagocytosis of apoptotic neutrophils (36).
SR-BI is a 509-amino-acid-long member of the CD36 superfamily of proteins with two transmembrane domains like CD36 but a quite different function. SRB-I and CD36 are fatty acylated proteins that cluster in caveola-like cholesterol-rich lipid domains in cultured cells (36). SR-BI is regarded as an HDL receptor, and mediates the selective uptake of HDL cholesterol by hepatocytes and steroidogenic cells (52). SR-BI can also function as a LDL receptor (binding and selective uptake). Although HDL does not bind as tightly as LDL, it binds preferentially when both ligands are present. CD36 can also bind HDL and LDL, but it cannot efficiently mediate CE uptake (178). The tissue distribution of SR-BI is that expected for an HDL receptor. It is highly expressed in liver and steroidogenic tissues, precisely those tissues that exhibit the highest levels of selective uptake of HDL-CE. In macrophages in atherosclerotic plaques, SR-BI is also present (178). The expression of SR-BI is coordinately regulated with cholesterol metabolism. Its expression in steroidogenic cells is regulated via the cAMP/protein kinase A signal transduction pathway that includes transcription factors such as CCAAT/enhancer-binding proteins (C/EBPs) and steroidogenic factor-1 (SF-1). The transcriptional regulation of SR-BI appears to be due to SR-BI promoter binding sites for a number of transcription factors including C/EBP, SF-1, and sterol regulatory element binding protein-1 (SREBP-1) (179).

SR-BI facilitates the cellular selective uptake of cholesterol (primarily in the form of CE) from the hydrophobic cores of lipoproteins, but not the apolipoprotein at the lipoprotein´s surface. It does not involve the sequential internalization of the intact lipoprotein particle and its subsequent degradation which is the case in the uptake of LDL via the LDLR (Fig. 2). (168). The detailed molecular mechanism underlying SR-BI-mediated selective lipid uptake has not yet been elucidated. In addition SR-BI can also mediate the bidirectional flux of unesterified cholesterol and phospholipids between HDL and cells.

Hepatic SR-BI mediates “reverse cholesterol transport” which implicates the transfer of cholesterol from plasma HDL to the bile for excretion. In atherosclerotic lesions of apoE-deficient mice, SR-BI is expressed in macrophages, and the expression is increased by peroxisome proliferator-activated receptors (PPARs), suggesting a contribution of SR-BI to the uptake of OxLDL by macrophages in loco (180).

Thus, SR-BI plays a key role in controlling the structure and amount of cholesterol in plasma HDL, steroidogenic and hepatic uptake of HDL cholesterol, and the use of HDL cholesterol for biliary cholesterol secretion.

7.1.3. SRs: classes D through G

CD68/macrosialin, classified as a class D receptor, is a member of the LAMP (lysosomal-associated membrane protein) family expressed on the endolysosomal compartments and partly on the cell surface of macrophages (181). It is demonstrated in macrophages and macrophage-derived foam cells in human and murine atherosclerotic lesions and was able to bind Ox-LDL in vitro (182;183). Lectin-like Ox-LDL receptor (LOX-1) and SR expressed by endothelial cells (SREC) are expressed on vascular endothelial cells and are classified as class E and class F, respectively (184;185). LOX-1 is also expressed on macrophages in humans and mice (185). It mediates endocytic uptake and subsequent lysosomal degradation of Ox-LDL. Binding of Ox-LDL to this receptor induces several cellular events such as activation of NFκB (186), upregulation of MCP-1 (187) and reduction in intracellular nitric oxide (186). Other ligands for LOX-1 include polyanionic compounds, aged/apoptotic cells (188), activated platelets (189) and bacteria (190). In addition, two other distinct novel SRs, SR for phosphatidylserine (PS) and Ox-LDL (PSOX, SR-G class) and PS receptor (PSR), have been identified (191;192). SR-PSOX recognizes PS and Ox-LDL and is predominantly expressed in lipidladen macrophages of human atherosclerotic lesions. This receptor does not share any structural homology with other Ox-LDL receptors. PSR is expressed not only in macrophages but also in fibroblasts and epithelial cells and is involved in the phagocytosis of apoptotic cells (192).

7.2. Uptake of lipoproteins by opsonin receptors including Fcγ- and complement receptors

Cellular uptake of lipids and lipoproteins by macrophages is either mediated by charge and motif receptors (scavenger receptors) directly recognizing non-opsonized ligands or by opsonization. Opsonization occurs by either non-specific opsonins (complement components or pentraxins including C-reactive protein (CRP), serum amyloid P (SAP), serum amyloid A (SAA), β-Amyloid and/or specific opsonins (immunoglobulins) prior to cellular uptake. Fcγ-receptors complement receptors and LRPs mediate uptake of opsonized lipoproteins.

Amyloid precursor protein (APP) is a type I integral membrane protein. The β-secretase-processed carboxyl-terminal fragment of APP is further processed to generate β amyloid peptide. Isoforms of APP containing the Kunitz proteinase inhibitor domain bind directly to LRP (193) and are internalized especially after the APP binds a natural target proteinase, such as epidermal growth factor-binding-protein (194). Potential modulation of APP transport and processing may involve apoE lipoproteins which may interfere with Kunitz-domain-mediated binding of APP to the extracellular domain of LRP. Therefore apoE could be regarded as an opsonine for APP binding to LRP receptors (195). APP is bridged to LRP-1 within the cytoplasm by FE65, a bifunctional adaptor protein which interacts with the NPxY motifs present in the cytoplasmic tails of LRP and APP (Fig. 8a) (196). This raises the possibility that LRP can modulate the intracellular trafficking of APP. Assembly of mammalian ena (Mena) on the cytoplasmatic tails of LRP and APP may function in the local reorganization of the cytoskeleton. Further tyrosine-phosphorylated mammalian Disabled protein 1 (mDab1) can recruit nonreceptor tyrosine kinases, such as src and ab1, to the cytoplasmic tails of the receptors to which it binds (e.g.: LDLR, LRP, APP) (Fig. 8a).

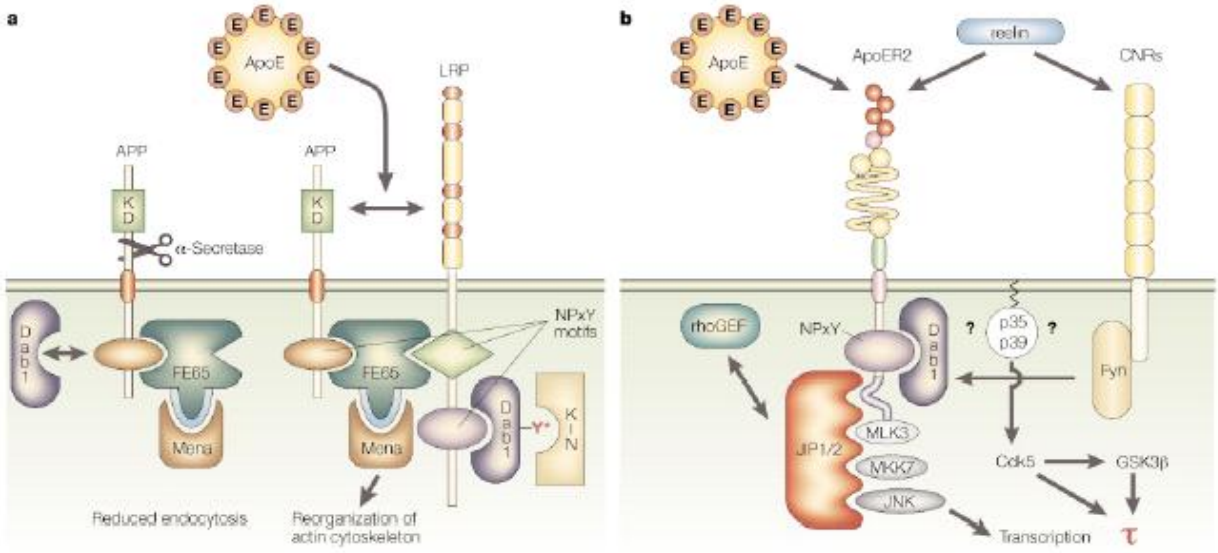

Fig. 8: Hypothetical models showing interactions of cytoplasmic neuronal adaptor and scaffold proteins with the LDL receptor family and APP (Herz, review, nature neuroscience 2000)

a. Interaction of Dab1, FE65, LRP and APP **b.** Hypothetical model of the reelin signalling pathway

Amyloid-β (Aβ) is a 4kDa hydrophobic polypeptide which is produced by proteolytic cleavages of the APP by the action of proteases called beta- and gamma secretases. Aβ deposition, the hallmark of Alzheimer disease (AD) (197) has been identified in brain parenchyma, within cerebral blood vessels (198) as well as in atherosclerotic plaques (199). Neurons poduce Aβ peptides of different sizes. The most prominent being 40 and 42 amino acids long ($A\beta_{40}$ and $A\beta_{42}$ respectively). The majority of all Aβ isoforms produced is $A\beta_{40}$ but about 10% is $A\beta_{42}$ (200). In AD-brains deposits of $A\beta_{42}$ are found more frequently in plaques and capillaries than $A\beta_{40}$ (201) which could be due to altered cellular processing of the APP with increased production or a reduced removal of cleavage products like $A\beta_{42}$ (202). Intracellular cholesterol regulates the generation of insoluble Aβ peptides, as increased concentrations of free cholesterol in membranes have been shown to stimulate Aβ production (203). Moreover Stanyer et al demonstrated that LDL and Ox-LDL interact with $A\beta_{40}$ and that these complexes were more readily internalized by SMCs than unbound peptide (204). Additionally fibrillar $A\beta_{42}$ binds to the class B scavenger receptor CD36 (205-207), the CD36/$\alpha_6\beta_1$-integrin/CD47 receptor complex (208) and also to LRP which is suggested to be involved in $A\beta_{42}$ binding and uptake, acting as an opsonin receptor (209). These findings strongly indicate a common link between Aβ and lipoproteins in the development of cerebrovascular disease as well as AD. However, the exact mechanism how capillary Aβ-deposits develop and whether macrophages and lipoproteins are involved in this process is still unknown. Several cellular processes or pathway in which neuronal apoE receptors are involved may affect the pathogenesis of AD. They include interactions with APP, modulation of Aβ clearance from the extracellular space and transmission of signals to neurons. Any of these functions may be modulated by binding of apoE to the extracellular domains of the different members of the LDL receptor family. The reelin signalling pathway is a downstream target of apoE induced neuronal signalling. A model is created (195) which suggests that binding of Dab1 to the cytoplasmatic tails of the VLDLR and apoE receptor 2 (ApoER2) is critical for the transmission of reelin signal to migrating neurons (Fig. 8b). An extended family of cadherin-related neuronal receptors (CNR) is also thought to participate in this process (Fig. 8b). CNRs have been shown to bind the non-receptor tyrosine kinase Fyn on their cytoplasmic tail and CNRs may interact with reelin bound to VLDLR or ApoER2 at the cell surface, resulting in tyrosine phosphorylation of Dab1. Coupling of p35, p39 and Cdk5 to the receptors and Dab1 on the plasma membrane may involve interactions with adaptor and scaffold proteins that bind to the cytoplasmic tails of the LDL receptor family (Fig.8b). Members of the JIP family of scaffold proteins bind to an alternatively spliced insert in the cytoplasmic tail of ApoER2. This may recruit stress-activated and mitogen-activated protein (MAP) kinases (for example, MLK3, MKK7 and JNK) and other cellular signalling

components (for example, rhoGEF) into the complex, resulting in the local reorganization of the cytoskeleton and modulation of gene transcription (Fig. 8b).

CRP, an innate recognition lectin is associated with coronary heart disease (210). Of particular importance might be calcium-dependent in vitro binding of CRP to E-LDL accompanied by an enhancement of complement activation (211). On monocytes, specific CRP binding occurs through FcγRI/CD64 (212) as well as FcγRIIA/CD32 (213). Previously it could be shown that cell surface ceramide is a prerequisite for recruitment of cross-linked FcγRIIA to rafts, which triggers the receptor tyrosine phosphorylation and signalling (214). Further the association of FcγRIIA with rafts leading to signalling events was described for platelets (215) and human neutrophils (216).

SAP is the second pentraxin present in human plasma, which also has been reported to locate to atherosclerotic lesions and bind to a variety of ligands such as C4b-binding protein, CRP, complement components C1q and C3bi, and human IgG in a calcium-dependent manner. SAP specifically interacts with HDL as well as VLDL but not with LDL (217) and can activate the complement system (218).

SAA, a family of acute-phase reactants, is found on HDL and displaces apolipoprotein AI from HDL particles and converts α-migrating mature HDL back to preβ$_1$-precursor HDL particles (219). Further functions of the SAAs include participation in detoxification, depression of immune responses, and interference with platelet functions (220).

Antibodies, as specific opsonines against different epitopes of lipids and lipoproteins (charge modified phospholipids, cholesterol or cryptic protein epitopes), have been demonstrated in human plasma. Human IgG1 and IgG3 autoantibodies reactive with Ox-LDL have been isolated from human plasma (221).

7.3. Phagocytosis

Phagocytosis is an actin dependent uptake of relatively large particles (>0.5 μm) into vacuoles by the cell. Two types of phagocytosis can be distinguished (Fig. 9):

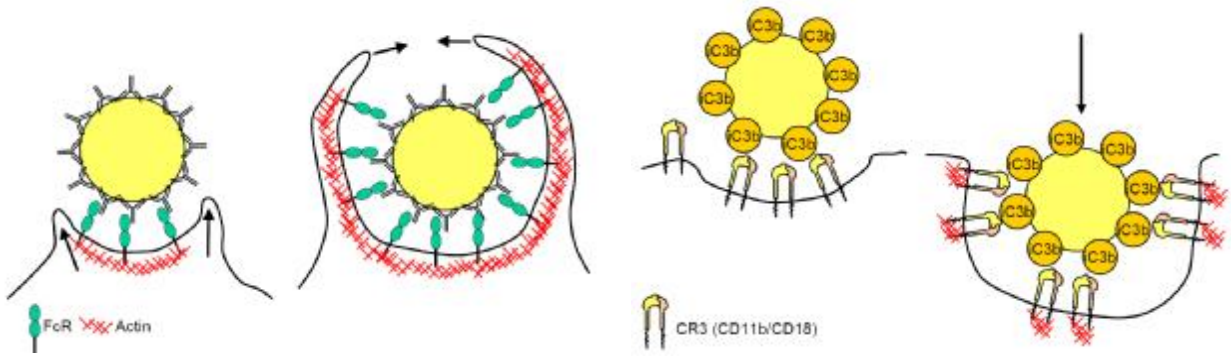

Fig. 9: Schematic view of type-I (engulfment) and type-II (sinking in) phagocytosis

Type-I phagocytosis (engulfment phagocytosis): This type of phagocytosis is mediated by Fcγ receptors (FcγRI/CD64, FcγRII/CD32 and FcγRIII/CD16) which bind to IgG-coated particles; it goes along with membrane ruffling and pseudopodia extension by a zippering mechanism and uses the Rho family GTP-ases Cdc42 and Rac (Fig. 9).

Type-II phagocytosis (sinking in phagocytosis): This type is complement receptor-mediated (CR3: CD11b/CD18, Mac-1, αMβ2) which binds C3bi-opsonized targets and particles sink into the cell. This mechanism uses only the GTP-ase RhoA (Fig. 9).
Previously it has been reported that CR3 mediates type-II and type-I phagocytosis during opsonic and nonopsonic phagocytosis, respectively (222). This suggests that CR3 triggers different intracellular signals which mediate distinct phagocytic processes.

Interaction between receptors and ligands on the particle results in signal transduction events that lead to actin polymerisation, particle engulfment and formation of the phagosome. During a maturation process, the phagosome interacts and fuses with early and late endosomes as well as with lysosomes transforming it into a phagolysosome where digestion takes place. The fusion processes are regulated by small GTP-binding proteins of the rab family.
FcRs recognize the Fc portion of antibodies and deliver signals when they are aggregated at the cell surface. FcRs can be functionally divided in two major types: FcRs that can trigger cell activation and FcRs that cannot. The aggregation of FcRs having immunoreceptor tyrosine-based activation motifs (ITAMs) activates sequentially src family tyrosine kinases and syk family tyrosine kinases that connect transduced signals to common activation pathways shared with other receptors. FcRs with ITAMs elicit cell activation, endocytosis and phagocytosis. There are four multichain FcRs with ITAMs: FcγRI, FcγRIIIA, FcεRI and FcαRI. FcRs having immunoreceptor tyrosine-based inhibition motifs (ITIMs) do not trigger cell activation. FcγRIIB are a family of single-chain low-affinity IgG receptors not containing ITAMs. FcγRIIB is a negative coreceptor of all receptors with ITAMs because coaggregation of antigen receptors or FcRs having ITAMs with FcRs having ITIMs negatively regulates cell activation (223).

8. Peroxisome proliferator-activated receptors (PPARs)

PPARs, nuclear receptors, are ligand-activated transcription factors that have been implicated to play an important role in obesity-related metabolic diseases such as hyperlipidemia, insulin resistance, and coronary artery disease. These orphan receptors are activated by fatty acids and derivatives and proposed to control lipid homeostasis by

regulating the expression of genetic networks involved in lipid metabolism, transport, storage and elimination (224).

PPAR bind, upon heterodimerisation with RXR (retinoid X receptor), to specific peroxisome proliferator response elements (PPRE) in the promoter of target genes, thus regulating the transcription of these genes. Both the formation of the PPAR/RXR heterodimer and the subsequent transcriptional activation of the target gene are ligand-dependent. Ligand binding may evoke conformational changes within the DNA-binding domain, thereby altering the potential to stimulate transcription of target genes.

The nuclear receptor subfamily of PPARs consists of isoforms α, γ and δ with distinct expression patterns and biological activities. Although these different members are encoded by separate genes, they have a similar protein structure.

PPARα is expressed in liver, heart, muscle, and kidney where it regulates fatty acid catabolism (225) and is the molecular target of the lipid lowering fibrates (e.g. fenofibrate and gemfibrozil), whereas PPARγ is highly enriched in adipocyte and macrophage and is involved in adipocyte differentiation, lipid storage, and glucose homeostasis (226). It mediates the activity of the insulin-sensitizing thiazolidinediones (e.g. rosiglitazone and pioglitazone). PPARδ is expressed ubiquitously with a less defined function. It has been implicated in keratinocyte differentiation and wound healing and, more recently in mediating VLDL signalling of the macrophage (227-229).

Furthermore, PPARs are expressed in atherosclerotic lesions and have been shown to affect transcription of genes in vascular endothelial cells, smooth muscle cells, monocytes, and monocyte-derived macrophages. The down-regulation of several atherogenic genes by PPAR activation suggests that stimulation of PPAR expression and/or activation may have beneficial effects on the progress of atherosclerotic disease.

The fact that dietary fatty acids are natural activators of this subfamily implies that lipoproteins serve as ligand carriers for PPARs, which in turn modulate lipid homeostasis of the body. PPAR activators have effects on both metabolic risk factors and on vascular inflammation related to atherosclerosis.

8.1. PPARγ and atheroslcerosis

PPAR-γ is present in virtually all vascular- and atheroma-associated cells seen in the vessel wall, including VSMCs, endothelial cells, monocytes, macrophages, T lymphocytes, and human atherosclerotic lesions (230). Its expression is significantly increased upon monocyte to macrophage differentiation and the PPAR-γ protein is present at high levels in the macrophage-derived foam cells of atherosclerotic lesions (231;232). PPAR-γ-regulated target genes are relevant to atherosclerosis and PPAR-γ agonists limit atherosclerosis in mouse

models (230). Furthermore PPARγ has been shown to regulate the expression of activation-dependent genes in macrophages (233).

8.2. PPARγ activators and agonists

PPARγ is activated by arachidonic acid metabolites derived from the cyclooxygenase and lipoxygenase pathways, e.g. 15-deoxy-Δ-12, 14-prostaglandin J2 (PG-J2) and 15-hydroxyeicosatetraenoic acid (15-HETE) (234-236). In addition, fatty acid-derived compounds of Ox-LDL, such as 9- and 13-hydroxyoctadecadienoic acid (9- and 13-HODE), activate PPARγ. Treatment of macrophages with Ox-LDL in vitro induces expression of both PPARγ and LXRα mRNAs (237). Internalization of Ox-LDL provides the cell with activators of PPARγ, such as oxidized fatty acids as well as with activators of LXRs such as 27- and 25-hydroxycholesterol (234;238). PPARγ ligands can also be produced locally in atherosclerotic lesions through the oxidation of fatty acids by 12/15 lipoxygenase (239).

Synthetic high affinity PPARγ ligands are the antidiabetic glitazones respectively thiazolidones (TZDs) (used in treatment of insulin resistance and type 2 diabetes) and the pharmacological non steroidal anti-inflammatory drugs (NSAIDs) indomethacin and ibuprofen.

8.3. Functions of PPARγ activators

PPARγ activators inhibit the expression of MMP-9 of human macrophages (240) and VSMCs, thus interfering with VSMC proliferation (241). The production of the inflammatory cytokines TNF-α, IL-6 and IL-1β by activated monocytes is inhibited by PPARγ (242) and the transcription of monocyte chemoattractant protein (MCP)-1 is decreased. The expression of inducible nitric oxide synthase (iNOS) and the scavenger receptor A in interferon (IFN)- γ-stimulated mouse macrophages (243) is inhibited by PPARγ. Activation of PPARγ has been shown to enhance CD36 expression of macrophages, which may indicate that PPARγ could stimulate uptake of oxidized LDL and contribute to foam cell formation (234;237). These CD36 effects may be compensated by increased expression of the putative cholesterol/phospholipid transporter ABCA1 and apoE in macrophages (244) through the activation of LXRα. LXRα forms a heterodimer with the retinoic-X-receptor (RXRα) and is a direct transcriptional target of PPARγ that promote cholesterol excretion and efflux by modulating expression of ABCA1 and apoE (245;246). Inhibition of the expression of the intracellular adhesion molecules ICAM-1 and VCAM-1 by troglitazone in human endothelial cells (247) and the induction of the scavenger receptor CLA-1/SR-BI by PPARγ in human macrophages (180) also suggests that PPARγ may influence monocyte recruitment and cholesterol efflux from foam cells.

Earlier results suggested that PPARγ is expressed at high levels in circulating human monocytes and its activation icreases the expression of macrophage-specific markers, such as CD14 and CD11b (237).

9. Retinoic-acid-receptors (RARs) and Retinoid-X-receptors (RXRs)

RXR are mainly activated by 9-cis retinoic acid, whereas RAR can be bound by 9-cis retinoic acid and all-trans retinoic acid (ATRA) (248). Although retinol and β-carotene are only marginally metabolized to ATRA and 9-cis RA, these retinoids display a very high biological activity. Upon activation, both receptors after heterodimerization are capable of binding to retinoic acid responsive elements (RARE) and thereby induce genes important for lipid metabolism including apolipoproteins (apoC-I, apoC-II, apoC-IV, apoE), the scavenger receptor CD36, steroid-27-hydroxylase CYP17A1, LXRα, and ABCA1 and ABCG1 (249). The heterodimeric complexes formed by RARs and RXRs are potent stimuli for apoA-I/ABCA1 dependent cholesterol efflux (249).

10. Genetic factors affecting macrophage lipid metabolism

10.1. ApoE polymorphism

In humans three common isoforms of apoE exist which differ from each other by single amino acid substitution. The most common isoform is apoE3/3 (cystein 112 and arginin 158) with a frequency of 77% in Caucasian population, apoE4/4 (arginin 112 and 158) has a frequency of 15% and apoE2/2 (cystein 112 and 158) a frequency of 8%. The apoE4/4 allele is known to be a risk factor for coronary atherosclerosis and Alzheimer´s disease (AD). The isoforms differ from each other in their binding affinity for the LDL and other apoE receptors (116). Thus the apoE polymorphism has a significant impact on plasma lipoprotein levels. The E4 allele results in a decrease in plasma HDL levels. Total and LDL cholesterol levels are greatest in persons carrying the apoE4 isoform, intermediate in those with the apoE3 isoform, and lowest in those with the apoE2 isoform (250). Because of the fact that apoE4 has two arginins (arginin 112 and 158) instead of apoE3 containing only one arginin (cystein 112 and arginin 158) as an ER retention domain it can be concluded, that apoE4 is trapped for a longer time by the ER and therefore its secretion and synthesis is decreased. There are higher levels of intracellular and secreted apoE during monocyte differentiation in apoE3/3 compared with apoE4/4 monocyte derived macrophages (MDM) and also immunological differences between the apoE3/3 and apoE4/4 monocytes could be found (25). So in lipid-free cultured monocytes which express apoE the expression of CD16 (Fcγ-receptor IIIa with phagocytosis-activity) is increased and the expression of CD40 (surface antigen for co-stimulation) is decreased in apoE4/4 cells. Thus the question raises if the different apoE3/3

and apoE4/4 monocyte differentiation correlate with the changed apoE-expression or with the phenotypic differences of the protein. Further it is known that apoE mediates cellular cholesterol efflux isoform-dependent which is modulated by cell surface proteoglycans (251). The apoE isoforms have a differential cellular cholesterol-modulating effect in macrophages, which would be due to the difference in their binding to proteoglycans. Compared with apoE3, apoE4 is less efficient in promoting cholesterol efflux in fibroblasts and astrocytes (252;253), indicating that apoE isoforms differentially affect the mobilization of cellular cholesterol. Heeren et al. demonstrated that HDL-induced recycling, of triglyceride rich lipoprotein-derived apoE4 is impaired compared with apoE3, and further associated with a decrease in cholesterol efflux and intracellular cholesterol accumulation (254). Thus, impaired apoE4 recycling could explain the low apoE protein and cholesterol content of HDL, which is associated with the human apoE4 allele (255-257). ApoE also protect cells against oxidant-mediated cellular death (258). The antioxidant effect was isoform-specific with the apoE2 protein isoforms demonstrating the highest level of antioxidant protection and apoE4, the lowest. ApoE modulates the production of RNOs in human MDMs and in RAW cells, a clonal mouse macrophage cell line, thus providing another means by which apoE and its protein product can modulate oxidative and nitrosative processes (259). ApoE regulates production of NO, a critical cytoactive factor released by immune active macrophages. Significantly more NO was produced in apoE4 mice compared to apoE3 transgenic mice that only express human apoE3 protein. MDM from humans carrying apoE4 gene alleles also produce significantly greater NO than those individuals with apoE3. Overall, greater NO production in apoE4 carriers where characteristically high levels of oxidative/nitrosative stress are found in diseases such as AD provides a mechanism that potentially explains the genetic association between apoE4 and human diseases (260-262).

10.2. Genetic HDL-deficiency syndrom, Tangier disease (TD)

TD is a genetic disorder of cholesterol transport named for the secluded island of Tangier, located in front of the coast of Virginia. TD was first identified in a five-year-old inhabitant of the island who had characteristic orange tonsils, very low levels of HDL and an enlarged liver and spleen.

Synonyms for Tangier disease are:

- Alpha High-Density Lipoprotein Deficiency
- Alphalipoproteinemia
- Analphalipoproteinemia
- Familial Alpha-Lipoprotein Deficiency
- Familial High-Density Lipoprotein Deficiency

TD is a rare autosomal codominant condition caused by mutations in both alleles of the ATP-binding cassette protein 1 (ABCA1) gene on chromosome 9q31 (263). ABCA1 is a key gatekeeper influencing intracellular cholesterol transport and it helps cells to get rid of excess cholesterol. This cholesterol is then picked up by HDL particles in the blood and carried to the liver, which processes the cholesterol to be reused in cells throughout the body. Mutations in ABCA1 lead to defective cholesterol efflux from macrophages, with rapid catabolism of HDL and increased apoA-I clearance (Fig.:3). This leads to low plasma levels of HDL cholesterol <5mg/dl and apoA-I. Cholesterol accumulation in the reticuloendothelial system results in enlarged, yellow-orange tonsils and hepatosplenomegaly (263). Intermittent peripheral neuropathy can also be seen due to cholesterol accumulation in Schwann cells (263). TD is probably associated with some increased risk of premature atherosclerotic vascular disease, but this risk does not seem to be proportional to the markedly decreased HDL cholesterol and apoA-I levels. Patients with TD have a pathologic accumulation of cholesterol in macrophages as well as in cells of the reticuloendothelial system (264). Heterozygotes have moderately reduced HDL and apoA-I levels and an increased risk of coronary artery disease (CAD), but they show no evidence of cholesterol accumulation (eg. tonsillar enlargement or hepatosplenomegaly) (264) and vice versa (Fig. 10).

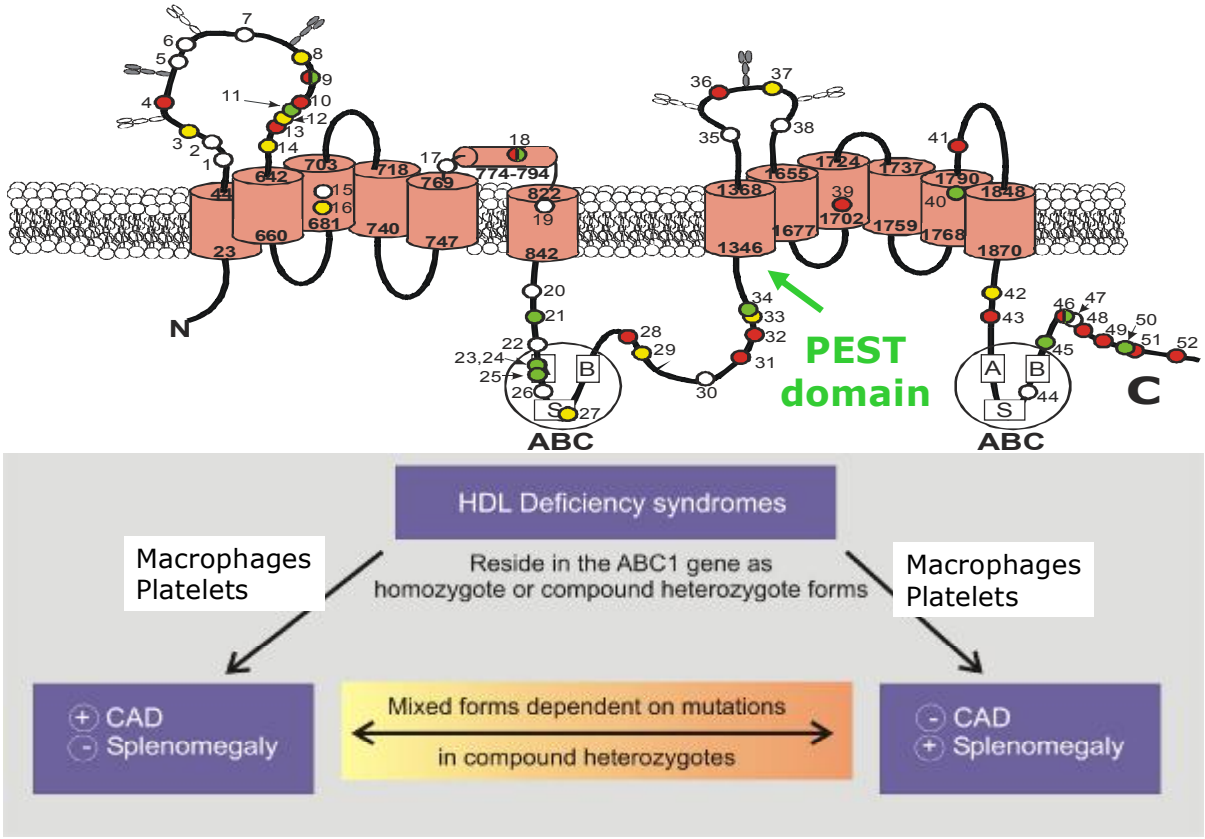

Fig. 10: ABCA1 structure and mutations in HDL deficiency syndromes

11. Sphingolipid and phospholipid metabolism

Atherosclerotic lesions accumulate glycosphingolipids (GSLs) (265) as well as ceramide and sphingolipids (SLs) which have emerged as a new class of lipid mediators of the atherogenic process. In response to various extracellular stimuli, SL turnover can be stimulated in vascular cells and cardiac myocytes. Subsequent generation of SL molecules such as ceramide (Cer), sphingosine, and sphingosine-1-phosphate (S1P), is followed by regulation of ion fluxes and activation of various signaling pathways leading to SMC proliferation, endothelial cell differentiation or apoptotic cell death, cell contraction, retraction or migration (266). Some SLs like S1P participate in the proliferation of vascular wall cells, favoring thickening and plaque stabilization (267). Further through an inflammatory response initiated by cytokines or Ox-LDL, lipids such as Cer, LacCer, or S1P can upregulate adhesion molecule expression and induce adhesion and migration of monocytes, which are crucial events in initiation and progression of atherogenesis (266). In addition SLs, eg. Cer or sphingosine derivatives, may promote cell death (mostly by apoptosis) in the vascular wall, a process implicated in plaque erosion and associated thrombosis. By modulating platelet activation and aggregation, glycolipids and sphingosine derivatives may favor thrombosis, as Cer could do by affecting tissue factor or plasminogen activator inhibitor (PAI)-1 release. A low plasma level of glucosylceramide (GlcCer) has also been proposed as a risk factor for venous thrombosis.

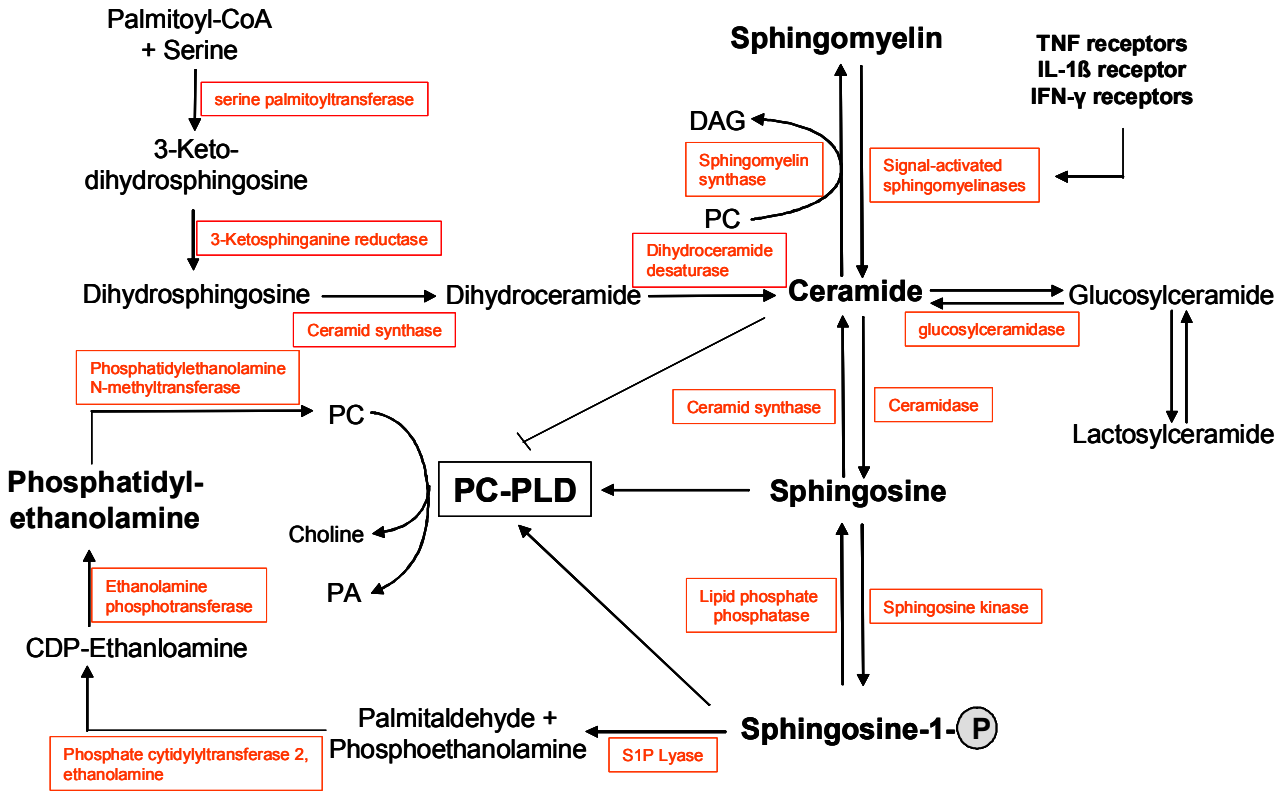

Fig.11: Interrelation between sphingolipid and phospholipid metabolism

11.1. Sphingomyelin (SM)

SM has been found to be an abundant constituent in the outer leaflet of the plasma membrane lipid bilayer of all tissues, as well as in the polar surface of circulating lipoproteins (268). Abnormalities in SM metabolism have been associated with atherosclerosis, cancer and genetic disorders (e.g. Niemann-Pick disease). The majority of SM is present in the plasma membrane, however a reasonable portion of cellular SM exists also in lysosomes, endosomes and the Golgi (269). Due to its unique physicochemical properties, SM is enriched in specialized lipid microdomains such as rafts and caveolae. Turnover of SM is a critical process and influences the maintenance of membrane integrity and synthesis of new membranes (270).

SM synthesized in the Golgi is transported to the plasma membrane via vesicular transport (271). SM synthesis *de novo* is mediated by SM synthase which transfers the phosphorylcholine moiety from phosphatidylcholine (PC) onto Cer forming SM and diacylglycerol (DAG) (Fig.11) (272). This enzyme is also able to catalyse the reverse reaction and generate PC from SM and DAG (273). Recently, a novel family of membrane proteins responsible for SM synthesis has been identified (274). Two members of this family SM synthase 1 (SMS1) and SM synthase 2 (SMS2) fulfill the criteria for functional SM synthases. SMS1 seems to represent the well-known Golgi-associated SM synthase while SMS2 is located to the plasma membrane. The presence of SM synthase in the plasma membrane may impair Cer signalling by converting Cer back to SM and generating DAG.

The degradation of SM leads to the release of Cer and free sphingosine, known signalling molecules. However, aside from generation of second messengers, stimulation of SM hydrolysis has been shown to induce cholesterol movement from cell surface to intracellular membranes (269). This suggests that SM metabolism plays an essential role not only in signalling pathways but also in the alteration of membrane physical properties.

SMases, enzymes catalysing hydrolysis of SM, have been classified into five categories based upon their pH optima, cellular localization, and cation dependence and are summarized in table 3.

Tab. 3: Different SMases

Sphingomyelinase (SMase)	**Localization**	**Unigene**	**Reference**
Ubiquitous acid SMase	Lysosome	Hs.77813	(Gatt et al. 1966; Kanfer et al. 1966)
Neutral Mg-dependent SMase	Membrane-bound	Hs.55235 Hs.283616	(Rao and Spence 1976)
Mg-independent SMase	Myelin sheath, cytosol of leukaemic cells		(Chakraborty et al. 1997) (Okazaki et al. 1994)
Neutral Mg-stimulated SMase	Nuclei of rat ascites cells	Hs.55235 Hs.283616	(Tamiya-Koizumi et al 1989)

Sphingomyelinase (SMase)	Localization	Unigene	Reference
Neutral SMase	Chromatin and envelope of rat liver cell nuclei	Hs.55235 Hs.283616	(Abi and Magni 1997; Alessenko and Chatterjee 1995)
Alkaline SMase	Bile and the digestive tract	Hs.114084	(Nyberg et al. 1996)
Acid secretory Zn-dependent SMase	Serum	Hs.77813	(Spence et. al. 1989) (Schissel et al. 1996a)
Acid SMase-like phosphodiesterase	Bladder tumors	Hs.277962 Hs.123659	(Wright et al. 2002)

Neutral membrane-bound Mg2+-independent neutral-SMase and lysosomal acid -SMase have been the best studied for their roles in Cer generation. An increase in neutral-SMase activity, a corresponding decrease in SM, and an increase in Cer have been demonstrated in response to TNFα, Fas ligand, 1α,25-dihydroxyvitamin D3 γ-interferon, chemotherapeutic agents, heat stress, ischemia/reperfusion, and interleukin-1 (275;276). In addition, both arachidonic acid and glutathione depletion have been shown to activate this enzyme (275;277).

The acid-SMase gene codes for both lysosomal (cation-independent) and secretory SMase (fully or partially dependent on Zn^{+2} for enzymatic activity) (278).

Lysenin a protein derived from coelomic fluid of the earthworm Eisenia foetida specifically recognizes SM (214;279). The specific binding of lysenin to SM makes it possible to use this protein as a unique tool to examine the distribution of cell surface and intracellular SM (279;280).

11.2. Ceramide (Cer)

Cer forms the backbone for all sphingolipids. *De novo*, biosynthesis of Cer, in the endoplasmic reticulum (ER), is initiated by the condensation of serine and palmitoyl-CoA (Fig.11), a reaction which is catalyzed by serine-palmitoyl CoA transferase (SPT). Mammalian SPT is a heterodimer of 35-kDa long-chain base gene 1 (LCB1) LCB1/SPT1 and 63-kDa long-chain base gene 2 (LCB2) LCB2/SPT2 subunits bound to the ER (281) and building the enzyme in a 1:1 ratio (282). SPT is the first and rate-limiting enzyme in the *de novo* pathway (283). The newly formed 3-ketosphinganine is subsequently reduced by NADPH-dependent ketosphinganine reductase to dihydrosphingosine. Afterwards dihydroceramide is formed by the amide linkage of fatty acyl groups to dihydrosphingosine through the action of ceramide synthase. Subsequently Cer is formed from dihydroceramide by the introduction of the *trans*-4,5-double bond. The reaction is catalyzed by dihydroceramide desaturase originating from the cytosolic side of the ER. At the state of cellular homeostasis, once formed, Cer is not accumulated but translocated to the Golgi where it serves as a starting point and metabolic precursor for all other sphingolipids such as

sphingomyelin (SM), glycosphingolipids (GSLs) of the lacto-, globo- and ganglioside series, and sulfatides. There are at least two pathways by which Cer is transported to the Golgi: an ATP- and cytosol-dependent major pathway and an ATP- or cytosol-independent minor pathway (284;285).

Recently, a gene called ceramide transfer protein (CERT) has been identified (286). CERT mediates the non-vesicular transport of Cer form the ER to the Golgi apparatus, where Cer is further converted to SM. This gene is a splice variant of the Goodpasture antigen-binding protein (GPBP-delta26) and codes for a cytoplasmic protein with a lipid-transfer catalysing START domain, a phosphoinositide-binding pleckstrin homology (PH) domain and two phenylalanines (FF) in an acidic tract (FFAT) motif. The FFAT motif is found on diverse human lipid binding proteins (287) and its combination with a PH domain which binds to the Golgi apparatus seems to predict the role of CERT. There are other proteins in mammalian cells with lipid- and organelle-binding domains that are similar to those in CERT. For example, STAR and MLN64 proteins recognize cholesterol (288;289), and phosphatidylcholine (PC)-transfer protein is capable of intermembrane transfer of PC in vitro (290).

Cer *de novo* synthesis is influenced by factors regulating the activity of serine palmitoyltransferase (SPT) and it has been documented that SPT mRNA expression and SPT activity increase in response to various inflammatory and stress stimuli. Interleukin-1ß (291), UVB radiation (292) fatty acids and cholesterol stimulate the activity of SPT resulting in the cytotoxic accumulation of palmitate accompanied by the elevation of intracellular Cer and induction of apoptosis. Cer is also generated at various subcellular locations by SM hydrolysis (293). This process of Cer formation is a receptor-operated pathway (294) which remained evolutionary unchanged and is induced by different environmental and physiological stimuli. At the plasma membrane, Cer is generated from SM hydrolysis by acidic and/or neutral sphingomyelinases (SMases) activated by diverse cytokines, death receptor ligands, differentiation factors or drugs (277). Stimulation of cells with 1,25-dihydroxy-vitamin D_3, TNFα and CD40 ligand activates a neutral SMase at the plasma membrane of cells, generating at the cytosolic side intracellular Cer and phosphocholine (295;296). Cer can also be formed through the action of an acidic SMase (see 10.1.1. ceramide and raft formation). Up till now, several SMases have been characterized in mammalian tissues and they differ from each other by their location, Mg^{+2} and Zn^{+2} dependence and pH optimum (277) (table 3).

Cer can follow several metabolic pathways. It can be reutilized for the synthesis of SM via SM synthase which transfers the phosphorylcholine moiety from phosphatidylcholine (PC) onto Cer forming SM and diacylglycerol (DAG) (272). Or Cer may be phosphorylated to form ceramide-1-phosphate. Cer catabolism can also be initiated by glucosylceramidase which

forms glucosylceramide (GlcCer) the starting substance of all the other GSLs. Another way of Cer degradation starts with a ceramidase catalysing the cleavage of Cer at the amide bond resulting in sphingosine and a free fatty acid. Three types of ceramidases have been described to date and classified according to pH optima as acid, neutral, or alkaline (297). The deficiency of acidic ceramidase, which is located in lysosomes, provides the genetic background for Farber's disease (298). Sphingosine released due to the action of ceramidase can be reacylated to Cer or posphorylated by sphingosine kinase (SphK) to sphingosine-1-phosphate (S1P) the precursor of phospholipid synthesis. Two SphK isotypes, type 1 and type 2 exist. Although highly similar in amino acid sequence and possessing five conserved domains, SphK type 1 is smaller than type 2 and expressed mainly in the cytosol, while SphK type 2 additionally has several transmembrane regions and a proline-rich SH-3-binding domain. This suggests different cellular functions and regulation mechanisms of the two isotypes (299). S1P is further metabolized by the enzyme S1P-lyase to palmitaldehyde and phosphoethanolamine. Afterwards the enzyme phosphate cytidyltransferase 2, ethanolamine leads to the formation of CDP-ethanolamine from which the aminoglycerophospholipid phosphatidylethanolamine is formed by ethanolamine phosphotransferase. Then phosphatdiylcholine is syntesized by adding one methyl residue with phosphatidylethanolamine N-methyltransferase. The originated phosphatidylcholine can be cleaved into the components choline and phosphatidic acid.

11.2.1. Cer and raft formation

Lipid rafts are originally defined as sphingolipid- and cholesterol- rich microdomains in the plasma membrane which play a role in a number of signalling processes involving specific receptors. According to Gulbins and Kolesnick (300) Cer might induce coalescence of sub-microscopic rafts into large-Cer-membrane macrodomains due to its capacity to self-associate through hydrogen bonding. These larger structures may serve as platforms for protein concentration and oligomerization, transmitting signals across the plasma membrane. Cer is generated by the action of acid SMase in response to diverse stress stimuli including chemotherapeutic drug treatment, factor withdrawal (e.g. IL3, NGF), radiation, UVA light, heat and ischemia. Cer then activates a variety of diverse protein kinase and protein phosphatase dependent signalling pathways which in most cases suppress cell growth and/or promote programmed cell death. This Cer-dependent organization of signalling domains in the membrane may relate to progression and treatment of diseases like cancer, degenerative disorders, pathogenic infections or cardiovascular disease. Sudden increases of Cer within the membrane have been shown to be involved in the regulation of cell apoptosis. Studies on CD95/Fas receptor have demonstrated that stimulation via this receptor triggers the translocation of the acid SMase from intracellular stores onto the

extracellular leaflet of the cell membrane. This surface acid SMase releases Cer from SM that rapidly forms Cer-enriched platforms in the cell membrane, which might serve as signalling platforms for the transmission of the apoptotic signal (301). Another example for Cer induced signalling is the finding that the generation of cell surface Cer through the action of acid SMase is a prerequisite for fusion of cross-linked FcγRII (CD32) and rafts, which triggers the receptor tyrosine phosphorylation and signalling (302).
Recently it has been shown that the formation of Cer-enriched domains in lipid particles enhances the binding of apoE and thus inhibits the SMase induced aggregation or fusion of the particles (110). Further it could be shown that surface SM reduced apoE mediated binding and uptake of lipid particles (111) suggesting a higher affinity of apoE to Cer than to SM.

11.2.2. Cer and its homology with lipopolysaccharide (LPS)

Cer shares some structural and functional similarities with the lipid A moiety of LPS, a lipid from the outer membrane of gramnegative bacteria. The cellular responses to LPS include changes in shape, metabolism, and gene expression but also induction of a variety of biological effects that are involved in systemic inflammation and sepsis (303). The initiation of these effects is due to the activation of monocyte/macrophages, leading to the secretion of proinflammatory cytokines such as TNFα, IL-1ß, IL-6 and IL-8. It has been suggested that LPS and Cer recognize the same intracellular molecules (304) and LPS was shown to mimick some Cer properties. Cer-activated protein kinase (CAPK) appears to be a common target and its activation by both agonists leads to the activation of MAP kinase and the translocation of activated NF-κB. Recent data emphasize that although LPS and Cer may share many signalling components, the signalling pathways are not identical (304).
In human monocyte derived macrophages exogenous Cer as efficiently as LPS induces the coassociation of the LPS receptor CD14 with complement receptor 3 (CD11b/CD18), the thrombospondin receptor CD36 and decay accelerating factor CD55 (30;305) (Fig.5). Thus clustering of signalling competent receptors may provide an interesting mechanism by which different ligands induce distinct cellular processes in systemic inflammation (SIRS or sepsis) and cardiovascular disease.

11.3. Sphingosine-1-phosphate (S1P)

The sphingosine metabolite S1P is produced upon phosphorylation of sphingosine by sphingosine kinase 1 and 2 (SPHK) (Fig.11). S1P can be further degraded to phosphoethanolamine and palmitaldehyde by S1P-lyase with the exception of platelets which lack S1P-lyase. S1P can be also converted back to sphingosine via the action of S1P phosphatase increasing the level of sphingosine in the cytosol and cell membranes. The

concentration of S1P is quite low, possibly reflecting the low expression of SPHK or the high lyase activity. Growth and survival factors, such as platelet derived growth factor (PDGF), serum, nerve growth factor (NGF) as well as muscarinic acetylcholine agonists and TNFα increase the intracellular concentration of S1P by activating SPHK. S1P is suggested to be involved in the regulation of cell shape changes, platelet aggregation, neurite retraction and smooth muscle cell chemotaxis (306) and it was implicated as a second messenger in cellular proliferation and survival. Through its high affinity G protein-coupled receptors, S1P is a physiological mediator regulating heart rate (307) coronary artery blood flow (308), blood pressure (309), endothelial integrity in the lung (310) and most recently it has been shown to regulate the recirculation of lymphocytes (311).

The intracellular targets of S1P have not been yet identified and it has been shown that S1P binding to its receptors stimulates SPHK to increase its own intracellular level (312). Up till now 5 receptors for S1P were identified and named according $S1P_1$ to $S1P_5$ receptors (313). All five receptors have been shown to bind S1P with high affinity and activate several intracellular processes related to angiogenesis, apoptosis, atherosclerosis, migration and proliferation (314;315). The receptors for S1P belong to the edg (endothelial differentiation gene) family of the seven transmembrane G protein-coupled receptor superfamily.

11.4. Regulation of cell death/survival by Cer and S1P

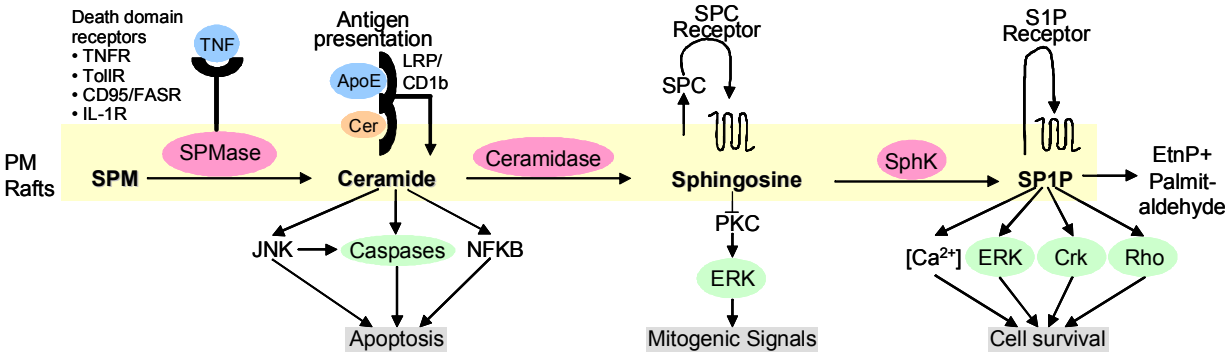

Fig. 12: The SM/Cer/Sph/S1P rheostat model

Cer has emerged as a lipid messenger of cell functions including differentiation and apoptosis. Cer can be generated by diverse kinds of stresses (ultraviolet, irradiation, heat shock and hypoxia) or biological factors (TNF-alpha, IFN-gamma and Fas antibody) through stimulation of the SM degrading enzyme SMase to execute apoptosis (316) (Fig.12). Cer is degraded with ceramidase to sphingosine, which is then phosphorylated by sphingosine kinase (SphK) to form S1P (317) (Fig.11/12), a molecule implicated in cell survival and cell growth. This suggests that the metabolic conversion of Cer into S1P could switch cells from an apoptotic state to a proliferative one. Therefore the balance between cellular

concentrations of Cer and S1P has been proposed to determine the physiological fate of the cell, which is also known as the “Cer-S1P-rheostat model” (Fig.12).
Intracellular Cer induces the caspase family and reactive oxygen intermediates (ROI), which are signals for inducing apoptosis, whereas S1P is known to extracellularly activate the phosphatidylinositol 3-kinase (PI3K) pathway through G-protein-binding EDG family receptors (318). Therefore S1P enhances the activation of protein kinase C, leading to the inhibition of Cer-induced apoptosis (319), which is activated via inhibition of PI3K activity/Akt kinase activity. Further PI3K potentiates inhibition of SMase activity and subsequently inhibits the ability to produce intracellular Cer in response to stress (320).
It can be concluded that Cer and S1P function interdependently and are deeply correlated with cell proliferation, cell survival and induction of apoptosis (321). Their interaction in the mechanism of maintaining a microdomain structure on the cell membrane is also becoming a subject of recent interest (300).

12. Glycosphingolipids (GSLs)

12.1. Structure and functions of GSLs

GSLs, amphipathic compounds consisting of sugar and Cer moieties, are ubiquitous components of the plasma membrane of all vertebrate cells. GSLs are considered to be receptors for bacteria, viruses and their toxins (e.g. Vibrio cholera, HIV), modulators of cell growth and differentiation, organizers of cellular attachment to matrices, play roles in cell-cell adhesion and receptor mediated signal transduction. Further glycolipids have been identified as tumor or differentiation antigens using monoclonal antibodies. More than 400 species of GSLs possessing different sugar structures have been reported, although only seven monosaccharides have mainly been found in vertebrate GSLs. GSLs show heterogeneity not only in their sugar chain but also in their Cer moieties. The biological significance of Cer heterogeneity is still not well understood. However, the structure of Cer, especially the fatty acid moieties, could influence the localization and functions of GSLs on the plasma membrane, possibly by direct interaction with cholesterol, phospholipids, and the transmembrane domains of receptor proteins. It is noteworthy that free Cer derived from GSLs, could mediate intracellular signal transduction.

12.2. GSLs and raft formation

The plasma membrane GSLs form clusters, called rafts, with cholesterol and relatively less phospholipids than other areas of the plasma membrane. The size of lipid rafts seems to range from “vanishingly small” <70 nm (322), to intermediate rafts ~100 nm scale (323), to larger-scale macrodomains (~500 nm or larger) (324;325). The partitioning of sphingolipids

into rafts allows the lipids themselves to be used as markers for rafts. For example, the GSL ganglioside GM1 that binds to the non-toxic β-subunit of cholera toxin is a commonly used raft marker. Theta Toxin (perfringolysin O), a thiol-activated cytolysin produced by Clostridium perfringens has been shown to bind to cholesterol in membrane microdomains that fulfill the biochemical criteria of rafts (326) and has been used as a cytochemical probe to evaluate the topology and distribution of cell surface rafts in intact cells (327;328). A recent study indicated a high distribution of the saturated, fluorescent phospholipid probe DMPE-TMR ([1,2-dimyristoyl-sn-glycero-3-phospho-ethanolamine]-tetramethyl-rhodamine) into membrane domains of the liquid ordered phase (329). It is very likely that DMPE-TMR represent the in vivo correlate of Triton resistant raft-microdomains because of the saturated side chain enabling and association with lipid ordered membrane domains such as rafts. The fluorophore is able to specifically intercalate with these domains and allows also the visualisation of the phagosome compartment. Rafts are extracted in low density fractions, insoluble in non-ionic detergents such as Triton X-100 and Lubrol WX and are called detergent-insoluble glycolipid-enriched complexes, or detergent insoluble GSL-enriched domains (DIGs).

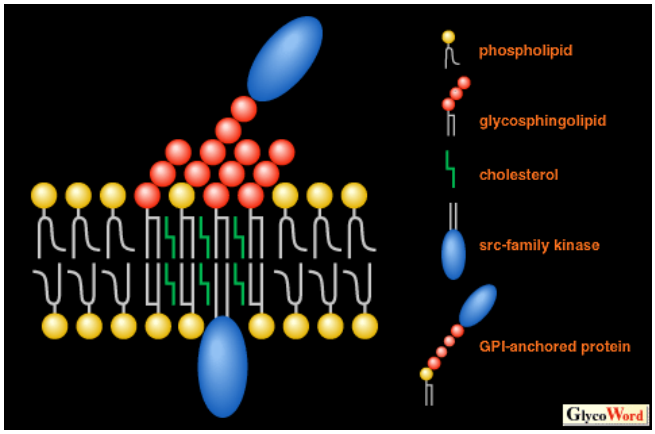

Fig. 13: Arrangement of GSLs in the plasma membrane

There are receptors for intercellular signal transducers such as glycosylphosphatdiylinositol (GPI)-anchored proteins on the exoplasmic face of the rafts and src family kinases on the cytosolic face. (Fig.13). Furthermore, endothelial growth factor (EGF) receptor and Ras are present in GSL microdomains. Also a specific association of protein kinase C alpha with GSL microdomains has been reported (330). Thus they play a role in transmembrane signaltransduction. Into this fraction, microinvaginated structures (diameter, around 50 nm) of the plasma membrane, caveolae, are also extracted. Caveolae also consist of GSLs, cholesterol, GPI-anchored proteins, src family kinases, trimeric G proteins, Ras, and a caveolae-specific membrane protein, caveolin, which associate themselves and bind to cholesterol and may take the invaginated shape. Caveolae are domains where endocytosis can occur. Rafts may be trapped in caveolae and the receptor molecules are clustered more

densely. This may improve efficiency of signal transduction. Recently, GSLs were found in caveolae, on the exoplasmic membrane, where signal transduction-related proteins are also concentrated. GSLs interact with receptor molecules and kinases, and modulate their functions. The general function of GSL microdomains in signal transduction may be to concentrate receptors and effectors on both sides of the membrane, thus speeding up binding during signalling and preventing inappropriate crosstalk between pathways (331;332). In table 4 some substances and antibodies are listed for raft detection.

Table 4: Detection of raft lipids (see also Materials and Methods for detailed information)

Raft Lipid	Substance/Antibodies for Detection
Cholesterol	Theta Toxin (perfringolysin O)
Sphingomyelin	Lysenin
Ceramide	Monoclonal antibody (IgM) mouse
LacCer (CDw17)	Monoclonal antibody
Gb_3Cer (CD77)	Monoclonal antibody and Shigatoxin
Dodecasaccharideceramide (CD65s)	Monoclonal antibody
Ganglioside GM1	Cholera Toxin

12.3. GSL-biosynthesis

In the pathway of GSL synthesis, the first step is transfer of glucose or galactose to a Cer from the endoplasmatic reticulum (ER) to produce glucosylceramide (GlcCer) or galactosylceramide (GalCer), respectively. This transfer reaction is catalyzed by glucosyltransferase (GlcT) (333;334) and galactosyltransferase (GalT), respectively (Fig. 12). Since over 400 different glycolipids are derived from GlcCer, GlcT-1 is an extremely important glycosylation enzyme. The catalytic domain of GlcT is located on the cytosolic side of the Golgi membrane, while that of GalT is on the lumen side of the ER. The rule of extension of sugar chains for GSLs is common in all mammals, i.e. a monosaccharide is sequentially transferred to a GlcCer or GalCer from a nucleotide sugar by one of a series of specific glycosyl transferases, all of which are localized on the lumen side of the Golgi membrane. In the lumen of the Golgi, GlcCer is galactosylated to lactosylceramide (LacCer) (Gal-Glc-Cer). Thus GlcCer produced on the cytosolic side of the Golgi membrane must be transferred (flip-flopped) to the lumen side by a putative enzyme. It appears most likely that glycolipid transfer protein (GLTP), a nonglycosylated protein with a molecular weight of 22.000 K, transfers by a carrier mechanism, glycolipids with a beta-glucosyl or beta-galactosyl residue directly linked to either Cer or diacylglycerol and participates in the intracellular traffic of GlcCer from the cytoplasmic side to the luminal side of the Golgi apparatus were glycosylation of GSLs occurs (335). Depending on the sugar that attaches to the nonreduced end of LacCer three synthetic pathways leading to the formation of lacto-series (neolacto-series), globo-series and ganglio-series have been defined (Fig.14). Above

all, the ganglio-series glycolipids contain many sialic acids, and are designated gangliosides. Most cells synthesize the ganglioside GM3, by the transfer of sialic acid to LacCer, but in addition make one other trihexosylceramide. GM3 ganglioside is sialylated to GD3, and GD3 to GT3 (Fig.14). The three involved sialyl-transferases (SIAT I, SIAT II and SIAT III) specifically recognize the acceptor substrate (336;337). GM3, GD3 and GT3 are the starting points for the “a-series”, “b-series” and “c-series” gangliosides, respectively. Along each series, non-specific N-acetylgalactosaminyl-transferase, galactosyl-transferase and SIAT IV introduce in sequence a residue of N-acetylgalactosamine, galactose and sialic acid, respectively, giving rise to more complex gangliosides. Further sialosylations can be accomplished by SIAT V. From LacCer, a further series of GSL ("O-series") can originate from the sequential action of N-acetylgalactosaminyl-transferase, galactosyl-transferase and sialyl-transferase IV and V (Fig. 14).

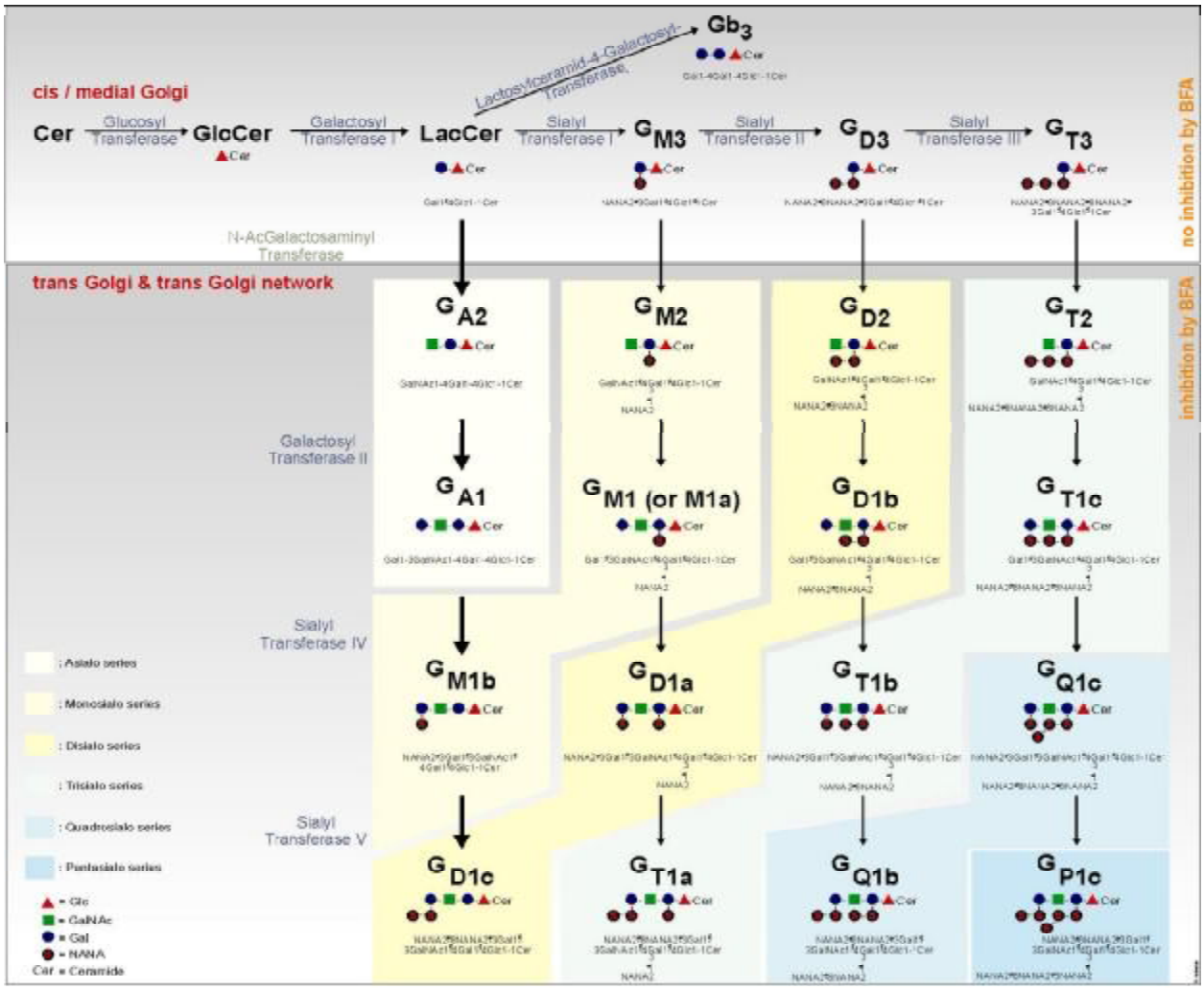

Fig. 14: Scheme of the de novo biosynthesis of the oligosaccharide moieties of gangliosides

The activity of galactosyltransferase, which catalyses the synthesis of LacCer, has been found increased in familial hypercholesterolemia and atherosclerosis (338;339). The increased levels of other GSLs in atherosclerotic lesions have been also reported (340).

Further LacCer is associated to plasma lipoproteins and various cell types such as endothelial cells and SMCs, monocytes and macrophages (265). LacCer may contribute to atherosclerosis as it was found in fatty streaks and intimal plaques (339;340). It stimulates also the proliferation of SMCs (341-343) and the expression of CD11b/CD18 on the surface of human neutrophils (344). LacCer participates in superoxide generation by induction of NADPH oxidase and is involved in removal of macromolecular antigens (345). Ox-LDL also stimulates specifically the biosynthesis of LacCer through enhanced activity of galactosyltransferase (343) while native LDL exerts an opposite effect (338;346). The neutral GSL globotriaosylceramide (Gb_3Cer) emerges as an anticoagulant (347) and transducer of apoptotic signals (348), eventually abrogating proinflammatory activities of lipid-loaden foam cells. The complex sialylated GSL dodecasaccharideceramide (CD65s) may function in adherence (349;350) and cellular activation (351). Moreover, the ganglioside GM1 plays an immunoregulatory and structural role in macrophages.

The biological functions of GSLs as well as the mechanism that regulates GSL metabolism in cells seems to still be a true mystery of the Sphinx, which is in fact the origin of the word 'Sphingolipid.' The recent remarkable progress that has been made in the gene cloning of glycosyltransferases and glycosylhydrolase should help provide an answer to this mystery.

To solve the riddle of glycolipid functions and to gain insight into the role of Cer glucosylation in whole animal, a method to eliminate a gene of glycolipid glycosyltransferase in mice has been developed and knock out mice have been generated. Since GlcCer is a central lipid as a precursor for numerous GSLs including brain gangliosides, the mice would be invaluable tools for understanding of the general functions of GSLs (331).

12.3.1. Inhibitors of GSL-biosynthesis

The experimental approach to deplete cellular GSLs with the specific inhibitors of GSL biosynthesis has the potential to identify functions of endogenous GSLs.

It has been demonstrated by Inokuchi and Radin that an analog of Cer, D-*threo*-1-phenyl-2-decanoylamino-3-morpholino-1-propanol (D-PDMP) inhibits the glucosyltransferase, which produces GlcCer. D-PDMP not only suppresses GSL biosynthesis, but also accumulates Cer and sphingoid bases. Therefore, one should consider carefully both effects of D-PDMP for interpretation of the results (352;353).

Recently, it was found that N-butyldeoxynojirimycin, known as an inhibitor against alpha-glucosidase I, also inhibits GlcCer synthase. Among various N-alkylimino sugars tested, N-butyldeoxygalactonojirimycin possesses no visible cytotoxicity and higher specificity for the inhibition of GlcCer synthesis. Much progress will be expected on the mechanism of GlcCer synthesis inhibition by these N-alkylimino sugars and on its medical application for treatment of Gaucher's disease.

12.4. Cellular distribution of GSLs

While their density in plasma membrane is high, two-thirds of the total GSLs are distributed in intracellular membrane such as Golgi apparatus, endosomes, lysosomes, nuclear membrane, ER and mitochondria. GSLs, along with other membrane components, circulate through these organelles. In Golgi apparatus, GSLs are newly synthesized by the addition of saccharides one by one and in lysosomes they are degraded by the removal of saccharides one by one. GSLs, which are incorporated by endocytosis, are sorted into lysosomes or Golgi apparatus from endosomes. Newly synthesized GSLs are sorted into plasma membranes through endosomes. A portion of endocytosed GSLs are returned back to the plasma membrane (Fig.15). One half of GSLs in plasma membrane were recycled and their composition in the plasma membrane remains constant. Most GSLs are transported between membranes as small vesicles maintaining a bilayer structure.

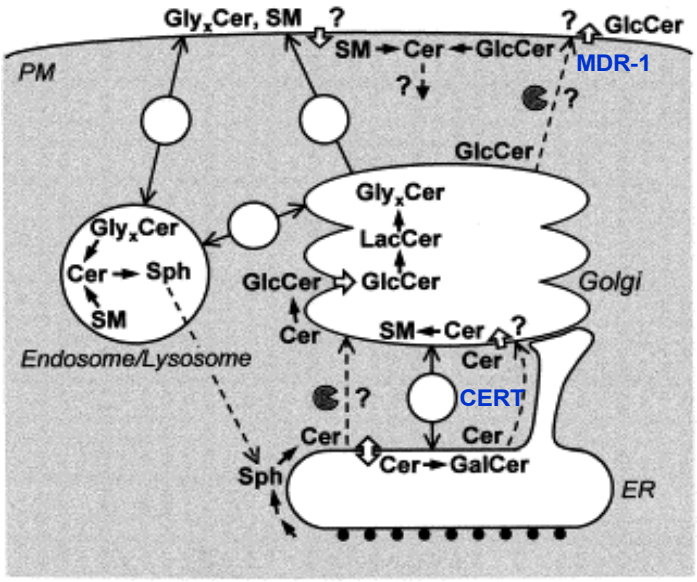

Fig. 15: Comprehensive view of sphingolipid transport from G. van Meer and J. C. M.

GSLs not only circulate between the plasma membrane and intracellular organs, but also move laterally over the exoplasmic membrane. Such migration could be conducted by the cholesterol-rich unit known as a 'raft.'

On the cytosolic surface of the Golgi, part of Cer is glucosylated to GlcCer. From here, GlcCer may follow three pathways, none of which can be excluded at present:

1) It can translocate across the Golgi membrane, evidence for which has been found in vitro, and can be (partially?) converted to higher GSLs GlcCer and the higher GSLs may then leave the Golgi on the lumenal side of transport vesicles (293) (Fig.15).

2) GlcCer may leave the Golgi on the cytosolic surface of secretory vesicles, and subsequently undergo tanslocation to the outer leaflet of the plasma membrane by multi drug resistant 1 (MDR1) P-glycoprotein. Alternatively, along the retrograde pathway, GlcCer might

be translocated across the ER membrane, after which it would have a fate similar to newly synthesized GalCer (293).

3) GlcCer might leave the cytosolic surface of Golgi membrane by desorption from the membrane and monomeric exchange with another organelle´s cytosolic surface. Good evidence has been presented that higher GSLs follow a vesicular transport pathway from their site of assembly in the lumen of the Golgi to the PM. This was demonstrated for the early ganglioside GM3, and for the late ganglioside GD 1a (354).

Ganglioside GM1 and globotriaosylceramide can act as receptors for the bacterial toxins cholera toxin (355) and Shiga toxin (356) respectively. These toxins need to reach the ER, where they translocate across the membrane to become active in the cytosol. Endocytotic transport of the toxin-GSL complex has provided information on vesicular transport pathways from SL domains on the plasma mebrane to the ER (357;358). Vesicular traffic of GSLs can be expected to display the full complement of properties that characterize vesicular transport of proteins, like dependence on energy and cytosolic proteins (coats, SNAREs, cytoskeleton).

12.5. Degradation of GSLs

GSL degradation occurs through the stepwise removal of individual sugar residues, starting from the non-reducing terminal unit, by acid exoglucosidases with the formation of Cer, which is eventually split into long chain base and fatty acid by ceramidase (336;337). Cer can leave the lysosome, reenter the biosynthetic pathway or be further degraded. Since GSLs have many of the same outer sugar sequences that are found in N- and O-glycans, many of the same glycosidases are used for their degradation. The degradation of plasma derived GSLs takes place in the lysosomes as the digesting organelles after internalization through the endocytic pathway. All the enzymatic steps of the degradative process require an acidic pH inside the organelle which is maintained by a proton pump that brings H^+ inside the organelle (336). However, specialized hydrolases are needed for cleaving the Glc-Cer and Gal-Cer bonds and other linkages near the membrane. Besides these specific enzymes, additional noncatalytic sphingolipid activator proteins (SAPs) (some called saposins) help present the substrate to the enzyme for cleavage. These proteins are necessary for the degradation of GSLs possessing short oligosaccharide chains where they mediate the interaction between the water-soluble enzymes and their membrane-bound substrates by forming water-soluble complexes, which lift out of the membrane (359). A total number of five SAPs are known, and they are encoded by only two genes. One gene codes for prosaposin 524-amino-acid precursor (pSAP) (360), which is proteolytically processed to four highly homologous proteins (SAP-A, -B, -C and –D). They are glycoproteins with molecular weights of 12-15 kDA, show highly homologous sequence identities to each other and have similar properties

but differ in their function and their mechanism of action. Sap-A and Sap-C both help b-glucosyl and b-galactosyl ceramidase degradation. Sap-B assists arylsulfatase A, α-galactosidase, α-sialidase, and β-galactosidase. Sap-D and Sap-B also assist in SM degradation by SMase. The second gene encodes GM2 activator protein (GM2AP), which acts on the degradation of ganglioside GM1 and GM2 (361). GM2AP forms a complex with either GM2 or GA2 and presents them to β-N-acetylhexosaminidase A for cleavage of terminal β-GalNAc. Sugars that lie too close to the lipid bilayer apparently have limited access to the soluble hexosaminidase. The activator protein binds a molecule of glycolipid, forming a soluble complex that can be cleaved by hexosaminidase. The resulting product is now inserted back into the membrane, and the activator presents the next GM2 molecule, and so on. Genetic loss of this activator protein causes the accumulation of GM2 and GA2, resulting in the AB variant of GM2 gangliosidosis. The activator is probably targeted to the lysosomes via the Mannose-6-Phosphate pathway.

All saposins may have more or less nonspecific stimulative effects on activities of lipid hydrolases by making more of the lipid substrates available to hydrolases (362). Since SAPs form water soluble complex with sphingolipids, as mentioned before, it can be assumed that SAPs may also function in lipid transport. Sandhoff and his colleagues showed that saposin B can transport gangliosides between liposomes (359).

The inherited deficiency of both lysosomal hydrolases and SAPs gives rise to sphingolipid storage diseases (Fig.16). Complete absence of prosaposin is lethal in humans. Glucocerebrosidase, also called β-glucoceramidase, is specific for the degradation of the Glc-Cer bond, and its loss causes Gaucher's disease, where GlcCer accumulates (363). A specialized β-galactosidase, called β-galactoceramidase, hydrolyzes the bond between Gal and Cer, and it can also cleave the terminal Gal from LacCer. Its loss produces Krabbe disease. GalCer is often found with a 3-sulfate ester (sulfatide), and thus a specific sulfatase, arylsulfatase A, is needed for its removal prior to β-galactosylceramidase action. Loss of this sulfatase causes metachromatic leukodystrophy and the accumulation of sulfatide but also additional glycolipids, e.g. globotriaosylceramide, accumulate owing to a blockage of degradation at several points in the catabolic pathway. Glycolipids terminated with α-galactosamine residues are degraded by a specific α-galactosidase and its loss causes Fabry disease (Fig.16).

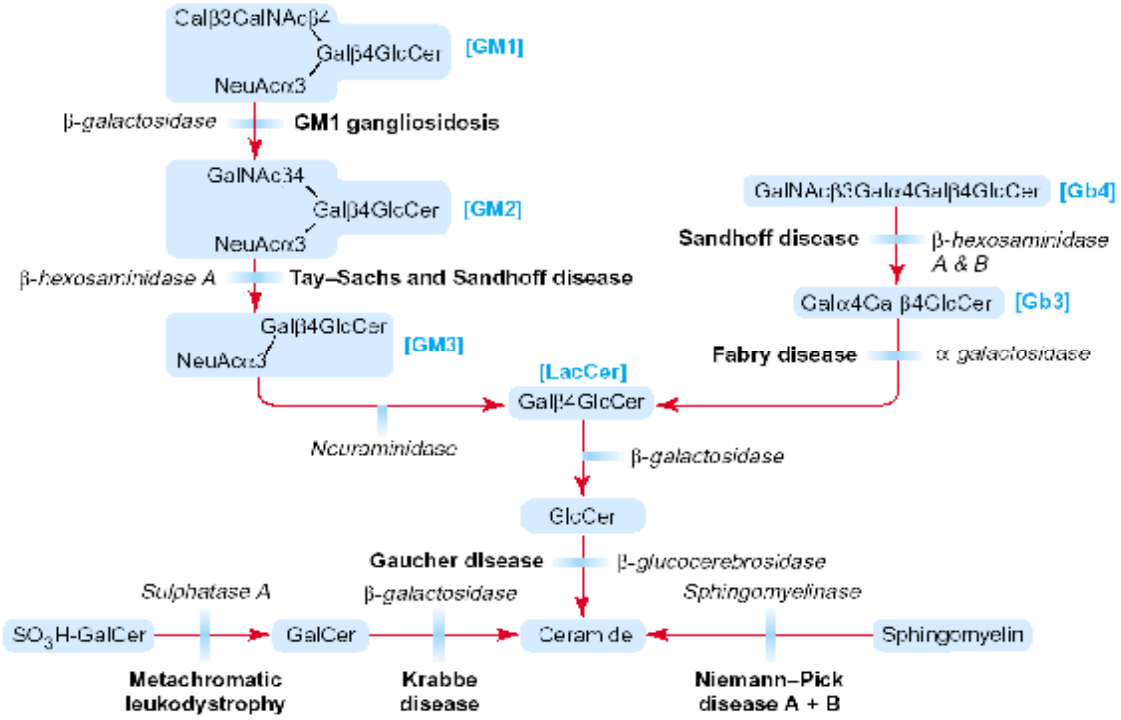

Fig. 16: GSL metabolism and disease (from Sillence D. J. et. al. 2003 (50))

13. Interrelation between apoE and ceramide metabolism

13.1. Enhanced binding of apoE on ceramide enriched microdomains

As reported recently, the formation of Cer-enriched domains in lipid particles enhances the binding of apoE and thus inhibits the SMase induced aggregation or fusion of the particles (110). In contrast to Cer, surface SM reduced apoE mediated binding and uptake of lipid particles (111) suggesting a higher affinity for apoE to Cer than to SM. These results indicate that the conversion of SM to Cer through the actions of SMases enhances the binding of apoE.

13.2. Induction of the monocyte innate immunity receptor cluster

Cer a component of atherogenic lipoproteins induces as efficiently as LPS the coassociation of the LPS receptor CD14 with complement receptor 3 (CD11b/CD18), the thrombospondin receptor CD36 and decay accelerating factor CD55 (30;305). Concerning the high binding affinity of apoE to Cer this apolipoprotein seems to be also involved in the regulation of this monocyte innate immunity receptor cluster.

13.3. Relationship between CRP, ceramide and apoE

CRP is known as an opsonin for the uptake of atherogenic lipoproteins by monocytes. On monocytes, specific CRP binding occurs through FcγRI/CD64 (212) as well as FcγRIIA/CD32

(213). Previously it could be shown that cell surface Cer is a prerequisite for recruitment of cross-linked FcγRIIA to rafts, which triggers the receptor tyrosine phosphorylation and signalling (214). ApoE which binds to Cer could also be involved in the process of FcγRIIA-raft generation and thereby triggering receptor-mediated endocytosis through a non-clathrin dependent mechanism.

13.4. ApoE mediates antigen presentation of ceramide-backbone-lipids

ApoE is able to bind lipid antigens and delivers them by receptor-mediated uptake into endosomal compartments containing CD1 in APCs (118;119). It could be shown that LRP and LDL-R are expressed on DCs and they are markedly upregulated during differentiation of monocytes to DCs and have a significant function in the uptake of apoE-lipid antigen complexes and presentation by CD1 (117). The delivery of lipids to the endosomal system can occur through three possible mechanisms (Fig.17). Either secreted or recycled apoE can capture lipid antigens (secretion-capture) or infected cells such as macrophages may shed lipid antigens associated with apoE that are delivered to bystander (uninfected) DCs (bystander acquisition) or serum lipoproteins (VLDL in the case of GGC) serve as a depot for lipid antigens and may stimulate a response far from the source of the antigen (Fig.17).

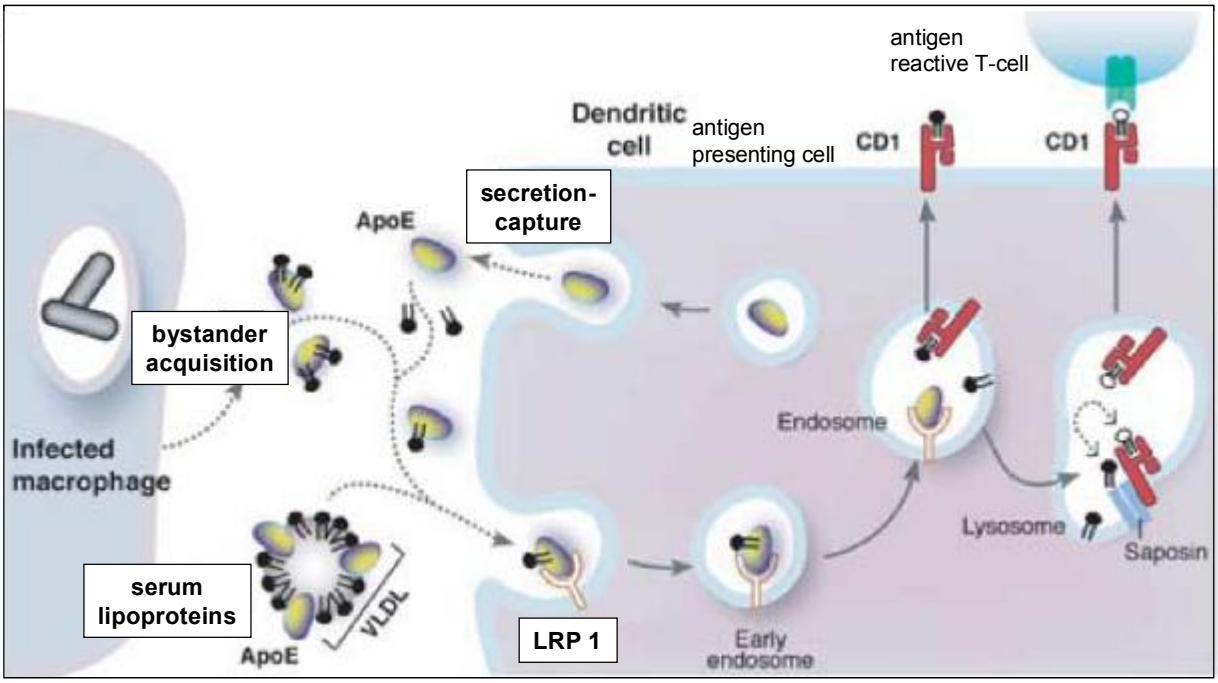

Fig. 17: Apolipoprotein-mediated pathways of lipid antigen presentation (Figure adapted from Van den Elzen, nature Vol 437 6 October 2005)

To investigate the role of lipoproteins in CD1 antigen presentation an in vitro model of human dendritic cells (DCs) was used with the CD1d-presented glycolipid, galactosyl(α1-2)galactosyl ceramide (GGC) in human serum (117). GGC strictly requires uptake and delivery to lysosomes where it is converted to the active antigenic form, α-galactosyl ceramide (α-GC) (364). The antigenic activity of GGC was distributed almost entirely in the VLDL fraction of human serum which includes apoB and apoE which independently participates in receptor-mediated uptake into cells (365). VLDL-mediated T-cell activity was effectively blocked by antibodies against apoE. This blockade was specific for VLDL-bound GGC which bind in the VLDL fraction of serum, and is acquired by DCs in an apoE-dependent manner, processed, and then presented to T cells. ApoE depleted serum incubated with GGC had a significantly lower capacity to stimulate T cells than normal serum, and the presenting capacity was recovered by adding back purified apoE. Therefore apoE might be the major factor in human serum mediating the presentation of GGC to CD1d-reactive T cells (117). ApoE has also a crucial function in the presentation of an exogenous lipid antigen in vivo because apoE-deficient mice showed a drastically reduced response to intravenously administered GGC although they have similar numbers of α-GC-reactive NK T cells as wild-type mice (117).

Further apoE specifically enhances T-cell responses to a variety of CD1-presented lipid antigens for multiple CD1 isoforms which is due to the apoE affinity for a wide diversity of lipid classes. T-cell responses to naturally occurring microbial lipid antigens were also enhanced in the presence of apoE for the presentation of glucose monomycolate (GMM), mycolic acid (CD1b-presented) and manosyl-phosphomycoketide (CD1c-presented) (366).

II. Aim of the thesis

The major aim of this thesis was to analyze the different effects of the two atherogenic modified lipoproteins, enzymatically modified LDL (E-LDL) and mildly oxidized LDL (Ox-LDL) on cellular cholesterol and phospholipid metabolism, raft microdomain generation and cell surface receptor expression during in vitro foam cell formation and HDL_3 dependent deloading. Experiments were performed with ApoE3/3 and apoE4/4 homozygous human monocyte-derived macrophages and macrophages obtained from ABCA1 deficient (Tangier) and hyperlipidemia patients.

Total cell analysis of lipid loaded and deloaded macrophages using lipidomics, genomics and proteomics based on mass spectrometry, Affymetrix microarray analysis, Taqman RT-PCR, flow cytometry, image microscopy and western blot analysis was applied. Mechanisms underlying the regulation of cellular lipid influx, raft formation, lipid efflux and storage as well as surface expression of ceramide, glycosphingolipids and receptors of the macrophage innate immunity cluster, involved in lipid uptake and processing should be unraveled. In this context proteins involved in cholesterol efflux like ABCA1, ApoE, ApoC-I, CETP and PLTP were also analyzed.

The results obtained from macrophages of the apoE3/3 genotype were compared with that of macrophages from the apoE4/4 genotype, ABCA1 deficient (Tangier) macrophages and macrophages of a patient with excessive hypertriglyceridemia and coronary heart disease in order to find out differences in the above mentioned analyzed pathways.

These investigations should contribute to the understanding of the consequences of the different lipoprotein modifications E-LDL and Ox-LDL on foam cell formation which is a hallmark in the pathogenesis of atherosclerosis.

Further macrophages were incubated with RXR and PPARγ agonists in order to modulate surface expression of receptors involved in lipid uptake and processing and to analyze expression of genes involved in macrophage lipid metabolism to elucidate influences of these agonists on atherogenesis.

III. Materials and Methods

1. Chemicals, Immunoreagents and Disposable Goods

Table 5: List of antibodies applied for flow cytometry and confocal microscopy

Antigen	clones	Provider	Label
CD14	MϕP9	Becton-Dickinson, Heidelberg, Germany	APC
CD45	2D1	Becton-Dickinson, Heidelberg, Germany	PerCP
Ceramide	MID15B4	Alexis, Grünberg, Germany	Goat anti mouse-FITC
CDw17	G035	Becton-Dickinson, Heidelberg, Germany	FITC
CD65s	VIM2	Caltag, Burlingham, California, USA	FITC
CD77	38-13	Coulter/Immunotech, Krefeld, Germany	Goat anti rat-PE
CD64	22	Coulter/Immunotech, Krefeld, Germany	FITC
CD32	2E1	Coulter/Immunotech, Krefeld, Germany	PE
CD16	3G8	Coulter/Immunotech, Krefeld, Germany	FITC
CD11a	25.3	Coulter/Immunotech, Krefeld, Germany	FITC
CD11b	D12	Becton-Dickinson, Heidelberg, Germany	PE
CD18	7E4	Coulter/Immunotech, Krefeld, Germany	FITC
CD36	FAG.152	Coulter/Immunotech, Krefeld, Germany	FITC
CD91	A2MR-α2	Becton-Dickinson, Heidelberg, Germany	FITC
CD163	GHI/61	Becton-Dickinson, Heidelberg, Germany	PE
CD47	B6H12	Becton-Dickinson, Heidelberg, Germany	FITC
CD55	IA10	Becton-Dickinson, Heidelberg, Germany	PE
apoCI	10-F4	ICN Biomedicals, Eschwege, Germany	Goat anti mouse-FITC
apoE	21-F3-D2	Biotrend, Köln, Germany	Goat anti mouse-FITC
CETP	ATM192	Dianova, Hamburg, Germany	Goat anti mouse-FITC
Adipophilin	AP125	Research Diagnostics, Flanders, USA	Goat anti mouse-FITC
Annexin V-Apoptosis detection kit		Becton-Dickinson, Heidelberg, Germany	FITC

Antigen	clones	Provider	Label
Secondary antibodies			
Goat F(ab)´2 anti mouse Ig		Becton-Dickinson	FITC
Goat F(ab)´2 anti rat IgM		Dianova	PE
Goat polyclonal to mouse IgG H&L		Abcam, Cambridge, UK	Cy5
Goat polyclonal to anti-rabbit		Calbiochem, Schalbach, Germany	Texas Red
Toxins			
Cholera toxin subunit B (recombinant) (GM1)		Molecular Probes Europe BV, Leiden, Netherland	Alexa Fluor 488
Cholera toxin subunit B (recombinant) (GM1)		Molecular Probes Europe BV, Leiden, Netherland	Alexa Fluor 555
Theta-Toxin (perfringolysin O)		Biotechnology workgroup of the Center of Excellence for Fluorescent Bioanalysis (KFB), Regensburg, Germany	FITC
Others			
DMPE-TMR (1,2-dimyristoyl-sn-glycero-3-phospho-ethanolamine-tetramethyl-rhodamine)		Avanti Polar Lipids, Inc., Alabama, USA	
POPC (1-palmitoyl-2-oleoyl-sn-glycero-3-phosphocholine)		Avanti Polar Lipids, Inc., Alabama, USA	
Lysenin		gift from Sobota A, Nencki Institute of Experimental Biology, Department of Cell Biology, Warsaw, Poland	
anti-His probe (H-15)		Santa Cruz Biotechnology, CA, USA)	

PE = Phycoerythrin, FITC = Fluorescein-isothiocyanate, PerCP = Peridin chlorophyll protein, APC = Allophycocyanin

Table 6: List of antibodies applied for western Blot analysis

Antibody	clone	provider	host	gel
ABCA1	AB.H10	Abcam, Cambridge, UK	mouse	
ApoE		Biodesign, Germany	goat	
ApoC-I	10-F4	ICN Biomedicals, Eschwege, Germany	mouse	
PLTP		kind gift from Jauhiainen M., National Public Health Institute, Department of Molecular Medicine, Helsinki, Finland	mouse	
ATP-synthase (β-chain)	3D5AB1	Acris, Hiddenhausen, Germany	mouse	
CD14		Santa Cruz, CA, USA	goat	non-reducing
CD11b		Santa Cruz, CA, USA	goat	
CD16	2H7	Serotec, Eching, Germany	mouse	non-reducing

CD47	BRIC126	Acris, Hiddenhausen, Germany	mouse	non-reducing
CD55		Santa Cruz, CA, USA	rabbit	
CD163	EDHu-1	Serotec, Eching, Germany	mouse	
CD64		Santa Cruz, CA, USA	goat	
CD32		Santa Cruz, CA, USA	goat	
CD11a		Santa Cruz, CA, USA	goat	
CD36		Santa Cruz, CA, USA	rabbit	

Medium, solutions and chemicals

Macrophage-SFM Medium, low endotoxin	Invitrogen, Karlsruhe, Germany
M-CSF, human (rec. from E. Coli)	R&D Systems, Minneapolis, Minnesota
PBS (w/o Ca2+, Mg2+)	Gibco BRL, Berlin, Germany
BSA (lipid free)	Sigma, Taufkirchen, Germany
FCS (Fetal calf serum)	Gibco BRL, Berlin, Germany
Saponin	Sigma, Taufkirchen, Germany
sodium azide	Sigma, Taufkirchen, Germany
formaldehyd	Sigma, Taufkirchen, Germany
$CuSO_4$	Sigma, Taufkirchen, Germany
DMSO	Sigma, Taufkirchen, Germany
SDS	Sigma, Taufkirchen, Germany
Cholesterol esterase	Roche, Basel, Switzerland
Trypsin	SAA, Basel, Switzerland
Trizol	Life Technologies, Karlsruhe, Germany
ALLN (N-acetyl-Leu-Leu-norleucinal)	Calbiochem, Schalbach, Germany
1,1`-Dioctadecyl-3,3,3´,3´-tetramethylindo-carbocyanine-perchlorate (Dil)	Sigma, Taufkirchen, Germany
9-cis-retinoic-acid all-trans-retinoic acid	Sigma, Taufkirchen, Germany
β-Carotene	Sigma, Taufkirchen, Germany
Rosiglitazone	Cayman Chemical, MI, USA
Ciglitazone	Cayman Chemical, MI, USA
Troglitazone	Cayman Chemical, MI, USA
Pioglitazone	Cayman Chemical, MI, USA
human plasma apolipoprotein A-I and apoE	Calbiochem, CA, USA

Kits

BCA, Protein Assay Kit	Pierce, Rockford, IL, USA
ECL Western Blotting Analysis System	Amersham, Braunschweig, Germany

Superscript II kit	Life Technologies, Karlsruhe, Germany
RNeasy MiniKit	Qiagen, Hilden, Germany
RNA 6000 Nano Chip	Agilent, Palo Alta, CA, USA
Reverse Transcription System	Promega, Madison, AL, USA
Enzo BioArray HighYield RNA Transcript Labeling Kit	Enzo Life, Farmingdale, NY, USA
Cy3, Cy5 Mono reactive dye pack	Amersham, NJ, USA
PD-10 columns	Amersham, NJ, USA

Microarray

Human Genome U133 Plus 2.0 Array	Affymetrix, Santa Clara, CA, USA

Cell culture dishes

Ultra low attachment 6-well plates	Costar Corning, Bodenheim, Germany
LAB-TEK borosilicate chamber slides	Nalge Nunc Int., Naprville, IL, USA
Falcon 6- well cell+	Becton Dickinson, NJ, USA
cell+ 10 cm tissue culture dishes	Sarstedt, Inc. Newton, USA

Instruments

Heraeus 6000 Incubator	Heraeus, Hanau, Germany
FACSCalibur flow cytometer	Becton Dickinson, Heidelberg, Germany
2100 Bioanalyzer, Caliper	Agilent, Palo Alto, CA, USA
ABI Prism 7900 HT Sequence Detection System (Taqman)	Perkin Elmer-Applied Biosystems, Darmstadt, Germany
TCS-4D confocal microscope equipped with a ArKr 75 mV mixed ion laser electrospray ionization tandem mass spectrometry (ESI-MS/MS)	Leica Lasertechnik, Omnichrom Heidelberg, Germany Melles Griot,
Thermocycler Gene Amp PCR System 9600	Perkin Elmer, Uberlingen, Germany
GeneQuant pro RNA/DNA Calculator	Amersham, Braunschweig,Germany
Gene Chip Fluidics Station 450	Affymetrix, Santa Clara, CA, USA
Gene Chip Scanner 3000	Affymetrix, Santa Clara, CA, USA
Affymetrix array scanner	Affymetrix, Santa Clara, CA, USA
ELISA reader	Tecan, Stuttgart, Germany

Analysis Software

Cellquest software for FACS Analysis	Becton Dickinson, Heidelberg,Germany
Affymetrix Microarray Suite (version 5.0)	Affymetrix, Santa Clara, CA, USA
ScanWare software package	Universal Imaging, Corp., PA, USA
Metamorph for microscopy image Analysis	Universal Imaging, Corp., PA, USA

Assays on Demand

gene-specific assays on demand were supplied by ABI.

Mastermix: 10 µl 2x TaqMan® Universal PCR Master Mix, 1 µl gene-specific probe-primer-mix and 4 µl sterile water

Mastermix for the endogenous control 18sRNA: 10 µl 2x TaqMan® Universal PCR Master Mix, 1 µl pre-developed TaqMan® assay reagents (PDAR) endogenous control kit and 4 µl sterile water

Table 7: Assays on demand

Assays on demand	**Assay ID**
sphingomyelin synthase 1	Hs00153716
sphingomyelin synthase 2	Hs00380453
acid sphingomyelinase like phosphodiesterase	Hs00205522
sphingomyelin phosphodiesterase 1 (acid SMase)	Hs00609415
neutral sphingomyelinase (neutral SMase) activation associated factor	Hs00182519
sphingomyelin phosphodiesterase 2 neutral SMase	Hs00162006
CD36	Hs00169627
glucosidase, beta;acid (includes glucosylceramidase)	Hs00400295
N-acylsphingosine amidohydrolase (acid ceramidase) 1	Hs00188842
UDP-glucose ceramide glucosyltransferase	Hs00326535
sphingosine kinase 1	Hs00184211
sphingosine kinase 2	Hs00219999
serine palmitoyltransferase, long chain base subunit 1	Hs00272311
serine palmitoyltransferase, long chain base subunit 2	Hs00191585

2. Preparation of samples

2.1. Donors

Leucocyte-enriched apheresates were obtained from healthy, normolipidemic volunteers bearing either the apolipoprotein E3/3 or the apolipoprotein E4/4 genotype after informed consent. Further patients with Tangier disease and hyperlipidemia were used for leukapheresis.

2.2. Elutriation of monocytes

Suspensions enriched in human peripheral blood leukocytes were isolated by leukapheresis in a Spectra cell-separator (Gambro BCT), supplemented with the anticoagulant ADCA and diluted with an equal volume of PBS (w/o Ca2+, Mg2+). The diluted apheresate was then subjected to counterflow centrifugation (J2-MC centrifuge with JE-6B Rotor, Beckmann) as described elsewhere (367).

The monocyte content of each fraction obtained during centrifugation was determined using flow cytometry based on the different scatter properties of lymphocytes, granulocytes and monocytes. Fractions that were devoid of granulocytes with a monocyte content of at least 90% of leukocytes were pooled, washed with PBS (w/o Ca2+, Mg2+) and resuspended in culture medium. The concentration of the suspension was determined with a sysmex counter.

2.3. Monocyte cell culture and harvesting

Elutriated monocytes were cultured either on dishes with Attachment Surfaces (Sarstedt, USA) or for analysis by flow cytometry on Ultra Low Attachment 6-well plates (Costar) to guarantee viability of the cells with minimal activation. They were seeded at 10^6 cells/ml in macrophage serum-free medium supplemented with monocyte-colony stimulating factor (MCSF, 50 ng/ml) (control) and incubated for up to 7 days at 37°C / 5 % CO_2 (Heraeus 6000 Incubator, Heraeus Instruments) to induce phagocytic differentiation as described previously (25). On the fourth day E-LDL (enzymatically degraded LDL) (40 μg/ml) respectively Ox-LDL (mildly oxidized LDL) (80 μg/ml) was added to the cells for 48 hours until day 6 (Fig.21) to generate foam cells resembling lipid-loaden cells within the atherosclerotic lesion. On day 6 macrophages were deloaded of cholesterol with HDL_3. Therefore medium was removed, cells were washed with PBS and new medium supplemented with MCSF and HDL_3 (100 μg/ml) was given to the cells for 24h (Fig.21). On the days 1, 4, 6 and 7 cells were harvested and experiments were performed.

3. Lipoproteins

3.1. Isolation of lipoproteins

Lipoproteins and lipoprotein-deficient serum were isolated from human plasma or serum by sequential preparative ultracentrifugation in KBr gradients according to (211;368) followed by extensive dialysis and filter sterilization. All lipoprotein concentrations mentioned are protein concentrations determined by Lowry´s method. Lipoprotein fractions were stored at 4^0C and used within two weeks from end of dialysis.

3.2. Enzymatic modification of LDL

E-LDL was generated under sterile conditions, of LDL isolated from plasma of healthy blood donors by dilution to 2 mg/ml protein in PBS (w/o Ca^{2+}, Mg^{2+}) and conduction of trypsin (8 µg/ml) and cholesterol esterase (60 µg/ml) for 48 h at 37°C.

3.3. Mildly oxidation of LDL

Mildly oxidized LDL was achieved by dialyzing purified LDL fractions (1 mg protein/ml) against 5 µM $CuSO_4$ for 36 h. The oxidation process was stopped by dialysis in PBS/EDTA. Further extensive dialysis in PBS was made. Afterwards, the Ox-LDL was sterile filtered and protein content was determined by Lowry-method. The mildly oxidation of LDL was controlled by electrophoresis.
Modified lipoproteins were stored at 4°C and used within a week.

3.3. Labelling of lipoproteins with DiI

5 µl of a 3 mg/ml solution of 1,1`-Dioctadecyl-3,3,3´,3´-tetramethylindo-carbocyanine-perchlorate (DiI) dissolved in DMSO were mixed with 500 µl lipoprotein deficient serum. Subsequent to lipoprotein modification 500 µl of lipoprotein solution (1 mg/ml) were added (369). After 12 h incubation at 37°C DiI-labelled lipoprotein solutions were separated from unbound chromophore by ultracentrifugation in KBr gradients ($d<1{,}063$ g/ml) followed by extensive dialysis.

4. Mass spectrometry analysis

4.1. Determination of the lipid composition of lipoproteins

Lipoproteins were conducted with 50 µl Luric-Plasma, internal standard and 1ml aqua dest..
Lipids were extracted according to the method of Bligh and Dyer (Chloroform/Methanol 1:2) (370). After addition of chloroform and water, the samples were centrifuged (20 min./4000 U RT). For the different lipid classes certain parts of the chloroform phase were separated and

after removing the solvent, acetylation for cholesterol determination respectively solubilisation in a phospholipid solvent was made. For quantification a standard curve with five spikes was created. Extracts were analyzed by electrospray ionization tandem mass spectrometry (ESI-MS/MS).

4.2. Determination of the cellular lipid content of macrophages

Cells were harvested on day 1 and day 4 of monocyte to macrophage differentiation, on day 6 after 48h E-LDL and Ox-LDL loading and on day 7 after 24h HDL_3 deloading. Cells were washed twice with PBS, lysed in 0.2 % SDS and lipids were extracted according to the method of Bligh and Dyer (370). Extracts were analyzed by electrospray ionization tandem mass spectrometry (ESI-MS/MS) as described previously (371;372).

4.3. Determination of the lipid composition of isolated membrane rafts

Cells were harvested at the time points according to 5.2.. They were washed twice with PBS and scrabbed on ice with TNE-Buffer supplemented with protease-inhibitor and centrifuged at 1200 rpm 7min, 4°C. The pellet was resuspended in TNE/protease-inhibitor-Buffer and homogenized. From this material membrane-fraction was prepared by centrifugation at 100000g, 1h, 4°C. The supernatant represents to cytosolic fraction and the pellet the crude membrane fraction. Afterwards Triton- respectively Lubrol-raft preparations were made using the OptiPrep^{TM} method with a iodixanol gradient as described under point 10 raft preparation. From these raft-preparations lipids were extracted according to the method of Bligh and Dyer and extracts were analyzed by ESI-MS/MS.

5. Flow cytometric analysis

5.1. Staining of cell surface antigens

Cells were detached by rinsing Ultra Low Attachment Surfaces with PBS. After washing with PBS (w/o Ca2+, Mg2+) cells were resuspended in PBS (w/o Ca2+, Mg2+), 0,5% BSA at $5x10^5$/100 µl and incubated for 15 minutes on ice with saturating concentrations of the antibodies. Antibodies used for detection were directly fluorochrome-conjugated or indirectly labelled by subsequent incubation with fluorochrome-conjugated secondary reagents after two washing steps with PBS, 0,5% BSA.

5.2. Staining for intracellular immunofluorescence

Cytoplasmatic antigens were detected using a modified version of Jung´s staining protocol. $5x10^5$ monocytes were incubated in 500 µl fixation buffer (PBS (w/o Ca^{2+}, Mg^{2+}), 4% (w/v) formaldehyd) for 15 min on ice. Cells were washed twice with permeabilization buffer (PBS

(w/o Ca $^{2+}$, Mg^{2+}), 1% (v/v) fetal calf serum, 0.1% (w/v) saponin, 0.1% (w/v) sodium azide) and labelled with primary antibodies for 15 min on ice followed by two washing steps with PBS (w/o Ca $^{2+}$, Mg^{2+}), 0.5% BSA. In case of unconjugated or biotin-conjugated primary antibodies labelled cells were washed twice with permeabilization buffer and incubated with the respective secondary reagents for 15 min on ice followed by two further washing steps with PBS (w/o Ca $^{2+}$, Mg^{2+}), 0.5% BSA.

5.3. Analysis of stained cells

The cellular light-scatter signals and three fluorescence signals of 20 000 cells per sample were analyzed in list mode at a channel resolution of 1024 with forward scatter as the trigger parameter on a FACSCalibur flow cytometer (excitation: 488 nm (argon) / 635 nm (diode); emission filters: 530/30 nm band pass (channel 1) / 585/47 nm band pass (channel 2) / 670 nm long pass (channel 3): 661/16 nm band pass (channel 4) (Fig.18); data acquisition was performed by Cellquest software (Becton Dickinson, Heidelberg, Germany). The photomultiplier gains were calibrated with polychromatic fluorescent reference beads (Polysciences). Compensation was adjusted with fluorochrome-coated microbeads (Becton Dickinson, Heidelberg, Germany). Gating of cultivated monocytes/monocyte-derived macrophages (MDM) was based on forward- and side-scatter dot plots as well as CD14 and CD45 antibodies. Mean fluorescence values were corrected for background by substraction of mean fluorescence of cells without antibody respectively if incubated with secondary antibody substraction of mean fluorescence in absence of the primary antibody.
For analysis of the list files the software CellQuest 2.0 (Becton Dickinson, Heidelberg, Germany) on a Macintosh G3 was used.
The mean and standard deviation of the mean fluorescence intensities of the independent experiments were calculated. Statistical significancy was tested by paired student´s t-test.

For analysis of surface membrane receptors during E-LDL and Ox-LDL loading, FACSCanto flow cytometer (BD Biosciences) the successor to FACSCalibur was used. It has two lasers, similar to the FACSCalibur (488nm and 633nm), however, the instrument was upgraded to detect 6-colors simultaneously (4-colors off the 488nm and 2-colors off the 633nm plus forward and side scatter). The FACSCanto has digital electronics and an octagon detection system. Data of these experiments were analyzed by FACSDiVa and CellquestPro softwares (both BD Biosciences).

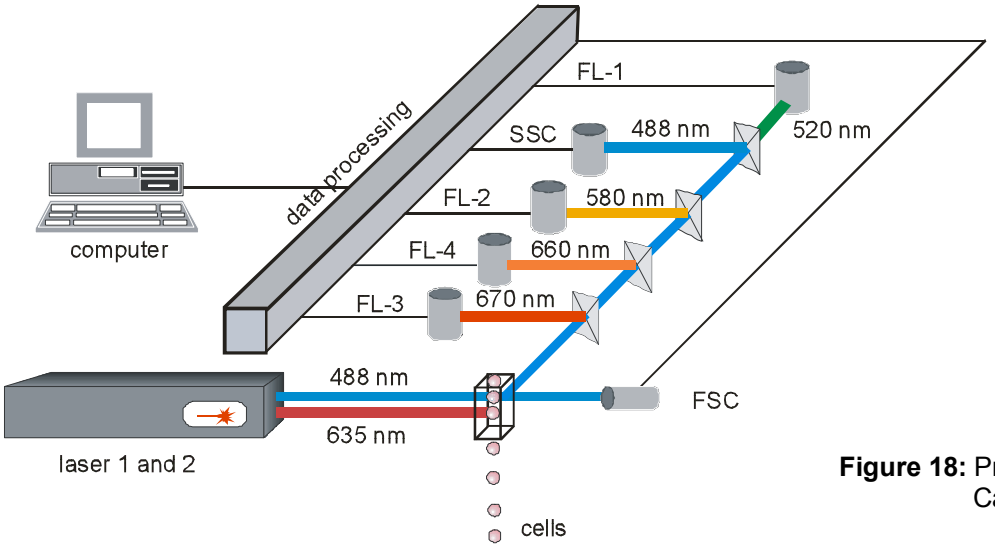

Figure 18: Principle of a FACS Calibur Flow Cytometer

5.4. Apoptosis-test with AnnexinV-FITC and Propidiumjodid (PI)

In the early stages of apoptosis, translocation of phosphatidylserine (PS) from the inner part of the plasma membrane to the outer layer takes place, by which PS becomes exposed at the external surface of the cell (373). AnnexinV is a Ca^{2+} dependent phospholipid-binding protein with high affinity for PS and is therefore suited to detect apoptotic cells. The simultaneous DNA stain with PI allows the discrimination of necrotic cells (Annexin V and PI positive) from apoptotic cells (Annexin V positive and PI negative).

Staining procedure:

After harvesting cells by gently rinsing costar plates with PBS, cells were washed twice with PBS and resuspended in AnnexinV Binding Buffer at a concentration of $1x10^6$ cells/ml. 100 µl of this solution ($1x10^5$ cells) were transferred to a 5 ml tube and 5 µl of AnnexinV-FITC and 5 µl of PI were added. Cells were gently vortexed and incubated at room temperature for 15 min in the dark. After adding 400 µl of AnnexinV Binding Buffer, samples were analyzed on a flow cytometer using 488 nm excitation and a 515 nm band-pass filter for fluorescein detection and a filter >600nm for PI detection. Ustained cells as well as cells stained with AnnexinV-FITC alone and cells stained with PI alone were used as controls to set up compensation and quadrants.

6. Microscopy

Cells were cultured in LAB-TEK borosilicate chamber slides, washed with PBS, fixed in 4% paraformaldehyde for 15 min, quenched with 50mM NH_4Cl/glycin for 15 min and then blocked with PBS/0.5% BSA for 15 min at RT.

For analysis of raft microdomains cells were incubated for 30 min at 4°C with saturated concentration of lipid vesicles in PBS, prepared from a mixture of 1-palmitoyl-2-oleyl-sn-

glycero-3-phosphocholine (POPC) and 1,2-dimyristoyl-sn-glycero-3-phospho-ethanolamine-tetramethyl-rhodamine (DMPE-TMR) at a ratio of 100:1 by sonication for 30 min as described by Schütz G. J. et al. (329). Afterwards cells were washed extensively with PBS and analyzed by confocal microscopy.

For differential raft analysis, cells were incubated with anti-ceramide mAB 15B4 (1:20) for 3h at 4°C and then labeled with goat anti mouse-Cy5 secondary antibody (1:150) for 1 h at 4°C, followed by incubation with theta-toxin-FITC (1:2000) for 20 min at 4°C for cholesterol staining or cholera toxin for GM1 ganglioside staining.

For sphingomyelin staining cells were incubated with lysenin (1:100) for 4h at 4°C. Afterwards anti-HIS antibody (1:150) for binding to the HIS of lysenin was added for 2h at 4°C followed by labelling with anti-rabbit texas-red antibody (1:150) for 30 min at 4°C.

Confocal images were acquired with an inverted TCS-4D confocal microscope (Leica, Heidelberg, Germany) equipped with a ArKr 75 mV mixed-ion laser (Melles Griot, Omnichrome, Carlsbad, CA, USA) and observed with an oil immersion objective 100x lens. Images were acquired with a 488 nm laser line (excitation) and detected with a 535/40m band pass filter (emission). Acquisition was performed with the Scan Ware software package of the instrument and analysis was done using the software Metamorph (Universal Imaging, Corp., PA, USA).

Fluorescence images were taken with HCS System Discovery-1 (Universal Imaging, Downingtown, PA, USA) which is a conventional high-end flourescence inverse microscope with 6-fold ojective-revolver consisting of a multiSpec-imager for emission beam splitting and a high end CoolSNAP HQ camera. The system is controlled by a high-end MetMorph imaging system for measurements and data handling.

The C-terminal domain (domain 4) of the θ-toxin (perfringolysin O) was synthesized by the biotechnology workgroup of the Center of Excellence for Fluorescent Bioanalysis (KFB, Regensburg, Germany) according to Shimada et al 2002 (374). FITC N-terminus labeling was carried out by a standard procedure, yielding in a product with absorbance and emission maxima of 490 nm and 520nm, respectively.

7. Preparation of fluorescent labeled ApoE and ApoA-I

Human plasma apolipoprotein A-I and apolipoprotein E were purchased from Calbiochem, CA, USA. Cy3 and Cy5 Mono-Reactive Dye Pack, as well as PD-10 columns were obtained from Amersham Pharmacia Biotech, New Jersey, USA. Protein labelling procedure was carried out as described by Mujumdar et al. (375). Briefly, the contents of 1 vial (for labelling of 1 mg protein) of Cy3- or Cy5-monofunctional dye was dissolved in 100 μL DMF. The amount of dissolved dye was calculated for the used protein concentration. Protein labelling reactions were carried out in 0,1 M carbonate buffer (pH 8,8-9,0). After 1 h of incubation at

4°C in the dark, the reaction was terminated by adding 20 μL of 10mM lysin solution. Unconjugated dye was separated from the labelled protein by gel permeation chromatography over Sephadex PD-10 column using PBS (pH 7,4) buffer as eluant. The dye/protein ratio for each sample was determined according to manufacturer`s instructions.

7.1. ApoE and ApoA-I binding assay by confocal microscopy

Cells were washed with PBS and subsequently incubated with 10μg/mL of fluorescent labelled apoE (Cy3) and apoA-I (Cy5) at 37°C or 4 °C to 5 min. After incubation, cells were washed twice with cold PBS containing 0,5% BSA and then with cold PBS alone. Subsequently fixation of cells was performed using 4% paraformaldehyde in PBS for 15 min on ice. Afterwards cells were washed three times with cold PBS and analyzed by confocal microscopy. By this method at 4°C only binding should occur while at 37°C binding and internalization should take place.

7.2. ApoE and ApoA-I time-kinetic binding assay by flow cytometry

Cells were harvested by smoothly washing the costar plates with a pipete. After washing with PBS, cells were resuspended in PBS containing 0,5% BSA at 5 x 10^6/ml. Cells were incubated with 10μg/mL of fluorescent labelled apoE (Cy3) and apoA-I (Cy5) at 37°C or 4 °C for 2, 5, 10 min. After incubation cells were washed three times with cold PBS buffer containing 0,5% BSA and analyzed by flow cytometry.

8. Affymetrix oligonucleotide array analysis

Total RNA of day1 monocytes, differentiated, E-LDL and Ox-LDL loaded and HDL_3 deloaded macrophages was extracted by TRIzol (Life Technologies). The RNA was quantified by measuring the spectrophotometric absorbance at 260 nm, the purity was determined by the use of the 2100 Bioanalyzer (Agilent technologies).

Double-stranded cDNA was synthesized by a Superscript II kit (Life Technologies) using T7-oligo(dT) as primer. Biotin-labeled cRNA was prepared by in vitro transcription reaction using an Enzo BioArray HighYield RNA Transcript Labeling Kit (Affymetrix, P/N 900182) based on the manufacturer's protocol. The Biotin-labeled cRNA was purified, fragmented and after addition of Control Oligonucleotide B2 (3nM) and 20X Eukaryotic Hybridization Controls (bioB, bioC, bioD, cre) hybridized to Affymetrix H-U133A GeneChips (Santa Clara, CA) for 16hrs at 45°C. The chips were stained with Streptavidin / Phycoerythrin (SAPE), and washed in the Fluidics Station 450 with protocol EukGE-WS2 which includes an antibody amplification step. The arrays were scanned on the Affymetrix array scanner and the data analysis was performed according to instructions and recommendations provided by Affymetrix using the Affymetrix statistical data analysis software, Affymetrix Microarray Suite

(version 5.0). For each gene, the gene expression of cells treated in different ways was compared. The comparison was based on a statistical analysis of probe sets consisting of 16 oligos recognizing different portions of the target gene. The probe sets were excluded if the detection call for both target and reference was absent; or if the change call gave no change (NC) in comparison analysis or if the signal log ratio between target and reference was between -1 and 1. Signal log ratio is used to describe the change between a target and reference array. The change is expressed as log2 ratio. Therefore, signal log ratio of 1 equals a fold change of 2.

Genes with significant up- and down-regulation (≥ 2 fold) by loading, deloading or differentiation were sorted into 73 categories based on literature search, data base analysis and unpublished data sets of our institute.

8.1. Principle of gene combining chromatin immunoprecipitation (Chip) analysis

The goal of comparative cDNA hybridization is to compare gene transcription in two or more different kinds of cells. GeneChip microarrays consist of small DNA fragments (referred to here as probes), chemically synthesized at specific locations on a coated quartz surface. The precise location where each probe is synthesized is called a feature, and millions of features can be contained on one array.

8.1.1. mRNA extraction and reverse transcription

mRNA for use in a microarray assay must be purified from total cellular contents. To prevent the experimental samples from being lost, they are reverse-transcribed back into more stable cDNA forms.

8.1.2. Fluorescent labelling of cDNA's

In order to detect cDNA's bound to the microarray, they must be labelled with reporter molecules like fluorescent dyes (fluors) which identifies their presence. A differently-colored fluor is used for each sample so that the two samples can be distinguished. The labeled cDNA samples are called probes. The choice of red and green colors is reminiscent of the emission wavelengths of commonly-used fluors, such as rhodamine and fluorescein or Cy3 and Cy5. To equalize the total concentrations of the two cDNA probes before applying them to the array, the probe solutions are diluted to have the same overall fluorescent intensity.

8.1.3. Hybridization to a DNA microarray

The two cDNA probes are tested by hybridizing them to a DNA microarray. The array holds hundreds or thousands of spots, each of which contains a different DNA sequence. If a probe contains a cDNA whose sequence is complementary to the DNA on a given spot, that cDNA

will hybridize to the spot, where it will be detectable by its fluorescence. In this way, every spot on an array is an independent assay for the presence of a different cDNA. There is enough DNA on each spot that both probes can hybridize to it at once without interference.

8.1.4. Scanning the hybridized array

Once the cDNA probes have been hybridized to the array and any loose probe has been washed off, the array must be scanned to determine how much of each probe is bound to each spot. The probes are tagged with fluorescent reporter molecules which emit detectable light when stimulated by a laser. The emitted light is captured by a detector, either a charge-coupled device (CCD) or a confocal microscope, which records its intensity. Spots with more bound probe will have more reporters and will therefore fluoresce more intensely. Each of the two fluorescent reporters (fluors) used has a characteristic excitation wavelength. The emitted light has a characteristic emission wavelength which is different from the excitation wavelength. If the emission wavelengths are different, light emitted from the two fluors can be selectively filtered to measure the amount emitted by each fluor separately. If the excitation wavelengths are different, the two fluors can be stimulated and scanned one at a time. If one of these conditions is not met, the scanned intensities can be contaminated by crosstalk between the two fluorescent channels.

8.1.5. Interpreting the scanned image

The end product of a comparative hybridization experiment is a scanned array image. The measured intensities from the two fluorescent reporters have been false-colored red and green and overlaid. Yellow spots have roughly equal amounts of bound cDNA from each cell population and so have equal intensity in the red and green channels (red + green = yellow). Spots whose mRNA's are present at a higher level in one or the other cell population show up as predominantly red or green. The intensities provided by the array image can be quantified by measuring the average or integrated intensities of the spots. The ratio of fluorescent intensities for a spot is interpreted as the ratio of concentrations for its corresponding mRNA in the two cell populations. Even after overcoming detection and calibration problems, the measured intensities for each spot only represent the ratio of cDNA's in each cell population.

9. TaqMan® polymerase chain reaction (PCR)

mRNA expression analysis was made from MCSF differentiated, E-LDL and Ox-LDL loaded as well as HDL_3 deloaded macrophages. Therefore TaqMan® PCR assays were performed on the ABI Prism 7900 HT Sequence Detection System (Perkin Elmer-Applied Biosystems, Darmstadt, Germany). The gene-specific assays on demand were supplied by ABI. For

quantitation of each gene, a mastermix containing 10 µl 2x TaqMan® Universal PCR Master Mix, 1 µl gene-specific probe-primer-mix and 4 µl sterile water was prepared and aliquoted in a 384-well optical plate. A mastermix for the endogenous control 18sRNA containing 10 µl 2x TaqMan® Universal PCR Master Mix, 1 µl pre-developed TaqMan® assay reagents (PDAR) endogenous control kit and 4 µl sterile water was treated similarly. Finally triplicates of cDNA templates equivalent to 50 ng of RNA were added to a final volume of 20 µl. The thermal cycling was performed for 2 min at 50°C and 10 min at 95°C followed by 45 cycles of 15 sec at 95°C and 1 min at 60°C.

Generation of standard curves - For quantification of the results obtained by real-time PCR we used the standard curve method. For this purpose a stock of total RNA from macrophages was serially diluted. A standard curve with 50, 25, 12.5, 6.25 and 3.125 ng total RNA was generated for all. The standard curves were used to determine the relative expression of genes and 18sRNA mRNA in each sample. Finally the results were normalized to the endogenous control 18sRNA.

9.1. The Taqman-principle

PCR is a fairly standard procedure now, and its use is extremely wide-ranging. At its most basic application, PCR can amplify a small amount of template DNA (or RNA) into large quantities in a few hours. This is performed by mixing the DNA with primers on either side of the DNA (forward and reverse), *Taq* polymerase (of the species *Thermus aquaticus*, a thermophile whose polymerase is able to withstand extremely high temperatures), free nucleotides (dNTPs for DNA, NTPs for RNA), and buffer. The temperature is then alternated between hot and cold to denature and reanneal the DNA, with the polymerase adding new complementary strands each time. “Real-time PCR” allows the scientist to actually view the increase in the amount of DNA as it is amplified.

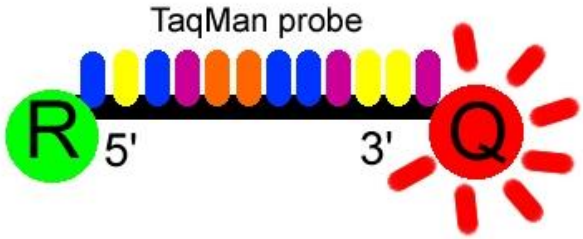

Figure 19: The Taqman probe. The red circle represents the quenching dye that disrupts the observable signal from the reporter dye (green circle) when it is within a short distance. *Image created by Dan Pierce.*

While the probe (Fig.19) is attached or unattached to the template DNA and before the polymerase acts, the **quencher (Q)** fluorophore (usually a long-wavelength colored dye, such as red) reduces the fluorescence from the **reporter (R)** fluorophore (usually a short-wavelength colored dye, such as green Green Fluorescent Protein (GFP)). This occurs

through Fluorescence Resonance Energy Transfer (FRET), which is the inhibition of one dye caused by another without emission of a proton. The reporter dye is found on the 5' end of the probe and the quencher at the 3' end.

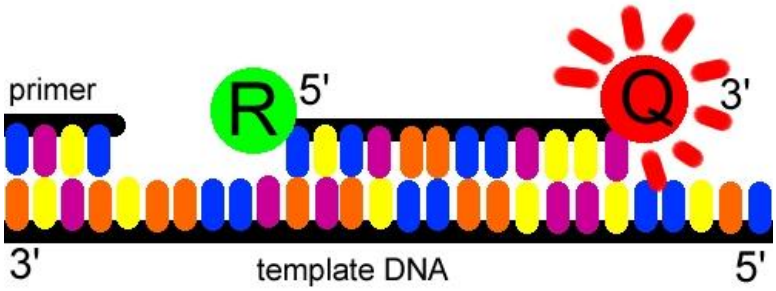

Figure 20: The TaqMan® probe binds to the target DNA, and the primer binds as well. Because the primer is bound, *Taq* polymerase can now create a complementary strand. *Image created by Dan Pierce.*

Once the TaqMan® probe has bound to its specific piece of the template DNA after denaturation (high temperature) and the reaction cools, the primers anneal to the DNA (Fig. 20). *Taq* polymerase then adds nucleotides and removes the Taqman® probe from the template DNA. This separates the quencher from the reporter, and allows the reporter to emit its energy (Fig.21). This is then quantified using a computer. The more times the denaturing and annealing takes place, the more opportunities there are for the Taqman® probe to bind and, in turn, the more emitted light is detected.

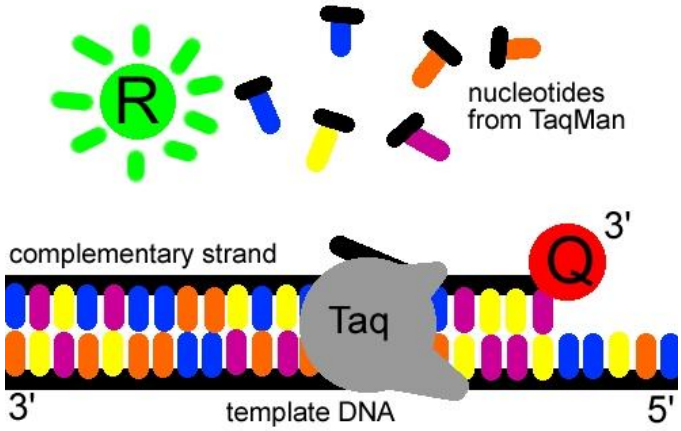

Figure 21: The reporter dye is released from the extending double-stranded DNA created by the Taq polymerase. Away from the quenching dye, the light emitted from the reporter dye in an excited state can now be observed. *Image created by Dan Pierce.*

The light emitted from the dye in the excited state is received by a computer and shown on a graph display, such as this, showing PCR cycles on the X-axis and a logarithmic indication of intensity on the Y-axis (Fig.22).

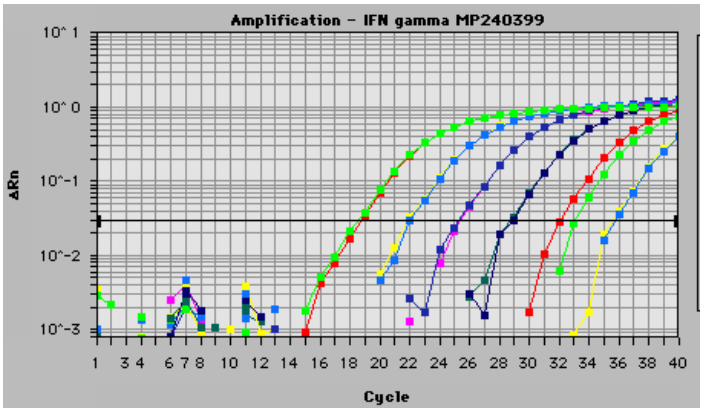

Figure 22: A graph print out of actual data found using the TaqMan® probe. Courtesy

10. Detergent lysis and flotation gradient

The basis for lipid raft isolation is their resistance to non-ionic detergents like Lubrol or Triton X-100. Using an iodixanol gradient the intact lipid rafts float to the top of the gradient while all the other detergent-solubilized membranes remain at the bottom.

Cells were harvested at the differentiated, E-LDL and Ox-LDL loaded and HDL_3 deloaded states, crude membrane fraction was isolated and Lubrol-WX rafts were prepared. In detail, cells were washed twice with PBS, scrabbed on ice with buffer A (TNE, 50 mM Tris, 150 mM NaCl, 5 mM EDTA, supplemented with protease-inhibitor set III, Calbiochem) and spun down at 1200 rpm 7 min, 4°C. The pellet was resuspended in buffer A and homogenized. From this material a crude membrane-fraction was prepared by centrifugation at 100000 *g*, 1 h, 4°C. The supernatant represents the cytosolic fraction and the pellet the crude membrane fraction (MF). MF was lysed in 300 µL buffer A containing 1% Lubrol-WX (Serva) on ice for 30 min. The detergent lysate was adjusted to 40% Iodixanol (Optiprep™, Axis-Shield) and therefrom 600 µL were given under a density gradient of 0, 20, 25, 30, and 35% Iodixanol (each 600 µl). After centrifugation in Beckman SW55Ti-rotor (160000 *g*, 4 h at 4°C) six 600 µL fractions were collected from the top of the gradient. Fraction 2 and 3 were considered as the raft-fractions and the fractions 4-6 as the non-raft fractions. For immunoblotting same volumes of each gradient-fraction were precipitated with chloroform/methanol.

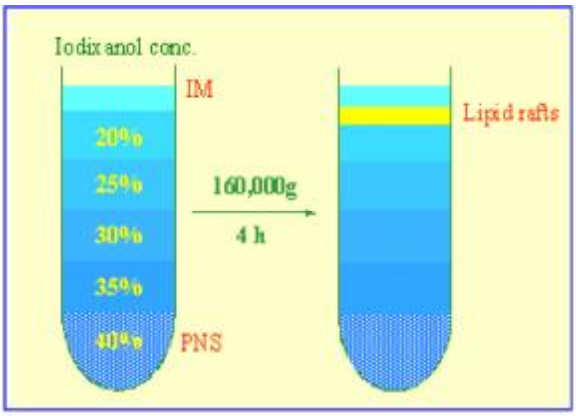

Figure 23: Isolation of lipid rafts by flotation from a postnuclear supernatant (PNS) in a discontinuous iodixanol gradient. IM =Isolation Medium.

From these raft fractions mass-spectrometry as well as immunoblotting was performed. For quantification of the blots with the lumi-imager the sum of the fractions 2 and 3 divided by the sum of the fractions 1-6*100 was considered as the raft–portion of the whole expression of the detected protein.

11. Western blot analysis

Cells were harvested at the differentiated, E-LDL and Ox-LDL loaded state, washed with PBS, frozen (-20°C). Cell debris was separated by centrifugation at 10.000 x g for 10min at 4°C. Proteins were separated by SDS-PAGE and transferred to PVDF (polyvinylindene fluoride) membranes. Incubations with antibodies were performed in 5% nonfat dry milk in PBS, 0.1% Tween. Detection of the proteins was carried out with the ECL Western blot detection system and following quantification with the lumi-imager.

12.ELISA

96 well plates were coated over night at 4-7°C with 200µl/well anti-apoC-I polyclonal respectively anti-apoE monoclonal antibody diluted 1:2000 with 10mM PBS. On the next day after washing with 400 µl/well PBS-0.1% Tween 20 (PBST0.1) plates were blocked with 200 µl/well PBS-1% Tween 20 (PBST1) for 45 min -1 h at 36-37°C and were washed again. Afterwards incubation with the supernatants of the cells in different concentrations follows diluted with PBST0.1 and with PBST0.1 alone as a blank (45 min-1 h at 36-37°C). Then plates were washed with PBST0.1 and subsequently incubated with the detection antibody anti-apoC-I (monoclonal) respectively anti-apoE (polyclonal) (45 min-1h, 36-37°C). The last step after washing with PBST0.1 was incubation with HRP-streptavidin-conjugat 1:5000 diluted in PBST0.1 (45 min-1h, 36-37°C) followed by addition of ABTS-colour reagent in ABTS-Buffer (30-45 min,36-37°C). Measuring of extinction was performed at 405 nm.

13. Cholesterol and choline phospholipid efflux

RAW264.7 cells were obtained from ATCC (Manassas, USA), cultured in RPMI 1640 medium (Sigma, St. Louis, USA) supplemented with 10% fetal calf serum (Gibco BRL), 100 U penicillin per ml, 100 µg of streptomycin per ml, and incubated in 10% CO_2 in air at 37°C. The cells were stimulated with 5 µM 9-cis RA, 5 µM ATRA, 5 µM β-carotene liposomes, or DMSO and PC liposomes as controls for 24 hours.

RAW264.7 mouse macrophages were maintained in RPMI containing 10% FCS in 12-well plates containing 400.000 cells per well. Cholesterol and choline phospholipids were labeled by incubation with 1.5 µCi/ml ^{14}C-cholesterol and 10 µCi/ml ^{3} H-choline chlorides for 2 days. As indicated for a part of the cells agonists were added for the last 24 h of the label phase. Cells were then rinsed with PBS and incubated for 24 h in DMEM containing 2 mg/ml BSA

with or without 10 µg/ml apoA-I and the indicated agonists. Efflux of ^{14}C-cholesterol and ^{3}H-choline phospholipids from cells was measured by the appearance of label in the medium. Lipids in the cells and the medium were extracted according to the method of Bligh and Dyer (370) and ^{3}H- and ^{14}C-radioactivity was measured by liquid scintillation counting. Lipid efflux was determined as percent fraction of the cpm (count per minute) in media over the total cpm (cpm in media + cpm in cells). Specific lipid efflux was calculated as lipid efflux in the presence of apoA-I $\pm$ the indicated agonist minus the efflux in the absence of apoA-I but the presence of the respective agonist.

IV. Results

1. The monocyte experimental system

1.1. Macrophage incubation protocol

Elutriated monocytes were cultured at 10^6 cells/ml in macrophage serum-free medium supplemented with monocyte-colony stimulating factor (M-CSF, 50 ng/ml) (control) and incubated for up to 7 days at 37°C/5 % CO_2 to induce phagocytic differentiation as described previously (25). On the fourth day E-LDL (enzymatically degraded LDL) (40 μg/ml) respectively Ox-LDL (mildly oxidized LDL) (80 μg/ml) prepared from the same donor LDL was added to the cells for 48 hours until day 6 (Fig.24) to generate foam cells resembling lipid-loaden cells within the atherosclerotic lesion. On day 6 macrophages were deloaded of cholesterol with HDL_3. Therefore medium was removed, cells were washed with PBS and new medium supplemented with MCSF and HDL_3 (100 μg/ml) was added to the cells for 24h (Fig.24). On the days 1, 4, 6 and 7 cells were harvested and experiments were performed.

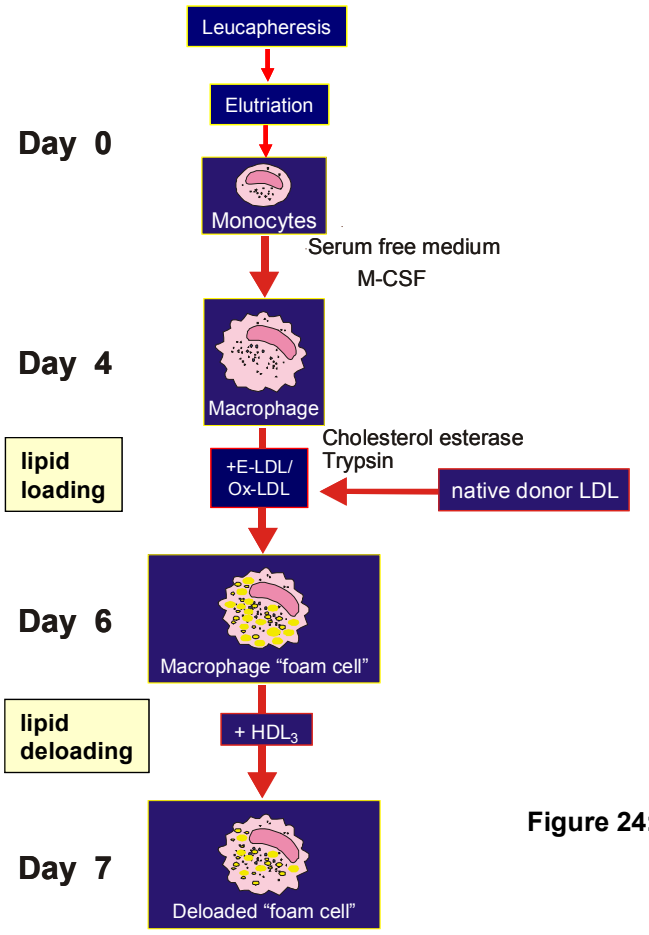

Figure 24: Incubation-scheme of human monocyte derived macrophages

1.2. Compositional analysis of modified lipoproteins

The lipid composition of LDL, E-LDL and Ox-LDL preparations of five different donors was analyzed by ESI-tandem mass spectrometry. The content of cholesteryl esters (CE) and free cholesterol (FC) was similar in LDL and Ox-LDL (Fig.25A). E-LDL however due to the treatment with cholesteryl ester hydrolase (acid lipase) contained a significantly higher amount of FC at the expense of CE as compared to LDL and Ox-LDL (Fig.25A). In Ox-LDL the CE fraction contained oxidized fatty acid moieties (data not shown). Considering the major phospholipid components, LDL showed the highest and Ox-LDL the lowest amount of phosphatidylcholine (PC) reflecting phospholipid oxidation and activation of phospholipase A2 (PLA2) (Fig.25B).

Acid lipase activity during the generation of E-LDL may also degrade small amounts of PC (Fig.25B). The amount of lysophosphatidylcholine (LPC) increased from LDL over E-LDL to Ox-LDL (Fig.25B). In Ox-LDL, this is likely due to the activation of platelet activating factor (PAF) acetylhydrolase a member of the PLA2 superfamily (37;158;376-379). The content of sphingomyelin (SPM) (Fig.25B) and ceramide (Fig.25C) was similar in LDL, E-LDL and Ox-LDL.

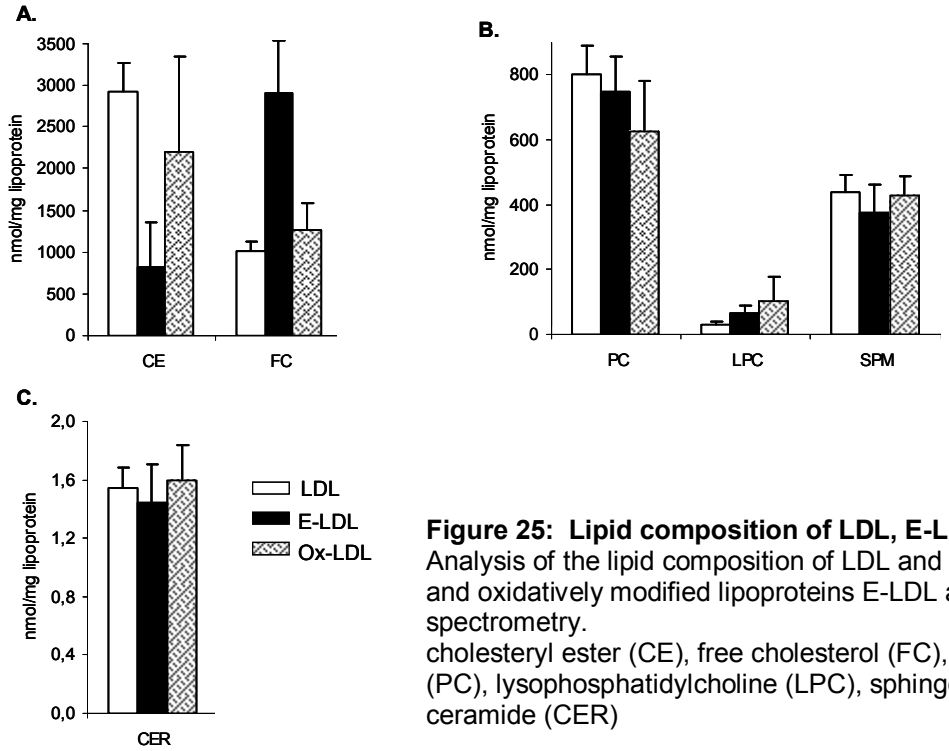

Figure 25: Lipid composition of LDL, E-LDL and Ox-LDL
Analysis of the lipid composition of LDL and the enzymatically and oxidatively modified lipoproteins E-LDL and Ox-LDL by mass spectrometry.
cholesteryl ester (CE), free cholesterol (FC), phosphatidylcholine (PC), lysophosphatidylcholine (LPC), sphingomyelin (SPM), ceramide (CER)

1.3. Viability tests for the cellular experiments

Cells were incubated according to the incubation protocol with MCSF, loaded with E-LDL (40 μg/ml) respectively Ox-LDL (80 μg/ml) on day 4 for 48h and deloaded with HDL_3 (100 μg/ml) on day 6 for 24h. At the days 6 and 7 cells were harvested and apoptosis test was performed with AnnexinV-FITC and propidiumjodid (PI) by flow cytometry (Fig.26A). Three individual experiments were performed and means and standard deviations of the percent of AnnexinV and PI positive cells were calculated. It could be observed that the percent of necrotic cells (PI and AnnexinV positive cells) was about 8 percent during MCSF, Ox-LDL, E-LDL and HDL_3 treatment. Only with HDL_3 deloading after E-LDL loading the amount of necrotic cells was 12%, which indicates also no critical concentration. Therefore it could be shown that the proposed incubation scheme assured viability of the cells for further experiments.

Moreover cells were incubated with different concentrations of Ox-LDL (20, 40, 50, 60 and 80 μg/ml) and subsequently tested for apoptosis with the same method (Fig.26B). The percentage of necrotic cells (PI and AnnexinV positive cells) of MCSF differentiated monocyte derived macrophages (MDM) and also of cells treated with different concentrations of Ox-LDL was in all cases negligible about 8%. Therefore an Ox-LDL concentration of 80 μg/ml can be taken to get lipid loaded cells.

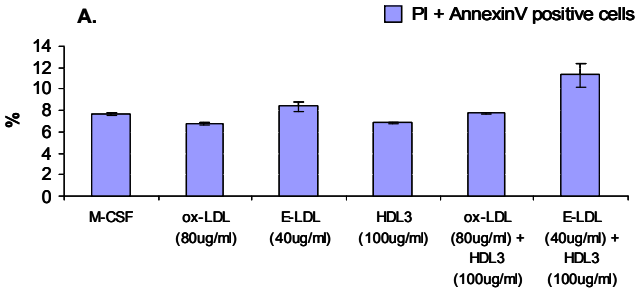

Figure 26A: Propidiumjodid (PI) and Annexin V positive cells in percent of total amount of cells measured by flow cytometry during MCSF differentiation, Ox-LDL and E-LDL loading and HDL_3 deloading of macrophages.

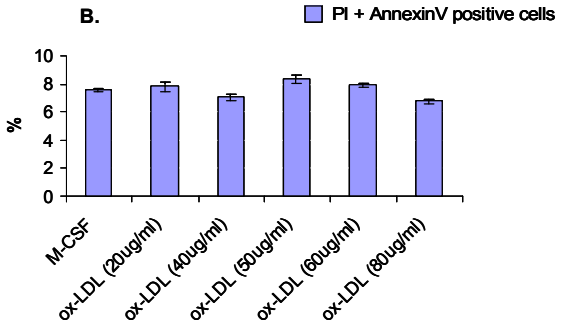

Figure 26B: Propidiumjodid (PI) and Annexin V positive cells in percent of total amount of cells measured by flow cytometry of macrophages incubated with MCSF and different concentrations of Ox-LDL

1.4. Discrimination of four different monocyte subpopulations by flow cytometry

It is possible to discriminate four different populations of peripheral blood monocytes with respect to their expression pattern of CD14 and CD16 by flow cytometry (Fig.27). Approximately 60% of monocytes belong to the subset 1 (MNP1) that is characterized by bright expression of CD14 and no or dim expression of CD16. The second (MNP2) and third (MNP3) subset have high capacity for phagocytosis and have bright expression of CD16 and bright (MNP2) or dim (MNP3) expression of CD14, respectively. The fourth subset (MNP4) is known to be a precursor subpopulation for antigen-presenting (dendritic) cells as they present only dim expression of CD14 and CD16.

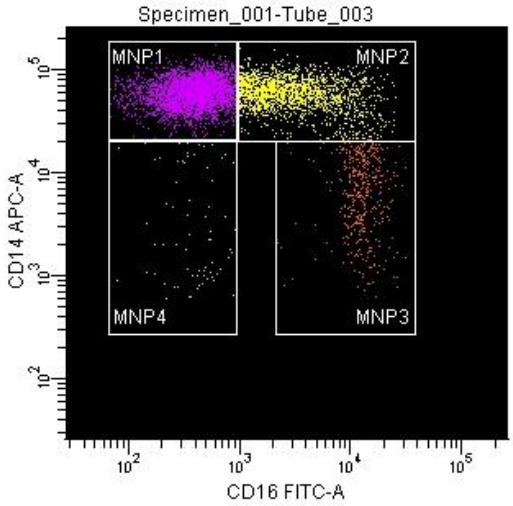

Figure 27: Four monocyte subsets can be distinguished on their expression patterns of CD14 and CD16. The dot plot illustrates the identification of peripheral blood monocyte subpopulations as discriminated by flow cytometry: MNP1 (CD14 high; CD16dim), MNP2 (CD14 high; CD16 high), MNP3 (CD14 dim; CD16 high) and MNP4 (CD14 dim; CD16 dim).

2. Analysis of MCSF differentiated, E-LDL and Ox-LDL loaded and HDL_3 deloaded human monocyte derived macrophages of the ApoE3/3 genotype

2.1. Changes in cellular lipid content determined by mass spectrometry

ESI-tandem mass spectrometry was used to measure cellular content of total, esterified and unesterified cholesterol, sphingomyelin, ceramide and sphingosine in four independent experiments and the results are shown in Fig.28. Total, esterified and unesterified cholesterol did not change during MCSF-induced differentiation (Fig.28A-C). However, monocyte derived macrophages loaded with E-LDL (40μg/ml) showed a 4-fold higher content of total cholesterol and a 99-fold increase of esterified cholesterol while Ox-LDL loaded cells (80μg/ml) showed only a 2.3-fold increase of total cholesterol and an 18-fold enhancement of esterified cholesterol (Fig.28A,B). Unesterified cholesterol increased with E-LDL and Ox-LDL loading to the same extent (Fig.28C). Cellular sphingomyelin content increased during monocyte to macrophage differentiation up to 1.7-fold and no further change could be observed during E-LDL and Ox-LDL loading (Fig.28D). The ceramide content during MCSF-induced differentiation showed no significant change (Fig.28E). Ox-LDL incubation however, led to a significant 3.6-fold increase in cellular ceramide content while E-LDL showed only a 1.4-fold increase (Fig.28E). As shown before, this effect was not due to higher ceramide content in Ox-LDL itself (Fig.25C). These data allow the conclusion that E-LDL loading predominantly increases cellular cholesterol content while Ox-LDL loading preferentially increases cellular ceramide content. Sphingosine content of the cells revealed a 1.6-fold upregulation during MCSF-dependent differentiation, an additional 1.2-/1.3-fold increase occurred with E-LDL and Ox-LDL respectively (Fig.28F). HDL_3-dependent deloading reversed the increase of cholesterol mass of both lipid loading agents (Fig.28A-C). Deloading of E-LDL loaded cells with HDL_3 diminished total cholesterol content up to 40% (Fig.28A), mostly (up to 140%) at the expense of esterified cholesterol (Fig.28B) while unesterified cholesterol decreased only by 2% (Fig.28C). HDL_3 deloading of Ox-LDL loaded cells led to a 20% decrease of total cholesterol (Fig.28A), a 10% decrease of esterified (Fig.28B) and a neglegible decrease of unesterifed cholesterol (Fig.28C). Sphingomyelin content however increased during HDL_3 deloading for both LDL-modifications up to 24% (Fig.28D) and cellular ceramide increased slightly during E-LDL deloading up to 13% (Fig.28E) while it decreased during Ox-LDL deloading up to 50%. Along with the decrease in ceramide, sphingosine increased with HDL_3 deloading of Ox-LDL loaded cells up to 130%. In E-LDL loaded cells however, HDL_3 did not affect sphingosine levels (Fig.28F).

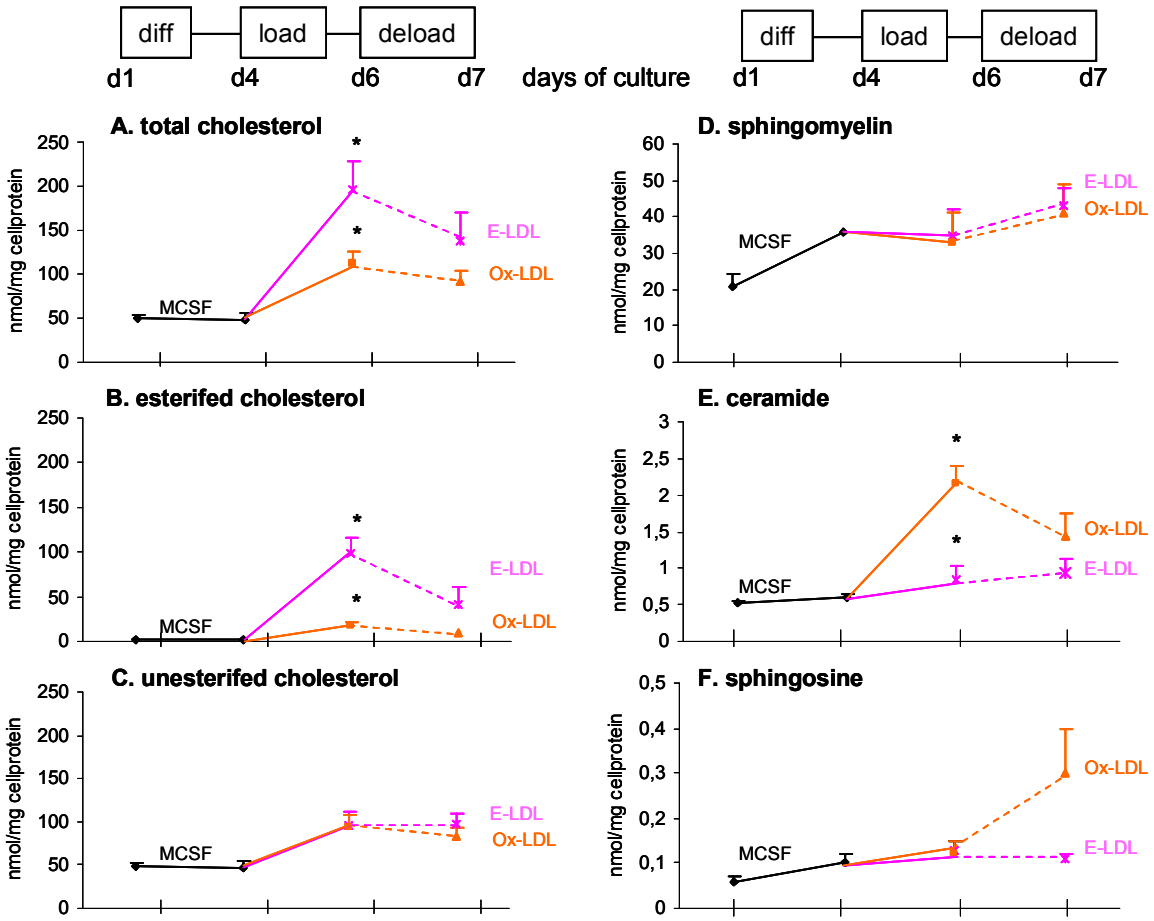

Figure 28: Cellular content of total, esterified and unesterified cholesterol, sphingomyelin, ceramide and sphingosine
Mass spectrometry was used to determine the cellular lipid content of human monocyte derived macrophages at the status of differentiation with MCSF (day 0 and day 4), during E-LDL and Ox-LDL loading after 48 hours and during HDL_3 deloading after 24 hours. The intracellular content of total cholesterol (A), esterified cholesterol (B), unesterified cholesterol (C), sphingomyelin (D), ceramide (E) and sphingosine (F) is shown.

2.2. RT-PCR analysis of enzymes involved in ceramide generation and degradation

To elucidate the reason for the Cer elevation during Ox-LDL loading, TaqMan realtime RT-PCR was performed for the enzymes involved in Cer generation and degradation of MCSF differentiated, E-LDL and Ox-LDL loaded and HDL_3 deloaded human monocyte-derived macrophages. During MCSF-dependent monocyte/macrophage differentiation, mRNA expressions of serine palmitoyltransferases 1+2 (SPTLC1+2), which are involved in Cer synthesis as well as the transcriptional levels of sphingomyelin synthases, 1 and 2 which convert Cer into sphingomyelin were downregulated (Fig.29A,B,C,D). Analysis of the sphingomyelinases, which convert sphingomyelin to Cer, revealed an upregulation of mRNA expression of acid sphingomyelinase (SMPD1) (2.8fold) and acid sphingomyelinase like phosphodiesterase (ASML3B) (3.5fold) (Fig.29E,F) whereas the mRNA expression of neutral sphingomyelinase (SMPD2) and neutral sphingomyelinase activation associated factor (NSMAF) was downregulated -1,5 fold during differentiation (Fig.29G,H). mRNA expression of glucosidase, beta; acid (GBA) which includes glucosylceramidase involved in the

degradation of glucosylceramide into Cer showed no change during differentiation (Fig.29I). UDP-glucose ceramide glucosyltransferase (UGCG) the enzyme which converts Cer to glucosylceramide and N-acylsphingosine amidohydrolase 1 (ASAH1) (acid ceramidase) degrading Cer to sphingosine showed an upregulation of mRNA expression (2 and 3.9 fold) during differentiation (Fig.29J,K).

During E-LDL loading SPTLC1 and SPTLC2 were 1.7 and 1.5 fold and during Ox-LDL loading 2.1 and 1.3 fold upregulated (Fig.29A,B). Sphingomyelin synthase 1 was 1.1 fold and sphingomyelin synthase 2 was 1.6 fold upregulated during both lipid loading agents (Fig.29C,D). SMPD1 and ASML3B mRNA expression was -1.7 and -1.8 fold downregulated during E-LDL loading. Ox-LDL loading however revealed a 3.1 fold upregulation of SMPD1 and a -2.3 fold downregulation of ASML3B compared to MCSF. mRNA expression of SMPD2 and NSMAF showed a stronger upregulation during Ox-LDL loading (5.2 and 2.2 fold) than during E-LDL loading (2.7 and 1.3 fold) (Fig.29G,H). The stronger upregulation of the sphingomyelinases SMPD1, SMPD2 and the activation factor NSMAF during Ox-LDL loading compared with E-LDL loading can be considered as causal for the Ox-LDL induced Cer elevation.

mRNA expression of GBA, was stronger upregulated during Ox-LDL than during E-LDL loading (3.7 vs 1.8 fold) (Fig.29I) while UGCG mRNA expression showed a higher upregulation during E-LDL loading (3.2 vs 2.2 fold) (Fig.29J). ASAH1 mRNA expression was -1.5 fold downregulated with E-LDL and Ox-LDL loading (Fig.29K).

E-LDL deloading with HDL_3 revealed almost no change of the mRNA expression of SPTLC1 and 2 (Fig.29A,B). With Ox-LDL deloading SPTLC1 decreased up to 1 fold (Fig.29A) while SPTLC2 levels remained unchanged (Fig.29B). Both sphingomyelinases, 1 and 2 were upregulated with HDL_3 after E-LDL deloading up to 2 fold (Fig.29C,D) With Ox-LDL deloading sphingomyelin synthase 1 increased 1.7 fold while sphingomyelin synthase 2 decreased 1.2 fold (Fig.29C,D). SMPD1, ASML3B as well as SMPD2 and NSMAF expression decreased with HDL_3 deloading compared to lipid loading, however from a higher level in Ox-LDL loaded cells (Fig.29E,F,G,H). HDL_3 deloading led also to a downregulation of GBA (Fig.29I), UGCG (Fig.29J) and ASHA1 (Fig.29K). These results show that all tested sphingomyelinases were strongly downregulated with HDL_3 deloading which reflects an inversion of the lipid loading effects of E- and Ox-LDL and a reduction of the enzymatic functions in converting sphingomyelin to ceramide to provide sphingomyelin for cholesterol efflux.

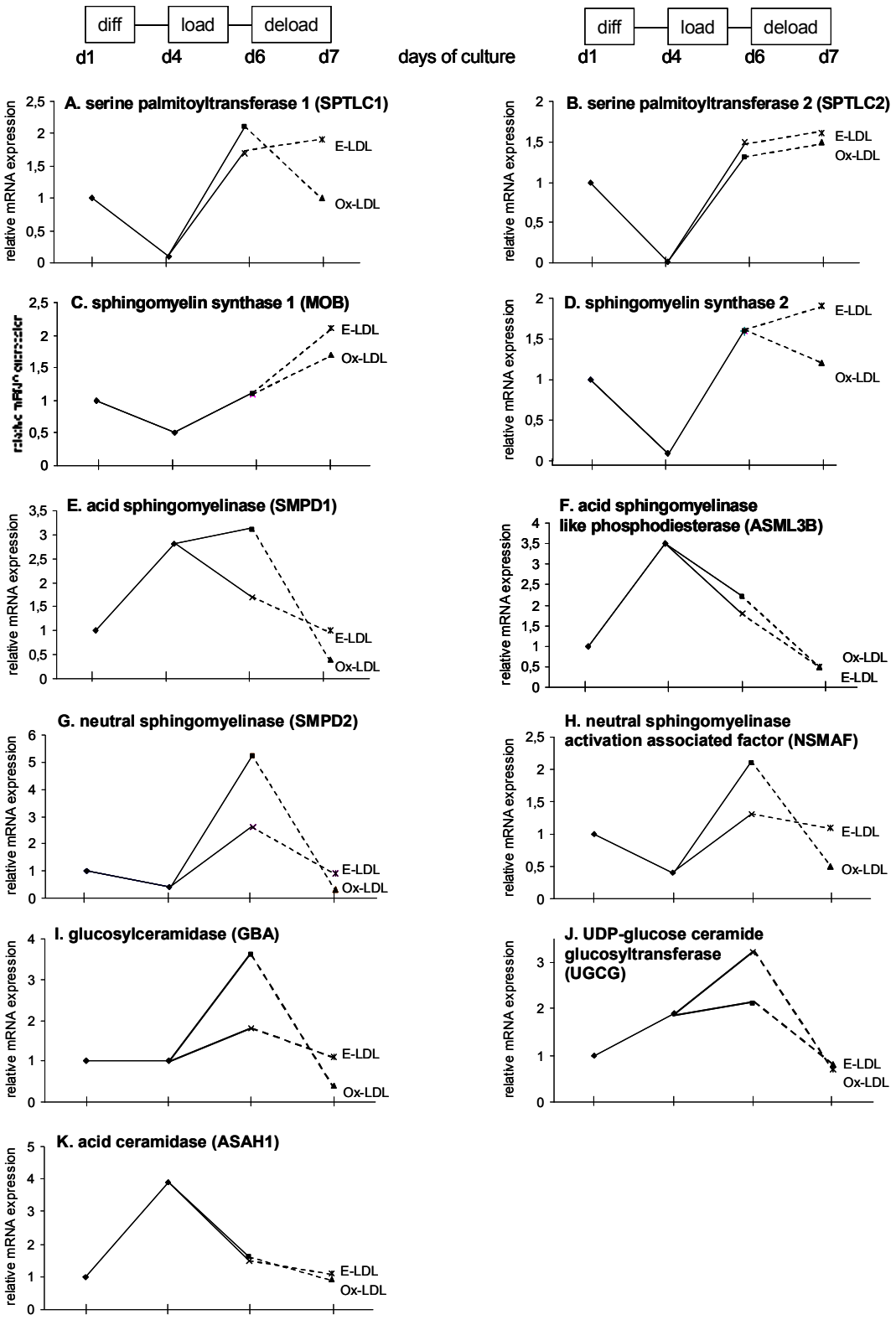

Figure 29. Taqman analysis of enzymes involved in ceramide synthesis and degradation
Using real time Taqman RT-PCR standardized to 18s rRNA as a reference, gene expression was monitored of 4 day differentiated macrophages, 48 hours E- and Ox-LDL loaded macrophages (day 4 to day 6) and 24 hours HDL_3 (day 6 to day 7) deloaded macrophages. Serine palmitoyltransferase 1 (SPTLC1) (A), serine palmitoyltransferase 2 (SPTLC2) (B), sphingomyelin synthase 1 (MOB) (C), sphingomyelin synthase 2 (D), acid sphingomyelinase (SMPD1) (E), acid sphingomyelinase like phosphodiesterase (ASML3B) (F), neutral sphingomyelinase (SMPD2) (G), neutral sphingomyelinase (N-SMase) activation associated factor (NSMAF) (H), glucosylceramidase (glucosidase beta acid) (GBA) (I), UDP-glucose ceramide glucosyltransferase (UGCG) (J), acid ceramidase (ASAH1)

2.3. Cell surface expression of sphingo- and glycosphingolipids

In order to analyze whether the increase of total cellular ceramide content during lipid loading of monocyte derived macrophages is paralleled by an increased surface expression of ceramide and ceramide derived glycosphingolipids, flow cytometric analysis with antibodies specific for ceramide, lactosylceramide (CDw17), globotriaosylceramide (CD77), dodeca-saccharideceramide (CD65s) and fluorescent labeled cholera toxin for GM1 ganglioside staining was performed and the results are shown in Fig.30. Means and standard deviations of mean fluorescence intensities of 6 independent experiments were calculated. Statistical significance was tested by a student´s t-test for paired samples. The asterisk indicates a significant difference with $p<0.05$ between MCSF differentiated and lipid loaded macrophages. Surface expression of ceramide (Fig.30A), globotriaosylceramide (Fig.30C) and GM1 ganglioside (Fig.30D) increased during MCSF-dependent differentiation while lactosylceramide (Fig.30B) and dodecasaccharideceramide (Fig.30E) decreased during the differentiation phase from day 1 to day 4, and following differentiation showed only a slight increase. Ox-LDL loading however, led to a significantly increased surface expression of ceramide, lactosylceramide, globotriaosylceramide, dodecasaccharideceramide and GM1 ganglioside while E-LDL loading only slightly increased their expression (Fig.30A-D). These data indicate that Ox-LDL in comparison to E-LDL not only increased total cellular ceramide content but also induced a higher cell surface expression of ceramide and ceramide-backbone glycosphingolipids. Neither ceramide, lactosylceramide nor globotriaosylceramide responded to HDL_3 in Ox-LDL loaded cells (Fig.30A-C) while dodecasaccharideceramide and GM1 ganglioside further increased (Fig.30D,E). E-LDL loaded cells responded to HDL_3 with a cell surface decrease in ceramide and lactosylceramide (Fig.30A,B) while globotriaosylceramide, dodecasaccharideceramide and GM1 ganglioside increased during HDL_3 exposure (Fig.30C-E).

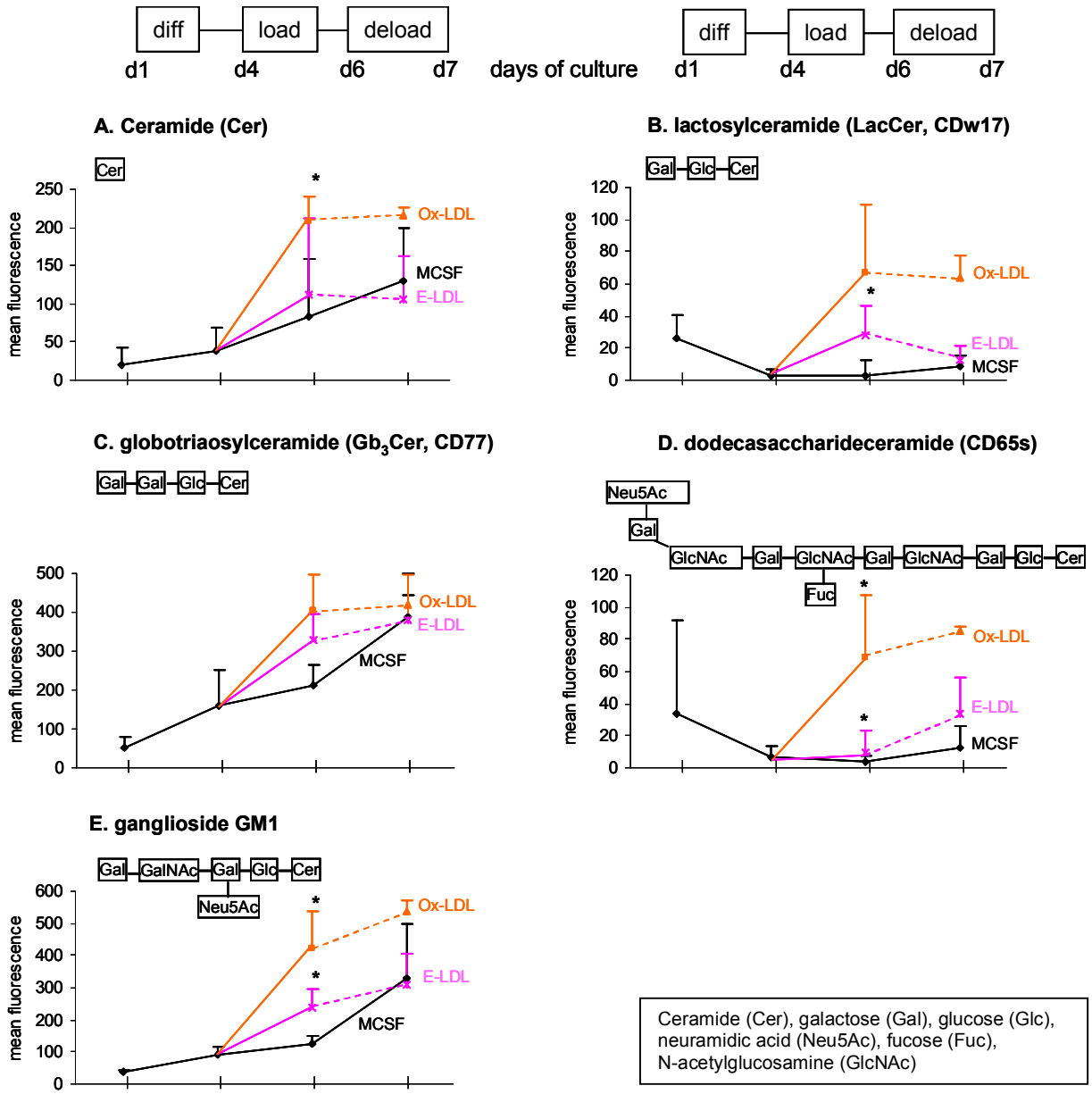

Figure 30: Surface expression of membrane ceramide, glycosphingolipids and GM1 ganglioside

The cell surface expression of membrane ceramide, glycosphingolipids and the GM1ganglioside was analyzed by flow cytometry.

Cellular surface expression of ceramide (Cer) (A), lactosylceramide (LacCer, CDw17) (B), globotriaosylceramide (Gb_3Cer, CD77) (C), dodecasaccharideceramide (CD65s) (D) and GM1 ganglioside (E) is shown.

2.4. Binding and uptake of apoE and apoA-I

Flow cytometric analysis of 4°C binding and 37°C binding and uptake of fluorescent labelled apoE and apoA-I demonstrated at 4°C higher apoE binding on surface Cer enriched Ox-LDL loaded cells as compared to E-LDL loaded cells (Fig.31A). In contrast to apoE, apoA-I showed similar binding capacity at 4°C to E-LDL and Ox-LDL loaded cells (Fig.31B). At 37°C, a higher binding and uptake of both, apoE and apoA-I was found to Cer enriched Ox-LDL loaded cells (Fig.31C,D) while apoA-I compared to apoE (Fig.31C) showed a smaller difference in the uptake and binding capacity between E-LDL and Ox-LDL loaded cells

(Fig.31D). These data strongly indicate that apoE not only has a high affinity to artificial liposomes enriched in Cer (110) but also to cell surface Cer enriched monocytes loaded with Ox-LDL.

It was also analyzed 37°C binding and uptake of fluorescent labelled apoE (Cy3-apoE) and apoA-I (Cy5-apoA-I) and their colocalization with Cer on Ox-LDL loaded macrophages by confocal microscopy and the results are shown in Fig.31 E-J. It could be demonstrated a higher binding and uptake of apoE on Cer enriched Ox-LDL loaded cells (Fig.31E) associated with an impaired colocalization of apoE and Cer compared to apoA-I (Fig.31H,I).

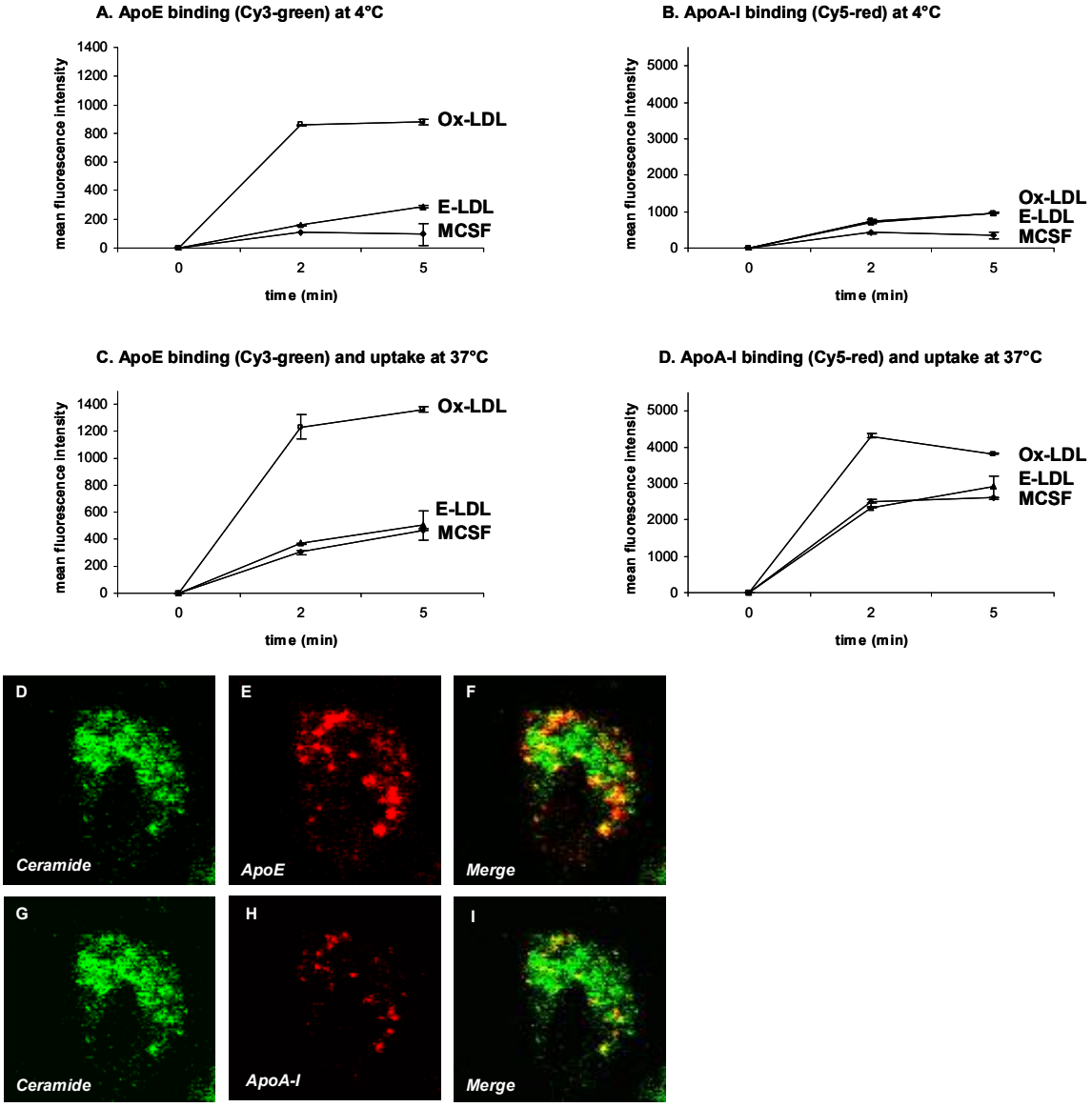

Figure 31. Binding and uptake of apoE and apoA-I determined by flow cytometry and confocal microscopy

At 4°C binding of fluorescent labeled apoE (Cy3-apoE) (A) and apoA-I (Cy5-apoA-I) (B) and at 37°C binding and uptake of apoE (C) and apoA-I (D) was analyzed by flow cytometry during 5 min of M-CSF differentiation as well as E-LDL and Ox-LDL loaded macrophages.

Ceramide expression and binding of fluorescent labeled apoE and apoA-I as well as colocalization between ceramide and apoE, apoA-I respectively (Merge) was analyzed in Ox-LDL loaded cells by confocal microscopy at 37°C.

2.5. Analysis of raft formation

2.5.1. Staining of raft-microdomains with DMPE-TMR

MCSF differentiated (6 days), E-LDL loaded (day 4-6) and HDL_3 deloaded (day 6-7) macrophages were stained with lipid vesicles prepared from a mixture of 1-palmitoyl-2-oleoyl-sn-glycero-3-phosphocholine (POPC) and 1,2-dimyristoyl-sn-glycero-3-phospho-ethanolamine-tetramethyl-rhodamine (DMPE-TMR) in order to find out differences in raft-microdomain formations during macrophage differentiation, E-LDL loading and HDL_3 deloading. DMPE is a phospholipid with a saturated side chain and therefore it specifically intercalates with highly lipid ordered membrane domains like rafts as described by Schütz G.J. et al. (329). In MCSF differentiated macrophages, a relatively homogenous distribution with weak fluorescence of DMPE-TMR on the cell membrane could be observed, which may represent small single lipid microdomains (Fig.32A). In contrast to this, macrophages loaded with E-LDL showed an inhomogenous distribution of DMPE-TMR staining and the formation of large raft-domains bearing intensive fluorescence on the cell surface (Fig.32B). This indicates that cholesterol loading promotes the confluence of relatively small rafts into larger domains. With HDL_3 deloading this phenomenon was reversed indicating a disruption of these large microdomains during HDL_3 deloading (Fig.32C).

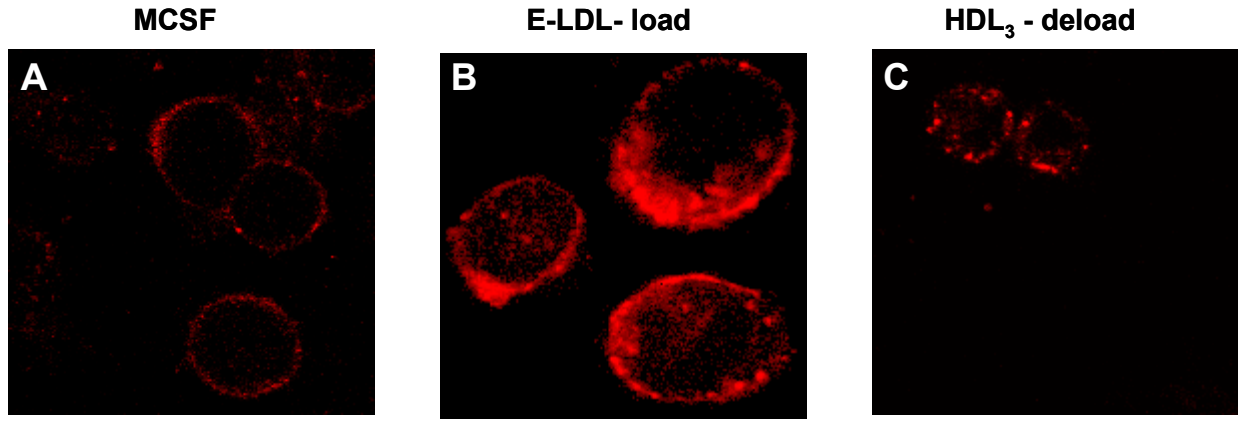

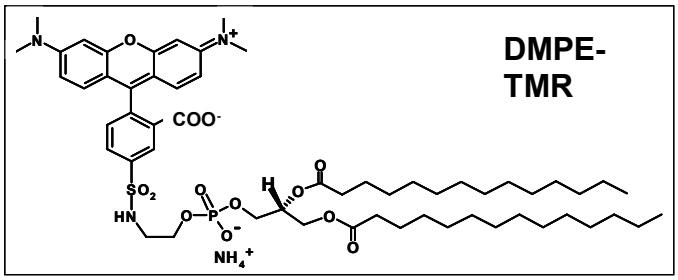

Figure 32: Analysis of raft formation with DMPE-TMR staining of MCSF differentiated (A), E-LDL loaded (B) and HDL_3 deloaded macrophages (C)

2.5.2. Staining of sphingomyelin- and Cer rafts and cholesterol-rich membrane microdomains

In addition to flow cytometry analysis of Cer surface expression and to the different formations of rafts found with DMPE staining during lipid loading and deloading, confocal microscopy was used as an additional method to analyze the distribution and raft formation of sphingomyelin (SM), cholesterol and Cer of MCSF differentiated, E-LDL and Ox-LDL loaded, as well as HDL_3 deloaded macrophages. Lysenin, labelled with anti-His antibody followed by incubation with anti-rabbit-Texas-Red antibody was used for SM staining, theta toxin-FITC for cholesterol staining and fluorescent labelled Cer antibody was used to analyze Cer rafts.

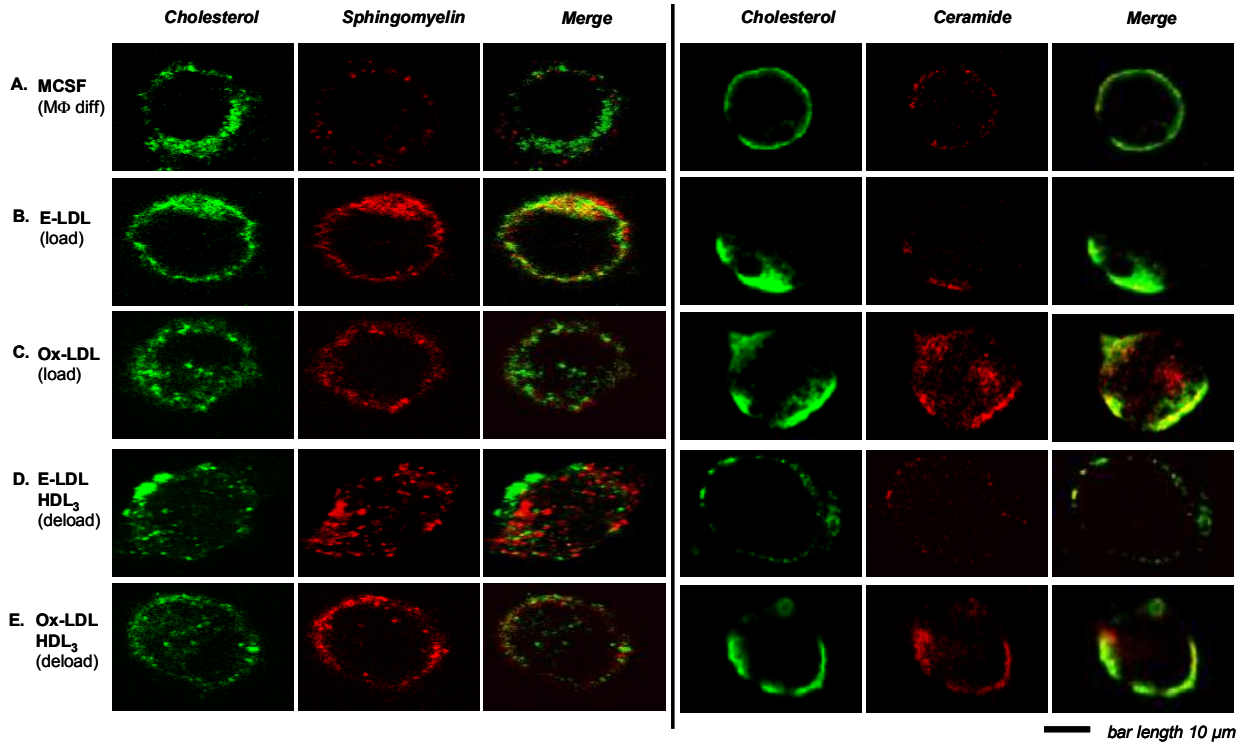

Figure 33: E-LDL promotes cholesterol/sphingomyelin rich membrane microdomains while Ox-LDL induces cholesterol/ceramide rafts
The surface expression of sphingomyelin (SM), cholesterol and ceramide (Cer) was analyzed by confocal microscopy with M-CSF, E-LDL and Ox-LDL loaded and HDL_3 deloaded macrophages (MΦ). Fluorescent theta toxin (FITC labeled, green staining, cholesterol column), lysenin (Texas-red-anti-rabbit; red staining, sphingomyelin column), and ceramide (Cy5-anti-mouse; red patches, ceramide column) were used to analyze the expression of SM, cholesterol and Cer rich microdomains. Overlap of cholesterol and SM respectively Cer was shown in the merge column. M-CSF treated MΦ (A), E-LDL loaded MΦ (B), Ox-LDL loaded MΦ (C), E-LDL deloaded MΦ (D), and Ox-LDL deloaded MΦ (E).

SM staining (red staining, sphingomyelin column) showed an induction during E-LDL loading (Fig.33B) compared to MCSF (Fig.33A) and Ox-LDL loading (Fig.33C). The formation of SM rich membrane microdomains during E-LDL loading is obvious from the staining pattern (Fig.33B). As compared to MCSF-differentiated cells (Fig.33A), theta toxin expression (green staining, cholesterol column) is similarly induced with E-LDL and Ox-LDL loading (Fig.33B,C) indicative for the formation of cholesterol enriched microdomains with both lipid loading

agents. The Cer expression (red staining, ceramide column) was lowest in MCSF treated macrophages as a control (Fig.33A) and E-LDL loaded macrophages (Fig.33B), while macrophages loaded with Ox-LDL showed a higher expression of Cer rich microdomains (Fig.33C). This is in accordance with the flow cytometric data which showed also the highest Cer surface expression during Ox-LDL loading (Fig.33A). Cer rich microdomains partially colocalize with the theta toxin labeled cholesterol rich microdomains (yellow overlay, Merge column).

With HDL_3 deloading a decrease of SM, cholesterol and Cer expression could be observed in E-LDL loaded cells (Fig.33D) and to a lower extent in Ox-LDL loaded cells (Fig.33E) indicating a differential deprivation of SM, cholesterol and Cer at the cell surface during HDL_3 deloading.

2.5.3. Mass spectrometry analysis of isolated lubrol-detergent resistant membranes

Tandem mass spectrometric analysis of isolated lubrol-detergent resistant membranes of MCSF differentiated, E-LDL and Ox-LDL loaded as well as HDL_3 deloaded macrophages, confirmed the induction of cholesterol/sphingomyelin rich membrane microdomains with E-LDL loading and cholesterol/ceramide rich rafts with Ox-LDL loading (table 8) as it was observed by confocal microscopy (Fig.33A-E). SM content was induced during E-LDL loading to a higher extent than during Ox-LDL loading (32 vs. 2 nmol/mg protein) compared with MCSF. During deloading, SM content increased more extensively after E-LDL than after Ox-LDL preloading (57 vs. 23 nmol/mg protein). Free cholesterol content (FC) increased with E-LDL and Ox-LDL loading (136 vs. 111 nmol/mg protein) in comparison to MCSF and decreased more extensively during Ox-LDL deloading (34 vs. 86 nmol/mg protein). The increased amount of Cer (4,0 vs. 0,6 nmol/mg protein) and glucosylceramide (GluCer) (1,6 vs. 0,3 nmol/mg protein) was higher during Ox-LDL than during E-LDL loading in comparison to MCSF.

	FC	SM	Cer	GluCer
MCSF (MΦ diff)	247+/-136	206+/-0	1.5+/-0.4	1.8+/-0.4
E-LDL (load)	**383+/-142**	**238+/-11**	2.1+/-0.6	2.1+/-0.8
E-LDL (deload)	**349+/-66** ↓	295+/-77 ↓	2.3+/-1.0	3.3+/-1.1
Ox-LDL (load)	**358+/-168**	**208+/-28**	**5.5+/-1.4**	**3.4+/-1.1**
Ox-LDL (deload)	**272+/-111** ↓	231+/-37 ↓	**2.0+/-0.3** ↓	**2.9+/-0.4** ↓

Table 8: Lipid content of lubrol rafts (nmol/mg membrane protein)
Analysis of free cholesterol (FC), sphingomyelin (SM), ceramide (Cer) and glucosylceramide (GluCer) content of isolated detergent resistant membranes (lubrol rafts) determined by ESI mass spectrometry.

2.6. Gene expression analysis

In order to elucidate potential mechanisms behind the differential effects of E-LDL and Ox-LDL, the gene expression profile of 4 day MCSF differentiated, E-LDL and Ox-LDL loaded, as well as HDL_3 deloaded human monocyte derived macrophages was analyzed by Affymetrix U133A Gene Chips™. The number and percentage of genes regulated under these conditions is shown in table 9. As indicated in table 9, E-LDL specifically downregulates (497 vs 105) while Ox-LDL upregulates (178 vs 20) more genes during lipid loading. With HDL_3 deloading of E-LDL loaded cells, a 3-4 fold higher number of genes was found upregulated than during deloading of Ox-LDL loaded cells (625 vs 166). The number of genes which were specifically downregulated during deloading is 54 in the case of E-LDL and 38 in the case of Ox-LDL deloading. The number of genes that were commonly induced during E-LDL and Ox-LDL loading was 29 vs 31. The commonly downregulated genes during E-LDL and Ox-LDL loading indicated a much higher number of regulated genes than during deloading (129 vs 1). This results indicate greatest dynamics in the gene regulation during HDL_3 deloading of E-LDL loaded cells which showed the highest number of upregulated genes.

Category	Number of genes		Percentage	
	E-LDL	Ox-LDL	E-LDL	Ox-LDL
Load Specific Up	20	178	0,5%	4,2%
Load Specific Down	497	105	11,7%	2,5%
Deload Specific Up	625	166	14,7%	3,9%
Deload Specific Down	54	38	1,3%	0,9%

Category	Number of genes		Percentage	
	Load	Deload	Load	Deload
Common Up	29	31	0,7%	0,7%
Common Down	129	1	3,0%	0,0%
Inversly regulated	16	113	0,4%	2,7%

Genes regulated during differentiation	1443	34,0%
Total significantly reglated genes	4240	

Table 9: Number and percentage of genes regulated in the E-LDL and Ox-LDL loaded, HDL_3 deloaded and differentiated status

In the next step the related in vitro results of the differential effects of E-LDL and Ox-LDL loading and deloading were related to in silico data of published detergent resistant membrane proteins that were identified by proteomic analysis and published by Li et al., Proteomics 2003 (380) and 2004 (381); Bae et al., Proteomics 2004 (382); Foster et al., PNAS 2003 (383) and Blonder et al., Electrophoresis 2004 (384). A gene list derived from this detergent resistant membrane proteins was matched with our gene array data analyzed by Affymetrix U133A Gene Chips™ of 4 day M-CSF differentiated, E-LDL and Ox-LDL

loaded, and HDL_3 deloaded human monocyte derived macrophages and genes were considered as significant with an up-(red color) or down- (blue color) regulation of ≥2.0 fold. This search list was extended with all significantly regulated membrane receptors and proteins present on the U133A Chip in order to further elucidate the differential plasma membrane receptor composition according to their specific, common or inverse regulation during E-LDL and Ox-LDL loading and deloading. In addition, proteins relevant for glycosphingolipid metabolism, lipid transfer proteins, apolipoproteins, ABC transport proteins and proteins involved in vesicular trafficking were attached and shown in table 10.

In the group of detergent resistant membrane proteins, three V-type ATPases (ATP6V1C1, ATP6V1D and ATP6V1G1) were found downregulated during E-LDL deloading and upregulated during Ox-LDL deloading which may reflect a compensatory increase in protonation due to the known impaired degradation of Ox-LDL (161). In contrast the ATPsynthase subunits (ATP5I, ATP5L, ATP5A1 and ATP50) were found upregulated during E-LDL deloading and showed no response upon Ox-LDL deloading. This regulation may relate to the recent observation that ApoA-I binds to the beta chain of ATP synthase at the plasma membrane and thereby triggers type II phagocytosis and generation of ADP (105) in clathrin independent vesicular processing which is relevant for E-LDL but not minimally Ox-LDL processing (161). These endocytotic processes also involve solute carriers and ion channels. The adenine nucleotide translocators SLC25A5, SLC25A6 as well as the citrate and oxyglutarate carriers SLC25A1 and SLC25A11, the voltage dependent anion channels VDAC3 and the sodium- and chloride-activated ATP-sensitive potassium channel SLICK showed the same regulation pattern as the ATPsynthase subunits with an upregulation during E-LDL deloading and no significant regulation during Ox-LDL deloading.

Most of the major histocompatibility complex related proteins like HLA-A, HLA-B, HLA-C, HLA-E, HLA-DMB, HLA-DPA1 and HLA-DPB1 showed an upregulation during E-LDL deloading but no regulation during Ox-LDL deloading. Others like HLA-DQA1 and HLA-DRA revealed no significant regulation during E-LDL loading but a downregulation during Ox-LDL loading. During E-LDL deloading no significant regulation while during Ox-LDL deloading an upregulation could be observed. These MHC class proteins were described by M. Desjardins and CV Harding (385;386) as a part of the phagosome compartment and involved in phagocytosis and clathrin independent MHC processing.

This compartment involves also part of the proteasome/ubiquinone protein processing system which was found not regulated during E-LDL loading and upregulated during Ox-LDL loading while deloading with HDL_3 led to an upregulation during E-LDL deloading and no regulation during Ox-LDL deloading. The ribosomal proteins showed a similar regulation pattern during deloading with an upregulation during E-LDL deloading and no regulation during Ox-LDL deloading. This indicates that E-LDL and Ox-LDL loading and deloading exert

differential effects on the degradation and translation machinery with a higher translational acitivation during E-LDL deloading.

In the group of membrane receptors relevant for innate immunity, the gene expression of CD32/Fcγ-receptor 2A was not significantly regulated during E-LDL loading but was downregulated during Ox-LDL loading. Decay acceleration factor CD55 was only upregulated with Ox-LDL loading. In relation to this raft associated membrane receptors, it was focused on the innate immunity receptor cluster described by Pfeiffer et al. (30) and other published ABCA1 pathway related proteins. This receptor cluster was induced by binding of ceramide and is involved in raft formation and signaling. The GPI-anchored LPS receptor CD14 was downregulated during lipid loading and upregulated during E-LDL deloading. The integrin associated pentaspan protein CD47 and the integrin CD11b were not significantly regulated during E-LDL deloading and upregulated during Ox-LDL deloading. The Fcγ-receptors CD64 and CD32 were not significantly regulated during E-LDL loading and downregulated during Ox-LDL loading while the Fcγ-receptor IIIa/CD16 was downregulated with both lipid loading agents. During HDL_3 deloading CD64 was upregulated with Ox-LDL deloading. The scavenger receptor CD36 was upregulated during E-LDL loading while the scavenger receptor cysteine rich/CD163 was downregulated during Ox-LDL loading. During E-LDL deloading CD163 and LRP1 were upregulated and CD163 was also upregulated during Ox-LDL deloading. Results of flow cytometric analysis of this innate immunity receptor cluster were shown in Fig.34.

ABCA1 and ABCG1 are proteins involved in lipid efflux of macrophages (387). ABCA1 was upregulated during E-LDL and Ox-LDL loading while ABCG1 was only significantly regulated during Ox-LDL loading. Both were not significantly regulated during HDL_3 deloading in the gene array data. ABCA1 related proteins like CDC42 which is involved in vesicular trafficking was not significantly regulated during E-LDL deloading and upregulated during Ox-LDL deloading reflecting a higher dynamic of vesicular trafficking during HDL_3 deloading of Ox-LDL loaded cells probably by abolishing the trapping of Ox-LDL in the lysosomal pathway. The proteins Sec6like 1 and the exocyst complex component 7 which is involved in the exocytotic vesicular pathway are upregulated during E-LDL deloading and downregulated respectively not significantly regulated during Ox-LDL deloading. This could indicate a higher dynamic of the exocytosis pathway during vesicular trafficking in E-LDL deloaded compared with Ox-LDL deloaded macrophages. The apolipoproteins C-I, C-II and C-IV were all upregulated during E-LDL deloading and not significantly regulated during Ox-LDL deloading indicating a higher lipid efflux and transport dynamic during E-LDL deloading. In addition apoC-II was downregulated during E-LDL loading while apoC-I and apoC-IV were upregulated during Ox-LDL loading.

2.6.1. Pathway specific analysis of microarray expression data

UniGene	Gene Title	Gene Symbol	Chrom Loc	E3 Mo_p	E3 Mo_Sig	E3_ELDL Load_p	E3_ELDL Load_FC	E3 ELDL Deload_p	E3 ELDL Deload_FC	E3 OxLDL Load_p	E3 OxLDL Load_FC	E3 OxLDL Deload_p	E3 OxLDL Deload_FC
	Raft proteins deduced from Li et al., Proteomics 2004, Bae et al., Proteomics 2004, Foster et al., PNAS 2003, Li et al., Proteomics 2003, Blonder et al., Electrophoresis 2004												
	ATPasen/synthasen												
Hs.86905	ATPase, H+ transporting, lysosomal 42kDa, V1 subunit C, isoform 1	ATP6V1C1	8q22.3	++	500	++	1,5	++	-2,8	++	1,4	++	4
Hs.272630	ATPase, H+ transporting, lysosomal 34kDa, V1 subunit D (Vacuolar ATP synthase catalytic s	ATP6V1D	14q23-q24.2	++	463	++	1,3	++	-2,1	++	1	++	2,5
Hs.90336	ATPase, H+ transporting, lysosomal 13kDa, V1 subunit G isoform 1	ATP6V1G1	9q32	++	1082	++	1,3	++	-3,2	++	-1,3	++	2,6
Hs.85539	ATP synthase, H+ transporting, mitochondrial F0 complex, subunit e	ATP5I	4p16.3	++	683	++	1	++	3,5	++	1,7	++	-1,5
Hs.107476	ATP synthase, H+ transporting, mitochondrial F0 complex, subunit g *S	ATP5L	11q23.3	++	2553	++	-1,5	++	2,6	++	1,2	++	1,1
Hs.298280	ATP synthase, H+ transporting, mitochondrial F1 complex, alpha subunit, isoform 1, cardiac m	ATP5A1	18q12-q21	++	2223	++	1,1	++	2,3	++	1,6	++	1,2
Hs.409140	ATP synthase, H+ transporting, mitochondrial F1 complex, O subunit (oligomycin sensitivity c	ATP5O	21q22.11	++	1444	++	-1,1	++	2,3	++	1,5	++	1,1
	Solute Carrier/Ion channels												
Hs.79172	Solute carrier family 25 (mitochondrial carrier; adenine nucleotide translocator), member 5	SLC25A5	xq24-q26	++	2961	++	-1,2	++	2	++	1,4	++	1,1
Hs.350927	solute carrier family 25 (mitochondrial carrier; adenine nucleotide translocator), member 6	SLC25A6	xp22.32 and yp	++	1768	++	-2,1	++	3,5	++	1,4	++	-1,2
Hs.111024	solute carrier family 25 (mitochondrial carrier; citrate transporter), member 1	SLC25A1	22q11.21	++	190	++	-2,5	++	1,9	++	-1,9	++	1,6
Hs.184877	solute carrier family 25 (mitochondrial carrier; oxoglutarate carrier), member 11	SLC25A11	17p13.3	++	520	++	-1,5	++	3	++	1,4	++	-1,1
Hs.439253	voltage-dependent anion channel 3	VDAC3	8p11.2	++	1396	++	1,1	++	2,3	++	1,6	++	-1,1
Hs.444376	Sodium- and chloride-activated ATP-sensitive potassium channel	SLICK	1q31.3	++	19	+	-3	++	4	+	-1,3	+	1,1
	Membrane Receptors/Proteins												
Hs.352642	Fc fragment of IgG, low affinity IIa, receptor for (CD32)	FCGR2A	1q23	++	285	++	-1,5	++	1,5	++	-2,1	++	1,4
Hs.408864	decay accelerating factor for complement (CD55, Cromer blood group system)	DAF	1q32	+	78	++	1,5	++	-1,6	++	2,3	++	-1,3
	HLA class I,II family												
Hs.181244	major histocompatibility complex, class I, A /// major histocompatibility complex, class I, C	HLA-A	6p21.3	++	6916	++	-1,3	++	2	++	1,1	++	1
Hs.77961	major histocompatibility complex, class I, B	HLA-B	6p21.3	++	7668	++	-1,1	++	2	++	1,2	++	-1,1
Hs.274485	major histocompatibility complex, class I, C /// major histocompatibility complex, class I, B	HLA-C	6p21.3	++	8347	++	-1,4	++	2,1	++	1,1	++	-1,1
Hs.381008	major histocompatibility complex, class I, E	HLA-E	6p21.3	++	2038	++	-1,4	++	2,1	++	1	++	1
Hs.1162	major histocompatibility complex, class II, DM beta	HLA-DMB	6p21.3	++	250	++	-1,2	++	1,9	++	-1,1	++	1,7
Hs.914	major histocompatibility complex, class II, DP alpha 1	HLA-DPA1	6p21.3	++	1010	++	-1,1	++	2,1	++	-1,3	++	1,3
Hs.368409	major histocompatibility complex, class II, DP beta 1	HLA-DPB1	6p21.3	++	540	++	-1,9	++	3	++	-1,9	++	1,2
Hs.387679	major histocompatibility complex, class II, DQ alpha 1	HLA-DQA1	6p21.3	+	67	++	-1,7	++	1,3	++	-3,7	++	2,6
Hs.409805	major histocompatibility complex, class II, DR alpha	HLA-DRA	6p21.3	++	1322	++	-1,4	++	1,1	++	-2,3	++	2,8
	Membrane Receptors/Proteins												
	GPI anchors/Pentaspans												
Hs.519624	CD14 antigen	CD14	5q31.1	++	1174	++	-3,5	++	3,5	++	-2,8	++	1,1
Hs.408864	decay accelerating factor for complement (CD55)	DAF	1q32	+	78	++	1,5	++	-1,6	++	2,3	++	-1,3
Hs.446414	CD47 antigen (Rh-related antigen, integrin-associated signal transducer)	CD47	3q13.1-q13.2	++	1010	++	-1,1	++	-1,1	++	-1,1	++	1,9
	Integrins/Complement Receptors												
Hs.172631	integrin, alpha M (complement receptor 3, alpha) CD11b	ITGAM	16p11.2	++	2204	++	-1,1	++	1,9	++	-1,6	++	2,3
	Fcg-Receptors												
Hs.534325	Fc fragment of IgG, high affinity Ia, receptor for (CD64)	FCGR1A	1q21.2-q21.3	++	208	++	-1,3	++	1	++	-3,7	++	4
Hs.126384	Fc fragment of IgG, low affinity IIa, receptor for (CD32)	FCGR2B	1q23	++	285	++	-1,5	++	1,5	++	-2,1	++	1,4
Hs.372679	Fc fragment of IgG, low affinity IIIa, receptor for (CD16)	FCGR3B/3A	1q23	++	131	++	-2,5	++	2	++	-3	++	1,9
	Scavenger Receptors												
Hs.443120	CD36 antigen (collagen type I receptor, thrombospondin receptor)	CD36	7q11.2	++	2864	++	2,3	++	-1,4	++	1,6	++	1,6
Hs.74076	CD163 antigen (scavenger receptor cysteine rich)	CD163	12p13.3	++	1354	++	-1,7	++	2,1	++	-2,8	++	2,1
Hs.162757	Low density lipoprotein-related protein 1 (alpha-2-macroglobulin receptor)	LRP1	12q13-q14	++	177	++	-1,5	++	2,6	++	-1,2	++	1,3
	Proteins involved in Glycosphingolipid Processing												
Hs.406455	prosaposin	PSAP	10q21-q22	++	4280	++	1,1	++	1,9	++	1,5	++	-1,2
Hs.387156	GM2 ganglioside activator	GM2A	5q31.3-q33.1	++	1065	++	1,1	++	1,9	++	1,5	++	1,1
Hs.381256	glycolipid transfer protein	GLTP	12q24.12	+	90	+	4	+	-3	+	2	++	2,6
	ABCA1and related Proteins												
Hs.147259	ATP-binding cassette, sub-family A (ABC1), member 1	ABCA1	9q31.1	++	130	++	2	++	-1,4	++	2	++	-1,2
Hs.355832	cell division cycle 42 (GTP binding protein, 25kDa)	CDC42	1p36.1	+	436	+	1,7	++	-1,1	++	1	++	2,5
Hs.134514	ATP-binding cassette, sub-family A (ABC1), member 7	ABCA7	19p13.3	++	67	++	-2,5	++	3,5	+	-1,5	+	-1,1
Hs.369055	ATP-binding cassette, sub-family G (WHITE), member 1	ABCG1	21q22.3	++	95	++	1,5	+	-1,2	++	2,5	++	-1,4
	Lipid Transfer Proteins and Apolipoproteins												
Hs.439312	phospholipid transfer protein	PLTP	20q12-q13.1	-	4	++	-1,4	++	1,1	++	-3	++	1,5
Hs.268571	apolipoprotein C-I	APOC1	19q13.2	+	47	++	1,1	++	2,5	++	1,6	++	-1,1
Hs.75615	apolipoprotein C-II	APOC2	19q13.2	+	109	+	-3,2	++	3,5	+	-4	+	1,3
Hs.491896	apolipoprotein C-IV	APOC4	19q13.2	++	268	++	-1,3	++	2,3	++	1,7	++	-1,1
Hs.110675	apolipoprotein E	APOE	19q13.2	++	200	++	-1,1	++	1,7	++	1,3	++	1,4
	Vesicular trafficking												
Hs.448580	SEC6-like 1 (S. cerevisiae)	SEC6L1	5p15.33	+	99	+	-1,7	++	**4,3**	++	1,7	++	**-2,3**
Hs.325530	exocyst complex component 7	EXOC7	17q25.1	++	221	++	-1,3	++	**2,1**	++	1,4	++	-1,1

Table 10: Raft proteins, membrane receptors/proteins, proteins for GSL degradation and ABCA1 and related proteins on U133 A

2.7. Analysis of gene expression, protein and surface expression of membrane receptors during E-LDL and Ox-LDL loading and HDL_3 deloading

In order to further elucidate the possible functions of the differential raft microdomain formations through E-LDL and Ox-LDL, the expression of membrane receptors and their downstream signaling elements were analyzed by Affymetrix chips (table 10). According to Pfeiffer et al., binding of Cer, that is present at the surface of atherogenic lipoproteins or apoptotic cells, induces a receptor cluster including the LPS receptor CD14, complement receptor 3 constituents CD11b/CD18, the Fcγ-receptors CD64, CD32 and CD16, scavenger receptor B CD36, integrin associated protein CD47 and decay acceleration factor CD55. Formation of this cluster leads to ligand dependent activation of downstream signaling pathways related to the receptor composition. In order to find out differential regulation of membrane receptors during E-LDL and Ox-LDL loading and HDL_3 deloading we focused on this known receptor cluster and also on the lipoprotein receptor CD91/LRP1 and the scavenger receptor cystein rich CD163.

In addition to Microarray analysis, surface and protein expression analysis of these receptors was performed by flow cytometry and Western Blot respectively. E-LDL and Ox-LDL loaded and HDL_3 deloaded human monocyte derived macrophages were analyzed.

E-LDL and Ox-LDL loading

In the ***Fcγ-receptor family*** (Fig.34A) surface and protein expression of CD64/FcγRI showed almost no change during E-LDL loading while CD32/FcγRIIA was increased. CD16/FcγRIII surface expression during E-LDL loading was decreased, which is in accordance with gene array data indicating a -2,5 fold decrease of CD16/FcγRIII during E-LDL loading, but it is in contrast to the protein expression which showed an increase of CD16/FcγRIII. Ox-LDL loading led to a decrease of the surface expression of all three FcγRs (Fig.34A). This corresponds with the chip data which showed a 3.7 fold decrease of CD64, a 2,1 fold decrease of CD32 and a 3 fold decrease of CD16 during Ox-LDL loading. With western blot analysis a decrease of CD64, CD32 and CD16 could not be clearly confirmed.

The surface expression of ***scavenger receptor B (SR-B), CD36*** showed an increase during E-LDL and a stronger increase during Ox-LDL loading while ***CD91/LRP1*** and ***CD163/SR*** were inversely regulated with an increase during E-LDL and a decrease during Ox-LDL loading (Fig.34B). The gene array data confirmed these results with a 2.3 fold upregulation of CD36 during E-LDL and 1.6 fold upregulation during Ox-LDL loading. In the case of CD163 a decrease of -2,8 fold during Ox-LDL loading was observed. The protein expression of CD36 showed also an upregulation with lipid loading which is stronger in the case of Ox-LDL. The protein expression of CD163 is also consistent with the data obtained by flow cytometry and gene analysis.

Cell surface expression of the ***integrins*** respectively ***complement receptor 3 (CD11a, CD11b) and CD18*** was increased during E-LDL but decreased during Ox-LDL loading (Fig.34C). This indicates that E-LDL in contrast to Ox-LDL activates complement. In the case of CD11a and CD11b an increase during E-LDL but not during Ox-LDL loading could be confirmed with western blot analysis. The ***integrin associated protein, pentaspan CD47*** surface expression was increased during E-LDL loading but decreased during Ox-LDL loading while the ***decay acceleration factor CD55*** was increased during E-LDL and Ox-LDL loading which could be confirmed by Western Blot (Fig.34D). The surface expression of ***LPS receptor CD14*** was decreased during E-LDL and Ox-LDL loading (Fig.34D). This could also be shown with western blot analysis and in the gene array data this could be confirmed with a decrease of -3.5 fold during E-LDL and -2.8 fold during Ox-LDL loading.

HDL_3 deloading

HDL_3 deloading showed a decrease of surface and protein expressions of ***FcγRs CD64***, ***CD32*** and ***CD16*** compared to MCSF (Fig.34A).

SR-B, CD36 surface and protein expression was increased with HDL_3 deloading compared to MCSF (Fig.34B). ***CD91*** and ***CD163*** were decreased during lipid deloading which could be confirmed by western blot analysis in the case of CD163. While gene array analysis showed an increase of CD163 during HDL_3 deloading (Fig.34B). ***CD11a*** was decreased during E-LDL and Ox-LDL deloading while ***CD11b*** was increased during E-LDL and decreased during Ox-LDL deloading (Fig.34C). ***CD18*** was increased during E-LDL and Ox-LDL deloading (Fig.34C).

CD47 and ***CD55*** surface expression was increased with E-LDL deloading and decreased with Ox-LDL deloading (Fig.34D). The LPS receptor ***CD14*** was increased during E-LDL and Ox-LDL deloading (Fig.34D). The increase of CD14 during lipid deloading could be confirmed by western blot and gene array analysis which showed an increase of 3.5 fold during E-LDL and 1.1 fold during Ox-LDL deloading.

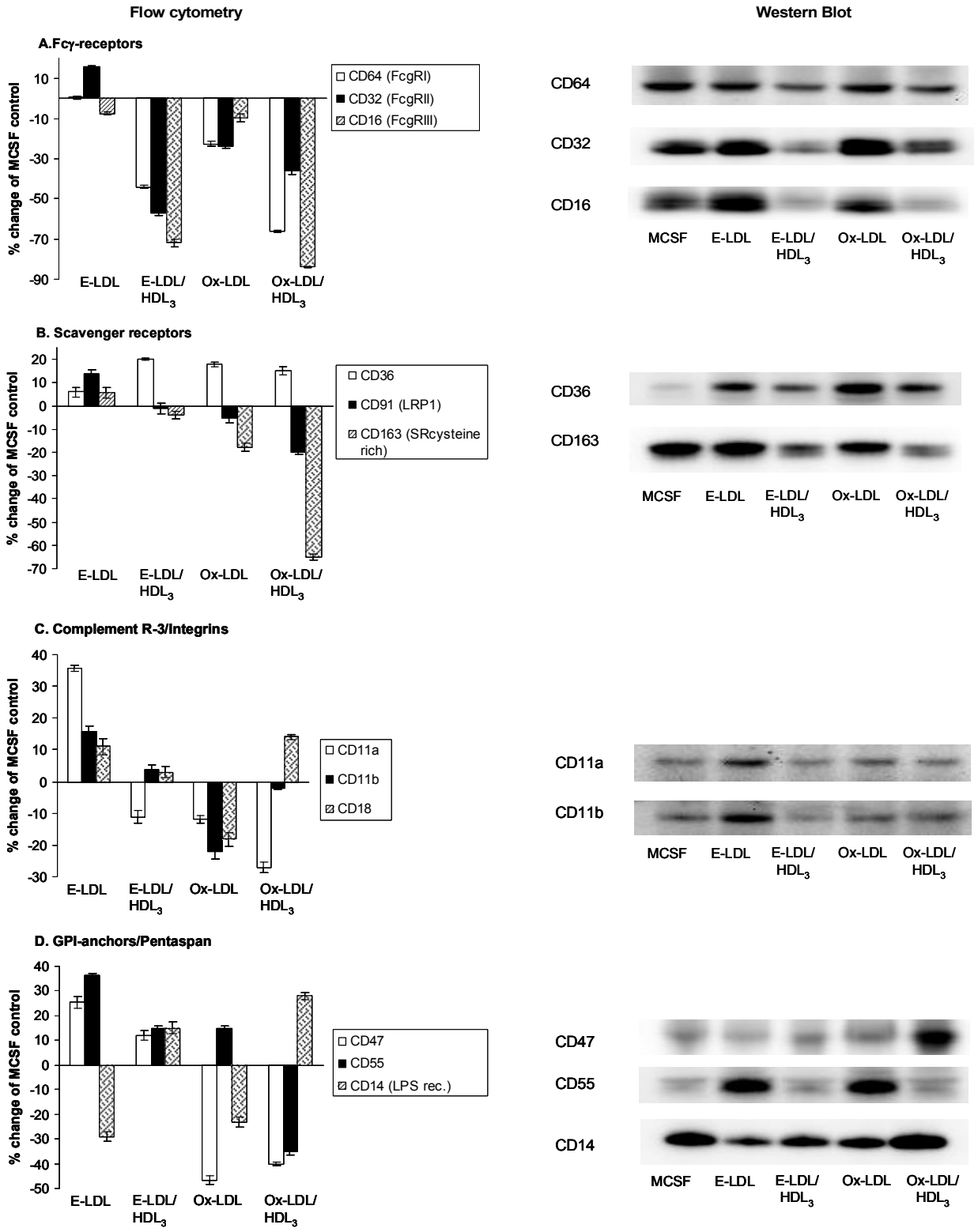

Figure 34: Flow cytometric and western blot analysis of membrane receptors
The surface expression of membrane receptors was analyzed by flow cytometry and the protein expression by western blot during E-LDL and Ox-LDL loading (48 h, day 4 to day 6) and HDL_3 deloading (24 h, day 6 to day 7) of macrophages. The mean fluorescence intensities of the receptor surface expressions were calculated in % of the mean fluorescence intensities of MCSF differentiated macrophages as a control. CD64/FcγRI, CD32/FcγRII, CD16/FcγRIII (A), CD36/SRBII, CD91/LRP1, CD163/Srcysteine rich (B), CD11a, CD11b, CD18 (C), CD47, CD55, CD14 (D)

2.8. Raft association of FcγRIIA /CD32

In a next step it should be analyzed if the different lipid loading agents E-LDL and Ox-LDL or HDL_3 deloading had influences on the raft association of FcγRIIA/CD32. This is in accordance with Shakor who published that cell surface Cer generation precedes and controls CD32 clustering in rafts (302). In our case Ox-LDL leads to a higher expression level of Cer which could influence CD32 raft association. Therefore lubrol-raft fractions respectively non raft fractions were isolated from membrane preparations of cells from the different incubation states and the protein expression of FcγRIIA/CD32 was analyzed in these fractions. Cells loaded with E-LDL showed a higher raft association of FcγRIIA/CD32 compared to MCSF differentiated macrophages and a lower raft association than Ox-LDL loaded cells (Fig.35). This raft association was partially reversed by HDL_3 deloading of the cells (Fig.35).

This result is reflecting a different receptor clustering associated with diverse raft formations during E-LDL and Ox-LDL loading and could lead to unequal signaling pathways activated by the different lipoproteins.

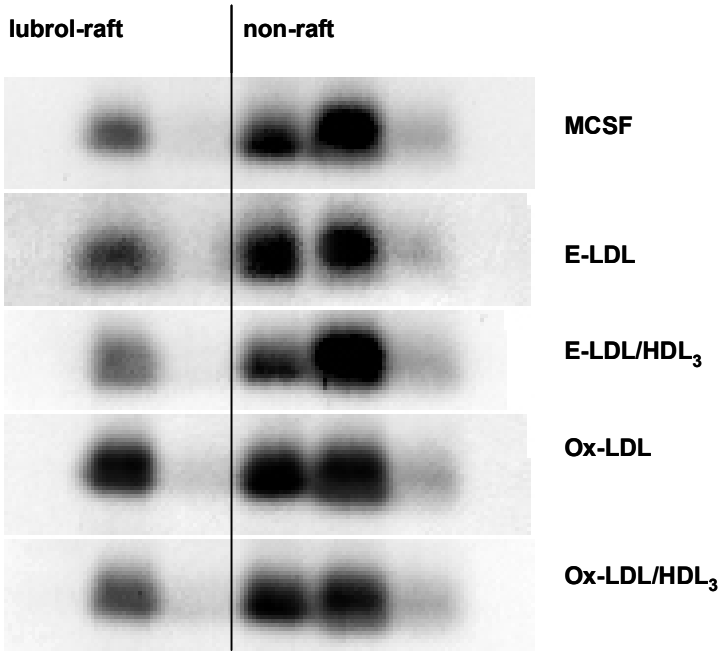

Figure 35: Raft association of FcγRIIA/CD32

2.9. Analysis of proteins involved in cholesterol metabolism

2.9.1. Gene expression analysis

The analysis of genes involved in cholesterol metabolism by Microarray analysis during E-LDL and Ox-LDL loading and also during HDL_3 deloading of macrophages revealed regulatory principles of the cholesterol metabolism during foam cell formation with the two different lipid loading agents E-LDL and Ox-LDL and cholesterol efflux with HDL_3 (table 10).

The LDL-receptor (LDLR), responsible for the binding and subsequent cellular uptake of apoB/E-containing lipoproteins plays a crucial role in cellular cholesterol homeostasis. The LDL-receptor is internalized via “clathrin coated pits” and following internalization of the LDL particles takes place. Cholesterol which is released into the cytoplasm suppresses cell surface expression of LDL receptors. This regulation corresponds with our chip data, which showed a -8.6 fold downregulation of the LDL receptor during E-LDL loading and a -4 fold downrgulation during Ox-LDL loading. During E-LDL deloading an upregulation of 3.2 fold and during Ox-LDL deloading an upregulation of 1.4 fold could be observed. The ABCA1 transporter responsible for cholesterol efflux was 2-fold upregulated during lipid loading indicating an enhanced amount of ABCA1 resulting in more effective cholesterol efflux due to an increase of cellular cholesterol.

2.9.2. Analysis of ABCA1

2.9.2.1. mRNA expression of ABCA1

The mRNA expression of ABCA1 determined with Taqman RT-PCR showed only a slight increase during E-LDL loading while upon Ox-LDL loading the mRNA expression was significantly induced. With HDL_3 deloading a reduction of ABCA1 mRNA expression took place (Fig.36). The gene array data reflect these findings partly with a 2 fold increase of ABCA1 gene expression during E-LDL and Ox-LDL loading and a decrease (-1.4 and -1.2 fold) during HDL_3 deloading (table 2).

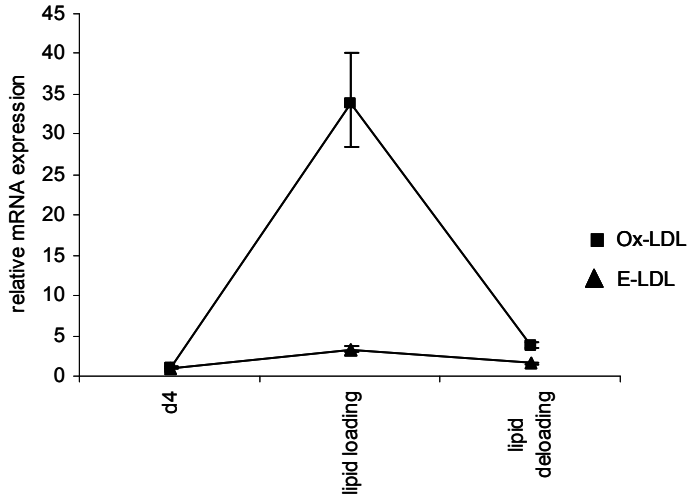

Figure 36: mRNA expression of ABCA1

2.9.2.2. Protein expression of ABCA1

Protein expression analysis of ABCA1 by Western Blot was performed to verify the Affymetrix gene array data with an additional method. Macrophages loaded with E-LDL and Ox-LDL showed in accordance with the gene array data an induction of ABCA1 total protein

expression compared to MCSF differentiated cells while the increase during Ox-LDL loading was stronger than the increase during E-LDL loading (Fig.37). This is in accordance to the mRNA expression of ABCA1 (Fig.36). The induction of ABCA1 protein expression was partially reversed during E-LDL deloading with HDL_3 and there was a stronger reduction of ABCA1 protein expression during Ox-LDL deloading with HDL_3 (Fig.37).

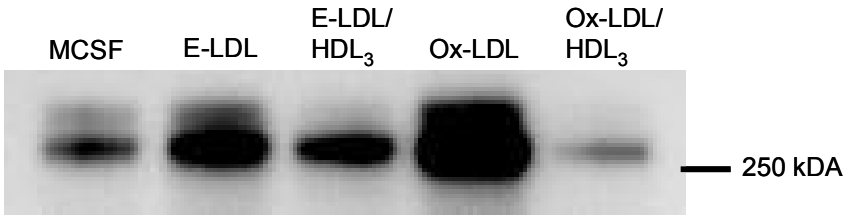

Figure 37: Protein expression of ABCA1

2.9.2.3. Analysis of membrane raft association of ABCA1

In a next step it should be analyzed whether the different lipid loading agents E-LDL and Ox-LDL or HDL_3 deloading have influences on the raft association of ABCA1. Therefore raft fractions respectively non raft fractions were isolated from membrane preparations of cells from the different incubation states and the protein expressions of ABCA1 in these fractions were analyzed.

During MCSF differentiation no raft association of ABCA1 could be detected while during E-LDL and Ox-LDL loading a slight raft association could be observed (Fig.38). Also during E-LDL and Ox-LDL deloading with HDL_3 a slight raft association was detectable. However the strongest raft association could be observed during Ox-LDL deloading (Fig.38).

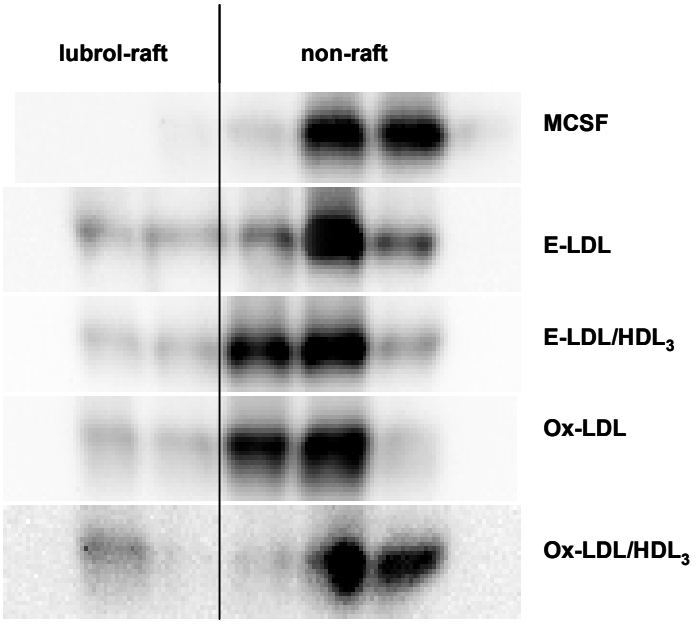

Figure 38: Raft association of ABCA1

2.9.3. Analysis of apoE

2.9.3.1. Protein expression of apoE

Total protein expression of apoE was analyzed with western-blot. Protein expression of apoE was only slightly induced during E-LDL and Ox-LDL loading compared to MCSF differentiated macrophages (Fig.39). Deloading with HDL_3 after E-LDL loading led to a stronger upregulation of apoE protein expression than after Ox-LDL loading compared to lipid loading (Fig.39).

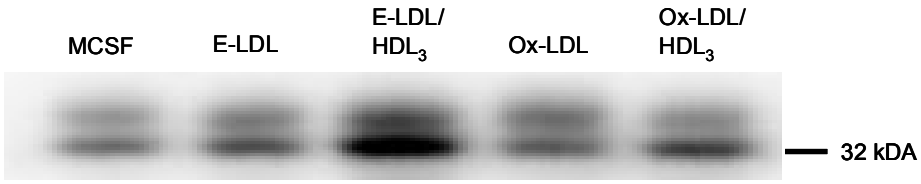

Figure 39: Protein expression of apoE

2.9.3.2. Extracellular (surface) and intracellular expression of apoE

Extracellular (surface) and intracellular expression of apoE was measured by flow cytometry of MCSF differentiated, E-LDL and Ox-LDL loaded and HDL_3 deloaded macrophages. In the differentiation phase with MCSF from day 1 to day 4 apoE surface expression was increased. From day 4 to day 6 no change and from day 6 to day 7 a further increase of apoE surface expression could be detected (Fig.40A). During lipid loading apoE surface expression increased with a stronger induction during E-LDL than during Ox-LDL loading (Fig.40A). This is in accordance with the protein expression of apoE (Fig.40). During HDL_3 deloading apoE surface expression was decreased compared to lipid loading (Fig.40A). Intracellular expression of apoE was increased during differentiation with MCSF from day 1 to day 6 and was decreased from day 6 to day 7. During E-LDL loading a slight increase and during Ox-LDL loading a decrease of apoE intracellular expression could be observed compared to MCSF differentiation (Fig.40B). HDL_3 deloading decreased intracellular apoE expression compared to lipid loading (Fig.40B).

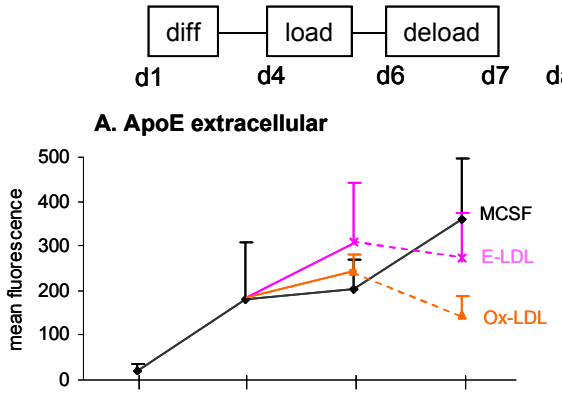

Figure 40A: ApoE surface expression analyzed by flow cytometry

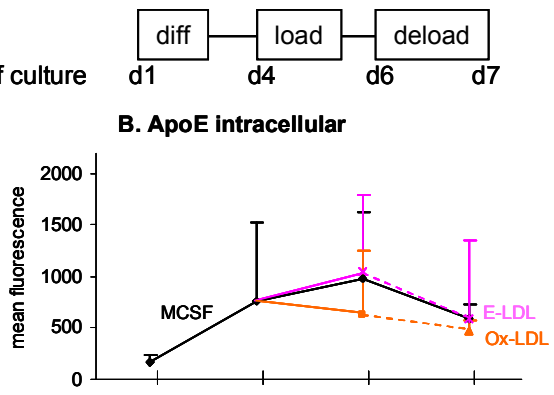

Figure 40B: ApoE intracellular expression analyzed by flow cytometry

2.9.4. Analysis of apoC-I

2.9.4.1. Protein expression of apoC-I

Protein expression of apoC-I was analyzed with western-blot. Protein expression of apoC-I was slightly reduced during E-LDL while it was induced during Ox-LDL loading compared to MCSF differentiated macrophages (Fig.41). E-LDL and especially Ox-LDL deloading with HDL_3 led to a stronger upregulation of apoC-I protein expression compared to lipid loading which is probably due to apoC-I as a constituent of HDL_3 (Fig.41).

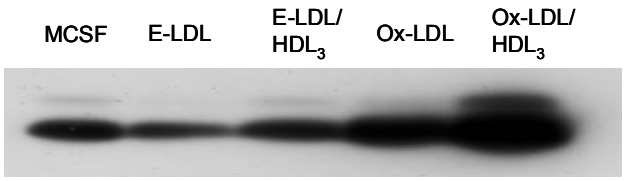

Figure 41: Protein expression of apoC-I

2.9.4.2. Extracellular (surface) and intracellular expression of apoC-I

Extracellular (surface) and intracellular expression of apoC-I was measured by flow cytometry of MCSF differentiated, E-LDL and Ox-LDL loaded and HDL_3 deloaded macrophages. ApoC-I surface and intracellular expression was increased during differentiation with MCSF from day 1 to day 4, was slightly decreased from day 4 to day 6 and was increased from day 6 to day 7 (Fig.42A). ApoC-I intracellular expression was much higher compared to extracellular expression, which is obvious from the higher mean fluorescence intensity. During E-LDL loading apoC-I surface expression was only slightly increased while during Ox-LDL loading it was strongly increased compared to MCSF (Fig.42A). E-LDL deloading with HDL_3 increased and Ox-LDL deloading slightly decreased apoC-I surface expression compared to lipid loading (Fig.42A).

Intracellular expression of apoC-I increased during lipid loading to a higher extent with Ox-LDL than with E-LDL loading compared to MCSF differentiated macrophages (Fig.42B). During Ox-LDL deloading with HDL_3 a slight decrease of apoC-I intracellular expression was observed while there was no change during E-LDL deloading compared to lipid loaded cells (Fig.42B).

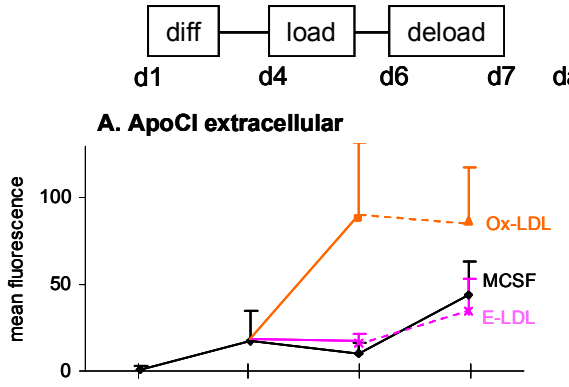

Figure 42A: ApoC-I surface expression analyzed by flow cytometry

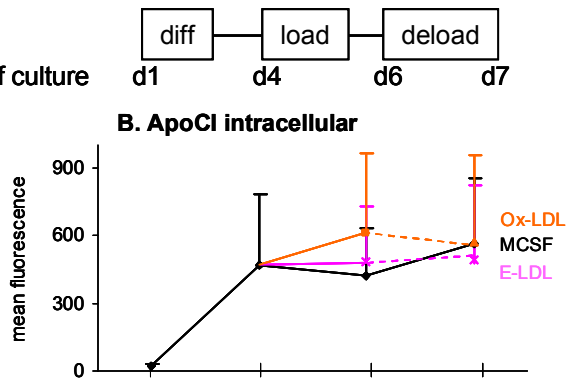

Figure 42B: ApoC-I intracellular expression analyzed by flow cytometry

2.9.5. Analysis of CETP

2.9.5.1. Extracellular (surface) and intracellular expression of cholesteryl ester transfer protein (CETP)

Extracellular (surface) and intracellular expression of CETP was measured by flow cytometry of MCSF differentiated, E-LDL and Ox-LDL loaded and HDL_3 deloaded macrophages. During differentiation with MCSF from day 1 to day 7 CETP surface expression was increased (Fig.43A). During lipid loading CETP surface expression was increased with E-LDL loading while it was decreased with Ox-LDL loading compared to MCSF (Fig.43A). During E-LDL deloading with HDL_3 CETP surface expression was slightly increased while during Ox-LDL deloading it was slightly decreased compared to lipid loading (Fig.43A).

Intracellular expression of CETP increased during differentiation with MCSF from day 1 to day 6 while no further change was observed from day 6 to day 7 (Fig.43B). During lipid loading intracellular expression of CETP was decreased compared to MCSF with a stronger decrease during Ox-LDL than during E-LDL loading (Fig.43B). HDL_3 deloading of E-LDL loaded cells increased while deloading of Ox-LDL loaded cells slightly decreased intracellular CETP expression compared to lipid loading (Fig.43B).

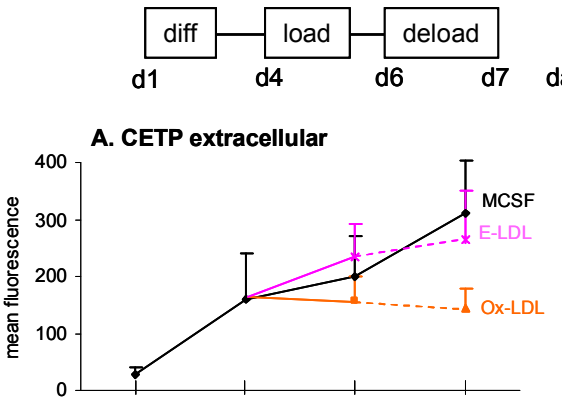

Figure 43A: CETP surface expression analyzed by flow cytometry

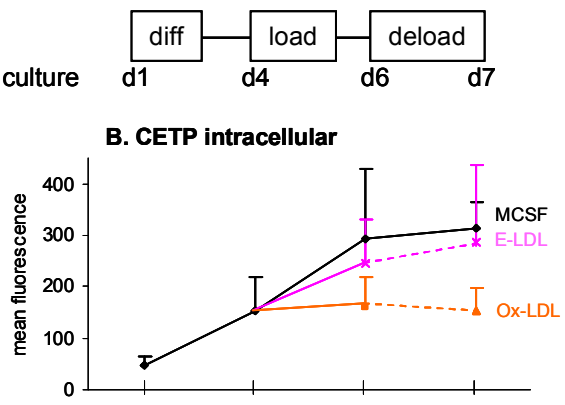

Figure 43B: CETP surface expression analyzed by flow cytometry

2.9.6. Analysis of PLTP

2.9.6.1. Protein expression of PLTP

Total protein expression of PLTP was analyzed with western-blot. Protein expression of PLTP was increased during E-LDL and Ox-LDL loading compared to MCSF differentiated macrophages (Fig.44). E-LDL deloading with HDL_3 led to an increase of PLTP protein expression while Ox-LDL deloading led to a decrease of PLTP protein expression compared

to lipid loading (Fig.44). Western Blot shows the two forms of PLTP with the molecular masses of 67kDa and 77kDa as described by Huuskonen et al. (388).

Figure 44: Protein expression of PLTP

2.9.7. Analysis of ATP-synthase (β-chain)

2.9.7.1. Protein expression of ATP-synthase (β-chain)

Total protein expression of ATP-synthase (β-chain) was analyzed with western-blot. Lipid loading with E-LDL and Ox-LDL revealed no change of ATP-synthase protein expression compared to MCSF (Fig.45). HDL_3 deloading after E-LDL loading led to a slight increase of ATP-synthase protein expression compared to lipid loading (Fig.45).

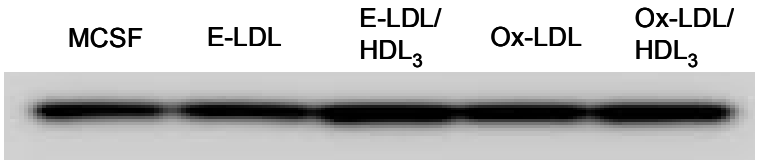

Figure 45: Protein expression of ATP-synthase (β-chain)

3. Incubation of ApoE3/3 macrophages with LDL, E-LDL and Ox-LDL alone and as opsonized complexes with Amyloidβ_{42}

3.1. Cell surface expression of sphingo- and glycosphingolipids

In these experiments it should be analyzed if incubation of macrophages with Amyloid β_{42} complexes (16μg/ml) of LDL, E-LDL and Ox-LDL (opsonized lipoproteins) compared to incubation of lipoproteins without Amyloid β_{42} have different effects on the surface expression of Cer and the GSLs LacCer (CDw17), Gb_3Cer (CD77), dodecasaccharideceramide (CD65s) and GM1 ganglioside. Therefore 4 day differentiated macrophages were treated with 40μg/ml LDL, E-LDL and Ox-LDL, respectively with the LDL/ßA_{42}, E-LDL/ßA_{42} and Ox-LDL/ßA_{42} complexes for 16h. The incubation protocol was established by our institute previously. Four different experiments were performed and means and standard deviations of the mean fluorescence intensities were calculated. Significance was tested by student's t-test and the asterisk indicates significance with $p<0.05$.

LDL loading of macrophages compared to MCSF differentiation slightly increased LacCer and CD65s surface expression (Fig.46B,D) while Cer, Gb_3Cer and GM1 surface expression was not affected by LDL loading (Fig.46A,C,E). Loading with the LDL/βA_{42} complex increased LacCer, Gb_3Cer and GM1 surface expression (Fig.46B,C,E) and decreased Cer and CD65s surface expression (Fig.46A,D) compared to LDL loading without βA_{42}. But none of these results reached statistical significance.

During E-LDL loading LacCer, Gb_3Cer and CD65s surface expression was clearly increased compared to MCSF (Fig.46B,C,D) whereas surface expression of Cer and GM1 was only slightly increased (Fig.46A, E). Loading the macrophages with the E-LDL/βA_{42} complex a significant increase of Cer, LacCer, Gb_3Cer and GM1surface expression could be observed compared with the non-opsonized E-LDL alone (Fig.46A,B,D,E). In contrast to this CD65s surface expression showed a slight decrease during loading with the E-LDL/βA_{42} complex compared with E-LDL (Fig.46D).

During Ox-LDL loading only slight changes could be observed compared to MCSF due to the small concentration of Ox-LDL (40μg/ml) used in these experiments. A small decrease of Cer (Fig.46A) and a small increase of GM1 surface expression (Fig.46E) could be detected while there was no change of LacCer, Gb_3Cer and CD65s surface expression (Fig.46B,C,D). Loading with the Ox-LDL/βA_{42} complex revealed a small increase of Cer, LacCer and GM1 surface expression (Fig.46A,B,E) while CD65s and Gb_3Cer surface expression was decreased (Fig.46C,D). But none of these results reached statistical significance.

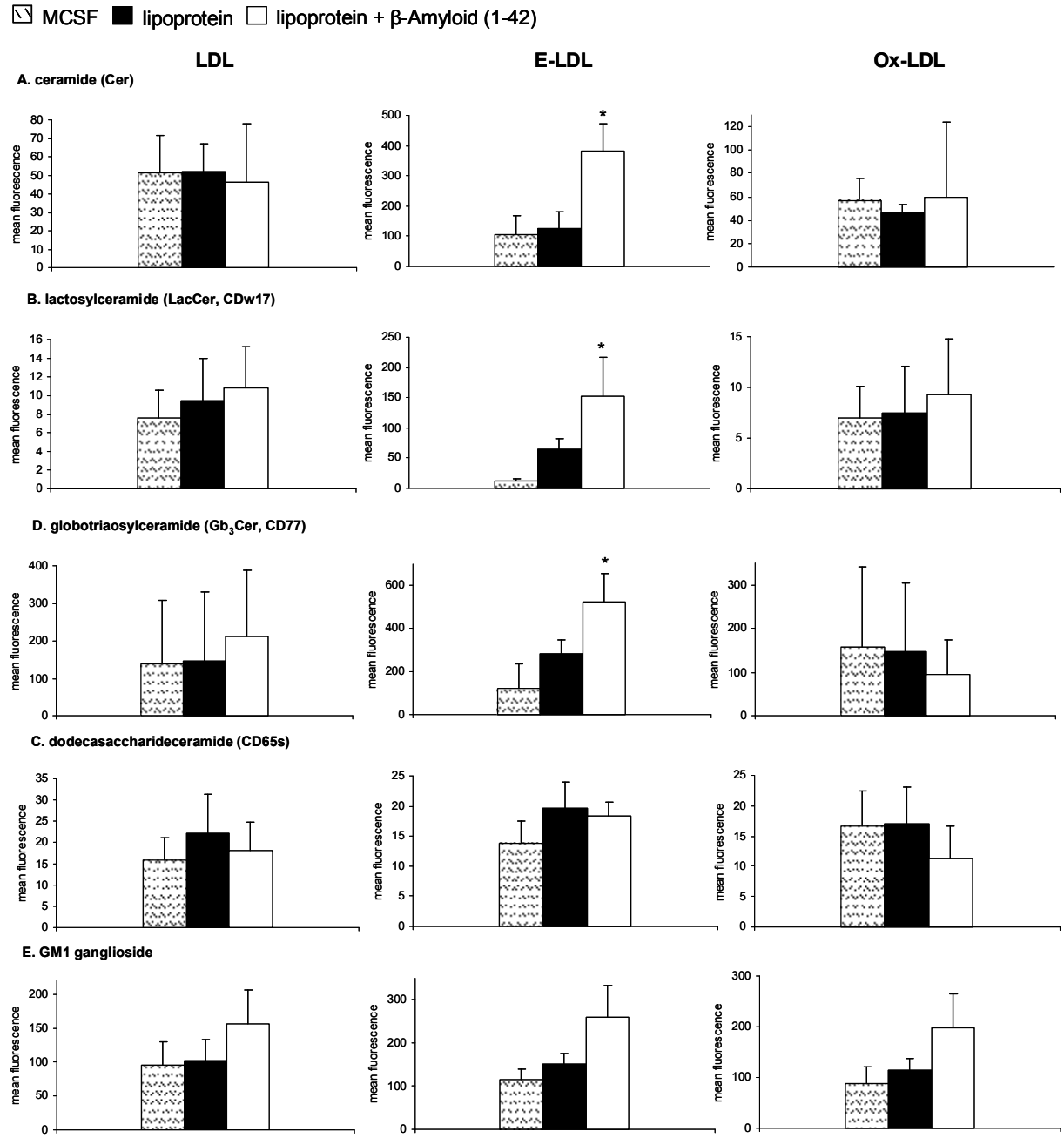

Figure 46: Determination of the surface expression of ceramide (A), lactosylceramide (CDw17) (B), dodecasaccharideceramide (CD65s), globotriaosylceramide (Gb_3Cer, CD77) (D) and GM1 ganglioside (C) by flow cytometry of macrophages incubated for 16h with LDL, E-LDL and Ox-LDL alone (black columns), with the lipoprotein-Amyloid β_{42} complex (white columns) or with MCSF as a control (columns with stripes).

3.2. Binding of DiI-LDL, DiI-E-LDL and DiI-LDL/Aβ$_{42}$, DiI-E-LDL/Aβ$_{42}$ complexes to monocyte subpopulations

The highest binding of DiI–LDL, DiI-E-LDL and their complexes with Amyloid β$_{42}$ could be observed on the CD14 high CD16 high monocyte subset (MNP2) (Fig.47A,B). Moreover Aβ$_{42}$-complexed LDL and E-LDL bound more efficiently to all subpopulations than the non-opsonized lipoproteins. Further E-LDL and the Aβ$_{42}$ complexed E-LDL bind to a higher extent to all subpopulations than LDL and the LDL complex with Aβ$_{42}$.

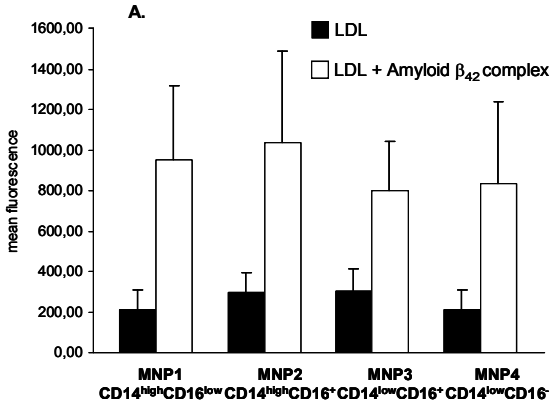

Figure 47A: Binding of DiI-LDL (black columns) and DiI-LDL/Aβ42 (white columns) to monocyte subpopulations as determined by flow cytometry.

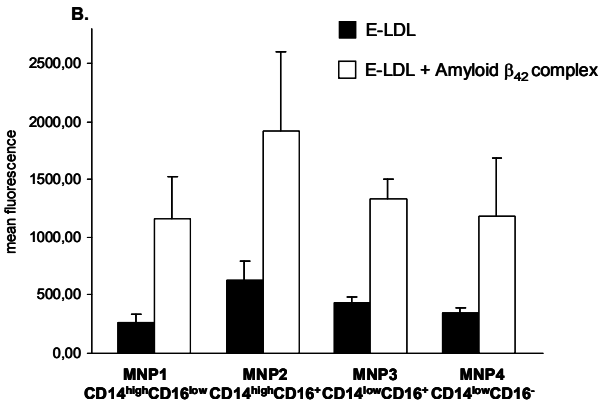

Figure 47B: Binding of DiI-E-LDL (black columns) and DiI-E-LDL/Aβ42 (white columns) to monocyte subpopulations as determined by flow cytometry.

4. Incubation of apoE3/3 macrophages during differentiation, E-LDL loading and HDL$_3$ deloading with the proteasomal inhibitor ALLN

In order to find out differences of the proteasomal degradation of apoE and CETP between the two genotypes apoE3/3 and apoE4/4, macrophages of the two genotypes should be treated with proteasomal inhibitors. Subsequently surface and intracellular expression of apoE and CETP should be analyzed by flow cytometry. Because of the interesting findings of different raft formations during E-LDL and Ox-LDL loading, there was only time to perform these experiments with apoE3/3 but not apoE4/4 macrophages.

Elutriated apoE3/3 monocytes were incubated after 1 day resting in serum free medium with 50μM of the proteasomal inhibitor ALLN respectively the solvent DMSO and MCSF as a control. On the fourth day of MCSF differentiation and ALLN treatment, macrophages were loaded with E-LDL (40μg/ml) and on day 6, E-LDL loaded cells were deloaded with HDL$_3$ (100μg/ml). Extracellular (surface) and intracellular expression of apoE and CETP was measured by flow cytometry during MCSF differentiation on days 4, 6 and 7 as well as after E-LDL loading on day 6 and after HDL$_3$ deloading on day 7. Three different experiments were performed and the means of mean fluorescence intensities of incubation with ALLN and the solvent DMSO were calculated in % change of MCSF, E-LDL, HDL$_3$ respectively as a control and results were shown for apoE in Fig.48 and for CETP in Fig.49.

4.1. Extracellular (surface) and intracellular expression of apoE

During all states of incubation ALLN treated cells had a higher surface expression of apoE compared to DMSO as a control. On days 4, 6 and 7 of MCSF differentiation surface expression of apoE was induced during incubation of ALLN compared to DMSO. During E-LDL loading and HDL_3 deloading apoE surface expression of cells treated with ALLN was reduced compared to MCSF differentiation. The difference between ALLN treatment and DMSO was greater during HDL_3 deloading than during E-LDL loading (Fig.48A).

ApoE intracellular expression of ALLN treated cells on day 4 of differentiation was stronger reduced than the expression of DMSO treated cells compared to MCSF. On day 6 of MCSF differentiation and on day 6 of E-LDL loading apoE intracellular expression was increased with ALLN treatment compared to DMSO treated cells (Fig.48B). On day 7 of differentiation almost no difference could be observed between ALLN and DMSO treated macrophages while during HDL_3 deloading apoE intracellular expression was stronger increased with ALLN treatment than with DMSO (Fig.48B).

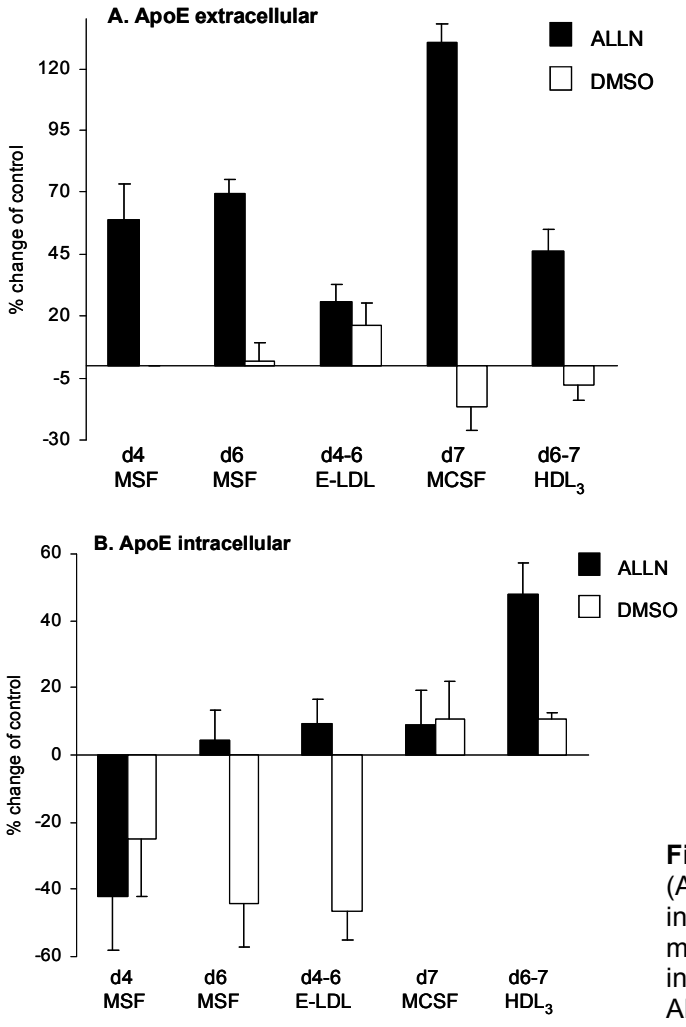

Figure 48: Extracellular (surface) expression (A) and intracellular expression (B) of apoE in % change of control (MCSF, E-LDL, HDL_3) measured by flow cytometry during incubation with the proteasomal inhibitor ALLN respectively DMSO as a solvent.

4.2. Extracellular (surface) and intracellular expression of CETP

Surface and intracellular expression of CETP of macrophages treated with the proteasomal inhibitor ALLN and DMSO as a solvent was similar to the expression profile obtained with apoE. Surface expression of CETP was during all incubation states (day 4, 6 and 7 differentiation, day 6 E-LDL loading and d7 HDL_3 deloading) increased in ALLN compared to DMSO treated macrophages. On day 7 of differentiation the strongest increase could be observed (Fig.49A).

Intracellular expression of CETP on the fourth day of differentiation was stronger decreased in DMSO treated cells than in cells incubated with ALLN compared to MCSF. On day 6 and day 7 of MCSF differentiated and on day 6 of E-LDL loaded cells CETP intracellular expression was increased with ALLN treatment compared to DMSO treated cells which showed a decrease. During HDL_3 deloading cells incubated with DMSO showed a stronger decrease than ALLN treated cells compared to MCSF (Fig.49B).

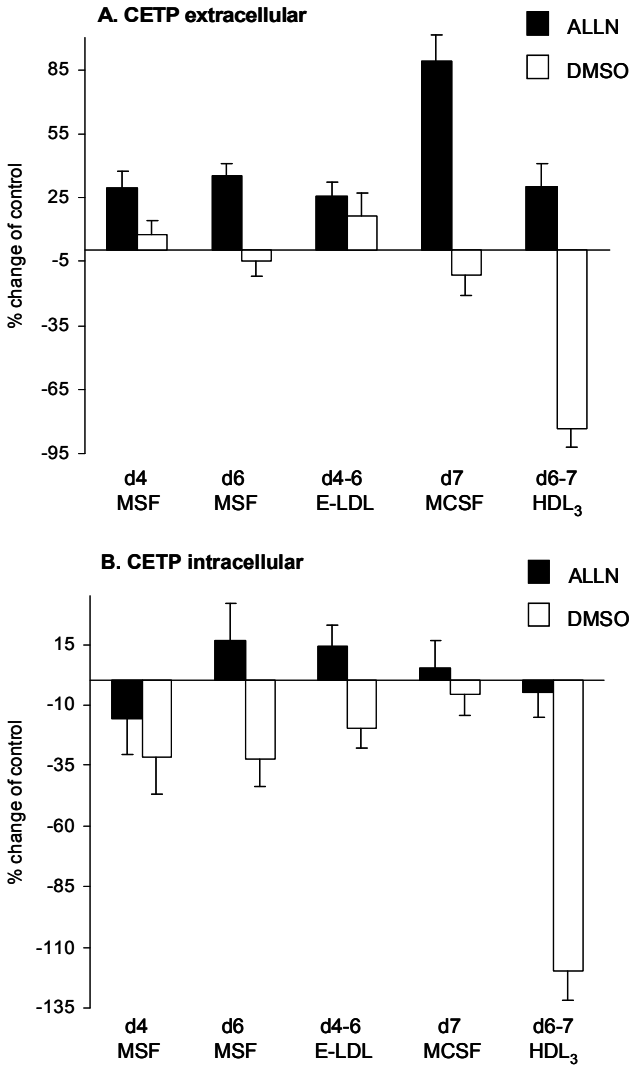

Figure 49: Extracellular (surface) expression (A) and intracellular expression (B) of CETP in % change of control (MCSF, E-LDL, HDL_3) measured by flow cytometry during incubation with the proteasomal inhibitor ALLN respectively DMSO as a solvent.

5. Analysis of MCSF differentiated, E-LDL and Ox-LDL loaded and HDL_3 deloaded human monocyte derived macrophages of the ApoE3/3 vs. the ApoE4/4 genotype

5.1. Analysis of the cellular lipid content with mass spectrometry

ESI-mass spectrometry was used to analyze cellular content of total, esterified and unesterified cholesterol (Fig.50); sphingomyelin (SM), ceramide (Cer) and sphingosine (Fig.51); phosphatidylethanolamine (PE), phosphatidylserine (PS), phosphatidylcholine (PC) and lysophosphatidylcholine (LPC) (Fig.52). MCSF differentiated, E-LDL and Ox-LDL loaded and HDL_3 deloaded macrophages of the apoE3/3 and the apoE4/4 genotype were analyzed. Four independent experiments of each genotype were performed and the results were compared between the apoE3 and the apoE4 genotype.

5.1.1. Analysis of total, esterified and unesterified cholesterol

The description is focused only on the differences between apoE3/3 and apoE4/4 macrophages because the results of apopE3/3 macrophages were described in detail earlier (s. 3.1.). The amount of total and unesterified cholesterol during Ox-LDL loading and deloading was lower in apoE4/4 compared with apoE3/3 macrophages (Fig.50A,B,E,F). During E-LDL loading and deloading the content of unesterified cholesterol was decreased in apoE4/4 macrophages (Fig.50A,B,E,F). The content of esterified cholesterol was the same in apoE3/3 and apoE4/4 macrophages during all incubation states (Fig.50C,D).

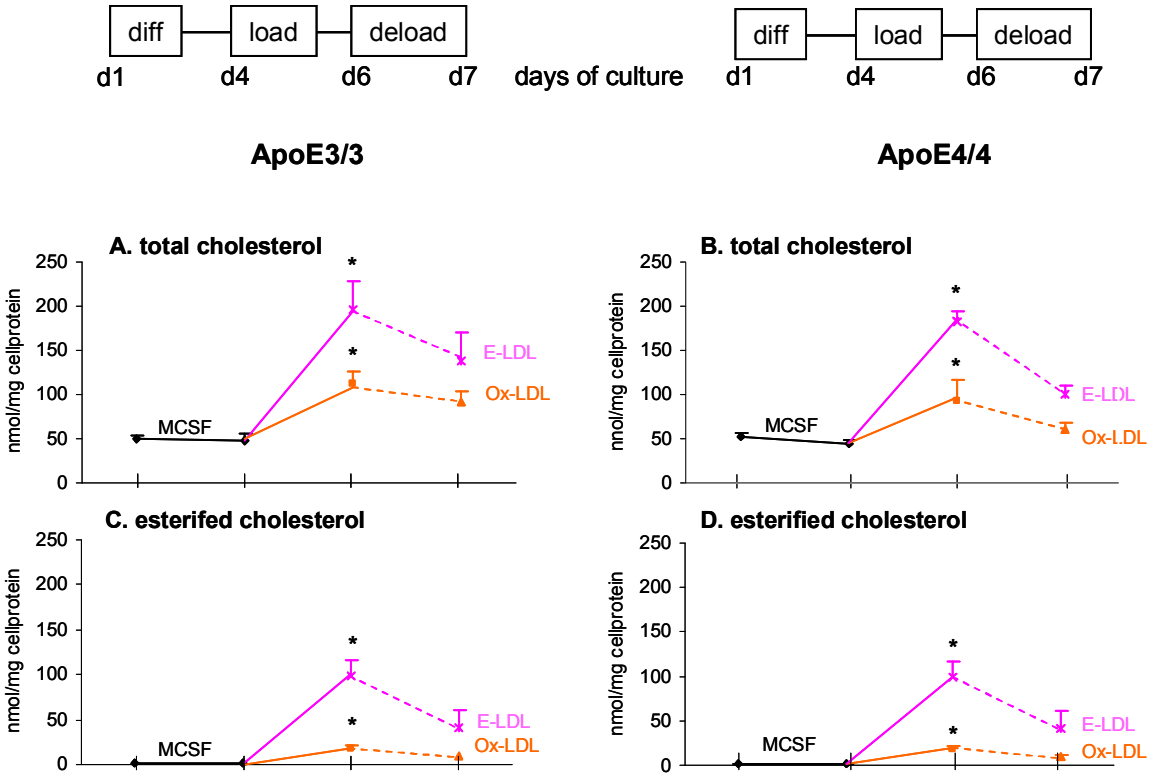

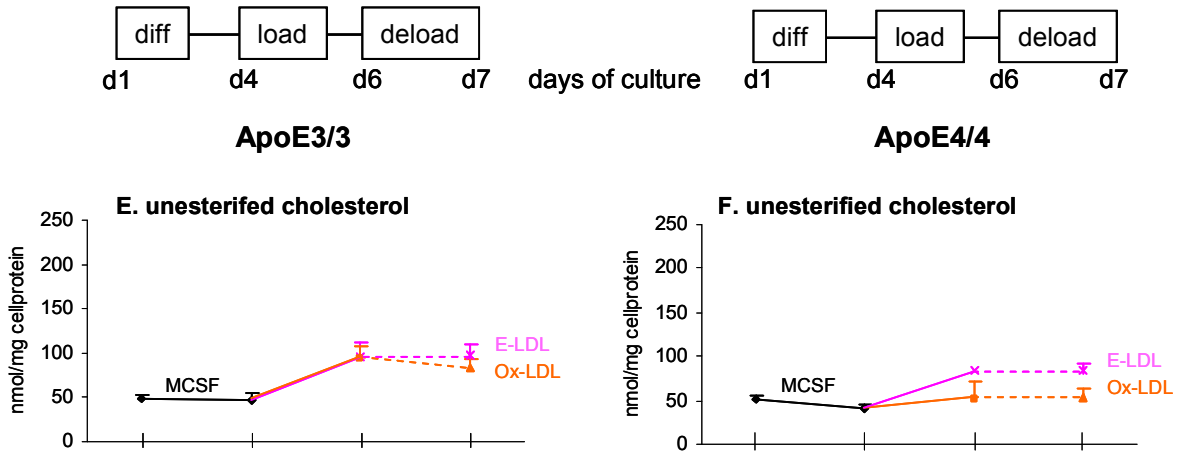

Figure 50: Cellular content of total cholesterol (A,B), esterified cholesterol (C,D) and unesterifed cholesterol (E,F) of apoE3/3 (left column) vs. apoE4/4 (right column) homozygous macrophages analyzed by mass spectrometry

5.1.2. Analysis of sphingomyelin (SM), ceramide (Cer) and sphingosine (Sph)

The description is focused only on the differences between apoE3/3 and apoE4/4 macrophages because the results of apoE3/3 macrophages were described in detail earlier (s. 3.1.). In apoE3/3 macrophages, SM content on day 1 was lower while on day 4 it was higher compared to apoE4/4 macrophages. During Ox-LDL loading SM content was stronger reduced in apoE4/4 than in apoE3/3 macrophages compared with MCSF differentiation (Fig.51A,B). During Ox-LDL deloading with HDL_3 an increase of SM content could be observed to a higher level in the apoE3 than in the apoE4 genotype (Fig.51A,B). During E-LDL loading and deloading no differences of SM content could be detected between the two genotypes (Fig.51A,B). Cer content during Ox-LDL loading and deloading was lower in the apoE4 genotype compared to the apoE3 genotype. No differences could be detected during the other incubation states (Fig.51C,D). The amount of Sph was increased during Ox-LDL deloading with HDL_3 to a higher level in apoE3/3 than in apoE4/4 macrophages (Fig.51E,F). The other incubation states showed no differences of Sph content between the apoE3 and the apoE4 genotype (Fig.51E,F). The described differences in the cellular SM, Cer and Sph content between apoE3/3 and apoE4/4 macrophages failed to be statistically significant. The difference in the Cer content between E-LDL and Ox-LDL loading in both genotypes was statistically significant with $p<0.05$ determined by a student´s t-test. The significance is indicated by an asterisk.

The lower amount of SM during Ox-LDL loading in apoE4/4 macrophages compared to apoE3/3 macrophages could lead to a lower Cer content which could result in a decreased synthesis of glucosylceramide and GSLs. This in turn could result in a decreased surface expression of Cer and GSLs during Ox-LDL loading.

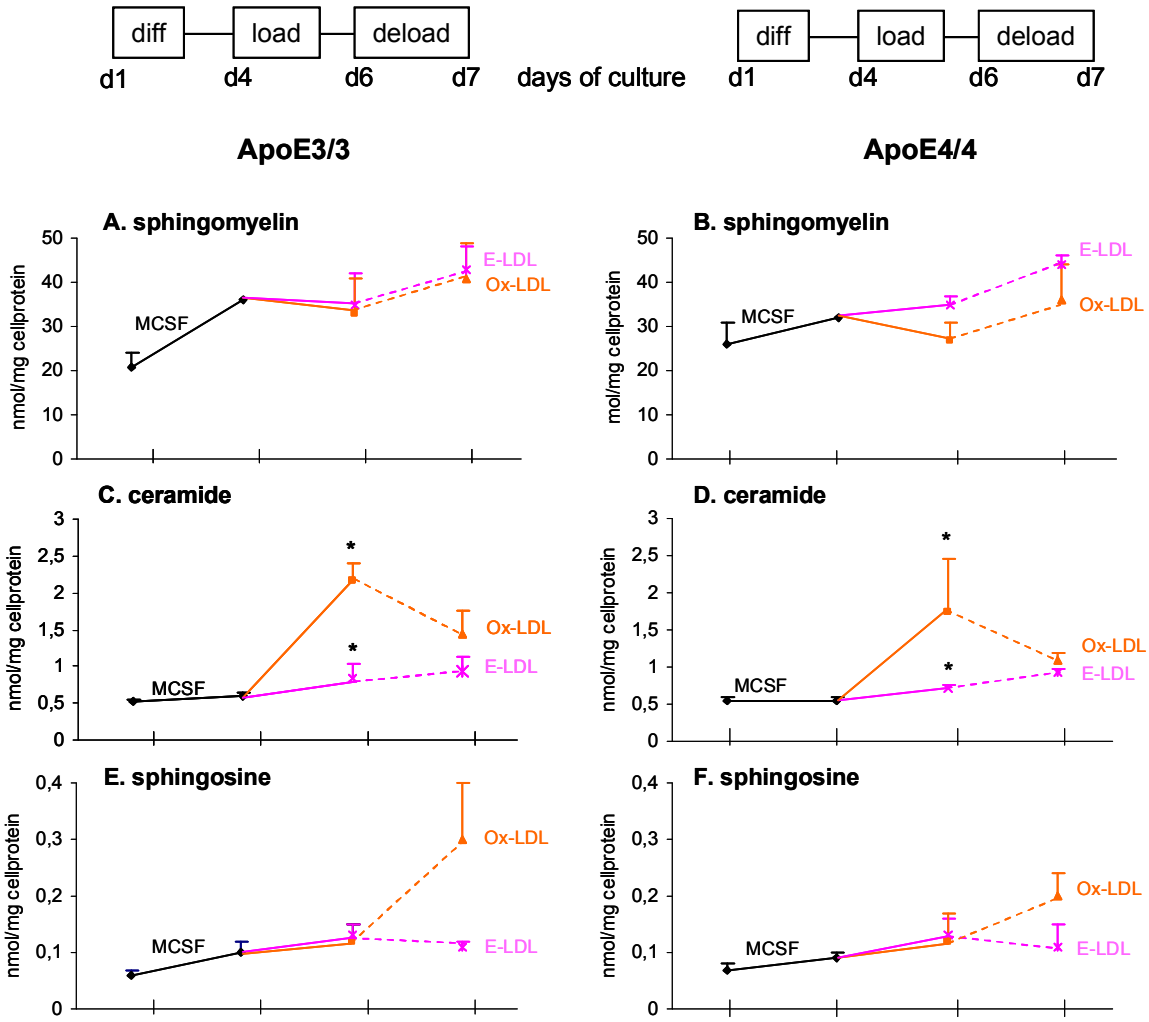

Figure 51: Cellular content of sphingomyelin (SM) (A,B), ceramide (Cer) (C,D) and sphingosine (E,F) of apoE3/3 (left column) vs. apoE4/4 (right column) homozygous macrophages analyzed by mass spectrometry

5.1.3. Analysis of phosphatidylethanolamine (PE), phosphatidylserine (PS), phosphatidylcholine (PC) and lysophosphatidylcholine (LPC)

ApoE4/4 macrophages had a higher PE content on day 1 compared with apoE3/3 macrophages (Fig.52A,B). PE content was increased during MCSF differentiation, decreased during E-LDL and Ox-LDL loading compared to MCSF and increased during HDL_3 deloading compared to lipid loading in both genotypes to the same extent (Fig.52A,B). PS content was increased during MCSF differentiation in apoE3/3 macrophages while it was decreased in apoE4/4 macrophages from a higher level on day 1 (Fig.52C,D). E-LDL loading increased PS content in apoE3/3 macrophages to a higher extent than in apoE4/4 macrophages. Ox-LDL loading decreased PS content in apoE4/4 macrophages to a higher extent than in apoE3/3 macrophages (Fig.52C,D). E-LDL deloading increased PS content in the apoE3 and to a higher extent in the apoE4 genotype compared to E-LDL loading. Ox-LDL deloading increased PS content to the same level in both genotypes compared to Ox-LDL loading (Fig.52C,D). PC content increased during MCSF differentiation in apoE3/3 while it didn't change in apoE4/4 macrophages which had a higher PC content than apoE3/3 macrophages (Fig.52E,F). Lipid loading increased PC content compared to MCSF. In the apoE3 genotype

PC content was higher during Ox-LDL loading while in the apoE4 genotype PC content was higher during E-LDL loading (Fig.52E,F). HDL_3 deloading increased PC content of both genotypes compared to lipid loading (Fig.52E,F). Altogether in apoE4/4 macrophages the PC content was higher during all stages of incubation compared to apoE3/3 macrophages (Fig.52E,F). LPC content increased during MCSF differentiation in both genotypes (Fig.52G,H). Ox-LDL loading led to an increase of LPC content in apoE3/3 while it didn´t change LPC content in apoE4/4 macrophages compared to MCSF (Fig.52G,H). E-LDL loading decreased LPC content in both genotypes compared to MCSF (Fig.52G,H). Ox-LDL deloading decreased while E-LDL deloading increased LPC content in both genotypes to a higher level in apoE3/3 than in apoE4/4 macrophages compared to lipid loading (Fig.52G,H)

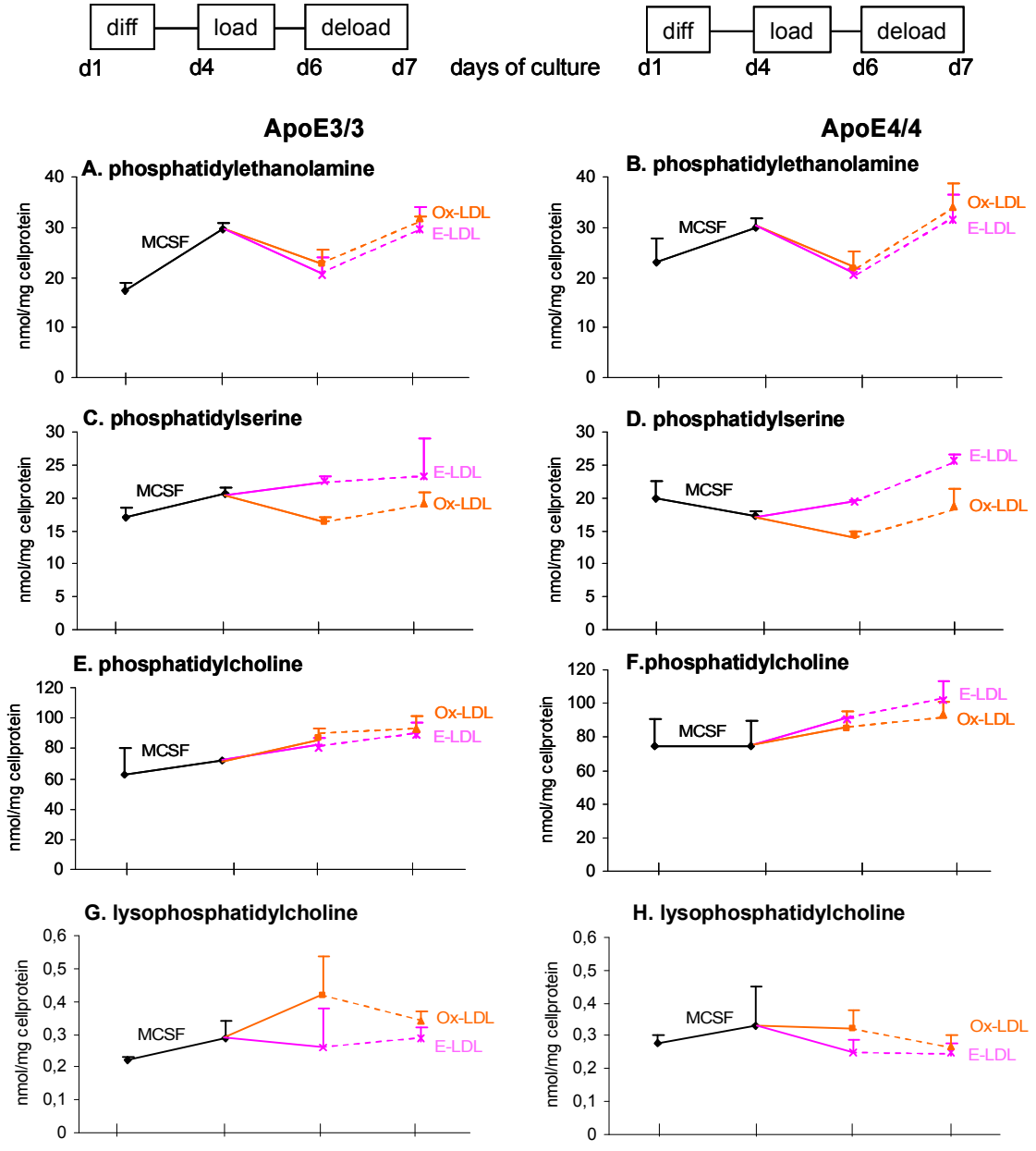

Figure 52: Cellular content of phosphatidylethanolamine (Ptdeth) (A,B), phosphatidylserine (PS) (C,D), phosphatidylcholine (PC) (E,F) and lysophosphatidylcholine (LPC) (G,H) of apoE3/3 (left column) vs. apoE4/4 (right column) homozygous macrophages analyzed by mass spectrometry

The described differences in the cellular PS, PC and LPC content measured by mass spectrometry between the apoE3/3 and apoE4/4 macrophages failed to be statistically significant tested by a student´s t-est for independent samples with $p<0.05$.

5.2. Cell surface expression of sphingo- and glycosphingolipids

In order to analyze wether there are differences in the surface expression of Cer, the GSLs lactosylceramide (LacCer, CDw17), globotriaosylceramide (Gb_3Cer, CD77), dodecasaccharideceramide (CD65s) and GM1 ganglioside between the apoE3/3 and apoE4/4 genotype, macrophages of the two different genotypes were loaded with E-LDL and Ox-LDL and deloaded with HDL_3 according to the previous experiments and surface expression was analyzed by flow cytometry. Four different experiments were performed and means and standard deviations of the mean fluorescence intensities were calculated. Differences between apoE3/3 and apoE4/4 macrophages that are significant at $p<0.05$ in a student's t-test for independent samples are indicated by an asterisk.

During differentiation of apoE3/3 and apoE4/4 macrophages with MCSF, Cer, Gb_3Cer, and GM1 ganglioside surface expression was increased from day 1 to day 7 (Fig.53A,C,E) while LacCer and CD65s surface expression was decreased from day 1 to day 4 and didn't change from day 4 to day 7 (Fig.53B,D). During E-LDL loading Cer, LacCer, CD65s and GM1 ganglioside surface expression was increased nearly to the same extent in both genotypes (Fig.53A,B,D,E) compared to MCSF differentiated cells. Gb_3Cer surface expression however was increased to a lower extent in apoE3/3 than in apoE4/4 macrophages during E-LDL loading compared to MCSF (Fig.53E,F). But during Ox-LDL loading cell surface expression of Cer, LacCer and CD65s (Fig.53A,B,D) was only significantly induced in apoE3/3 but not in apoE4/4 macrophages compared to MCSF differentiated cells. Also Gb_3Cer and GM1 surface expression was higher induced in apoE3/3 than in apoE4/4 macrophages during Ox-LDL loading but the differences were not statistically significant (Fig.53E,F,I,J).

During HDL_3 deloading of E-LDL loaded cells no change of Cer and LacCer surface expression could be observed between the two genotypes (Fig.53A,B,C,D) while surface expression of Gb_3Cer, CD65s and GM1 ganglioside was increased in apoE3/3 and decreased in apoE4/4 macrophages during HDL_3 deloading (Fig.53E,F,G,H,I,J). Ox-LDL deloading with HDL_3 showed no change of LacCer, Gb_3Cer and CD65s surface expression between the two genotypes (Fig.53C,D,E,F,G,H). Cer surface expression was increased (Fig.53A,B) and GM1 ganglioside surface expression was decreased (Fig.53I,J) in apoE4/4 macrophages compared with apoE3/3 macrophages during Ox-LDL deloading with HDL_3.

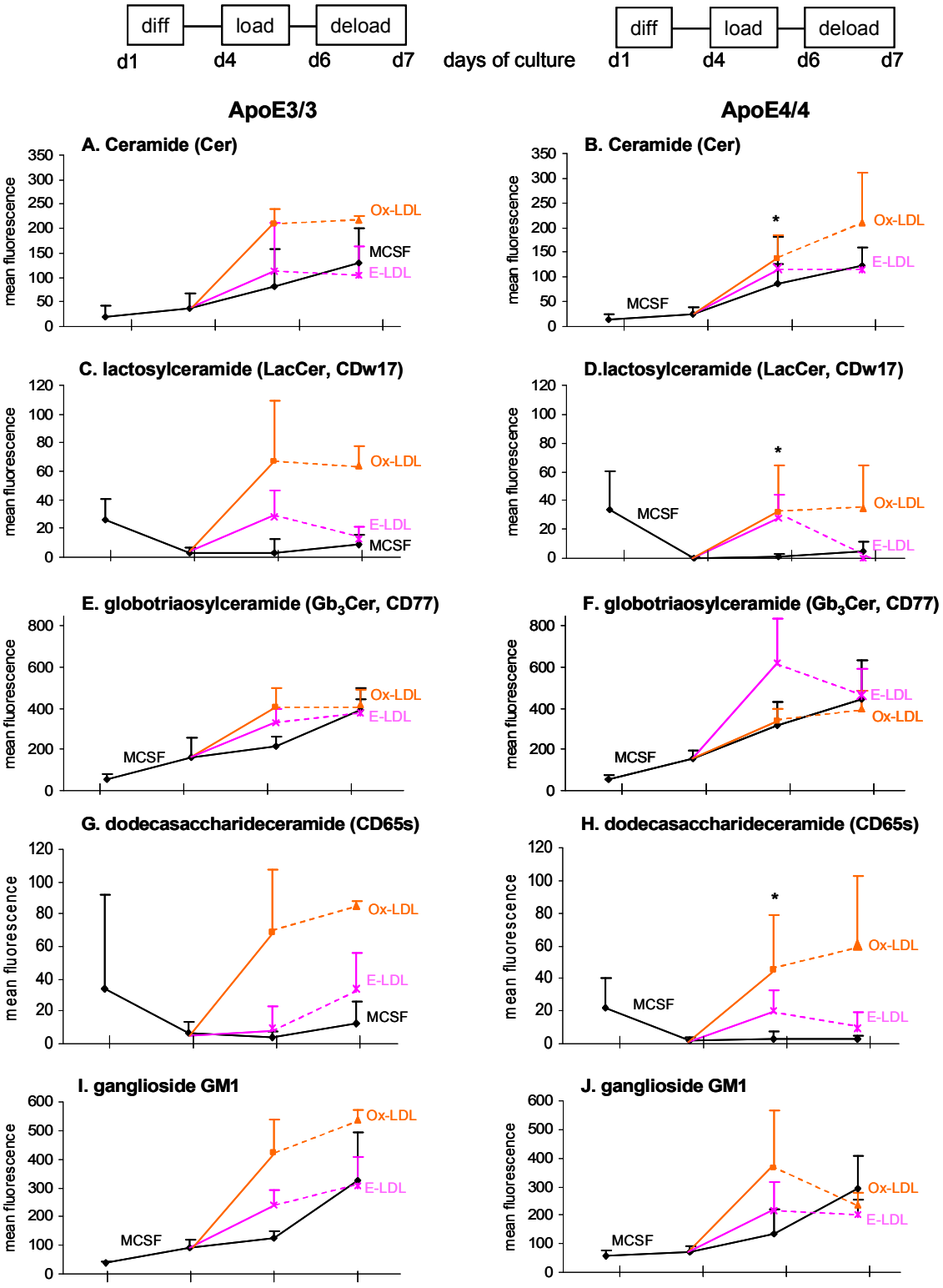

Figure 53: Surface expression of membrane ceramide, glycosphingolipids and GM1ganglioside of ApoE3/3 vs. ApoE4/4 macrophages
Cell surface expression of ceramide (A,B), lactosylceramide (C,D), globotriaosylceramide (E,F), dodecasaccharideceramide (G,H) and GM1 ganglioside (I,J) of apoE3/3 (left column) vs. apoE4/4 homozygous macrophages (right column) measured by flow-cytometry

5.3. Pathway specific analysis of microarray expression data – sphingolipid metabolism

UniGene	Gene Title	Gene Symbol	Chrom Loc	E3 MF_p	E3 MF_Sig	E3_ELDL Load_p	E3_ELDL Load_FC	E3 ELDL Deload_p	E3 ELDL Deload_FC	E3 OxL DL Load_p	E3 OxL DL Load_FC	E3 OxL DL Deload_p	E3 OxL DL Deload_FC	E4 MF_p	E4 MF_Sig	E4 ELDL Load_p	E4 ELDL Load_FC	E4 ELDL deload_p	E4 ELDL deload_FC	E4 OxL DL Load_p	E4 OxL DL Load_FC	E4 OxL DL deload_p	E4 OxL DL deload_FC
	Sphingomyelinases																						
Hs.277962	sphingomyelin phosphodiesterase, acid-like 3A	SMPDL3A	6q22.31	++	594,0	++	1,1	++	-1,5	++	1,7	++	-1,5	++	485,0	++	2,0	++	**-2,8**	++	1,7	++	-1,3
Hs.77813	sphingomyelin phosphodiesterase 1, acid lysosomal (acid sphingomyelina	SMPD1	11p15.4-p15	++	295,0	++	-1,6	++	**2,8**	++	1,1	++	1,1	++	209,0	++	-1,1	++	-1,1	++	-1,9	++	1,5
Hs.372000	neutral sphingomyelinase (N-SMase) activation associated factor	NSMAF	8q12-q13	++	631,0	++	1	++	1,2	++	1,6	++	-1,3	++	895,0	++	-1,1	++	1,1	++	1,7	++	-1,2
Hs.324808	N-acylsphingosine amidohydrolase (acid ceramidase) 1	ASAH1	8p22-p21.3	++	4612,0	++	1,0	++	1,5	++	1,5	++	-1,1	++	5104,0	++	1,0	++	1,5	++	1,1	++	1,1
Hs.282997	glucosidase, beta; acid (includes glucosylceramidase)	GBA	1q21	++	492,0	++	-1,1	++	1,6	++	1,5	++	1,3	++	593,0	++	1,0	++	1,6	++	**-2,0**	++	1,2
Hs.408273	galactosylceramidase (Krabbe disease)	GALC	14q31	++	562,0	++	-1,1	++	1,7	++	-1,1	++	1,7	++	988,0	++	-1,1	++	1,1	++	**-2,0**	++	1,2
	Glucosyltransferase																						
Hs.432605	UDP-glucose ceramide glucosyltransferase	UGCG	9q31	++	716,0	++	1,1	++	**-4,0**	++	**-1,9**	++	**3,0**	++	704,0	++	**2,1**	++	-1,4	++	**2,0**	++	**-4,9**
	Galactosyltransferases																						
Hs.396798	UDP-Gal:betaGlcNAc beta 1,4- galactosyltransferase, polypeptide 1	B4GALT1	9p13	++	216,0	+	**-2,3**	++	**3,2**	++	1,7	+	**-2,0**	+	147,0	+	1,0	+	-1,1	++	-1,3	++	1,4
Hs.534404	UDP-Gal:betaGlcNAc beta 1,3-galactosyltransferase, polypeptide 4	B3GALT4	6p21.3	++	257,0	++	**-3,0**	++	2,6	++	-1,2	++	-1,6	++	259,0	++	-2,0	++	-1,1	++	**-2,8**	++	1,9
	Acetylglucosaminyltransferases																						
Hs.173203	UDP-GlcNAc:betaGal beta-1,3-N-acetylglucosaminyltransferase 1	B3GNT1	2p15	+	105,0	++	**2,1**	+	**-3,7**	+	-1,2	++	**7,0**	++	111,0	++	**3,5**	++	-1,7	++	1,7	++	-1,7
Hs.69009	UDP-GlcNAc:betaGal beta-1,3-N-acetylglucosaminyltransferase 3	B3GNT3	19p13.1	+	145,0	++	**-2,1**	++	1,5	+	-1,4	+	1,2	++	78,0	+	1,2	+	-2,6	+	-2,0	+	2,1
Hs.8526	UDP-GlcNAc:betaGal beta-1,3-N-acetylglucosaminyltransferase 6	B3GNT6	11q13.2	++	184,0	++	**-2,0**	++	**4,6**	++	1,1	++	1,1	++	202,0	++	1,1	++	-1,4	++	-1,7	++	1,5
	Sialyltransferases																						
Hs.2554	sialyltransferase 1 (beta-galactoside alpha-2,6-sialyltransferase)	SIAT1	3q27-q28	++	402,0	++	**-2,3**	++	2,1	++	-1,3	++	1,0	++	258,0	++	-1,1	++	-1,2	++	-1,6	++	1,4
Hs.288215	sialyltransferase 7 ((alpha-N-acetylneuraminyl-2,3-beta-galactosyl-1,3)-N-	SIAT7B	17q25.1	-	30,0	+	2,3	+	1,6	+	**7,0**	+	-1,1	+	102,0	+	**2,0**	+	**-6,5**	++	1,9	+	-1,7
Hs.415117	sialyltransferase 9 (CMP-NeuAc:lactosylceramide alpha-2,3-sialyltransfera	SIAT9	2p11.2	++	433,0	++	-1,2	++	1,9	++	-1,4	++	**2,0**	++	273,0	++	1,6	++	1,1	++	-1,2	++	2,8
Hs.440913	sialyltransferase 10 (alpha-2,3-sialyltransferase VI)	SIAT10	3q12.1	++	134,0	++	1,9	++	**-2,3**	++	-1,4	++	**3,0**	++	134,0	++	**2,0**	++	-1,1	++	1,5	++	1,3
	Glycosphingolipid Degradation																						
Hs.69089	galactosidase, alpha	GLA	xq22	++	1655,0	++	-1,3	++	1,9	++	1,5	++	1,1	++	2082,0	++	1,1	++	-1,6	++	-1,1	++	1,1
Hs.387156	GM2 ganglioside activator	GM2A	5q31.3-q33.	++	6001,0	++	1,1	++	1,9	++	1,5	++	1,1	++	6053,0	++	1,2	++	-1,1	++	-1,4	++	1,7
Hs.411157	hexosaminidase A (alpha polypeptide)	HEXA	15q23-q24	++		++	**-1,6**	++	2,0	++	1,4	++	-1,3	++		++	1,0	++	**-2,0**	++	-1,7	++	1,4
Hs.69293	hexosaminidase B (beta polypeptide)	HEXB	5q13	++	3785,0	++	1,1	++	1,6	++	1,7	++	1,1	++	4770,0	++	1,1	++	-1,1	++	-1,2	++	1,7
Hs.406455	prosaposin (variant Gaucher disease and variant metachromatic leukodys	PSAP	10q21-q22	++	8013,0	++	1,1	++	1,9	++	1,5	++	-1,2	++	10790,0	++	-1,1	++	-1,1	++	-1,2	++	1,1
	Phospholipid Metabolism																						
Hs.24678	sphingosine-1-phosphate phosphatase 1	SGPP1	14q23.2	++	43,0	++	1,1	+	**-2,0**	++	1,0	++	**4,3**	++	43,0	++	**3,2**	++	-1,4	++	**2,1**	++	-1,4
Hs.77221	choline kinase alpha	CHKA	11q13.2	+	76,0	++	-1,4	++	**2,5**	++	1,6	++	1,3	+	53,0	+	1,5	+	1,0	++	1,1	++	1,3
Hs.68061	sphingosine kinase 1	SPHK1	17q25.2	++	277,0	++	**-1,9**	++	1,9	++	1,0	++	-1,2	+	125,0	+	1,6	+	-1,4	++	1,7	++	-1,1
Hs.186613	sphingosine-1-phosphate lyase 1	SGPL1	10q21	++	809,0	++	-1,5	++	1,5	++	-1,1	++	1,1	++	1001,0	++	-1,4	++	-1,1	++	**-3,0**	++	**2,1**
Hs.77329	phosphatidylserine synthase 1	PTDSS1	8q22	++	1462,0	++	-1,3	++	2,3	++	1,5	++	-1,1	++	1267,0	++	1,0	++	1,1	++	-1,1	++	**2,1**
Hs.12851	phosphatidylserine synthase 2	PTDSS2	11p15	+	68,0	+	-1,1	+	2,3	+	**1,9**	+	**-1,9**	+	67,0	-	**-3,2**	-	-1,3	+	**-2,0**	+	**2,1**
Hs.15192	phosphatidylethanolamine N-methyltransferase	PEMT	17p11.2	+	74,0	+	-1,1	+	2,1	++	1,5	+	1,2	+	27,0	+	2,5	+	-1,1	+	2,3	++	1,4
Hs.120439	ethanolamine kinase 1	ETNK1	12p12.1	++	156,0	++	1,1	++	1,2	++	1,0	++	**2,3**	++	199,0	++	1,4	++	1,7	++	**2,3**	++	1,1
Hs.18858	phospholipase A2, group IVC (cytosolic, calcium-independent)	PLA2G4C	19q13.3	++	357,0	+	-1,7	+	**3,0**	++	**2,0**	++	-1,7	+	366,0	+	1,1	+	-1,2	+	-1,7	+	**2,0**
Hs.93304	phospholipase A2, group VII (platelet-activating factor acetylhydrolase, pla	PLA2G7	6p21.2-p12	++	1977,0	++	**1,9**	++	-1,1	++	**2,8**	++	1,1	++	3121,0	++	1,1	++	1,1	++	-1,1	++	**2,0**
Hs.127958	1-acylglycerol-3-phosphate O-acyltransferase 4 (lysophosphatidic acid ac	AGPAT4	6q26	+	113,0	+	-1,5	+	2,5	++	**2,1**	+	-1,1	+	66,0	+	1,5	+	**-2,5**	+	1,3	++	1,4
Hs.77221	choline kinase alpha	CHKA	11q13.2	+	76,0	++	-1,4	++	**2,5**	++	1,6	++	1,3	+	53,0	+	1,5	+	1,0	++	1,1	++	1,3

Table 11: Genes involved in glycosphingolipid and lipid metabolism of apoE3/3 and apoE4/4 macrophages

Pathway specific analysis of genes involved in Cer and sphingolipid metabolism revealed some regulatory differences between the apoE3/3 and the apoE4/4 genotype which could explain the decreased Cer and GSL expression on the cell surface of apoE4/4 macrophages (Fig.53) and the decreased cellular phospatidylserine (PS) and lysophosphatidylcholine (LPC) content as well as the increased cellular phosphatidylcholine (PC) content of apoE4/4 macrophages (Fig.52C-H) during lipid loading. Gene-expression data obtained from microarray analysis of E-LDL and Ox-LDL loaded and HDL_3 deloaded macrophages of the apoE3/3 and the apoE4/4 genotype were compared.

UDP-glucose ceramide glucosyltransferase (UGCG) which catalyses the formation of glucosylceramide (GlcCer) from Cer didn´t change during E-LDL loading in apoE3/3 macrophages and was 2.1 fold upregulated in apoE4/4 macrophages. During Ox-LDL loading UGCG was -1.9 fold downregulated in apoE3/3 macrophages while in apoE4/4 macrophages it was 2.0 fold upregulated. This shows that GlcCer, the starting substance of the GSLs was probably synthesized to a higher extent in apoE4/4 macrophages during E-LDL and Ox-LDL loading. Therefore the fact that GSLs cannot be detected at the cell surface

of apoE4/4 macrophages during Ox-LDL loading seems to be due to a defect in transporting the GSLs from the Golgi to the cell surface.

Enzymes involved in GSL degradation like galactosidase alpha, GM2 ganglioside activator, hexosaminidase B and prosaposin were downregulated during Ox-LDL loading in apoE4/4 macrophages but upregulated in apoE3/3 macrophages. This could be due to a lower level of GSLs on the cell surface of apoE4/4 macrophages which should not be further reduced by degradation. During E-LDL deloading also an inverse regulation of GSL-degradation-enzymes could be observed. While the enzymes were increased in apoE3/3 macrophages they were decreased in apoE4/4 macrophages.

Glycolipid transfer protein which transports glucosylceramide was inversely regulated during HDL_3 deload between apoE3/3 and apoE4/4 macrophages. In apoE3/3 macrophages it was -3.0 fold downregulated during E-LDL deloading and 2.6 fold upregulated during Ox-LDL deloading while in apoE4/4 macrophages it was 2.0 fold upregulated during E-LDL deloading and -5.7 fold downregulated during Ox-LDL deloading.

From the genes involved in phospholipid metabolism, the phosphatidylserine synthases 1 and 2 (PTDSS1 and 2) which are involved in phosphatidylserine (PS) synthesis from phosphatidylcholine (PC) and phospatidylethanolamine (PE) respectively were differentially regulated between apoE3/3 and apoE4/4 macrophages. During E-LDL loading PTDSS1 was -1.3 fold downregulated in apoE3/3 and 1.0 fold regulated in apoE4/4 macrophages and PTDSS2 was -1.1 fold downregulated in apoE3/3 and significantly -3.2 fold downregulated in apoE4/4 macrophages. During Ox-LDL loading PTDSS1 was 1.5 fold and PTDSS2 1.9 fold upregulated in apoE3/3 macrophages while in apoE4/4 macrophages PTDSS1 was -1.1 fold and PTDSS2 -2.0 fold downregulated. It is concluded that the significant downregulations of PTDSS1 and 2 during lipid loading in the apoE4/4 but not in the apoE3/3 genotype could lead to a lower synthesis of PS and could explain the decreased amount of cellular PS in apoE4/4 macrophages during lipid loading as detected with mass spectrometry (Fig.52C,D).

Phosphatidylethanolamine N-methyltransferase (PEMT) which forms PC from PE was -1.1 fold downregulated during E-LDL loading in apoE3/3 and 2.5 fold upregulated in apoE4/4 macrophages. During Ox-LDL loading PEMT was 1.5 fold upregulated in apoE3/3 and 2.3 fold upregulated in apoE4/4 macrophages. The greater upregulation of PEMT during lipid loading in apoE4/4 compared to apoE3/3 macrophages could explain the increased cellular amount of PC in apoE4/4 macrophages found with mass spectrometry (Fig.52E,F).

Phospholipases A2, group IVC and VII and lysophospholipid acyltransferase involved in LPC processing were significantly upregulated during Ox-LDL loading in apoE3/3 macrophages but not significantly regulated in apoE4/4 macrophages which may explain the decreased cellular LPC content in apoE4/4 compared with apoE3/3 macrophages (Fig.52G,H).

5.4. Taqman analysis of enzymes involved in Cer generation and degradation

To verify the gene array data and to get informations about the regulation of further enzymes involved in Cer generation and degradation, Taqman realtime PCR was performed. ApoE3/3 and apoE4/4 macrophages during E-LDL and Ox-LDL loading and HDL_3 deloading were used and enzymes involved in sphingolipid metabolism were analyzed. In the following results fold changes are related to the non differentiated state of the monocytes.

Serine palmitoyltransferase 1 and 2, which were not present on the chip were decreased during differentiation in both genotypes (Fig.54A,B). During lipid loading both serine palmitoyltransferases were stronger upregulated in apoE4/4 than in apoE3/3 macrophages. In apoE3/3 macrophages serine palmitoyltransferase 1 was 1.7 fold increased during E-LDL and 2.1 fold during Ox-LDL loading (Fig.54A) while in apoE4/4 macrophages serine palmitoyltransferase 1 was 4.7 fold increased during E-LDL and 3.8 fold increased during Ox-LDL loading (Fig.54B). Serine palmitoyltransferase 2 was 1.3 fold upregulated during E-LDL and 1.5 fold upregulated during Ox-LDL loading in apoE3/3 macrophages (Fig.54C) while in apoE4/4 macrophages serine palmitoyltransferase 2 was 2.4 fold upregulated during E-LDL and 4.3 fold during Ox-LDL loading (Fig.54D). ***Sphingomyelin synthase 1 and 2 (SMS1 and 2)*** were decreased during differentiation in both genotypes (Fig.54E,F). During lipid loading SMS1 and 2 were stronger upregulated in apoE4/4 than in apoE3/3 macrophages. ApoE3/3 macrophages showed a 1.5 fold upregulation of SMS1 during E-LDL and a 1.3 fold upregulation during Ox-LDL loading (Fig.54E) and SMS2 was 1.6 fold upregulated during E-LDL and Ox-LDL loading (Fig.54G). Whereas in apoE4/4 macrophages SMS1 was 4.6 fold upregulated during E-LDL and 1.6 fold during Ox-LDL loading (Fig.54F) and SMS2 increased up to 5.9 fold during E-LDL loading and 3.8 fold during Ox-LDL loading (Fig.54H). ***Acid Sphingomyelinase (acidSMase)*** showed only a significant regulation in apoE3/3 macrophages (Fig.54I). It was induced during differentiation up to 2.8 fold. E-LDL loading led to a -1.7 fold decrease while Ox-LDL loading led to a 3.1 fold increase (Fig.54I). In apoE4/4 macrophages during differentiation a 1.4 fold increase of acid SMase could be observed with no further changes during lipid loading (Fig.54J). The increase during Ox-LDL loading in apoE3/3 macrophages of acid SMase which degrade SM to Cer could lead to an increased Cer formation in apoE3/3 but not in apoE4/4 macrophages. ***Neutral SMase*** was regulated similarly in both genotypes (Fig.54K,L). It was decreased during differentiation and increased during lipid loading. During E-LDL loading the upregulation was lower than during Ox-LDL loading with 2.6 fold in the apoE3 and 3.9 fold in the apoE4 genotype while with Ox-LDL loading it was 5.2 fold in the apoE3 and 4.7 fold in the apoE4 genotype (Fig.54K,L). ***Neutral SMase activation associated factor (NSMAF)*** was decreased during differentiation in both genotypes (Fig.54M,N). During lipid loading it was stronger induced in apoE4/4 compared with apoE3/3 macrophages. E-LDL loading of apoE3/3 macrophages showed a

1.3 fold upregulation of NSMAF while in apoE4/4 macrophages were 7.2 fold upregulated (Fig.54M,N). Ox-LDL loading led to a 2.3 fold upregulation of NSMAF in apoE3/3 and to a 11 fold upregulation in apoE4/4 macrophages (Fig.54M,N). ***Acid ceramidase*** was increased during differentiation in apoE3/3 macrophages while it was slightly decreased in apoE4/4 macrophages (Fig.54O,P). During lipid loading acid ceramidase was 1 fold decreased in the apoE3 genotype compared to MCSF while it was 11.8 fold increased in the apoE4 genotype during E-LDL loading and 7.9 fold during Ox-LDL loading (Fig.54O,P). The increase of acid ceramidase during lipid loading in the apoE4 genotype could enhance ceramide degradation leading to a lower level of Cer with decreased generation of GSLs. ***Glucosylceramidase*** was not regulated during differentiation in both genotypes (Fig.54Q,R). During E-LDL loading it was 1.8 fold upregulated in apoE3 and 1.3 fold in apoE4 macrophages. During Ox-LDL loading it was 3.6 fold upregulated in apoE3/3 macrophages while in apoE4/4 macrophages it was only 1.6 fold upregulated (Fig.54Q,R). This could lead to a stronger increase of GlcCer during Ox-LDL loading in apoE4/4 than in apoE3/3 macrophages. This could allow the conclusion that there may be a defect in the traffic of Cer and GSLs from the Golgi to the cell surface as a reason for the lower Cer and GSL surface expression in the apoE4 genotype. ***UDP-glucose ceramide glucosyltransferase*** was not regulated during differentiation but during E-LDL and Ox-LDL loading the upregulation was higher in apoE4/4 than in apoE3/3 macrophages (Fig.54S,T). E-LDL loading led in apoE3/3 macrophages to a 2.1 fold upregulation while in apoE4/4 macrophages a 13 fold upregulation could be observed. Ox-LDL loading of apoE3/3 macrophages led to a 3.2 fold upregulation while Ox-LDL loading of apoE4/4 macrophages led to 15.2 upregulation of UDP-glucose ceramide glucosyltransferase (Fig.54S,T). Upregulation of UDP-glucose ceramide glucosyltransferase which transfers Cer to GlcCer could lead to an increased degradation of Cer with an increase of GlcCer in apoE4/4 macrophages. These data could also lead to the conclusion that there may be a defect in the traffic of Cer and GSLs from the Golgi to the cell surface.

With ***HDL_3 deloading*** of E-LDL loaded cells of the apoE3/3 genotype almost no change could be observed of ***serine palmitoyltransferase 1 and 2*** mRNA expression (Fig.54A,C). While in the apoE4/4 genotype the mRNA expression of serine palmitoyltransferase 1 and 2 was decreased from 4.7 and 4.3 fold respectively up to 1.3 fold (Fig.54B,D). Deloading of Ox-LDL loaded cells led in the case of apoE3/3 macrophages to a decrease from 2.1 to 1 fold of serine palmitoyltransferase 1 while no change of serine palmitoyltransferase 2 mRNA expression could be observed (Fig.54A,C). In the case of apoE4/4 macrophages during Ox-LDL deloading an increase from 4.7 fold to 5.4 fold of serine palmitoyltransferase 1 (Fig.54B) and an increase from 2.4 fold to 7 fold of serine palmioyltransferase 2 (Fig.54D) could be detected. ***SMS1*** was upregulated in apoE3/3 macrophages during E-LDL deloading from 1.1 fold to a 2.1 fold while there was no change of ***SMS2*** mRNA expression (Fig.54E,G). In

apoE4/4 macrophages during E-LDL deloading a decrease of mRNA expression of SMS1 from 4.6 fold to 1.2 fold and in the case of SMS2 from 5.9 fold to 1.7 fold could be observed (Fig.54F,H). During Ox-LDL deloading SMS1 was upregulated from 1.1 fold to 1.7 fold and SMS2 was decreased from 1.6 fold to 1.2 fold in apoE3/3 macrophages (Fig.54E,G). While in the apoE4 genotype an upregulation from 1.6 fold to 3.5 fold of SMS1 and a decrease from 3.8 fold to 3 fold of SMS2 could be observed during Ox-LDL deloading (Fig.54F,H). The mRNA expression of ***acid SMase*** was decreased in the apoE3 genotype from 1.7 fold to 1 fold during E-LDL deloading (Fig.54I) while in the apoE4 genotype acid SMase was slightly increased during E-LDL deloading from 1.5 fold to 1.8 fold (Fig.54J). During Ox-LDL deloading a decrease of acid SMase from 3.1 fold to 0.4 fold could be observed in apoE3/3 (Fig.54I) and from 1.5 fold to 0.9 fold in apoE4/4 macrophages (Fig.54J). With HDL_3 deloading the mRNA expression of ***neutral SMase*** was decreased in both genotypes. In the apoE3 genotype during E-LDL deloading from 2.6 fold to 0.9 fold (Fig.54K) and in the apoE4 genotype from 3.9 to 1 fold (Fig.54L). During Ox-LDL deloading a decrease from 5.2 fold to 0.3 fold took place in the apoE3 (Fig.54K) and from 4.7 fold to 1.3 fold in the apoE4 genotype (Fig.54L). ***NSMAF*** decreased during Ox-LDL deloading with HDL_3 from a higher level in apoE4/4 macrophages (Fig.54M,N). During E-LDL deloading almost no change could be observed in the apoE3 genotype while NSMAF was downregulated in the apoE4 genotype (Fig.54M,N). ***Acid ceramidase*** was decreased during HDL_3 deloading from a higher level in apoE4/4 than in apoE3/3 macrophages (Fig.54O,P). The upregulation of ***glucosylceramidase*** in apoE3/3 macrophages was reversed with HDL_3 deloading (Fig. 54Q,R). During E-LDL deloading from 1.8 fold to 1.1 fold and during Ox-LDL deloading from 3.6 to 0.4 fold (Fig.54Q) while in apoE4/4 macrophages almost no change of glucosylceramidase mRNA expression could be detected during E-LDL and Ox-LDL deloading (Fig.54R). ***UDP-glucose ceramide glucosyltransferase*** was decreased during HDL_3 deloading. In apoE3/3 macrophages during E-LDL deloading from 3.2 fold to 0.8 fold and during Ox-LDL deloading from 2.1 fold to 0.7 fold (Fig.54S). In apoE4 macrophages UDP-glucose ceramide glucosyltransferase was decreased from a higher level during HDL_3 deloading. During E-LDL deloading it was decreased from 15.2 fold and during Ox-LDL deloading from 13 fold up to 1.1 fold (Fig.54T).

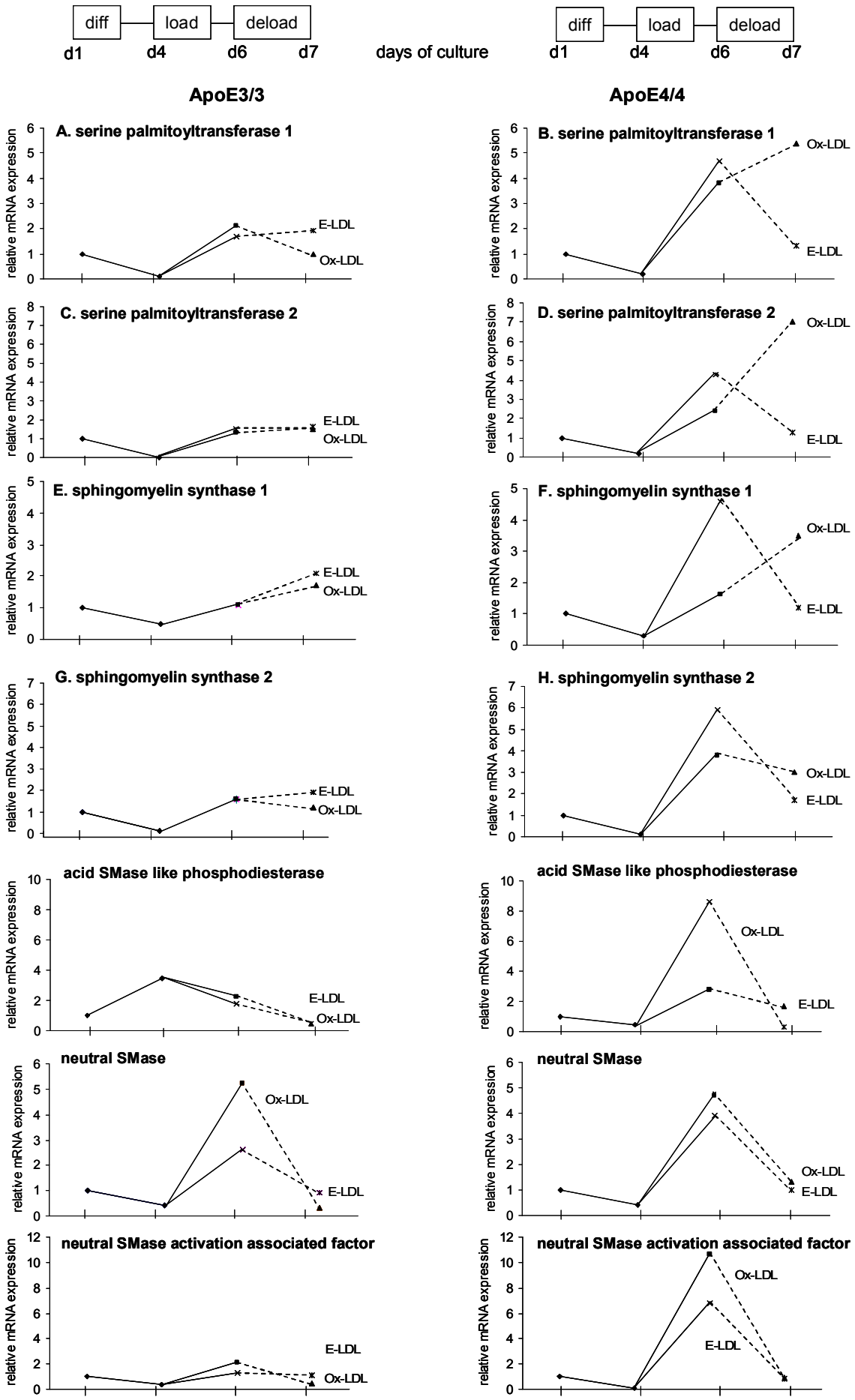
diff
load
deload
d1
d4
d6
d7
days of culture
ApoE3/3
ApoE4/4
A. serine palmitoyltransferase 1
B. serine palmitoyltransferase 1
C. serine palmitoyltransferase 2
D. serine palmitoyltransferase 2
E. sphingomyelin synthase 1
F. sphingomyelin synthase 1
G. sphingomyelin synthase 2
H. sphingomyelin synthase 2
acid SMase like phosphodiesterase
neutral SMase
neutral SMase activation associated factor
relative mRNA expression
E-LDL
Ox-LDL

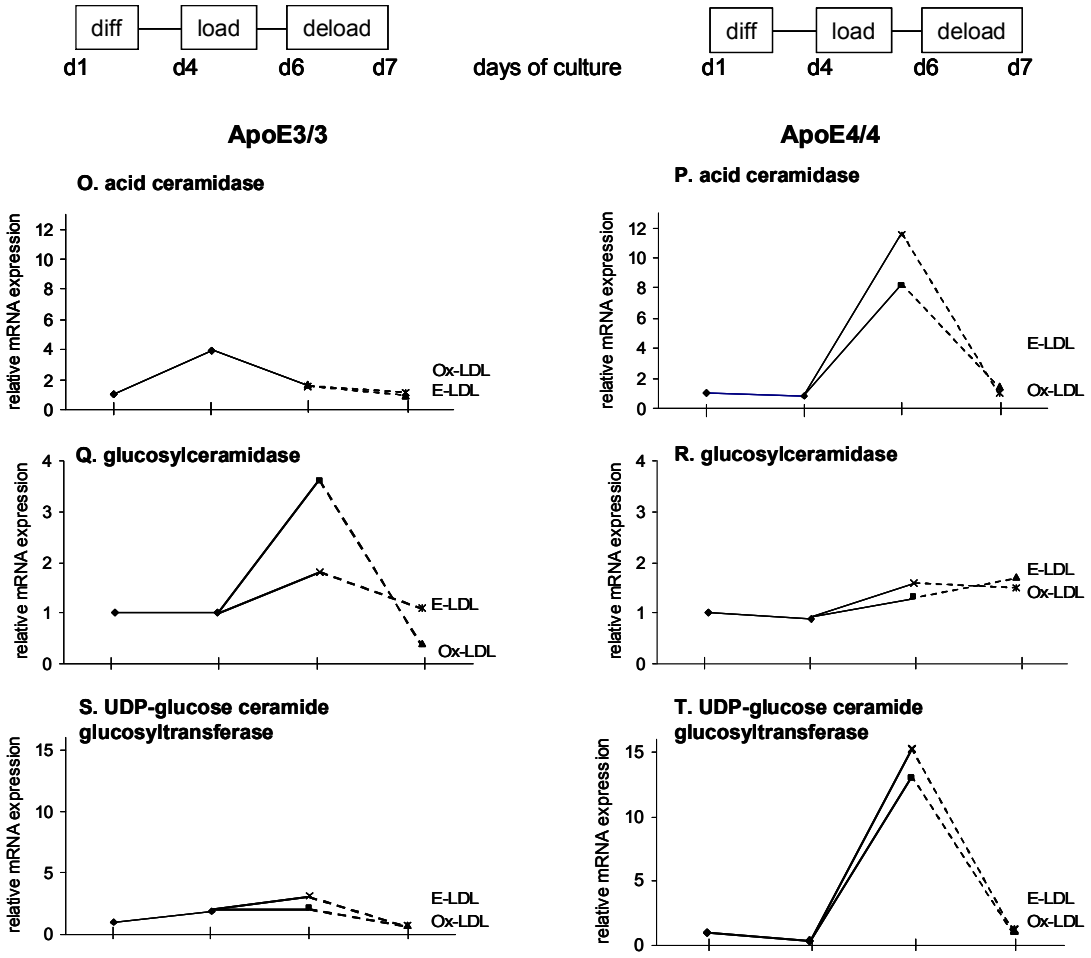

Figure 54: Taqman analysis of enzymes involved in sphingolipid metabolism
Macrophages of apoE3/3 (left column) and apoE4/4 (right column) genotype; serine palmitoyltransferase 1 (A,B), serine palmitoyltransferase 2 (C,D), sphingomyelin syntase 1 (E,F), sphingomyelin synthase 2 (G,H), acid sphingomyelinase (I,J), neutral sphingomyelinase (K,L), neutral sphingomyelinase activation associated factor (M,N), acid ceramidase (O,P), glucosylceramidase (Q,R), UDP-glucose ceramide glucosyltransferase (R,T)

5.5. Analysis of proteins involved in cholesterol metabolism

5.5.1. Analysis of mRNA expression of apoE and apoC-I

The mRNA expression of apoE and apoC-I obtained by microarray data analysis was increased during differentiation to a higher extent in apoE3/3 than in apoE4/4 macrophages.

ApoE mRNA expression of apoE3/3 macrophages was at all incubation states, except of E-LDL loading, higher than apoE mRNA expression of apoE4/4 macrophages (Fig.55A).

ApoC-I mRNA expression pattern was similar to that of apoE. ApoC-I mRNA expression of apoE3/3 macrophages was at all incubation states higher than apoC-I mRNA expression of apoE4/4 macrophages. The highest mRNA expression of apoC-I was observed in apoE3/3 macrophages during E-LDL deloading and Ox-LDL loading (Fig.55B).

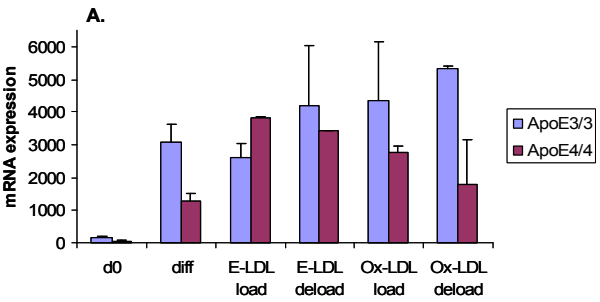

Figure 55A: mRNA expression of apoE

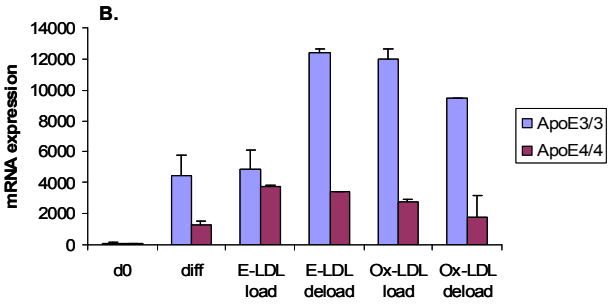

Figure 55B: mRNA expression of apoC-I

5.5.2. Analysis of secreted apoE and apoC-I

In a next step, the amount of secreted apoE and apoC-I in the culture media was analyzed. Therefore culture media of 6 day differentiated and of E-LDL respectively Ox-LDL loaded macrophages (day 4 to day 6) of the apoE3/3 and the apoE4/4 genotype were collected and the amounts of apoE and apoC-I were determined by ELISA. Because serum-free culture medium without apoE and apoC-I was used in these experiments, the measured apoE respectively apoC-I concentrations correlate directly with the apoE and apoC-I secretion of the cells.

In both genotypes it could be observed that the amount of secreted apoE was decreased during E-LDL and was further decreased during Ox-LDL loading compared with MCSF differentiated macrophages (Fig.56A). ApoE3/3 macrophages secreted more apoE than apoE4/4 macrophages during all incubation states (Fig.56A).

ApoC-I was increased in both genotypes to a higher extent during E-LDL than during Ox-LDL loading compared with MCSF differentiated macrophages (Fig.56B). The amount of secreted apoC-I of the different genotypes was almost the same during MCSF differentiation while it was higher in apoE3/3 than in apoE4/4 macrophages during E-LDL and Ox-LDL loading (Fig.56B).

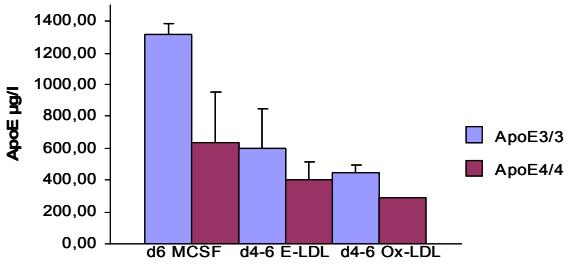

Figure 56A: amount of secreted apoE determined by ELISA

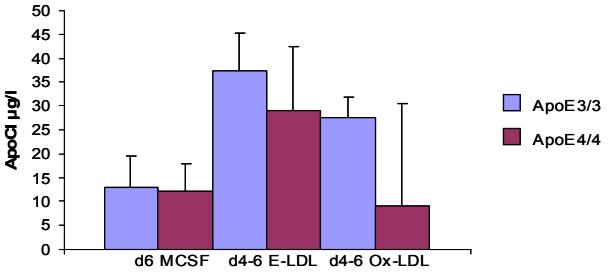

Figure 56B: amount of secreted apoC-I determined by ELISA

5.5.3. Extracellular (surface) and intracellular expression-analysis of proteins involved in cholesterol metabolism

Flow cytometry was used to analyze the extracellular (surface) and intracellular expression of apoE, apoC-I and CETP. ApoE3/3 and apoE4/4 macrophages were analyzed during MCSF differentiation (day 1-7), E-LDL and Ox-LDL loading (48h, day 4-6) and HDL_3 deloading (24h, day 6-7). Six different experiments were performed and means and standard deviations of the mean fluorescence intensities were calculated.

5.5.3.1. ApoE

During MCSF differentiation of apoE3/3 macrophages apoE surface expression was increased from day 1 to day 4, didn't change from day 4 to day 6 and was further increased from day 6 to day 7 (Fig.57A). In the apoE4 genotype apoE surface expression during MCSF differentiation increased from day 1 to day 6 and showed almost no change from day 6 to day 7 (Fig.57B). During lipid loading apoE surface expression was increased compared to MCSF in both genotypes. In the apoE3 genotype the increase was stronger during E-LDL loading than during Ox-LDL loading while in the apoE4 genotype a stronger increase could be observed during Ox-LDL than during E-LDL loading (Fig.57A,B). HDL_3 deloading of apoE3/3 macrophages decreased apoE surface expression compared to lipid loading (Fig.57A). ApoE4/4 macrophages showed also a decrease of apoE surface expression during Ox-LDL deloading while there was no change during E-LDL deloading compared to Ox-LDL and E-LDL loading (Fig.57B).

The intracellular expression of apoE during MCSF differentiation was increased in both genotypes from day 1 to day 6 and was decreased from day 6 to day 7 (Fig.57C,D). During Ox-LDL loading apoE intracellular expression decreased compared to MCSF in both genotypes to the same extent while during E-LDL loading a slight increase in the apoE3 genotype and a slight decrease in the apoE4 genotype could be detected (Fig.57C,D). HDL_3 deloading led to a decrease of apoE intracellular expression in apoE3/3 macrophages compared to lipid loading while in apoE4/4 macrophages during E-LDL deloading a decrease

and during Ox-LDL deloading an increase could be observed compared to E-LDL and Ox-LDL loading (Fig.57C,D).

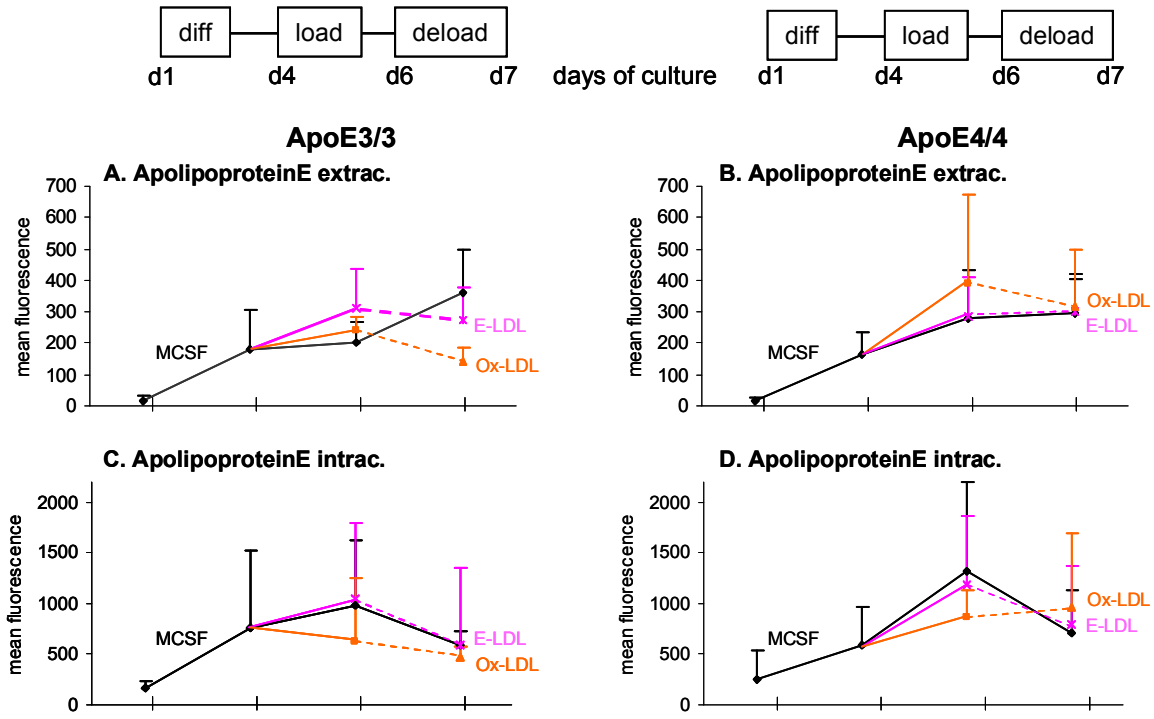

Figure 57: ApoE expression extracellular (Fig.51A,B) and intracellular (Fig.51C,D) of apoE3/3 (left column) and apoE4/4 (right column) homozygous macrophages.

5.5.3.2. ApoC-I

During differentiation apoC-I surface expression was similar regulated in both genotypes with almost no change from day 1 to day 6 and an increase from day 6 to day 7 (Fig.58A,B). During lipid loading apoC-I surface expression increased compared to MCSF in both genotypes to a higher extent during Ox-LDL than during E-LDL loading (Fig.58A,B). E-LDL deloading of the apoE3 genotype increased apoC-I surface expression compared to E-LDL loading while during Ox-LDL deloading apoC-I surface expression didn't change compared to Ox-LDL loading (Fig.58A). In the apoE4 genotype E-LDL deloading decreased while Ox-LDL deloading increased apoC-I surface expression compared to lipid loading (Fig.58B).

The intracellular expression of apoC-I was higher in apoE4/4 than in apoE3/3 macrophages during all incubation states. During differentiation apoC-I was upregulated from day 1 to day 4 to a higher level in apoE4/4 than in apoE3/3 macrophages and showed almost no further change from day 4 to day 7 in both genotypes (Fig.58C,D). During lipid loading an upregulation of apoC-I could be observed which was higher during Ox-LDL than during E-LDL loading in both genotypes (Fig.58C,D).

During HDL_3 deloading almost no change of intracellular apoC-I expression could be observed in apoE3/3 macrophages compared to lipid loading (Fig.58C). In apoE4/4

macrophages intracellular apoC-I expression was increased during E-LDL deloading and didn't change during Ox-LDL deloading compared to E-LDL and Ox-LDL loading (Fig.58D).

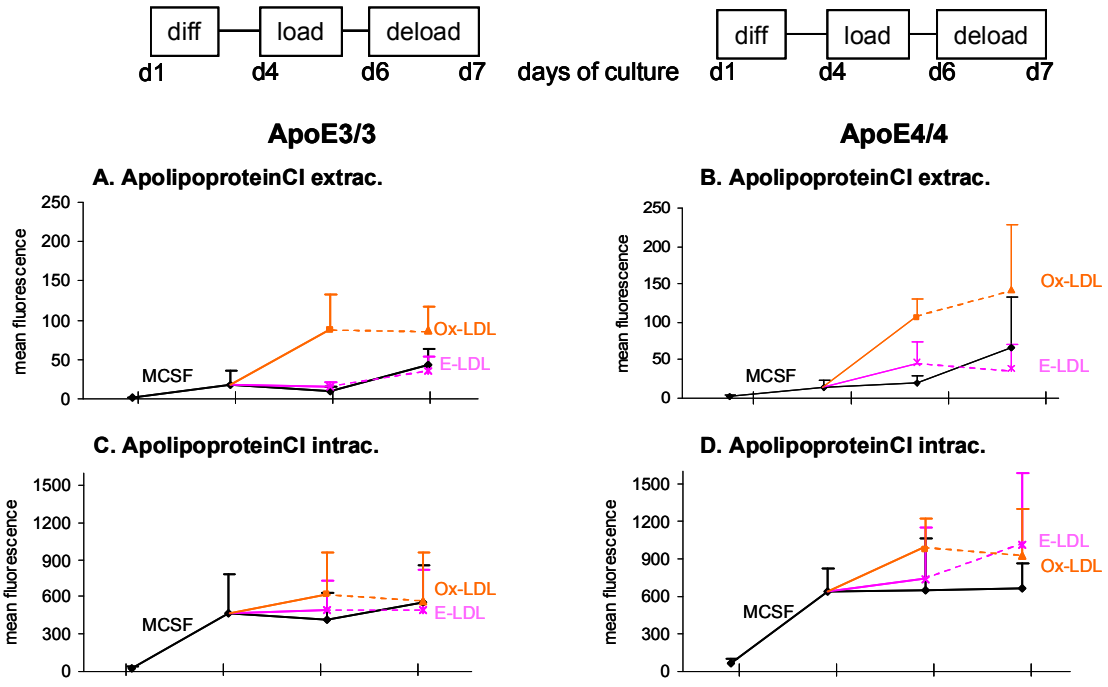

Figure 58: ApoC-I expression extracellular (Fig.52A,B) and intracellular (Fig.52C,D) of apoE3/3 (left column) and apoE4/4 (right column) homozygous macrophages.

5.5.3.3. CETP

Surface expression of CETP was increased during MCSF differentiation from day 1 to day 6 in both genotypes while from day 6 to day 7 it was increased in apoE3/3 macrophages and didn't change in apoE4/4 macrophages (Fig.59A,B). During E-LDL loading CETP surface expression was increased in the apoE3 genotype while it was slightly decreased in the apoE4 genotype compared to MCSF. Ox-LDL loading led to a decrease of CETP in both genotypes compared to MCSF (Fig.59A,B). During E-LDL deloading with HDL_3 both genotypes showed a small increase of CETP surface expression. During Ox-LDL deloading apoE3/3 macrophages showed a decrease and apoE4/4 macrophages an increase of CETP surface expression compared to lipid loading (Fig.59A,B).

Intracellular expression of CETP was increased during MCSF differentiation from day 1 to day 6 to a higher level in apoE4/4 than in apoE3/3 macrophages (Fig.59C,D). From day 6 to day 7 of differentiation apoE3/3 macrophages showed almost no change of CETP intracellular expression while in apoE4/4 macrophages a decrease could be observed (Fig.59C,D). Lipid loading led in both genotypes to a decrease of intracellular CETP expression compared to MCSF with a stronger decrease during Ox-LDL loading than during E-LDL loading (Fig.59C,D) compared to MCSF. HDL_3 deloading led to almost no changes in CETP intracellular expression of the apoE3 genotype while in the apoE4 genotype a decrease could be observed compared to lipid loading (Fig.59C,D).

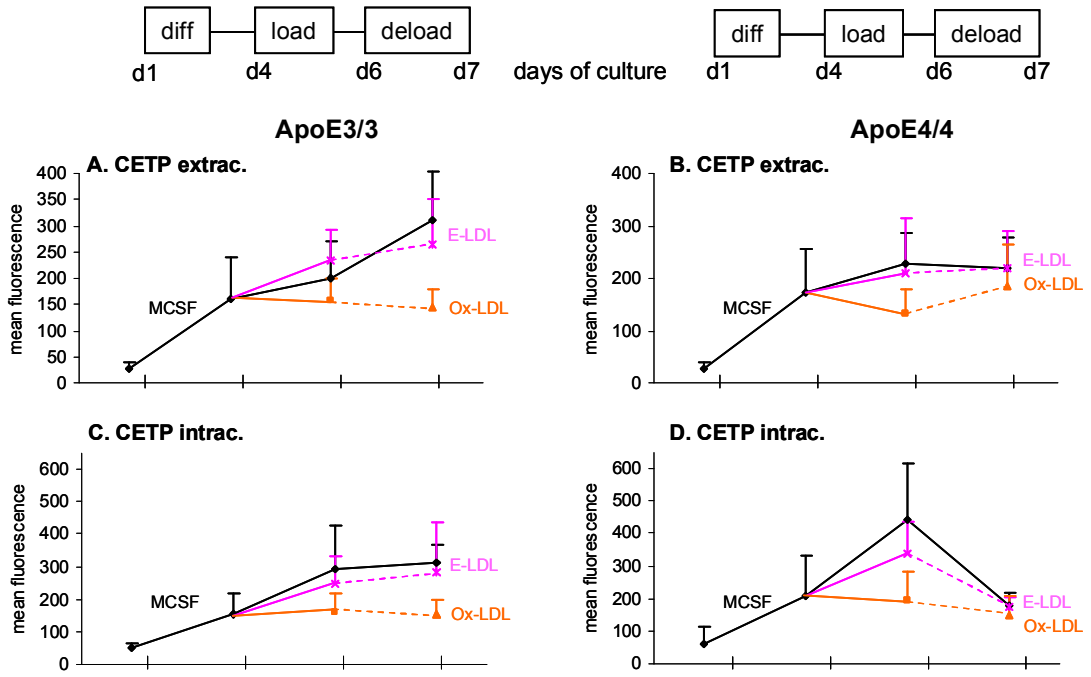

Figure 59: CETP expression extracellular (Fig.53A,B) and intracellular (Fig.53C,D) of apoE3/3 (left column) and apoE4/4 (right column) homozygous macrophages

5.6. Intracellular expression-analysis of adipophilin

Intracellular expression of adipophilin, a protein associated with intracellular lipid storage droplets and further a marker for lipid loading was analyzed on fixed and permeabilized cells during MCSF differentiation (day 1-7), E-LDL and Ox-LDL loading (day 4-6) and HDL_3 deloading (day 6-7).

During MCSF differentiation from day 1 to day 4 adipophilin expression didn't change while from day 4 to day 7 the expression increased in both genotypes. During E-LDL loading an increase of adipophilin expression could be observed which was stronger in apoE3/3 than in apoE4/4 macrophages. Ox-LDL loading showed almost no change of adipophilin expression in the apoE3 genotype and a small increase in the apoE4 genotype. During E-LDL deloading with HDL_3 adipophilin expression decreased while during Ox-LDL deloading with HDL_3 adipophilin expression increased in both genotypes compared to lipid loading (Fig.60A,B).

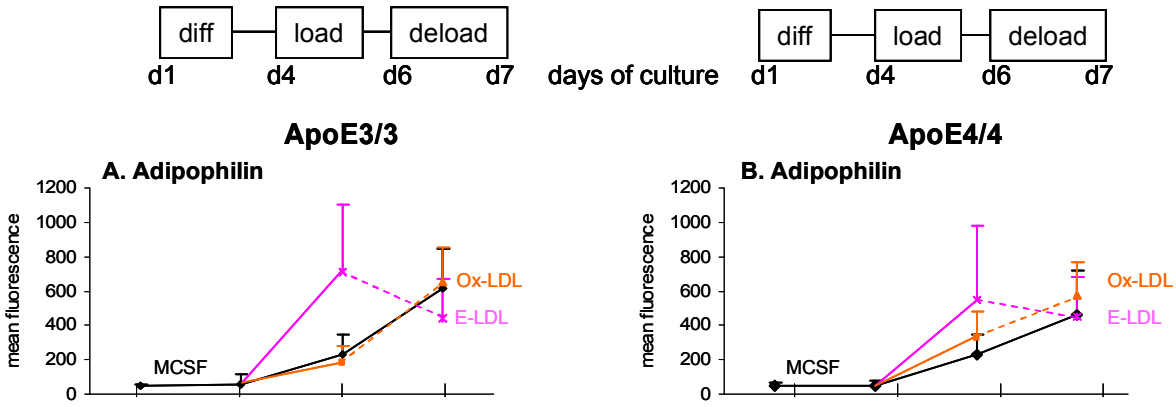

Figure 60: Intracellular expression analysis of adipophilin of apoE3/3 (A) and apoE4/4 macrophages (B)

5.7. Gene expression analysis of receptors involved in lipid uptake and processing

Unigene	Name	Gene Symbol	Chrom Loc	E3 MF_p	E3 MF_Sig	E3_ELDL Load_p	E3_ELDL Load_FC	E3 ELDL Deload_p	E3 ELDL Deload_FC	E3 OxLDL Load_p	E3 OxLDL Load_FC	E3 OxLDL Delad_p	E3 OxLDL Deload_FC	E4 MF_p	E4 MF_Sig	E4 ELDL Load_p	E4 ELDL Load_FC	E4 ELDL deload_p	E4 ELDL deload_FC	E4 OxLDL Load_p	E4 OxLDL Load_FC	E4 OxLDL deload_p	E4 OxLDL deload_FC
0	**LDL Receptor and Related Proteins**																						
Hs.213289	Low density lipoprotein receptor (familial hypercholesterolen	LDLR	19p13.3	++	491,0	+	**-8,6**	++	**3,2**	++	**-4,0**	++	1,4	++	639,0	++	**-6,1**	++	2,1	++	**-7,5**	++	1,5
Hs.162757	Low density lipoprotein-related protein 1 (alpha-2-macroglob	LRP1	12q13-q14	++	417,0	++	-1,5	++	**2,6**	++	-1,2	++	1,3	++	382,0	++	1,4	++	**-2,0**	++	-1,9	++	1,9
Hs.75140	low density lipoprotein receptor-related protein associated p	LRPAP1	4p16.3	++	1785,0	++	-1,4	++	**2,5**	++	**2,0**	++	-1,2	++	1520,0	++	-1,1	++	-1,5	++	**-2,0**	++	**2,1**
Hs.210343	Low density lipoprotein receptor-related protein 6	LRP6	12p11-p13	++	92,0	+	**-3,0**	+	2,6	++	-1,1	+	-1,2	+	11,0	+	4,6	+	-1,4	+	3,5	+	-1,1
Hs.410784	Low density lipoprotein receptor-related protein 8, apolipopr	LRP8	1p34	++	86,0	+	**-2,0**	++	1,7	++	-1,2	++	1,9	+	53,0	+	1,1	++	1,7	++	1,1	++	1,1
Hs.438159	Sortilin-related receptor, L(DLR class) A repeats-containing	SORL1	11q23.2-q24.2	++	618,0	++	**-6,5**	++	**3,7**	++	**-4,0**	++	-1,1	++	213,0	++	1,2	++	-1,9	++	**-2,3**	++	1,5
Hs.445299	Oxidised low density lipoprotein (lectin-like) receptor 1	OLR1	12p13.2-p12.3	++	79,0	++	1,0	++	1,0	++	**-2,1**	++	1,6	++	35,0	++	**2,1**	++	-1,1	++	-1,3	++	1,2
Hs.370422	very low density lipoprotein receptor	VLDLR	9p24	++	78,0	++	-1,6	+	1,4	++	1,0	++	1,0	++	39,0	++	1,9	++	-1,9	++	**3,0**	++	-1,6
Hs.1239	alanyl (membrane) aminopeptidase (aminopeptidase N, am	ANPEP	15q25-q26	++	705,0	++	**-2,3**	++	2,3	++	-1,1	++	1,0	++	672,0	++	-1,1	++	-1,4	++	**-7,5**	++	**2,0**
0	**LPS-/Toll-like Receptors**																						
Hs.519624	CD14 antigen	CD14	5q31.1	++	6150,0	++	**-3,5**	++	**3,5**	++	**-2,8**	++	1,1	++	5168,0	++	-1,9	++	-1,7	++	**-7,0**	++	**2,6**
Hs.111805	toll-like receptor 1	TLR1	4p14	++	132,0	++	1,0	++	1,1	++	-1,2	++	1,5	++	151,0	++	1,1	++	-1,1	++	1,1	++	1,1
Hs.519033	toll-like receptor 2	TLR2	4q32	++	663,0	++	-1,3	++	1,1	++	**-2,0**	++	1,3	++	613,0	++	-1,5	++	-1,4	++	**-3,7**	++	**2,6**
Hs.174312	toll-like receptor 4	TLR4	9q32-q33	++	128,0	++	-1,1	++	-1,2	++	-1,4	++	**4,0**	++	92,0	++	**2,3**	++	-1,6	++	1,0	++	-1,5
Hs.114408	toll-like receptor 5	TLR5	1q41-q42	++	383,0	++	-1,7	++	1,7	++	-1,7	++	1,6	++	433,0	++	-1,3	++	-1,1	++	**-2,0**	++	-1,2
Hs.179152	toll-like receptor 7	TLR7	xp22.3	++	236,0	++	-1,7	++	**2,3**	++	**-3,0**	++	1,2	++	350,0	++	-1,2	++	-1,2	+	**-18,4**	++	**5,3**
Hs.272410	toll-like receptor 8	TLR8	xp22	-	7,0	+	4,0	+	**-3,7**	+	-1,4	+	6,1	+	59,0	++	1,9	+	**-2,0**	+	-2,3	-	-2,5
0	**Fcg-Receptors**																						
Hs.534325	Fc fragment of IgG, high affinity Ia, receptor for (CD64)	FCGR1A	1q21.2-q21.3	++	972,0	++	-1,3	++	1,0	++	**-3,7**	++	**4,0**	++	1220,0	++	1,1	++	-1,7	++	**-6,5**	++	**3,7**
Hs.352642	Fc fragment of IgG, low affinity IIa, receptor for (CD32)	FCGR2A	1q23	++	958,0	++	-1,5	++	1,5	++	**-2,1**	++	1,4	++	1266,0	++	-1,1	++	-1,1	++	**-9,2**	++	**3,2**
Hs.372679	Fc fragment of IgG, low affinity IIIa, receptor for (CD16)	FCGR3B /FC	1q23	+	114,0	+	-2,5	+	1,1	-	-10,6	+	**13,9**	+	123,0	++	**2,5**	++	-1,4	+	**-3,0**	-	-2,1
0	**Scavenger Receptor**																						
Hs.443120	CD36 antigen (collagen type I receptor, thrombospondin rec	CD36	7q11.2	++	1088,0	++	**2,8**	++	1,1	++	**2,5**	++	1,7	++	730,0	++	**3,0**	++	1,9	++	**2,5**	++	**2,3**
Hs.349656	scavenger receptor class B, member 2	SCARB2	4q21.1	++	231,0	++	**2,0**	++	**-2,8**	++	**-2,3**	++	**6,1**	++	185,0	++	**2,6**	++	1,6	++	**2,0**	++	**-2,0**
Hs.436887	macrophage scavenger receptor 1	MSR1	8p22	++	692,0	++	**2,6**	++	-1,1	++	1,9	++	1,6	++	877,0	++	**2,6**	++	1,6	++	**2,3**	++	1,0
Hs.74076	CD163 antigen (scavenger receptor cysteine rich)	CD163	12p13.3	++	3754,0	++	-1,7	++	**2,1**	++	**-2,8**	++	**2,1**	++	5881,0	++	**-2,1**	++	1,2	++	**-7,0**	++	**4,9**
0	**Integrins/Complement Receptors**																						
Hs.172631	integrin, alpha M (complement component receptor 3, alpha	ITGAM	16p11.2	++	1427,0	++	-1,1	++	1,9	++	-1,6	++	**2,3**	++	1405,0	++	1,2	++	1,9	++	**-2,5**	++	**4,3**
Hs.408864	decay accelerating factor for complement (CD55, Cromer bl	DAF	1q32	++	139,0	++	1,5	++	-1,6	++	**2,3**	++	-1,3	++	147,0	++	1,5	++	**-2,1**	++	**2,8**	++	**-2,3**
Hs.446414	CD47 antigen (Rh-related antigen, integrin-associated signa	CD47	3q13.1-q13.2	++	1211,0	++	-1,1	++	-1,1	++	-1,1	++	1,9	++	1685,0	++	-1,2	++	1,2	++	-1,7	++	**2,0**
0	**Signal Regulators of Fc Receptors**																						
Hs.387579	CD9 antigen (p24)	CD9	12p13.3	++	2653,0	++	1,3	++	1,1	++	1,1	++	1,9	++	3244,0	++	1,5	++	1,0	++	-1,2	++	1,6
Hs.287692	CD33 antigen-like 3	CD33L3	18q12.3	++	238,0	++	-1,7	+	**-2,1**	++	1,3	++	1,3	++	196,0	++	-1,2	++	1,6	++	**3,7**	++	**-9,2**
Hs.83731	CD33 antigen (gp67)	CD33	19q13.3	++	134,0	++	-1,4	++	1,7	+	1,5	++	1,3	++	164,0	+	**-2,3**	+	-1,5	+	**-2,8**	++	**4,0**
0	**Genes involved in Fc Receptor Signalling**																						
Hs.352554	CDC42 effector protein (Rho GTPase binding) 3	CDC42EP3	2p21	++	257,0	++	1,2	++	-1,6	++	1,7	++	1,6	++	292,0	++	1,0	++	-1,1	++	**2,0**	++	**-2,6**
Hs.355832	cell division cycle 42 (GTP binding protein, 25kDa)	CDC42	1p36.1	++	414,0	++	1,7	++	-1,1	++	1,0	++	**2,5**	++	664,0	++	1,5	++	1,9	++	-1,1	++	-1,7
Hs.372800	Rac/Cdc42 guanine nucleotide exchange factor (GEF) 6	ARHGEF6	xq26	++	375,0	++	**-2,0**	++	**2,6**	++	-1,4	++	1,1	++	301,0	++	-1,4	++	1,1	++	**-3,7**	++	**3,5**
Hs.528296	activated Cdc42-associated kinase 1	ACK1	3q29	++	227,0	+	**-2,6**	++	**2,8**	++	-1,5	+	-1,4	++	176,0	++	-1,1	++	-1,4	+	**-3,7**	++	**3,2**
Hs.185140	phosphoinositide-binding protein PIP3-E	PIP3-E	6q25.2	+	33,0	+	-1,5	++	1,9	+	1,2	+	-1,1	+	27,0	+	1,5	+	1,4	+	-1,2	+	-1,1
Hs.239818	phosphoinositide-3-kinase, catalytic, beta polypeptide	PIK3CB	3q22.3	++	343,0	++	-1,1	++	2,0	++	1,9	++	-1,5	++	364,0	++	1,0	++	-1,1	++	1,1	++	1,5
Hs.249235	Phosphoinositide-3-kinase, class 2, alpha polypeptide	PIK3C2A	11p15.5-p14	++	161,0	++	1,1	++	-1,2	++	1,1	++	**2,0**	++	211,0	++	1,2	++	1,3	++	1,9	++	-1,2
Hs.306747	phosphoinositide-3-kinase, regulatory subunit 4, p150	PIK3R4	3q21.3	++	143,0	++	-1,2	++	-1,1	++	1,0	++	1,7	++	147,0	++	1,1	++	1,1	++	1,4	++	1,1
Hs.418150	phosphoinositide-3-kinase, class 3	PIK3C3	18q12.3	++	199,0	++	1,1	++	1,4	++	1,9	++	-1,1	++	234,0	++	1,1	++	1,1	++	1,2	++	1,2
Hs.426967	phosphoinositide-3-kinase, catalytic, delta polypeptide	PIK3CD	1p36.2	++	948,0	++	-1,1	++	**2,1**	++	1,6	++	-1,3	++	1074,0	++	-1,3	++	-1,1	++	-1,9	++	**2,0**
Hs.85701	phosphoinositide-3-kinase, catalytic, alpha polypeptide	PIK3CA	3q26.3	++	94,0	++	-1,1	+	-1,7	++	-1,2	++	**2,6**	++	89,0	++	1,7	++	-1,1	++	1,1	++	-1,1
0	**Integrins/Complement Receptors**																						
Hs.97199	Complement component 1, q subcomponent, receptor 1	C1QR1	20p11.21	++	341,0	++	**-3,5**	++	2,6	+	**-2,5**	+	1,3	++	375,0	++	**-2,5**	++	-1,3	+	**-6,1**	+	1,9
Hs.134012	complement component 1, q subcomponent-like 1	C1QL1	17q21	++	147,0	++	**-2,5**	++	3,0	++	-1,1	++	1,1	++	109,0	++	1,1	++	-1,2	++	-1,1	++	1,1
Hs.155935	Complement component 3a receptor 1	C3AR1	12p13.31	++	2009,0	++	1,1	++	1,2	++	**-2,3**	++	**2,3**	++	3666,0	++	-1,1	++	1,0	++	**-11,3**	++	**8,0**
Hs.334019	Complement component (3b/4b) receptor 1, including Knop	CR1	1q32	++	138,0	++	-1,9	++	**2,5**	++	-1,2	++	1,0	++	102,0	++	-1,1	++	-1,2	++	-1,5	++	1,2
Hs.389133	Integrin, alpha E (CD103, human mucosal lymphocyte antig	ITGAE	17p13	++	738,0	++	-1,4	++	**2,1**	++	1,9	++	-1,3	++	470,0	++	1,5	++	-1,2	++	1,6	++	1,6
Hs.287797	Integrin, beta 1 (fibronectin receptor, CD29)	ITGB1	10p11.2	++	1695,0	++	1,5	++	-1,2	++	1,5	++	1,2	++	1678,0	++	1,4	++	1,3	++	1,5	++	1,1
Hs.408468	integrin beta 1 binding protein 1	ITGB1BP1	2p25.2	++	383,0	++	1,6	++	1,9	++	**3,5**	++	-1,2	++	343,0	++	1,7	++	-1,2	++	1,9	++	**2,0**
Hs.265829	Integrin, alpha 3 (CD49c, alpha 3 subunit of VLA-3 receptor	ITGA3	17q21.33	+	69,0	+	1,1	+	3,2	+	**2,1**	++	1,6	-	13,0	+	**9,8**	+	-1,1	+	**8,0**	+	1,4
Hs.145140	Integrin, alpha 4 (antigen CD49D, alpha 4 subunit of VLA-4	ITGA4	2q31-q32	++	86,0	++	-2,1	++	1,4	+	**-2,5**	++	1,6	++	46,0	++	1,9	++	-1,3	++	-1,4	++	-1,1
Hs.149846	Integrin, beta 5	ITGB5	3q21.2	++	537,0	++	1,5	++	1,9	++	1,1	++	1,5	++	657,0	++	1,3	++	1,7	++	**-2,5**	++	**4,0**
Hs.212296	integrin, alpha 6	ITGA6	2q31.1	++	143,0	++	1,7	++	1,0	++	**2,1**	++	1,1	+	30,0	++	**7,0**	++	-1,3	++	1,9	++	**2,5**
Hs.524484	Integrin, alpha 7	ITGA7	12q13	-	16,0	-		-		-		-		+	13,0	-		-		-		-	
Hs.385521	integrin, alpha X (antigen CD11C (p150), alpha polypeptide	ITGAX	16p11.2	++	742,0	++	-1,6	++	**3,0**	++	1,7	++	-1,6	++	300,0	++	1,7	+	**-2,8**	++	-1,4	++	**4,9**
Hs.92033	integrin-linked kinase-associated serine/threonine phosphat	ILKAP	2q37.3	++	132,0	++	-1,2	++	**2,5**	++	1,4	++	-1,2	++	84,0	++	1,0	++	1,1	++	-1,1	++	1,4
0	**Chemokines**																						
Hs.78913	Chemokine (C-X3-C motif) receptor 1	CX3CR1	3p21.3	++	170,0	+	**-8,6**	-	-1,4	-	**-10,6**	-	-1,1	+	21,0	-	-1,4	+	3,0	+	-1,7	-	3,5
Hs.159553	Chemokine-like receptor 1	CMKLR1	12q24.1	++	164,0	++	-1,7	++	**2,3**	+	-1,7	++	1,9	++	298,0	+	**-2,6**	++	-1,2	+	**-3,7**	++	**2,1**
Hs.511794	chemokine (C-C motif) receptor 2	CCR2	3p21	++	429,0	+	**-7,0**	+	2,0	+	**-4,3**	+	-1,7	+	86,0	+	1,1	+	-1,1	+	-1,7	+	1,2
Hs.198252	chemokine (C-X-C motif) receptor 3	CXCR3	xq13	+	48,0	+	**-2,3**	+	-1,3	+	1,3	+	1,2	+	53,0	+	-1,2	++	1,6	+	-1,2	+	-1,9
Hs.421986	chemokine (C-X-C motif) receptor 4	CXCR4	2q21	++	877,0	++	**-2,1**	++	-1,1	++	-1,2	++	**2,0**	++	906,0	++	1,5	++	**-2,3**	++	1,1	++	**-2,6**
Hs.1652	chemokine (C-C motif) receptor 7	CCR7	17q12-q21.2	+	134,0	-	**-18,4**	+	**9,8**	+	**-2,0**	+	-1,5	+	28,0	+	1,0	-	1,0	+	**2,6**	+	-6,5
Hs.89714	chemokine (C-X-C motif) ligand 5	CXCL5	4q12-q13	++	315,0	+	**-12,1**	+	3,0	+	**-4,0**	+	-1,4	++	318,0	+	**-4,6**	+	-1,1	++	**-10,6**	++	2,0
Hs.164021	chemokine (C-X-C motif) ligand 6 (granulocyte chemotactic	CXCL6	4q21	+	51,0	+	**-3,5**	++	3,2	++	1,1	++	-1,3	++	22,0	++	1,5	++	-1,3	++	-1,3	++	2,3
Hs.271387	chemokine (C-C motif) ligand 8	CCL8	17q11.2	++	275,0	++	-1,1	++	1,0	+	**-3,2**	++	**2,0**	++	417,0	++	**-2,0**	++	1,5	+	**-10,6**	++	**18,4**
Hs.413924	chemokine (C-X-C motif) ligand 10	CXCL10	4q21	+	143,0	+	-1,6	+	1,7	+	-1,3	++	**2,0**	+	73,0	+	1,6	+	1,1	+	-1,1	++	**5,7**
Hs.16530	chemokine (C-C motif) ligand 18 (pulmonary and activation-	CCL18	17q11.2	++	333,0	++	**-2,5**	++	3,7	+	**-2,6**	++	1,7	++	306,0	++	**-2,0**	++	1,0	++	**-2,8**	++	**3,2**
Hs.458425	putative chemokine receptor	GPR109B	12q24.31	++	138,0	++	**4,9**	+	**-8,0**	++	**4,3**	++	1,2	+	50,0	++	**3,2**	+	**-5,3**	+	**-2,0**	++	**4,9**
0	**Purinergic Receptors**																						
Hs.41735	purinergic receptor P2X, ligand-gated ion channel, 1	P2RX1	17p13.3	++	160,0	+	**-2,1**	++	1,7	+	-1,6	++	1,6	++	174,0	++	1,1	+	-1,5	+	**-3,0**	++	1,4
Hs.321709	purinergic receptor P2X, ligand-gated ion channel, 4	P2RX4	12q24.32	++	523,0	++	1,9	++	**-2,3**	++	1,4	++	**2,5**	++	515,0	++	**2,3**	++	**-2,0**	++	-1,1	++	-2,1
Hs.528636	purinergic receptor P2X, ligand-gated ion channel, 7	P2RX7	12q24	++	241,0	++	**2,0**	+	**-8,0**	++	-1,9	++	**2,6**	++	187,0	++	1,7	++	**-2,3**	++	1,1	+	**-6,1**
Hs.113275	purinergic receptor P2X-like 1, orphan receptor	P2RXL1	22q11.21	++	141,0	+	-1,7	+	2,1	+	-1,1	++	1,0	++	103,0	+	1,4	+	-1,2	++	-1,3	+	1,2
Hs.386296	purinergic receptor P2Y, G-protein coupled, 13	P2RY13	3q24	+	108,0	+	-1,7	+	1,4	-	**-9,8**	++	**21,1**	+	153,0	++	1,5	++	-1,6	-	**-21,1**	+	**9,8**

Table 12: Genes involved in regulation of membrane receptors

The LDL receptor was downregulated during E-LDL and Ox-LDL loading and upregulated during HDL_3 deloading in both genotypes. The low density lipoprotein-related protein (LRP) 1, 6 and 8 as well as the sortilin-related receptor, L (SORL1) and the very low density lipoprotein receptor (VLDLR) were downregulated during E-LDL loading in apoE3/3 macrophages but upregulated in apoE4/4 macrophages. Also E-LDL deloading with HDL_3 led to an inverse regulation of these receptors except of LRP8 but including the LDL receptor

related protein 1 (LRPAP1) with an upregulation in apoE3/3 but a downregulation in apoE4/4 macrophages. This indicates a differential response of apoE4/4 compared to apoE3/3 macrophages upon cholesterol loading. While apoE3/3 macrophages showed the expected regulation of LDL receptors with a downregulation during lipid loading to protect cells from an excess of cholesterol and an upregulation during lipid deloading, apoE4/4 macrophages showed the vice versa regulation. This could lead to cholesterol overloading of the cells leading to a higher risk of developing atherosclerosis.

LPS receptor CD14, as well as toll-like receptor 2 (TLR2), which is involved in CD14 signal transduction were inversely regulated between the two genotypes during E-LDL deloading. In apoE3/3 macrophages they were upregulated while in apoE4/4 macrophages they were downregulated during E-LDL deloading. TLR4 which is also involved in CD14 receptor signalling was downregulated during E-LDL and Ox-LDL loading in apoE3/3 macrophages while it was upregulated in apoE4/4 macrophages. During Ox-LDL deloading TLR4 was 4 fold upregulated in apoE3/3 macrophages but -1.5 fold downregulated in apoE4/4 macrophages.

The Fcγ-receptors Ia, IIa, IIIa (CD64, CD32 and CD16) were inversely regulated during E-LDL deloading with HDL_3 between the apoE3 and the apoE4 genotype. They were increased in apoE3/3 macrophages while they were decreased in apoE4/4 macrophages during E-LDL deloading. CD64 and CD16 were also inversely regulated during E-LDL loading between the two genotypes. While they were decreased in apoE3/3 macrophages they were increased in apoE4/4 macrophages during E-LDL loading. This could indicate an enhanced phagocytosis activity of apoE4/4 macrophages which could lead to an increased uptake of E-LDL through phagocytosis. During Ox-LDL deloading CD16 was 13.9 fold increased in apoE3/3 macrophages while it was -2.1 fold decreased in apoE4/4 macrophages.

Scavenger receptor class B, member 2 (SCARB2) was inversely regulated during Ox-LDL loading as well as during E-LDL and Ox-LDL deloading between the apoE3 and the apoE4 genotype. It was -2.3 fold downregulated during Ox-LDL loading in apoE3/3 macrophages while it was 2.0 fold upregulated in apoE4/4 macrophages. During E-LDL deloading it was -2.8 fold downregulated and during Ox-LDL deloading 6.1 fold upregulated in apoE3/3 macrophages. In apoE4/4 macrophages SCARB2 was 1.6 fold upregulated during E-LDL deloading and -2.0 fold downregulated during Ox-LDL deloading.

Most of the integrins/complement receptors showed a differentially regulation between apoE3/3 and apoE4/4 macrophages during E-LDL deloading. In the apoE3/3 macrophages they were upregulated during E-LDL deloading while in the apoE4/4 macrophages they were downregulated. All the receptors can be found in table 12.

6. ApoE3/3 macrophages compared with macrophages obtained from patients with ABCA1 deficiency (Tangier disease (TD))

6.1. Cell surface expression of sphingo- and glycosphingolipids

In a next set of experiments the surface expression of Cer, GSLs and GM1 ganglioside was compared between apoE3/3 macrophages and macrophages obtained from patients with ABCA1 deficiency (Tangier disease). The same protocol as in the previous experiments was used, with MCSF differentiation (day 1-7), E-LDL and Ox-LDL loading (day 4-6) and HDL_3 deloading (day 6-7) and cell surface expression of Cer, lactosylceramide (LacCer, CDw17), globotriaosylceramide (Gb_3Cer, CD77), dodecasaccharideceramide (CD65s) and GM1 ganglioside was analyzed by flow cytometry. Four different experiments were performed and means and standard deviations of the mean fluorescence intensities were calculated. Differences between apoE3/3 and Tangier macrophages that are significant in a student's t-test for independent samples at $p<0.05$ were indicated by an asterisk.

During the differentiation phase with MCSF from day 1 to day 7 the surface expression of Cer, Gb_3Cer and also GM1 ganglioside was lower in Tangier macrophages compared to apoE3/3 macrophages (Fig.61A,B;E,F;I,J) while the surface expression of LacCer and CD65s during MCSF differentiation was nearly the same in apoE3/3 and Tangier macrophages. (Fig.61C,D;G,H). During E-LDL loading of apoE3/3 and Tangier macrophages the surface expression of Cer, Gb_3Cer and GM1 ganglioside was slightly induced compared to MCSF differentiated cells (Fig.61A,B;E,F;I,J) while CD65s showed no induction during E-LDL loading (Fig.61G,H). However LacCer surface expression was reduced in Tangier compared to apoE3/3 macrophages during E-LDL loading (Fig.61C,D). During Ox-LDL loading cell surface expression of all measured cell surface markers Cer, CDw17, CD65s, CD77 and GM1 ganglioside was compared to MCSF differentiated cells only significantly induced in apoE3/3 but not in ABCA1 deficient (Tangier) macrophages (Fig.61A-J).

During HDL_3 deloading no significant changes between apoE3/3 and Tangier macrophages could be observed.

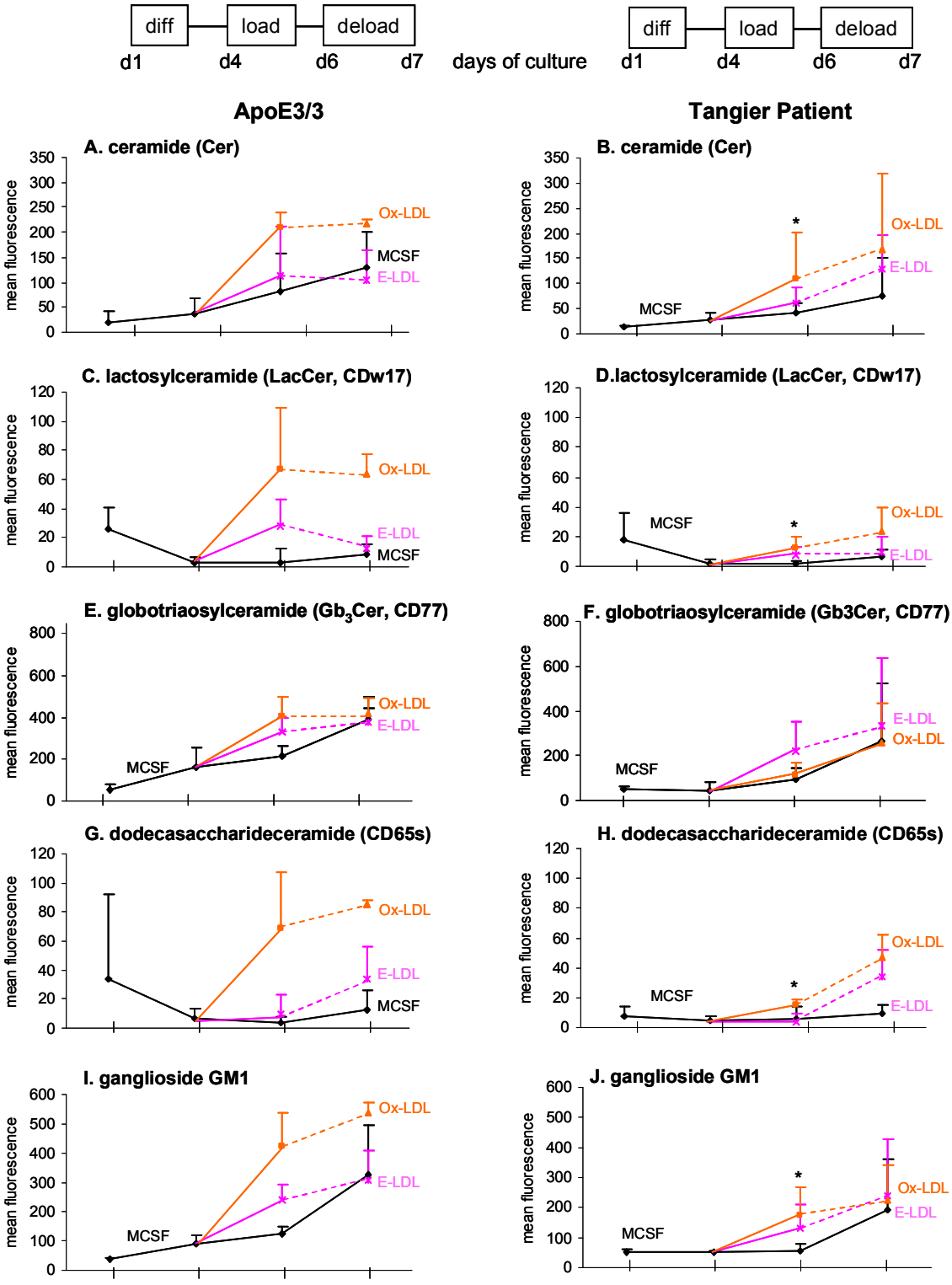

Figure 61: Surface expression of membrane ceramide, glycosphingolipids and GM1 ganglioside of ApoE3/3 vs. Tangier macrophages
Cell surface expression of ceramide (A,B), lactosylceramide (C,D), globotriaosylceramide (E,F), dodecasaccharideceramide (G,H), and ganglioside GM1 (I,J) of apoE3/3 homozygous macrophages vs. macrophages obtained from tangier patients measured by flow-cytometry.

6.2. Extracellular (surface) and intracellular expression-analysis of proteins involved in cholesterol metabolism

In order to find out differences in the expression of proteins involved in cholesterol metabolism between apoE3/3 macrophages and macrophages obtained from Tangier-patients, extracellular (surface) and intracellular expression of apoE, apoC-I and CETP were measured by flow cytometry. Macrophages were analyzed during MCSF differentiation (day 1-7), E-LDL and Ox-LDL loading (48h, day 4 to day 6) and HDL_3 deloading (day 6 to day 7). Four independent experiments were performed and means and standard deviations of the mean flourescence intensities were calculated.

6.2.1. ApoE

ApoE surface expression was increased from day 1 to day 4 in apoE3/3 and in Tangier macrophages (Fig.62A,B). From day 4 to day 6 almost no change could be observed in the apoE3 genotype while there was an increase of apoE surface expression in “Tangier”-macrophages (Fig.62A,B). From day 6 to day 7 in apoE3/3 and Tangier macrophages an increase could be observed which was higher in apoE3/3 macrophages (Fig.62A,B). During lipid loading apoE surface expression increased in apoE3/3 macrophages to a higher extent with E-LDL than with Ox-LDL loading compared to MCSF (Fig.62A). In Tangier macrophages apoE surface expression was only increased with E-LDL loading but not to the level of the apoE3 genotype and there was no change during Ox-LDL loading compared to MCSF (Fig.62B). During HDL_3 deloading in apoE3/3 and Tangier macrophages a decrease of apoE surface expression could be observed compared to lipid loading (Fig.62A,B).

Intracellular expression of apoE was lower in Tangier macrophages compared to apoE3/3 macrophages at all states of incubation. It increased from day 1 to day 6 in apoE3/3 macrophages to a higher level than in Tangier macrophages and decreased from day 6 to day 7 (Fig.59C). In Tangier macrophages apoE intracellular expression was only slightly increased from day 1 to day 4 and almost no change occured from day 4 to day 6 while it was increased from day 6 to day 7 (Fig.62D). During E-LDL loading of apoE3/3 macrophages apoE intracellular expression was slightly increased while it was decreased during Ox-LDL loading (Fig.62C). In Tangier macrophages almost no change of intracellular apoE expression could be observed during lipid loading and the apoE expression was much lower compared with apoE3/3 macrophages (Fig.62D). During HDL_3 deloading apoE intracellular expression was decreased in apoE3/3 macrophages while it was slightly increased in Tangier macrophages compared with lipid loading (Fig.62C,D).

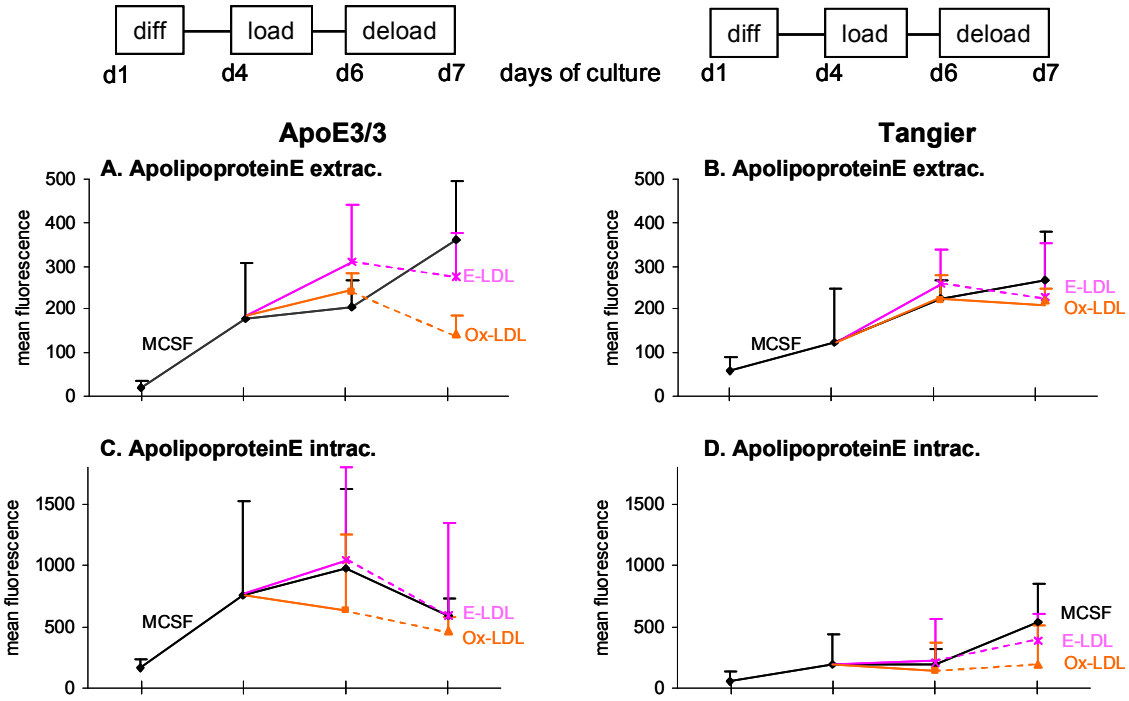

Figure 62: Extracellular (surface) (A,B) and intracellular expression (C,D) of apoE in apoE3/3 (left column) and Tangier macrophages (right column) measured by flow cytometry.

6.2.2. ApoC-I

In apoE3/3 macrophages apoC-I surface expression was slightly increased during MCSF differentiation from day 1 to day 4, slightly decreased from day 4 to day 6 and increased from day 6 to day 7 (Fig.63A). ApoC-I surface expression in Tangier macrophages showed almost no regulation during MCSF differentiation from day 1 to day 6 but it was increased from day 6 to day 7 (Fig.63B). During Ox-LDL loading a strong increase of apoC-I surface expression could be observed in apoE3/3 macrophages compared to MCSF while in Tangier macrophages the increase was lower (Fig.63A,B). E-LDL loading led in apoE3/3 and in Tangier macrophages to a slight increase of apoC-I surface expression (Fig.63A,B). Ox-LDL deloading with HDL_3 of apoE3/3 macrophages didn't change the surface expression of apoC-I while E-LDL deloading led to an increase of apoC-I surface expression compared to lipid loading (Fig.63A). HDL_3 deloading of Tangier macrophages led to an increase of apoC-I surface expression compared to E-LDL and Ox-LDL loading (Fig.63B).

Intracellular expression of apoC-I during MCSF differentiation was similar in apoE3/3 and Tangier macrophages (Fig.63C,D). It increased from day 1 to day 4, didn't change from day 4 to day 6 and increased again from day 6 to day 7 (Fig.63C,D). During Ox-LDL loading an increase of apoC-I surface expression could be observed compared to MCSF in apoE3/3 as well as in Tangier macrophages to the same extent (Fig.63C,D). E-LDL loading showed a slight increase in apoE3/3 macrophages but a slight decrease in Tangier macrophages compared to MCSF (Fig.63C,D). HDL_3 deloading didn´t change the intracellular expression of apoC-I in apoE3/3 macrophages while in Tangier macrophages during E-LDL deloading an

increase of apoC-I intracellular expression could be observed compared to lipid loading (Fig.63C,D).

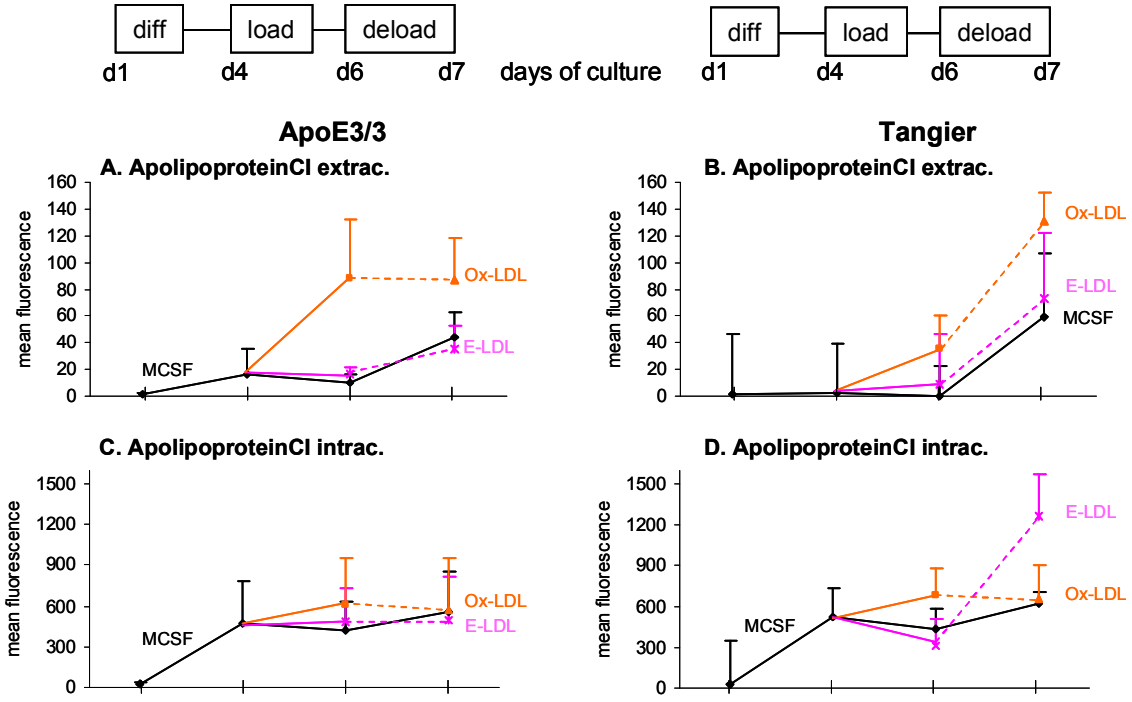

Figure 63: Extracellular (surface) (A,B) and intracellular expression (C,D) of apoC-I in apoE3/3 (left column) and Tangier macrophages (right column) measured by flow cytometry.

6.2.3. CETP

CETP surface expression was increased during MCSF differentiation from day 1 to day 7 to a higher level in apoE3/3 than in Tangier macrophages (Fig.64A,B). E-LDL loading increased CETP surface expression in apoE3/3 macrophages while there was no change of CETP surface expression in Tangier macrophages compared to MCSF (Fig.64A,B). Ox-LDL loading led in apoE3/3 and in Tangier macrophages to a decrease of CETP surface expression compared to MCSF (Fig.64A,B). E-LDL deloading with HDL_3 led to a slight increase while Ox-LDL deloading led to a slight decrease of CETP surface expression in apoE3/3 macrophages compared to lipid loading (Fig.64A). HDL_3 deloading of Tangier macrophages increased CETP surface expression compared to E-LDL and Ox-LDL loading (Fig.64B).

Intracellular expression of CETP was increased during differentiation with MCSF from day 1 to day 6 in apoE3/3 and in Tangier macrophages (Fig.64C,D). From day 6 to day 7 almost no change of CETP intracellular expression could be observed in apoE3/3 macrophages while an increase was observed in Tangier macrophages (Fig.64C,D). Lipid loading decreased intracellular CETP expression in both genotypes with a stronger decrease during Ox-LDL than during E-LDL loading (Fig.64C,D). E-LDL deloading of apoE3/3 macrophages increased while Ox-LDL deloading decreased CETP intracellular expression slightly compared to lipid loading (Fig.64C). In Tangier macrophages a strong increase during E-LDL deloading and a

strong decrease during Ox-LDL deloading could be observed compared to E-LDL and Ox-LDL loading (Fig.64D).

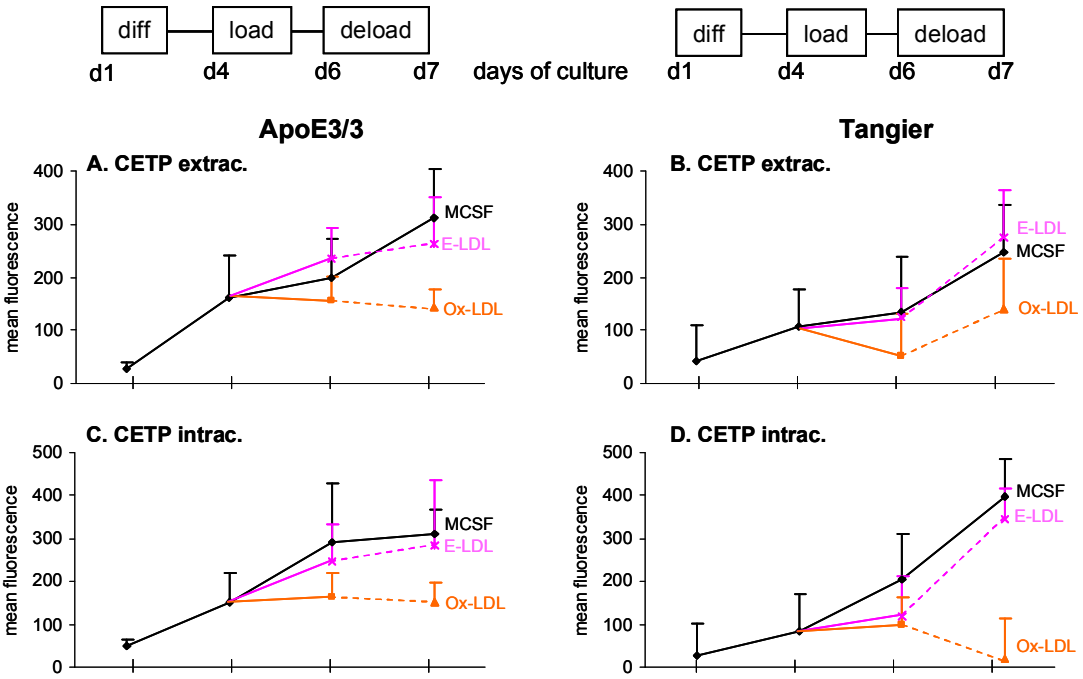

Figure 64: Extracellular (surface) (A,B) and intracellular expression (C,D) of CETP in apoE3/3 (left column) and Tangier macrophages (right column) measured by flow cytometry.

6.3. Intracellular expression analysis of adipophilin

Intracellular expression of adipophilin didn't change from day 1 to day 4 of MCSF differentiation and increased from day 4 to day 7 in apoE3/3 and Tangier macrophages (Fig.65A,B). E-LDL loading increased adipophilin expression to a higher level in Tangier than in apoE3/3 macrophages (Fig.65A,B) compared to MCSF. Ox-LDL loading didn´t change adipophilin expression in apoE3/3 macrophages while it decreased adipophilin expression in Tangier macrophages (Fig.65A,B) compared to MCSF. E-LDL deloading with HDL_3 decreased adipophilin expression in apoE3/3 macrophages while it increased adipophilin expression in Tangier macrophages compared to E-LDL loading. Ox-LDL deloading with HDL_3 increased adipophilin expression in apoE3/3 and in Tangier macrophages compared to Ox-LDL loading (Fig.65A,B).

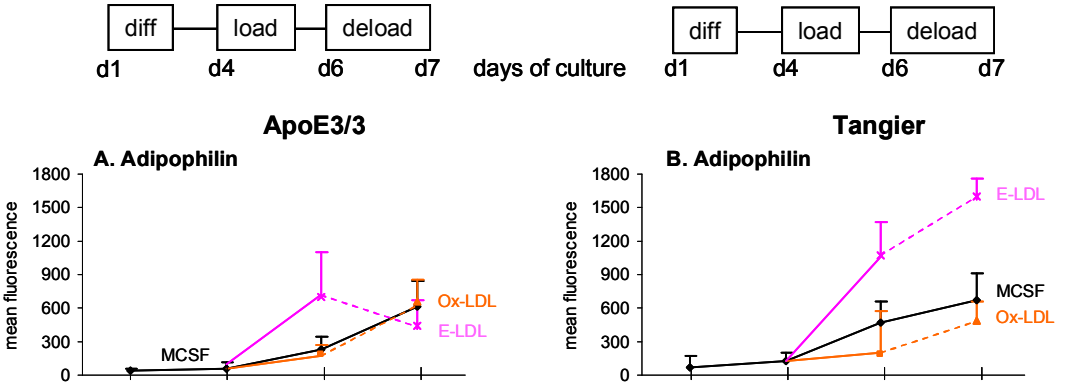

Figure 65: Intracellular expression of adipophilin in apoE3/3 (A) and Tangier macrophages (B)

7. ApoE3/3 macrophages compared with macrophages obtained from a patient with Hypertrigylceridemia (normal HDL, high VLDL and LDL) and coronary heart disease

In contrast to macrophages obtained from Tangier patients which have low HDL and normal VLDL and LDL , macrophages obtained from a patient with hypertriglyceridemia (HTG) with normal HDL but high VLDL and LDL (like familial hyperlipidemia) were analyzed. Macrophages of the HTG patient were isolated by elutriation, differentiated with MCSF up to 4 days, loaded with E-LDL (day 4-6) and deloaded with HDL_3 (day 6 to day 7). The surface expression of Cer, GSLs and GM1 ganglioside was analyzed by flow cytometry. Further surface- and intracellular expression of proteins which are involved in cholesterol transport namely apoE, apoC-I and CETP, and also of adipophilin a marker for lipid loading was analyzed by flow cytometry. The results were compared to that obtained from apoE3/3 macrophages which were considered as the healthy control group.

7.1. Cell surface expression of sphingo- and glycosphingolipids

The surface expression of membrane Cer, lactosylceramide (LacCer, CDw17), globotriaosylceramide (Gb_3Cer, CD77), dodecasaccharideceramide (CD65s) and GM1 ganglioside was analyzed by flow cytometry during differentiation with MCSF (day 1-7), E-LDL loading (day 4-6) and HDL_3 deloading (day 6-7). The experiment was performed of a patient with hypertriglyceridemia (HTG) and compared to the results obtained from macrophages of the apoE3/3 genotype.

During differentiation with MCSF, macrophages of the patient with HTG, showed no change of Cer surface expression during day 1 to day 4 while it was increased from day 4 to day 6 and decreased from day 6 to day 7. In apoE3/3 macrophages Cer surface expression increased during differentiation from day 1 to day 7 (Fig.66A). E-LDL loading led to an increase of Cer surface expression compared to MCSF in apoE3/3 macrophages but not in macrophages obtained from the patient with HTG (Fig.66A). During E-LDL deloading with HDL_3, Cer surface expression increased compared to E-LDL loading in macrophages of the HTG while it was decreased in apoE3/3 macrophages (Fig.66A). LacCer surface expression was decreased during differentiation from day 1 to day 4, showed almost no change from day 4 to day 6 and increased from day 6 to day 7 in apoE3/3 and HTG macrophages (Fig.66B). E-LDL loading compared to MCSF differentiation led in apoE3/3 macrophages to a higher increase of LacCer surface expression compared with macrophages obtained from the HTG patient which showed only a slight increase of LacCer surface expression (Fig.66B). HDL_3 deloading led to a decrease of LacCer surface expression in apoE3/3 macrophages compared to E-LDL loading while in HTG macrophages HDL_3 deloading further increased LacCer surface expression (Fig.66B). Gb_3Cer surface expression increased during MCSF differentiation from day 1 to day 7 to a higher level in apoE3/3 than in HTG macrophages

(Fig.66C). E-LDL loading led in both types of macrophages to an increase of Gb_3Cer surface expression (Fig.66C). HDL_3 deloading slightly increased Gb_3Cer expression in apoE3/3 macrophages while it didn´t change Gb_3Cer surface expression of HTG macrophages (Fig.66C). A higher surface expression level of CD65s was observed in macrophages of the HTG patient compared with apoE3/3 macrophages. From day 1 to day 4 of differentiation, CD65s surface expression was decreased in HTG and apoE3/3 macrophages and from day 4 to day 7 almost no further changes could be observed (Fig.66D). CD65s surface expression didn´t change during E-LDL loading while it was increased during HDL_3 deloading in both types of macrophages (Fig.66D). GM1 ganglioside surface expression didn't change during MCSF differentiation in macrophages of the HTG patient (Fig.66E), while in apoE3/3 macrophages GM1 ganglioside surface expression increased during differentiation from day 1 to day 7 (Fig.66E). E-LDL loading compared to MCSF led in apoE3/3 macrophages to an increase of GM1 ganglioside surface expression while in HTG macrophages no change could be observed (Fig.66E). HDL_3 deloading led in both types of macrophages to an increase of GM1 ganglioside expression with the highest level in apoE3/3 macrophages (Fig.66E).

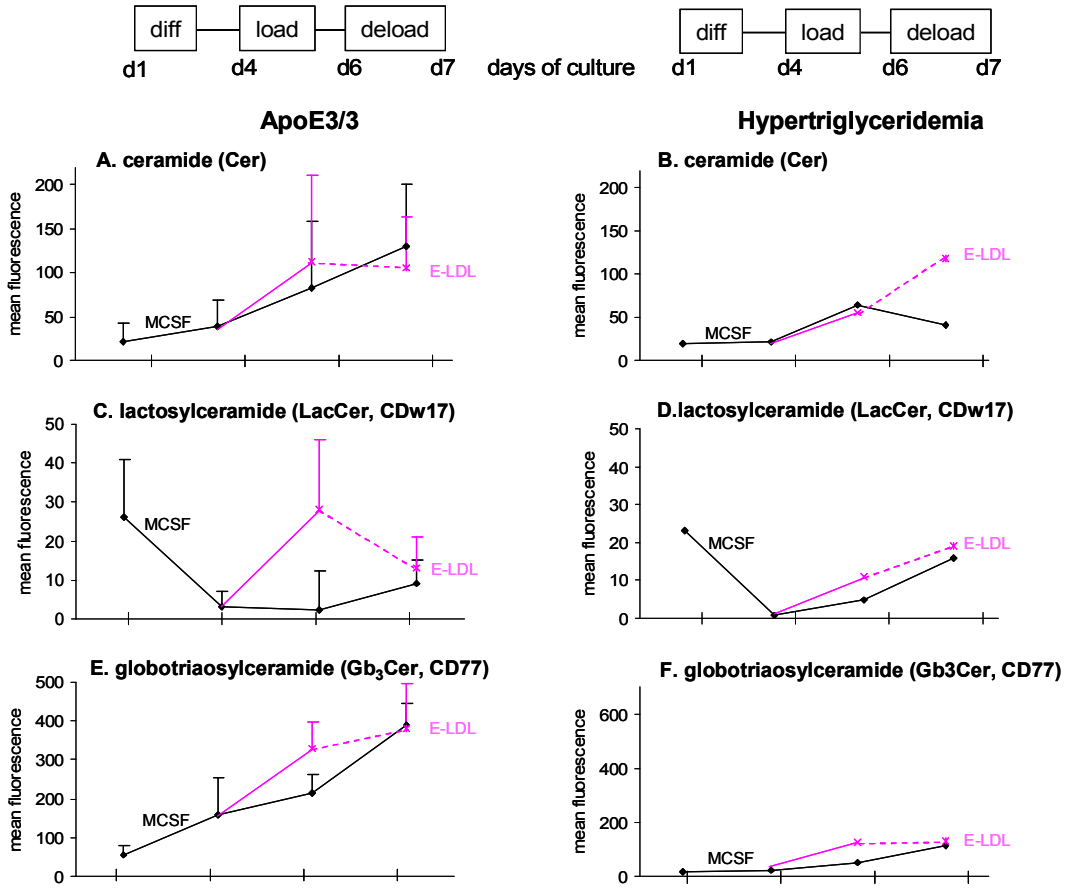

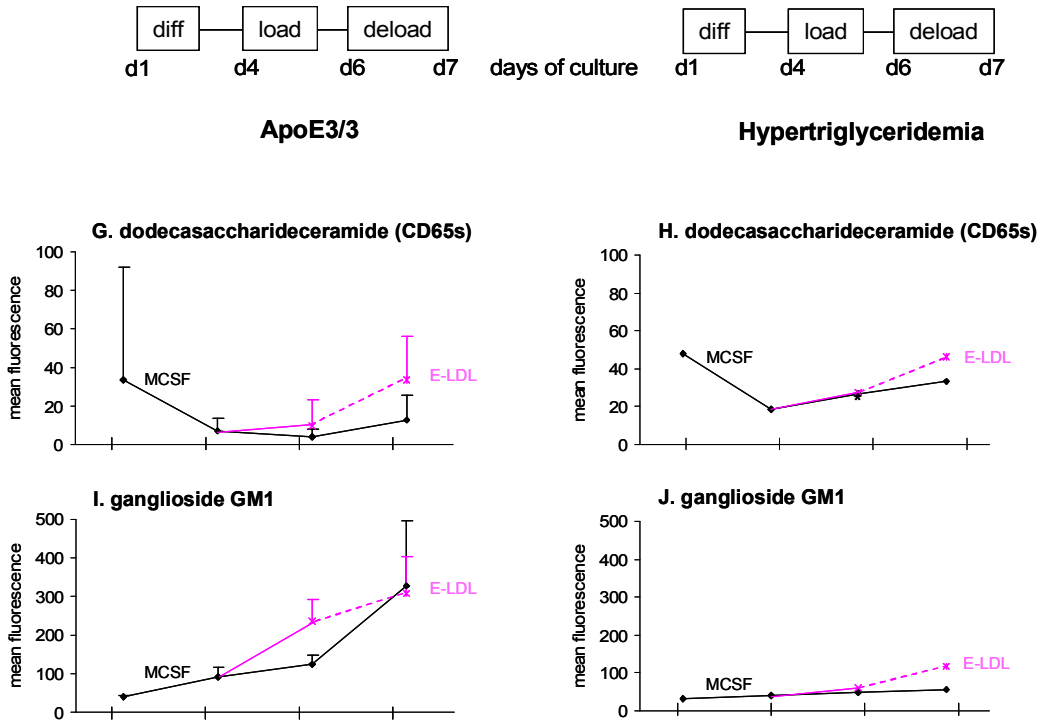

Figure 66: Surface expression of membrane ceramide (Cer), glycosphingolipids (GSLs) and GM1 ganglioside of macrophages obtained from macrophages of the apoE3/3 genotype and patient with hypertriglyceridemia (HTG)
Surface expression of Ceramide (Cer) (A), lactosylceramide (LacCer,CDw17) (B), globotriaosylceramide (Gb_3Cer, CD77) (C), dodecasaccharideceramide (CD65s) (D) and GM1 ganglioside (E) was analyzed by flow cytometry.

7.2. Extracellular (surface) and intracellular expression analysis of proteins involved in cholesterol metabolism

Further extracellular- and intracellular expression of proteins involved in cholesterol metabolism namely apoE, apoC-I and CETP was analyzed by flow cytometry. The experiment was performed like the previous described under 7.2.1. without Ox-LDL loading and deloading.

7.2.1. ApoE

During MCSF differentiation from day 6 to day 7 apoE surface expression was increased to a higher level in apoE3/3 compared to HTG macrophages (Fig.67A,B). E-LDL loading of apoE3/3 macrophages led to an increase of apoE surface expression compared to MCSF, while macrophages of the HTG revealed no change (Fig.67A,B). E-LDL deloading with HDL_3 decreased apoE surface expression of apoE3/3 macrophages while there was almost no change of apoE surface expression of HTG macrophages compared to E-LDL loading (Fig.67A,B).

ApoE intracellular expression increased during MCSF differentiation from day 1 to day 6 in apoE3/3 and HTG macrophages (Fig.67C,D). During day 6 to day 7 of differentiation apoE intracellular expression decreased in apoE3/3 macrophages while it further increased in HTG macrophages (Fig.67C,D). E-LDL loading compared to MCSF didn´t change apoE intracellular expression of apoE3/3 macrophages while it slightly increased apoE intracellular expression of HTG macrophages (Fig.67C,D). During E-LDL deloading with HDL_3 apoE intracellular expression of apoE3/3 and HTG macrophages was decreased (Fig.67C,D).

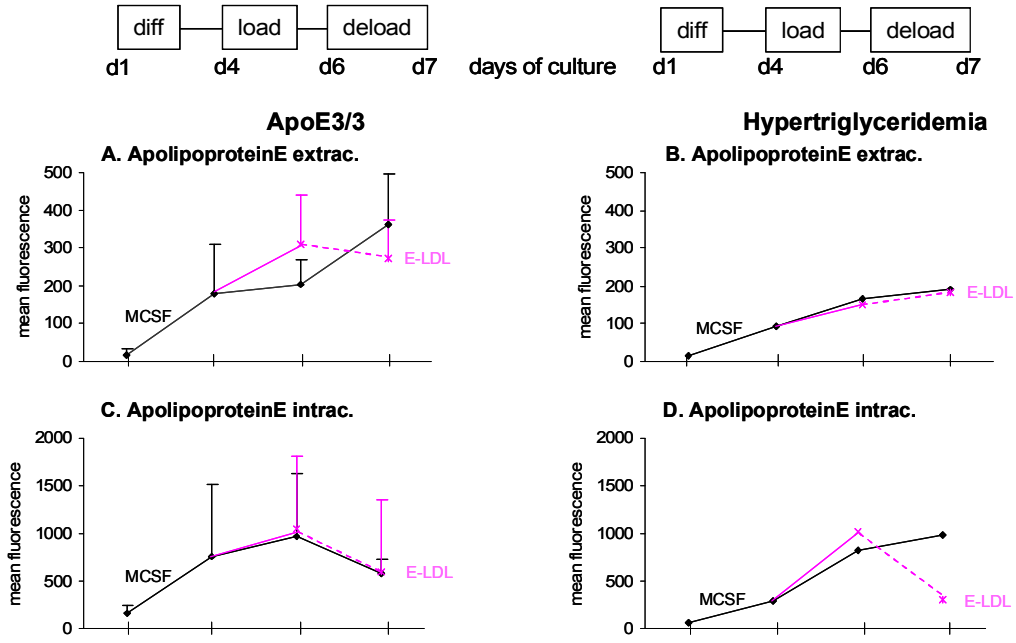

Figure 67: Extracellular (surface) (A) and intracellular expression (B) of apoE.
Macrophages obtained from the apoE3/3 genotype and from a patient with hypertriglyceridemia (HTG)

7.2.2. ApoC-I

ApoC-I surface expression of apoE3/3 macrophages was increased from day 1 to day 4 of MCSF differentiation while in HTG macrophages it was decreased (Fig.68A,B). From day 4 to day 6 of MCSF differentiation it was decreased and from day 6 to day 7 of MCSF differentiation it was increased in both types of macrophages (Fig.68A,B). E-LDL loading of apoE3/3 macrophages led to a slight increase of apoC-I surface expression while in macrophages of the HTG patient no change of apoC-I surface expression could be observed compared to MCSF (Fig.68A,B). During HDL_3 deloading both types of macrophages showed an increase of apoC-I surface expression compared to E-LDL loading (Fig.68A,B).

ApoC-I intracellular expression of apoE3/3 macrophages showed an increase during day 1 to day 4 of MCSF differentiation, a slight decrease during day 4 to day 6 and a slight increase during day 6 to day 7 of MCSF differentiation (Fig.68C). No apoC-I surface expression could be detected on HTG macrophages during day 1 to day 4 while it was increased during day 4 to day 7 of MCSF differentiation. The apoC-I intracellular expression was slightly increased

during E-LDL loading in both types of macrophages compared to MCSF. HDL_3 deloading led to no further changes of apoC-I intracellular expression (Fig.68B).

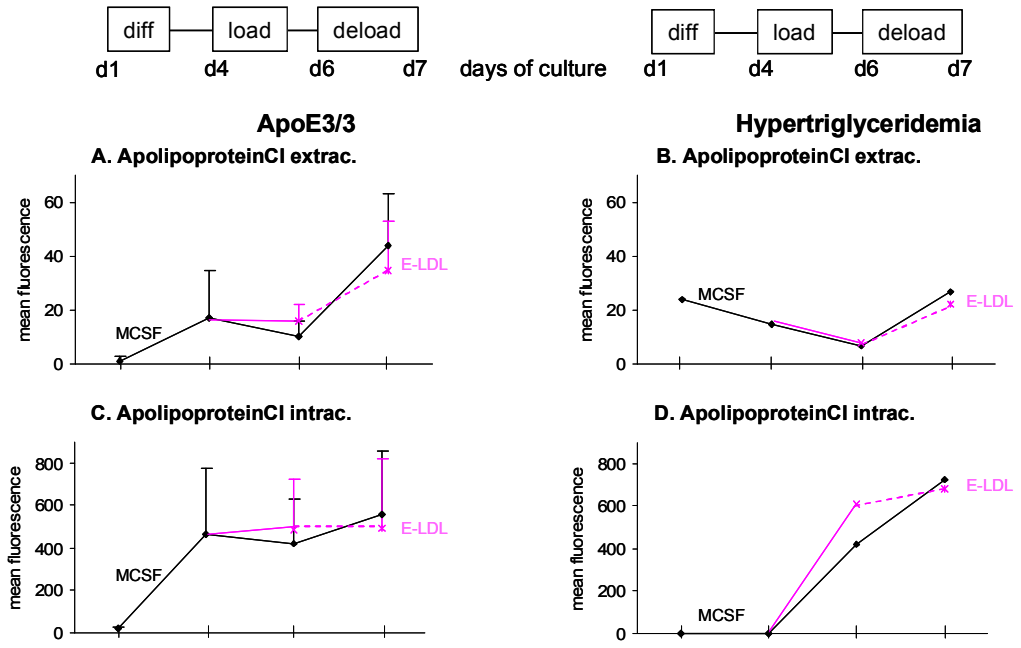

Figure 68: Extracellular (surface) (A) and intracellular expression (B) of apoC-I.
Macrophages obtained from the apoE3/3 genotype and a patient with hypertriglyceridemia (HTG)

7.2.3. CETP

CETP surface expression increased during differentiation from day 1 to day 4 in both types of macrophages (Fig.69A,B). During day 4 to day 7 of MCSF differentiation in apoE3/3 macrophages CETP surface expression was further increased while in macrophages of HTG patient almost no further change of CETP surface expression could be observed (Fig.69A,B). E-LDL loading led in apoE3/3 macrophages to an increase of CETP surface expression compared to MCSF while in HTG macrophages a slight decrease could be observed (Fig.69A,B). HDL_3 deloading slightly increased CETP surface expression of HTG and apoE3/3 macrophages compared to E-LDL loading (Fig.69A,B).

CETP intracellular expression was increased during MCSF differentiation from day 1 to day 6 to a higher level in apoE3/3 macrophages. From day 6 to day 7 CETP intracellular expression didn´t change in apoE3/3 macrophages while in HTG macrophages it was further increased. E-LDL loading led in apoE3/3 macrophages to a decrease of CETP intracellular expression while in HTG macrophages an increase of CETP intracellular expression compared to MCSF could be observed. HDL_3 deloading led in apoE3/3 macrophages to a slight increase of CETP intracellular expression while in HTG macrophages a decrease of CETP intracellular expression could be observed compared to E-LDL loading (Fig.69B).

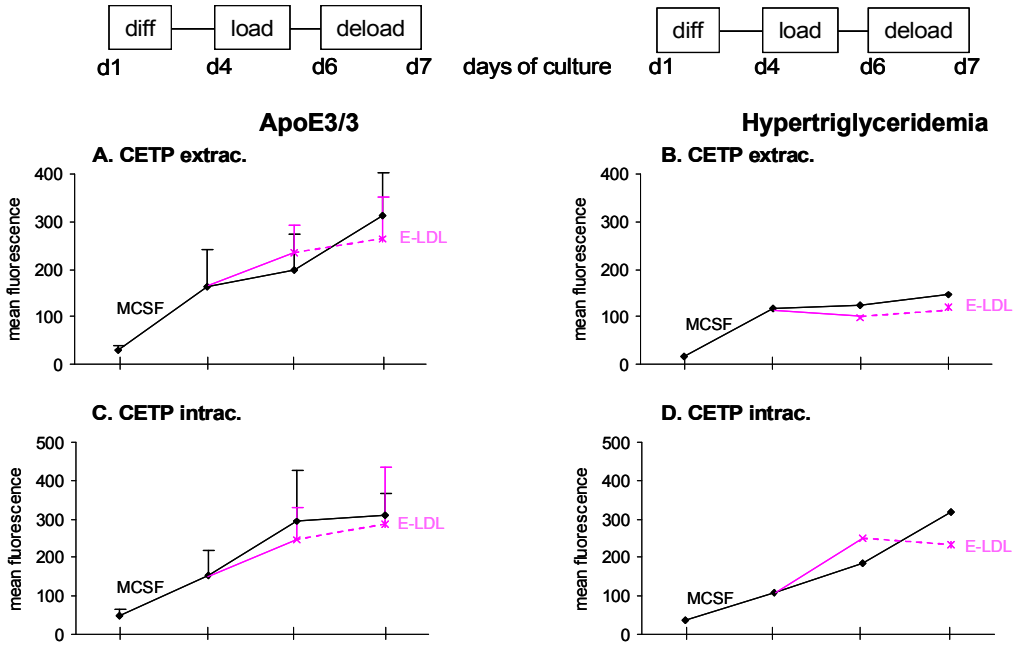

Figure 69: Extracellular (surface) (A) and intracellular expression (B) of CETP.
Macrophages obtained from the apoE3/3 genotype and a patient with hypertriglyceridemia (HTG)

7.3. Intracellular expression analysis of adipophilin

During MCSF differentiation from day 1 to day 4 almost no change of adipophilin expression could be observed in both types of macrophages (Fig.70A,B). During day 4 to day 6 of MCSF differentiation adipophilin expression was increased in apoE3/3 macrophages while it was slightly decreased in HTG macrophages. During day 6 to day 7 of differentiation adipophilin expression was increased in both types of macrophages (Fig.70A,B). E-LDL loading led to an increase of adipophilin expression compared to MCSF differentiation to a higher extent in apoE3/3 than in HTG macrophages (Fig.70A,B). HDL_3 deloading decreased adipophilin expression in apoE3/3 macrophages while it slightly increased it in HTG macrophages compared to E-LDL loading (Fig.70A,B).

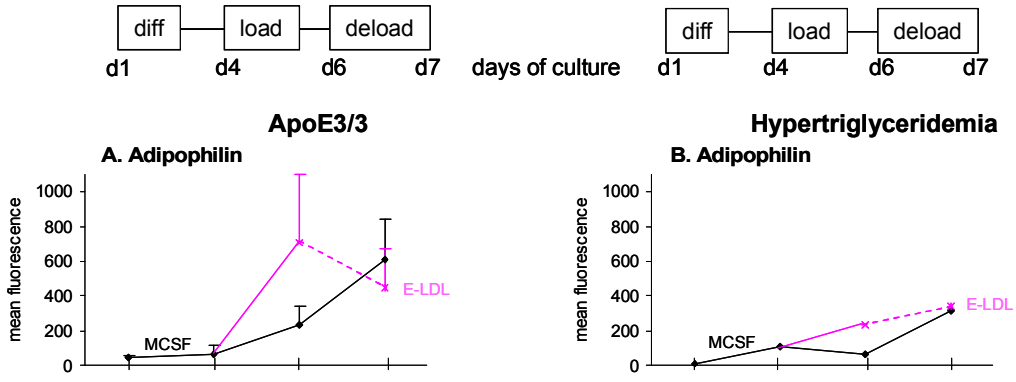

Figure 70: Intracellular expression of adipophilin.
Macrophages obtained from the apoE3/3 genotype and a patient with hypertriglyceridemia (HTG)

8. Incubation of ApoE3/3 macrophages with PPARγ and RXR agonists

8.1. Analysis of CD36 and apoE expression after incubation with PPARγ agonists

In a next set of experiments the influence of different PPARγ agonists on the surface expression of scavenger receptor CD36 (SRCD36) and on the surface and intracellular apoE expression was analyzed. SRCD36 was chosen because it is known that PPARγ induces SRCD36 and therefore it seems to be a key component of lipid uptake and apoE is known to be a direct target of LXR and therefore PPARγ sensitive. Monocytes were incubated from day 1 to day 4 with different glitazones solubilized in ethanol. The same amount of ethanol (Etoh) without glitazones was taken as a control. Three different experiments were performed and means of the mean fluorescence intensities and standard deviations were calculated. It could be observed that the surface expression of CD36 was upregulated during incubation with the different glitazones in comparison to Etoh as a control (Fig.71A). But no significant differences in the intensities between the different glitazones could be observed. However pioglitazone in a concentration of 5μM showed the greatest induction of CD36 (Fig.71A).

The apoE expression extracellular as well as intracellular was also induced during incubation with the different glitazones compared to Etoh as a control but no significant differences in their intensities could be detected (Fig.71B,C).

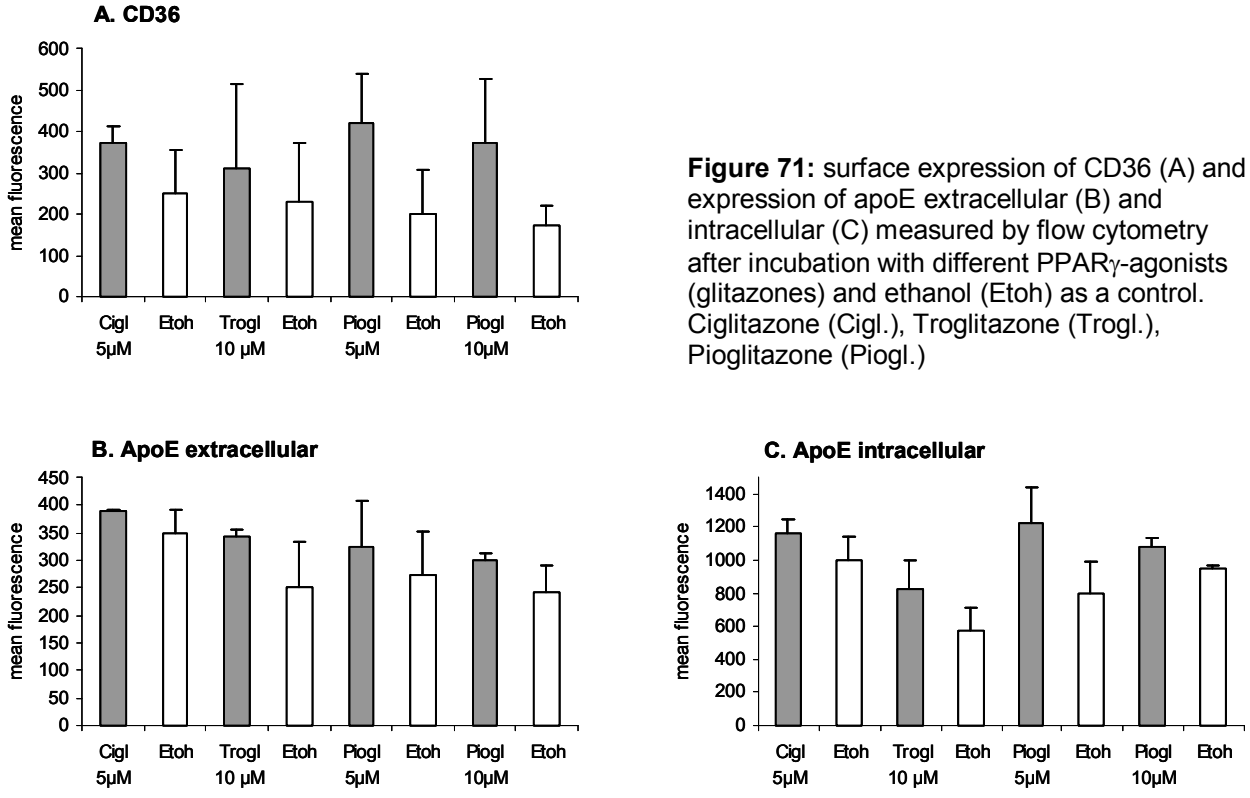

Figure 71: surface expression of CD36 (A) and expression of apoE extracellular (B) and intracellular (C) measured by flow cytometry after incubation with different PPARγ-agonists (glitazones) and ethanol (Etoh) as a control. Ciglitazone (Cigl.), Troglitazone (Trogl.), Pioglitazone (Piogl.)

8.2. Expression-analysis of cell surface receptors involved in lipid uptake and processing after incubation with RXR- and PPARγ-agonists

Further receptors involved in the monocyte innate immunity cluster and also other receptors involved in adhesion and signalling processes relevant for atherosclerosis were analyzed during incubation with RXR- and PPARγ-agonists. Monocytes were differentiated from day 1 to day 4 with MCSF. On day 4 they were incubated for 24h with the RXR agonists β-Carotene (5 μM), cis-retinoic-acid (10 μM) and all-trans-retinoic-acid (10 μM) as well as with the PPARγ-agonist rosiglitazone (30 μM). As a control MCSF differentiated cells respectively cells incubated with phosphatidylcholine (PC)-liposomes as the solvent for β-carotene or DMSO as the solvent for the other substances were taken. After 24h of incubation with the RXR- and PPARγ-agonists, respectively cells were harvested and cell surface expression of receptors involved in lipid uptake and processing was analyzed by flow cytometry. Results are shown in % change of MCSF as a control.

As examples of receptors which are involved in lipid uptake, the scavenger receptor class B CD36 and the phagocytosis receptors Fcγ-receptor III CD16 and Fcγ-receptor II CD32 were analyzed (Fig.72A,B,C). Incubation with the RXR agonist beta-carotene showed a decrease of cell surface expression of all three receptors compared with PC-liposomes which were used as a solvent (Fig.72A,B,C). Cis-retinoic-acid decreased surface expression of CD36 and CD32 compared to DMSO (Fig.72A,C). The surface expression of CD16 was slightly increased with cis-retinoic-acid compared to DMSO (Fig.72B). All-trans-retinoic-acid decreased the surface expression of CD36 and CD32 while there was no change of CD16 surface expression compared to DMSO (Fig.72A,C,B). The PPARγ-agonist rosiglitazone increased CD36 and CD16 expression but decreased surface expression of CD32 compared to DMSO (Fig.72A,C,B). Compared with MCSF only the incubation with rosiglitazone increased in the case of CD36 cell surface receptor expression while all the other stimuli revealed a decrease of cell surface receptor expression (Fig.72A,B,C).

The LPS receptor CD14 and the toll like receptors (TLRs) 2 and 4 which are involved in CD14 signalling were also analyzed (Fig.72D,E,F). During beta-carotene stimulation CD14 surface expression was increased while TLR 2 and 4 were decreased compared to incubation with PC-liposomes (Fig.72D,E,F). Cis-retinoic-acid led to a small decrease of CD14 surface expression and to a strong decrease of TLR 2 and 4 while all-trans-retinoic-acid decreased CD14 as well as TLR 2 and 4 almost to the same extent (Fig.72D,E,F). The PPARγ agonist rosiglitazone also decreased the surface expression of CD14 and the TLRs 2 and 4 (Fig.72D,E,F).

The adhesion molecules integrin-β2/CD18, integrin-αL/CD11a and integrin-αM/CD11b were also analyzed (Fig.72G,H,I). They play an important role in the adhesion of monocytes to the endothelium and following extravasation into the tissue with progression of atherosclerosis.

As the α subunit of the β2-integrin, CD11b forms a heterodimer complex with CD18 on the surface of granulocytes and monocyte/macrophages that is important in a variety of adherence-related activities and as a complement receptor which mediates the phagocytosis of opsonized particles. During incubation with beta-carotene CD18 and CD11b (complement receptor 3) were decreased while CD11a was slightly increased compared to incubation with PC-liposomes (Fig.72G,H,I). Incubation with cis-retinoic-acid and all-trans-retinoic-acid decreased cell surface expression of CD18, CD11a and CD11b compared to incubation with DMSO (Fig.72G,H,I). The PPARγ-agonist rosiglitazone increased expression of CD18 while the surface expression of CD11a and CD11b was slightly decreased compared to DMSO (Fig.72G,H,I).

The tetraspanin CD81, CD33 a member of the sialoadhesion family and CD95 the prototypical cell death receptor a member of TNF receptor family were decreased during incubation with beta-carotene compared to PC-liposomes (Fig.72J,K,L). Also the incubation with cis-retinoic-acid and all-trans retinoic acid decreased the surface expression of CD81, CD33 and CD95 compared to DMSO (Fig.72J,K,L). Rosiglitazone decreased CD81 and CD95 expression but had almost no influence on CD33 surface expression compared to DMSO (Fig.72J,K,L).

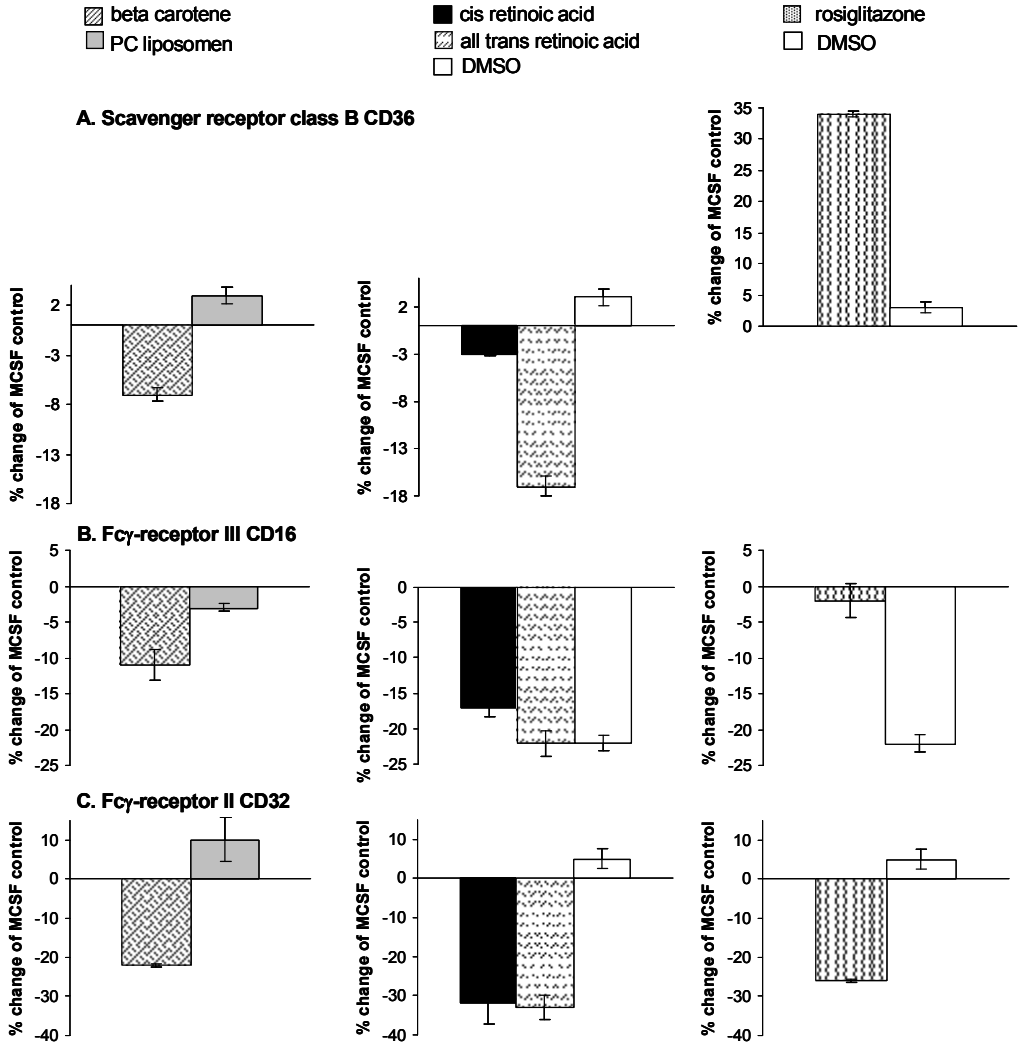

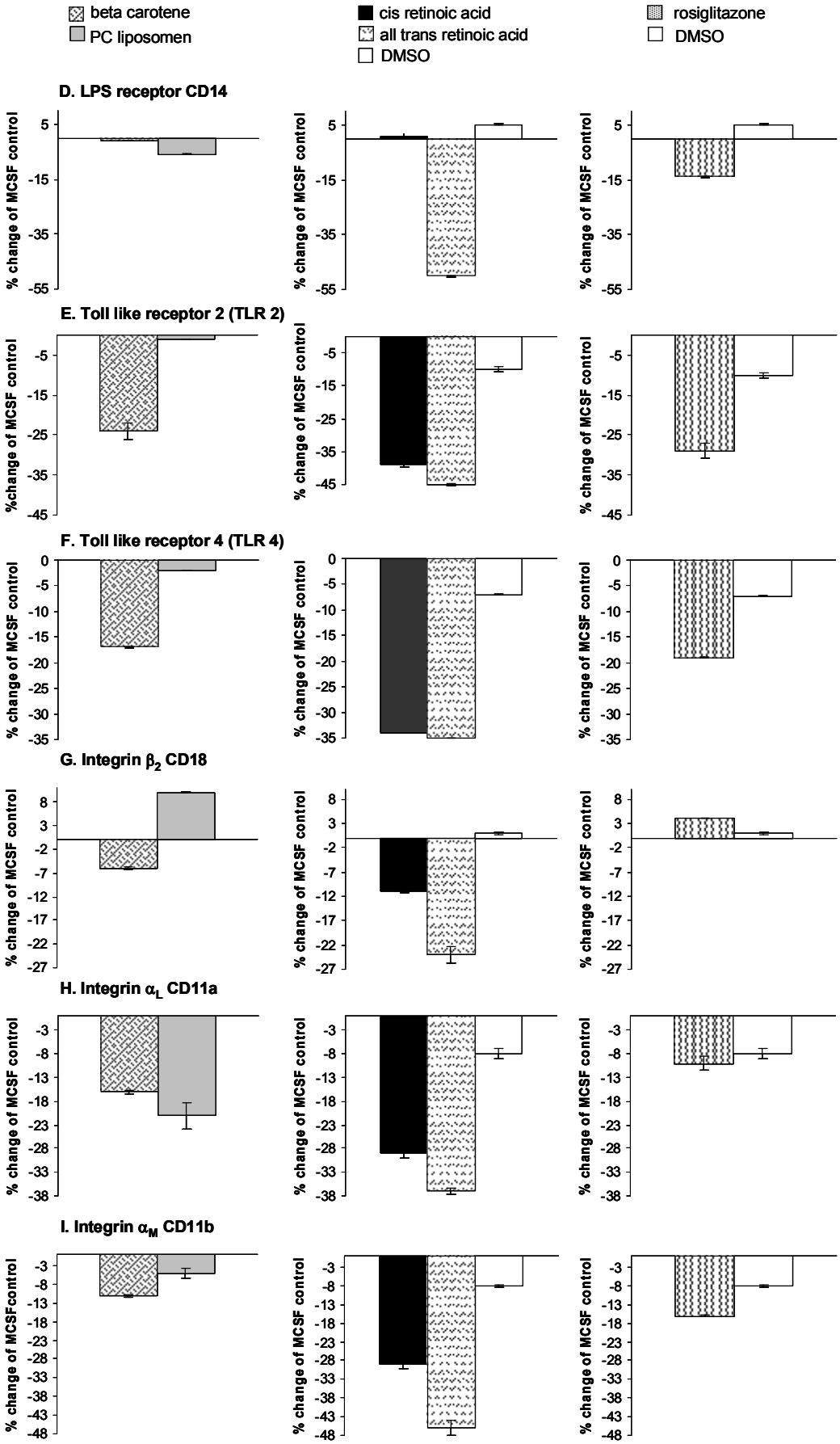
beta carotene
PC liposomen
cis retinoic acid
all trans retinoic acid
DMSO
rosiglitazone
DMSO
D. LPS receptor CD14
E. Toll like receptor 2 (TLR 2)
F. Toll like receptor 4 (TLR 4)
G. Integrin β2 CD18
H. Integrin αL CD11a
I. Integrin αM CD11b
% change of MCSF control
%change of MCSF control
% change of MCSFcontrol

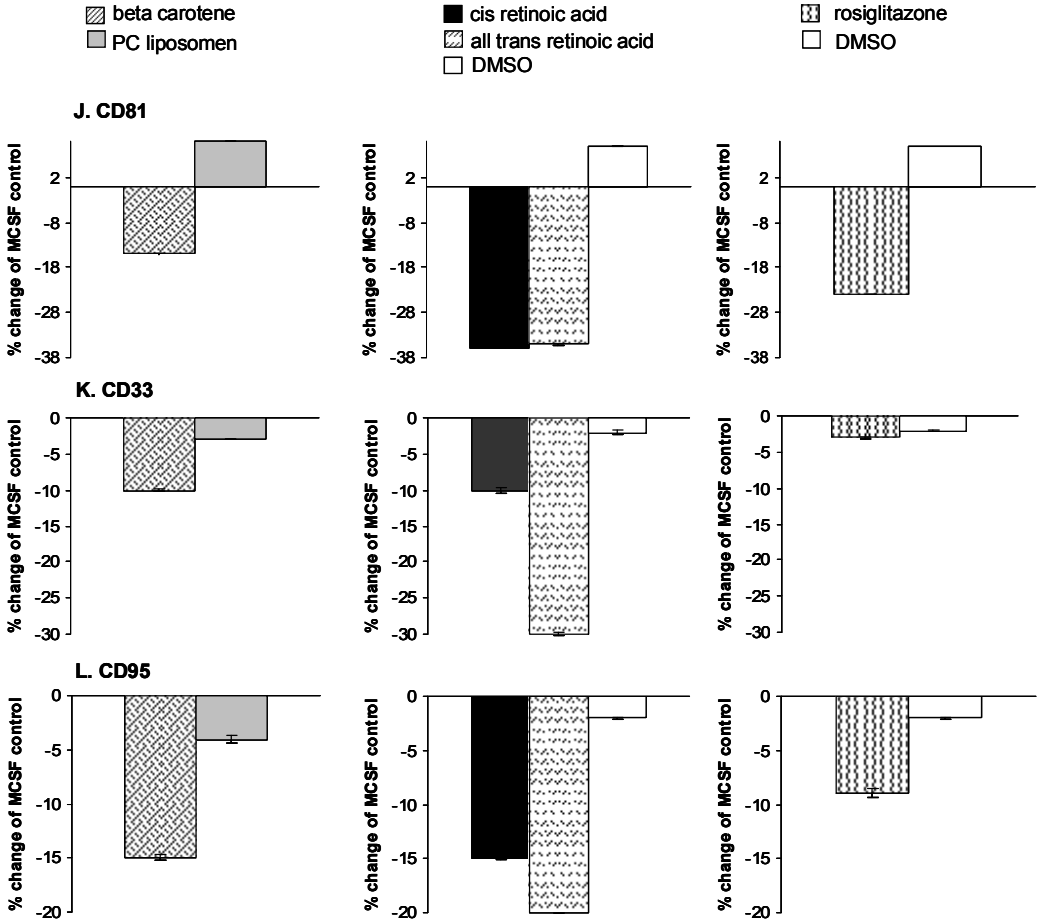

Figure 72: Surface expression analysis after incubation with the RXR agonists beta carotene, cis retinoic acid and all trans retinoic acid and the PPARγ agonist rosiglitazone compared with the solvents PC liposomes and DMSO as a control. Results are shown in % of MCSF as control.
CD36 (A), CD16 (B), CD32 (C), CD14 (D), TLR2 (E), TLR4 (F), CD18 (G), CD11a (H), CD11b (I), CD81 (J), CD33 (K), CD95 (L)

8.3. Retinoids induce genes of lipid metabolism in human monocytes/macrophages

Human monocytes and macrophages were stimulated in vitro with the retinoids β-carotene, 9-cis retinoic acid and all-trans retinoic acid and gene expression was analyzed by Affymetrix U133A GeneChips™. As indicated in table 13, genes involved in cellular lipid metabolism were significantly induced by these retinoids. β-carotene had the lowest effects, whereas 9-cis RA and ATRA where nearly equally potent in inducing genes of fatty acid metabolism, cholesterol metabolism, apolipoproteins and lipid-related transcription factors. Interestingly, both cell types, undifferentiated monocytes and in-vitro differentiated macrophages displayed a signifcant upregulation of mRNA levels of lipid genes even without prior cholesterol loading, which is a known potent stimulus of transcription for these genes including the ABC transporters ABCA1 and ABCG1, and apoE, which implies that retinoids have a strong impact on gene expression in human monocytes and macrophages.

Unigene	Title	Symbol	Chrom Location	1d_MCSF_p	1d_MCSF_Sig	1d_b Car_p	1d_b Car_FC	1d_9cisRA_p	1d_9cisRA_FC	1d_ATRA_p	1d_ATRA_FC	5d_MCSF_p	5d_MCSF_Sig	5d_b Car_p	5d_b Car_FC	5d_9cisRA_p	5d_9cisRA_FC	5d_ATRA_p	5d_ATRA_FC
	Fatty acid metabolism																		
Hs.83190	Fatty acid synthase	FASN	17q25	++	283	++	1,1	++	1,9	++	1,6	++	113	++	1,1	++	1,6	++	1,2
Hs.388164	fatty acid desaturase 2	FADS2	11q12-q13.1	++	446	++	1,2	++	2,0	++	1,4	++	337	+	1,0	++	1,7	++	1,1
Hs.119597	Stearoyl CoA desaturase	SCD	10q23-q24	++	699	++	1,1	++	2,5	++	2,1	++	779	++	-1,1	++	3,0	++	3,0
Hs.268012	Fatty-acid-Co A-ligase, long-chain 3	FACL3	2q34-q35	++	408	++	1,1	++	2,0	++	1,9	++	364	++	1,0	++	2,0	++	1,6
Hs.391561	fatty acid binding protein 4	FABP4	8q21	++	2219	++	-1,1	++	1,0	++	1,0	++	268	+	-1,3	++	2,3	++	1,6
Hs.409826	monoglyceride lipase	MGLL	3q21.3	++	311	++	1,6	++	2,6	++	2,3	++	667	++	1,1	++	-1,3	++	-1,3
Hs.416385	insulin induced gene 1	INSIG1	7q36	++	1128	++	1,3	++	1,9	++	1,9	++	521	++	1,0	++	1,3	++	1,3
Hs.443120	CD36	CD36	7q11.2	++	839	++	1,3	++	1,6	++	1,6	++	467	++	-1,1	++	2,5	++	1,9
	Cholesterol metabolism																		
Hs.11899	HMG-CoA reductase	HMGCR	5q13.3-q14	++	282	++	1,2	++	1,6	++	1,4	++	92	+	-1,1	++	1,1	++	1,0
Hs.252457	mevalonate decarboxylase	MVD	16q24.3	-	33	-	1,6	++	2,3	++	1,6	-	44	-	1,0	+	1,4	-	1,0
Hs.76038	Isopentenyl-diphosphate delta isomerase	IDI1	10p15.3	++	412	++	1,0	++	1,9	++	1,3	++	199	++	-1,1	++	1,1	++	-1,1
Hs.11806	7-dehydrocholesterol reductase	DHCR7	11q13.2-q13.5	++	166	++	1,1	++	1,6	++	1,2	+	128	+	1,1	++	1,7	+	1,3
Hs.213289	LDL-receptor	LDLR	19p13.3	++	393	++	1,1	++	1,7	++	1,4	++	234	++	-1,1	++	1,4	++	1,2
Hs.446331	Acyl-Co A: cholesterol acyltransferase	SOAT1	1q25	++	119	++	1,5	++	1,1	++	1,3	++	157	++	1,2	++	1,4	++	1,3
Hs.82568	steroid 27-hydroxylase	CYP27A1	2q33-qter	++	234	++	2,6	++	4,6	++	3,5	++	1678	++	1,2	++	1,3	++	1,3
Hs.139851	Caveolin 2	CAV2	7q31.1	+	16	-	1,1	+	-1,4	+	-1,3	-	14	+	2,5	+	1,5	+	1,4
Hs.404930	Niemann-Pick disease, type C1	NPC1	18q11-q12	++	181	++	1,0	++	1,4	++	1,5	++	971	++	-1,2	++	-1,4	++	-1,3
Hs.433222	Niemann-Pick disease, type C2	NPC2	14q24.3	++	2226	++	1,3	++	1,5	++	1,5	++	3119	++	1,1	++	1,0	++	1,1
Hs.147259	ATP-binding cassette transporter A1	ABCA1	9q31.1	++	186	++	1,1	++	3,5	++	4,0	++	371	++	-1,1	++	2,5	++	2,3
Hs.369055	ATP-binding cassette transporter G1	ABCG1	21q22.3	++	37	++	1,2	++	5,3	++	4,6	++	120	++	-1,1	++	4,6	++	4,6
	Apolipoproteins																		
Hs.268571	apolipoprotein C-I	APOC1	19q13.2	++	778	++	1,1	++	2,8	++	2,6	++	2069	++	1,1	++	1,9	++	1,9
Hs.75615	apolipoprotein C-II	APOC2	19q13.2	-	129	-	1,1	+	1,6	+	1,6	+	428	+	1,2	+	2,3	+	2,6
Hs.110675	apolipoprotein C-IV	APOC4	19q13.2	+	244	++	1,1	++	2,3	++	1,9	++	3226	++	1,1	++	1,1	++	1,2
Hs.169401	apolipoprotein E	APOE	19q13.2	++	238	++	1,4	++	2,8	++	3,5	++	3831	++	-1,1	++	1,2	++	1,1
	Transcription factors																		
Hs.426528	sterol regulatory element binding factor 1	SREBF1	17p11.2	+	152	+	1,0	++	2,3	++	2,0	+	131	++	1,1	++	2,1	++	1,9
Hs.108689	sterol regulatory element binding factor 2	SREBF2	22q13	+	133	++	1,2	++	1,6	++	1,4	++	187	+	1,0	+	1,1	++	1,1
Hs.361071	retinoic acid receptor, alpha	RARA	17q21	+	44	-	1,0	+	1,6	++	1,5	+	61	+	-1,1	++	1,4	+	1,5
Hs.387667	peroxisome proliferative activated receptor, gamma	PPARG	3p25	++	86	++	1,6	++	1,9	++	1,7	++	118	++	-1,1	++	1,3	++	1,5
Hs.438863	Liver X receptor, alpha	NR1H3	11p11.2	++	122	++	1,6	++	4,9	++	4,3	++	581	++	-1,1	++	1,7	++	1,7

Table 13: Changes of gene expression in human lipid metabolism by retinoids

8.3.1. Verification of microarray results in human monocytes stimulated with retinoids

To evaluate the results obtained with DNA microarrays with an independent and more sensitive technique, TaqMan realtime RT-PCR was performed for selected candidate genes in human monocytes incubated in the presence of β-carotene, 9-cis RA and ATRA (Fig.73). Among the genes of fatty acid metabolism, mRNAs of fatty acid desaturase 2 (FADS2), stearoyl-CoA desaturase, monoglyceride lipase (MGLL), and CD36 were clearly inducible by 9-cis RA and ATRA, whereas β-carotene could not significantly upregulate mRNA levels of these genes (Fig.73a.). The level of gene induction was generally higher with 9-cis RA compared to ATRA. The insulin induced gene 1 (INSIG), which was slightly upregulated in DNA microarrays (table 13, 1.9 fold), was not induced in these experiments compared to control conditions. In the group of cholesterol metabolism genes, a strong upregulation of ABCA1, ABCG1, steroid-27 hydroxylase (CYP27A1) and liver X receptor α (LXRα) could be observed (Fig.73b.) with 9-cis RA and ATRA. Interestingly, CYP27A1 mRNA levels were considerably increased by β-carotene, which confirms the results from DNA microarrays. As shown in Fig.73c, the remarkable induction of mRNA expression of apolipoprotein genes after incubation with 9-cis RA and ATRA was confirmed by TaqMan RT-PCR.

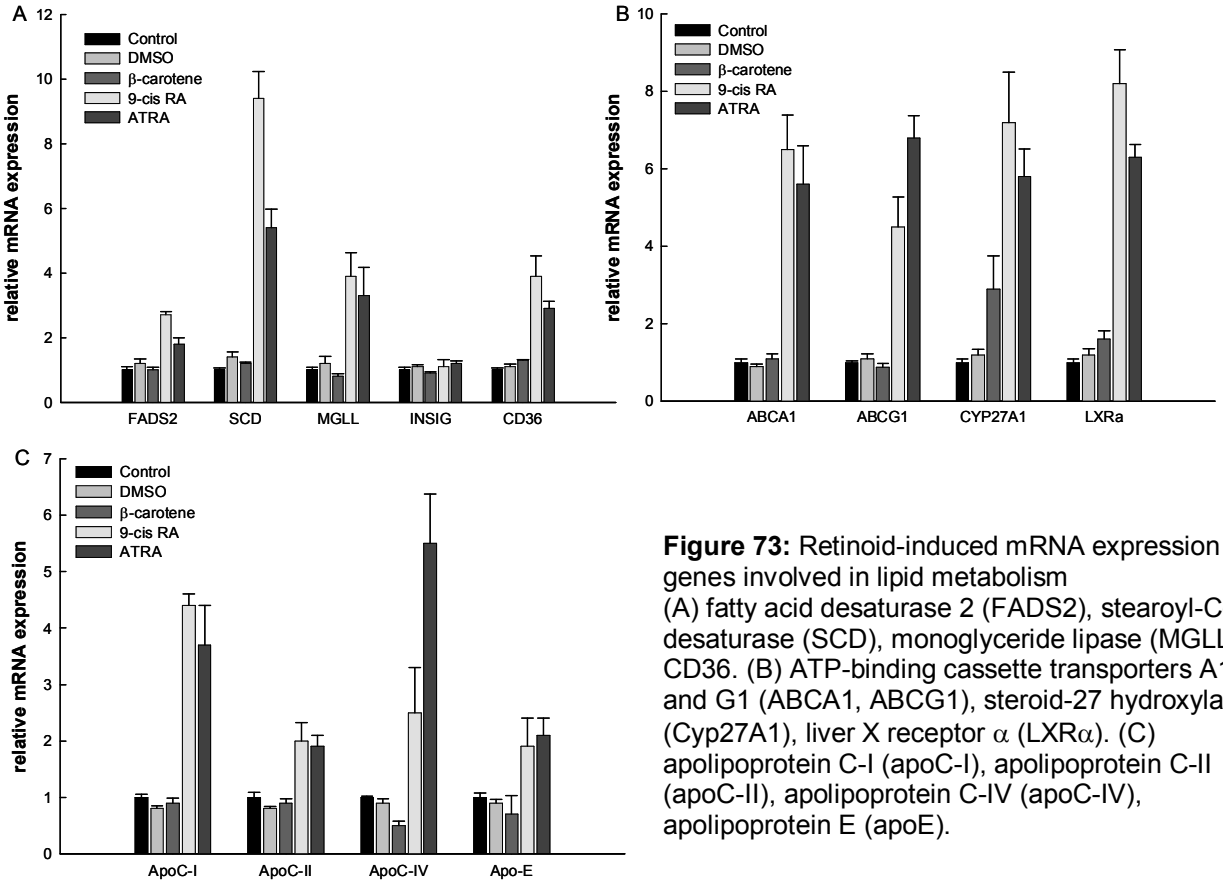

Figure 73: Retinoid-induced mRNA expression of genes involved in lipid metabolism
(A) fatty acid desaturase 2 (FADS2), stearoyl-CoA desaturase (SCD), monoglyceride lipase (MGLL), CD36. (B) ATP-binding cassette transporters A1 and G1 (ABCA1, ABCG1), steroid-27 hydroxylase (Cyp27A1), liver X receptor α (LXRα). (C) apolipoprotein C-I (apoC-I), apolipoprotein C-II (apoC-II), apolipoprotein C-IV (apoC-IV), apolipoprotein E (apoE).

8.3.2. Retinoids increase macrophage phospholipid and cholesterol efflux

In order to analyze whether the increase in gene transcription of important regulators of intracellular cholesterol trafficking by retinoids causes functional consequences, lipid efflux of RAW264.7 macrophages was monitored. Therefore, cells were stimulated with 9-cis RA and ATRA for two different time points (24h and 48h) and the apoA-I specific phospholipid and cholesterol efflux was investigated. The analyzed retinoids significantly induced the efflux of both lipid species to apoA-I as acceptor particle (Fig.74). Remarkably, the retinoid-response of cholesterol efflux (Fig.74B.) was larger than the influence on phospholipid efflux (Fig.74A.). Furthermore, 9-cis RA was more potent in modulating specific efflux levels than ATRA. These results reveal that the increase in mRNA levels of lipid genes activated by retinoids parallels with a functional response of macrophages as related to cholesterol and phospholipid efflux.

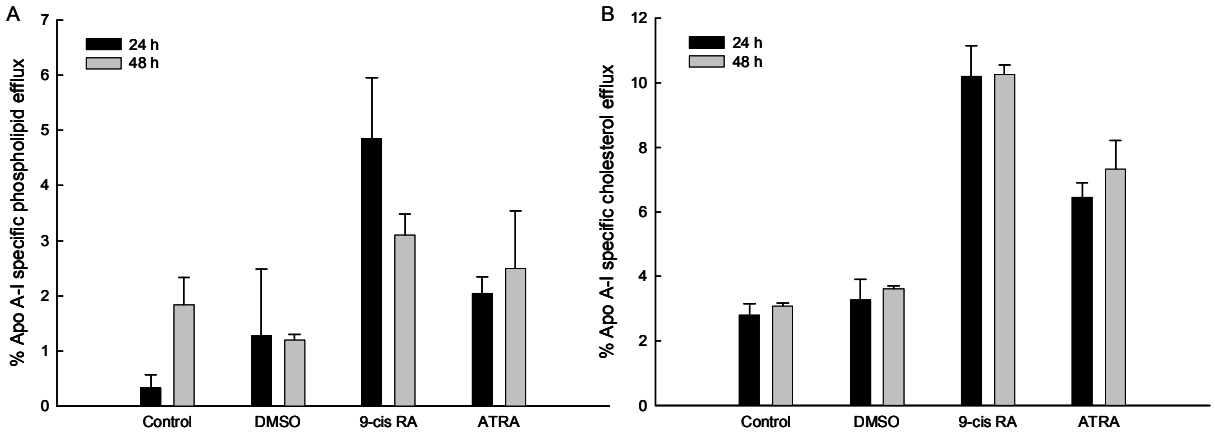

Figure 74: Retinoids stimulate lipid efflux in macrophages. RAW264.7 macrophage cells were either incubated in the presence of vehicle (DMSO) or lipid agonists (5μM 9-cis RA or 5μM ATRA) for 24h or 48h and apoA-I-specific phospholipids efflux (A) or apoA-I-specific cholesterol efflux (B) was monitored.

V. Discussion

In the first part of the thesis, the differential effects of the atherogenic modified lipoproteins E-LDL and mildly Ox-LDL and the antiatherogenic lipoprotein HDL_3 on the cholesterol and sphingolipid metabolism and on raft microdomain constituents during in vitro foam cell formation of apoE3/3 human monocyte derived macrophages have been investigated. The differential composition as well as the differential uptake mechanisms of E-LDL and Ox-LDL could contribute to the specific effects of these lipoproteins concerning cholesterol and sphingolipid metabolism. E-LDL is internalized via CD36, Fcγ-receptor and complement receptor dependent phagocytosis (149), while minimally oxidized LDL is known to be internalized mainly via the LDL receptor coated-pit pathway when exposed to macrophages (389). The degradation of esterified cholesterol by acid lipase treatment converts LDL to coreless liposome like E-LDL. That does not occur in Ox-LDL and is in accordance to in-vivo detection of large lipoprotein particles within the vessel wall (390;391). E-LDL in contrast to Ox-LDL, rapidly induces foam cell formation which is also present in vivo with extensive extracellular deposition of E-LDL already in the earliest stages of human atheriosclerotic lesions accompanying the onset of monocyte infiltration (152). The results obtained by mass spectrometry demonstrate that E-LDL induces total cellular cholesterol especially esterified cholesterol content due to the high free cholesterol content of E-LDL which leads inside the cell to rapid reesterification and foam cell formation. In contrast to E-LDL, Ox-LDL is poorly able to induce cytoplasmic cholesteryl ester accumulation since the oxidation processes lead to the formation of oxysterols from cholesterol and fatty acyl groups of core cholesteryl esters, rendering them resistant to lysosomal hydrolysis and trapping them within these organelles (161;392). Ox-LDL loading of macrophages leads to an upregulation of intracellular ceramide (Cer) content. Mass spectrometry analysis of the modified lipoproteins revealed that the Cer content of E-LDL and Ox-LDL is similar, indicating that cellular Cer elevation is not due to a higher Cer level in the oxidative modified lipoprotein itself. However it can not be excluded that macrophages have a higher capability to take up Cer from Ox-LDL than from E-LDL. It has been shown previously that Ox-LDL induces the sphingomyelin (SM)-Cer pathway by stimulation of neutral and acid sphingomyelinase (SMase) (393) and that minimally Ox-LDL enhances Cer generation via induction of acid SMase (394) while in MCSF deprived macrophages Ox-LDL blocks Cer generation in part by inhibiting acid SMase (395). In this thesis an upregulation of relative mRNA expression of acid SMase, neutral SMase and neutral SMase activation associated factor during Ox-LDL but not during E-LDL loading could be demonstrated which could result in a rapid increase in Cer levels in which a large fraction of cellular SM is converted to Cer (396;397). Further the acitvity of acid SMase is mainly determined by its expression (398) and acid SMase translocates into and generates Cer within distinct plasma membrane sphingolipid-enriched microdomains (300). Sudden

increases in Cer levels due to the action of SMase upon the plasma membrane have important effects in bacterial pathogenesis, cholesterol homeostasis, and apoptosis (399-403). Further a greater upregulation of relative mRNA expression of glucosylceramidase which degrades glucosylceramide to Cer could be detected during Ox-LDL loading compared with E-LDL. This suggests also a Cer elevation upon glucosylceramide degradation to a higher extent during Ox-LDL than during E-LDL loading.

HDL_3 deloading reverses the increase of cholesterol during E-LDL loading and the Cer increase resulting from Ox-LDL loading. This is due to the function of HDL_3 as a cholesterol acceptor. However in contrast to a decrease in Cer, sphingosine levels increased during HDL_3 deloading after Ox-LDL loading. Considering the formation of S1P from sphingosine, this diverse effect could be due to the differential effects of Cer and S1P concerning the Cer-S1P rheostat regulating apoptosis and survival.

In addition to an increase of cellular Cer content during Ox-LDL loading, an increase of cell surface Cer and from Cer derived glycosphingolipids (GSLs) and GM1 ganglioside could also be detected. The increased expression of GSLs on the cell surface during Ox-LDL loading could reflect either their increased net synthesis due to the increase in Cer content during Ox-LDL loading or an enhancement of their translocation from the Golgi to the plasma membrane. An inhibited degradation of the GSLs or their decreased endocytosis could also be responsible. The activities of the GSL degradation enzymes undergo a complex regulation by sphingolipid activator proteins (SAP-A to SAP-D and the GM2 activator) and it might be possible that these regulatory proteins may also be involved in regulating the net amount of GSL expression on the cell surface.

Cer enriched Ox-LDL loaded macrophages compared to E-LDL loaded and MCSF differentiated macrophages bind more effectively apoE compared to apoA-I at 4°C. This increased binding of apoE during Ox-LDL loading of macrophages could be due to an enhanced surface expression of Cer and to the formation of Cer-enriched microdomains during Ox-LDL loading. This is supported by the recent observation that apoE prefers binding on Cer-enriched domains compared to SM-enriched domains exposed on emulsion particle surfaces (110) while further incorporation of SM into emulsion surfaces decreased binding of apoE and reduced apoE-mediated uptake (111). At 37°C binding and uptake of both, apoE and apoA-I was enhanced in Ox-LDL loaded macrophages. This effect could also be due to the higher plasma membrane Cer content in these cells and is in accordance with the higher expression of ABCA1 during Ox-LDL loading which could lead to enhanced cholesterol efflux with increased demand for the efflux mediating HDL constituent apoA-I.

In accordance with the finding of increased apoE binding on Cer enriched microdomains in liposomes which decreases with SM enrichment is the formation of cholesterol/Cer rich rafts in Ox-LDL loaded macrophages which avidly bind apoE while E-LDL loaded macrophages

generate cholesterol/SM rich microdomains. Cer location within lipid rafts is an important factor in Cer action (399-401;404). Cer both stabilizes and associates strongly with lipid rafts (405;406). It can also induce the formation of unusually large raft domains ("platforms") in plasma membranes (400) which can be detected by a monoclonal Cer antibody which has been used in the experiments (300). Raft composition could have marked effects upon raft structure, receptor clustering and function (407). In this regard certain previously observed physiological processes may be a result of raft composition. Recently it could be found that cholesterol and SM levels of the plasma membrane control γ-secretase activity in amyloid precursor protein (APP) cleavage which results in amyloid β 40 (Aβ40) and Aβ42 respectively (408). Because of the fact that the accumulation of Aβ is one of the main characteristics of Alzheimers´s disease (AD) and is associated with neurodegeneration it seems possible that differential raft formation could be associated with the development of AD.

Differential effects on cell surface expression of the monocyte innate immunity receptor cluster resulting in different signaling pathways could also be ascribed to the differential formation of raft domains through Ox-LDL and E-LDL. Previously it could be shown that Cer induces the monocyte innate immunity receptor cluster including Fcγ-receptors (FcγRs) and LRP1 important for lipid uptake, complement constituents for immune regulation and the LPS receptor CD14 (30). According to this receptor cluster it could be demonstrated in this thesis that these receptors are differentially regulated during E-LDL and Ox-LDL loading. The FcγRs CD32 and CD64 increase during E-LDL loading but decrease during Ox-LDL loading compared to M-CSF, indicating an involvement of the phagosomal compartment during E-LDL uptake and a stimulation of type I phagocytosis during E-LDL loading. Fcγ-RII/CD32 shows a raft association in Cer enriched Ox-LDL loaded cells which is in accordance to the fact that cell surface Cer precedes and controls Fcγ-RII/CD32 clustering in rafts (302). It was also shown that CD32 is a constituent of detergent resistant membranes (DRMs) in human platelets and neutrophils (215;216) and the lupus-associated FcγRIIb polymorphism $Fc\gamma RIIbT_{232}$ excludes CD32 from sphingolipid rafts rendering CD32 unable to fulfill its proposed function of inhibiting activatory receptors (409) resulting in an enhancement of inflammatory processes and an exacerbation of the disease.

Scavenger receptor (SR) class B CD36 increases during E-LDL and Ox-LDL loading while LRP1/CD91 and SR cysteine rich/CD163 increase during E-LDL but decrease during Ox-LDL loading. SRs with charge and motif recognition are well known to be involved in uptake of modified lipoproteins in particular ac- and Ox-LDL. Especially CD36 as the major class B SR is considered to be relevant for E-LDL induced foam cell formation (36) and the uptake of E-LDL appears to be mediated in part by CD36 (149). The induction of CD36 surface expression during E-LDL and Ox-LDL loading as an autoamplifying internalization loop for enhanced lipid uptake indicate an involvement of CD36 in the uptake of both modified

lipoproteins. The stronger upregulation of CD36 during Ox-LDL loading could be due to an activation of PPARγ with oxysterols derived from Ox-LDL. CD91 and CD163 increase during E-LDL loading which is probably due to a participation of these receptors in the phagocytic uptake of E-LDL. The importance of CD163 for phagocytosis was shown previously by Buechler et al. who demonstrated an upregulation of CD163 in phagocytic macrophages but not in dendritic cells (410). The upregulation of CD11a, CD11b and CD18 (complement receptor 3) during E-LDL loading but not during Ox-LDL loading indicates an induction of complement as well as type II pagocytosis during E-LDL but not during Ox-LDL loading. The enhanced complement activity of E-LDL has been previously described by Klouche et. al. (154) while Ox-LDL shows only minor complement activation (411). Cer inhibits IgG-dependent phagocytosis in human pylymorphonuclear leukocytes (412) and phagocytosis is enhanced through inhibition of de novo Cer synthesis (413). This implicates an inhibitory effect of Cer in phagocytosis which could explain the decrease of phagocytotic receptors in Cer enriched Ox-LDL loaded macrophages. Upregulation of integrins on the cell surface lead to enhanced phagocytosis, adhesion and migration of monocytes with increased risk of developing atherosclerosis. Enhanced presence of CD11b at the cell surface may reflect an unspecific cellular activation (414). The integrin associated protein CD47 is also increased during E-LDL but decreased during Ox-LDL loading. Decay acceleration factor CD55 is increased during E-LDL and Ox-LDL loading. The LPS receptor CD14 a GPI-linked raft associated receptor was decreased during E-LDL and Ox-LDL loading. It has been demonstrated that minimally modified Ox-LDL bind to CD14 and lead to cytoskeletal rearrangements and pro-inflammatory gene expression (415). Because of the similar regulation of CD14 with Ox-LDL and E-LDL, probably the same effect could be assumed for E-LDL. The downregulation of CD14 during lipid loading could be due to a compensatory effect to protect the cell against pro-inflammatory stimuli. This differential regulation of the surface expression of the monocyte innate immunity receptor cluster during E-LDL and Ox-LDL loading and deloading could lead to the conclusion that differential formation of rafts with the different atherogenic lipoproteins are accompanied by certain receptors resulting in specific signal transduction events for E-LDL and Ox-LDL loading and deloading. Further influences on the cholesterol and sphingolipid trafficking could be a result of different raft domains accompanied by different receptor clustering and could cause disturbances in cholesterol homeostasis. In this thesis it could be shown that ATP cassete transporter ABCA1, a lipid transporter which is responsible for cholesterol efflux from cells is differentially regulated with E-LDL and Ox-LDL loading. Ox-LDL induces protein and mRNA expression of ABCA1, to a higher extent than E-LDL. This could be due to an activation of LXR, a subfamily of nuclear receptors through oxysterols as components of Ox-LDL which in turn activate ABCA1. A possible explanation for the increased ABCA1 protein content by Ox-LDL

could also be due to the enhanced Cer content of Ox-LDL loaded cells which could lead either to enhanced synthesis or delayed degradation of ABCA1 resulting in a specific cellular regulation of ABCA1 content and ABCA1 mediated cholesterol efflux. In this regard it could be shown previously that Cer enhances cholesterol efflux to apoA-I by increasing cell surface presence of ABCA1 (416) which could also happen in Cer enriched Ox-LDL loaded cells in contrast to E-LDL loaded cells. The upregulation of ABCA1 during lipid loading is reversed with HDL_3 deloading of the cells leading to a depriviation of cholesterol and Cer and in turn to a downregulation of ABCA1. HDL which function as a cholesterol scavenger serve as depository for apoA-I, apoE and apoC-I. ApoE protein expression shows an upregulation during lipid loading compared to MCSF differentiation and a further upregulation during HDL_3 deloading which is probably reflecting the apoE content of HDL_3 itself. ApoE surface and intracellular expression measured by flow cytometry is higher during E-LDL than during Ox-LDL loading. However HDL_3 deloading leads to a decrease of apoE surface and intracellular expression. Recently it could be shown that apoE respectively apoE-rich lipoproteins like VLDL contribute to antigen presentation of lipid antigens by high affinity binding of endogenous or exogenous antigens mainly Cer derived GSLs (117). The uptake of these lipid antigens takes place via LRP1 by antigen presenting cells and after processing they are presented to lipid antigen-reactive T-cells on the cell surface by CD1. Therefore induction of apoE by E-LDL could also lead to a promotion of inflammatory processes which is reversed with HDL_3.

In contrast to apoE, apoC-I surface and intracellular expression measured by flow cytometry as well as apoC-I protein expression shows a higher increase during Ox-LDL than during E-LDL loading. This could be a compensatory effect of the cell because apoC-I activates lecithin cholesterol acyl transferase (LCAT) (75) which catalyze the esterification of free cholesterol in plasma and cholesteryl ester enrichment of HDL and apoC-I is also described as an inhibitor of phospholipase A2 (PLA2) (79) which amplifies atherogenic processes by liberating potent pro-inflammatory lipid mediators and by generating pro-atherogenic LDL (80). On the other side apoC-I inhibits lipoprotein lipase an enzyme involved in lipoprotein processing (78) which leads to high plasma TG levels and low HDL levels which are considered as pro-atherogenic factors (417).

Surface and intracellular expression of cholesterol ester transfer protein (CETP), a member of the lipopolysaccharide binding protein (LBP) gene family increases during MCSF differentiation which was reported previously (131). With E-LDL loading surface CETP increases and with Ox-LDL loading it decreases compared to MCSF and the intracellular expression of CETP decreases with E-LDL and to a higher extent with Ox-LDL compared to MCSF. This is a contradictory result to the known functions of CETP which would suggest an increase of CETP with cholesteryl ester accumulation and further an induction of CETP like

ABCA1 via LXR induced by oxysterols as components of Ox-LDL. A possible explanation for this fact could be a compensatory effect of CETP in response to the upregulation of ABCA1 upon Ox-LDL loading.

Analyzing the impact of apoE polymorphism and Tangier disease on cholesterol, sphingolipid and GSL metabolism, it could be demonstrated that monocytes of the apoE3/3 and apoE4/4 genotype develop both foam cell morphology and accumulate lipids but show differences in the cellular lipid profile upon E-LDL and Ox-LDL loading. While analysis with mass spectrometry reveals no changes of the esterified and unesterified cholesterol content between the two genotypes, phosphatidylserine (PS) and lysophosphatidylcholine (LPC) content is decreased and phosphatidylcholine (PC) content is increased in apoE4/4 compared to apoE3/3 macrophages during lipid loading.

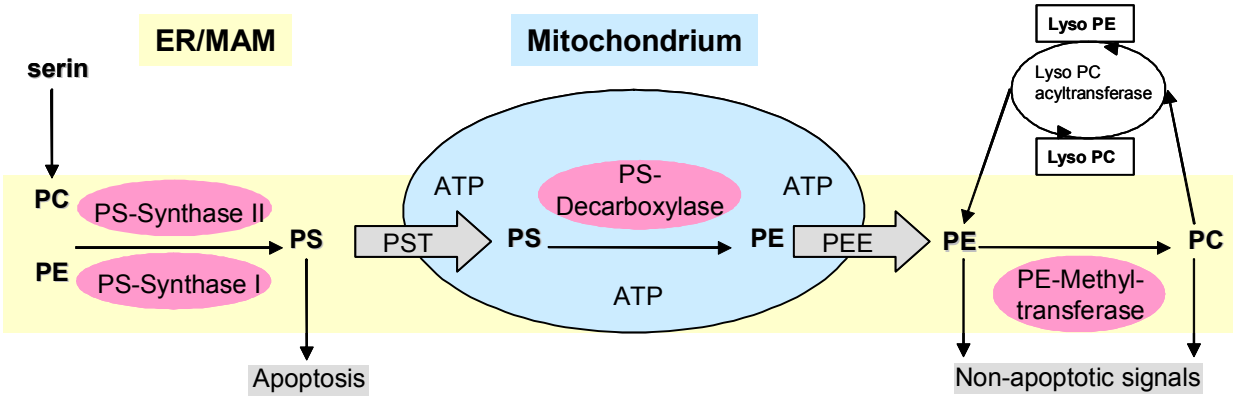

Fig. 75: The Phosphatidylcholine/ Phosphatidylserine/ Phosphatidylethanolamine Rheostat

The decrease of PS content in apoE4/4 macrophages could be due to a downregulation of gene expression of the PS generating enzymes PS-synthases I and II in the apoE4 genotype and to the additional Arg-X-Arg (RXR) endoplasmatic reticulum (ER) retention domain in the apoE4/4 genotype leading to a prolonged retention of PS in the ER associated with impaired ER to Golgi trafficking and translocation to the plasma membrane. In contrast to PS the PC content is increased in apoE4/4 compared to apoE3/3 macrophages which could be explained by upregulation of PE-N-Methyltransferase gene expression in apoE4/4 macrophages during lipid loading but not by increased PE content which shows no differences between the two genotypes. The decrease in LPC during Ox-LDL loading in apoE4/4 compared with apoE3/3 macrophages could be explained by an upregulation of gene expression of the LPC processing enzymes phospholipase A2, group IVC and VII and lysophospholipid acyltransferase in apoE3/3 but not in apoE4/4 macrophages. Another explanation for LPC increase could be the additional RXR domain in the apoE4/4 genotype leading to retention of PC in the ER and impaired LPC synthesis. The differences in lipid content of apoE3/3 and apoE4/4 macrophages affect the PC/PS/PE rheostat (Fig.75). The lower PS content in apoE4/4 macrophages could lead to decreased apoptosis while the

higher PC content could lead to an increase in non-apoptotic signals in apoE4/4 macrophages. In summary the PC/PS/PE rheostat switches apoE4/4 macrophages compared to apoE3/3 cells to the “nonapoptotic” side during lipid loading. This may allow the conclusion that foam cells of the apoE4 genotype could execute proinflammatory effects for a prolonged time and thereby promotes lesion progression as compared to apoE3/3 macrophages which could exert controlled apoptosis.

SM and Cer content is decreased upon Ox-LDL loading in apoE4/4 compared to apoE3/3 macrophages and the sphingosine content is decreased during HDL_3 deloading of apoE4/4 compared to apoE3/3 macrophages. The lower amount of SM during Ox-LDL loading of apoE4/4 compared with apoE3/3 macrophages could lead to a lower content of Cer, which is derived from either SM or degradation of glycosyl-Cer species, and could lead to decreased synthesis of glucosylceramide and GSLs. This could be a possible explanation for the reduced surface expression of Cer and GSLs upon Ox-LDL loading in apoE4/4 macrophages found in this thesis by flow cytometry analysis compared with apoE3/3 macrophages. Taqman RT-PCR analysis of sphingomyelin synthases 1 and 2, involved in SM synthesis and also of serine palmitoyltransferases 1 and 2, involved in Cer synthesis shows a higher relative mRNA expression during lipid loading of apoE4/4 compared with apoE3/3 macrophages which could be a compensatory effect of the apoE4/4 macrophages to balance the lower SM and Cer content. Enhanced degradation of Cer indicated by increased mRNA expression of acid ceramidase during lipid loading could also be a reason for decreased surface expression of Cer and Cer derived GSLs. Other reasons for the decreased surface expression of Cer in apoE4/4 macrophages could be defects in the trafficking pathways of Cer and GSLs from the ER to Golgi and following translocation to the plasma membrane due to the additional RXR-retention domain in the apoE4/4 genotype. A compensatory effect to defects in this transport pathway and the resulting low amount of Cer and GSL surface expression could lead to increased mRNA expression of Cer generating enzymes during lipid loading of apoE4/4 compared to apoE3/3 macrophages.

Decreased surface expression of Cer and GSLs during lipid loading of apoE4/4 and Tangier macrophages compared to apoE3/3 macrophages could indicate differential capacities of activation, apoptosis and survival with consequences in signal transduction. This could contribute as a risk factor for inflammatory response during atherogenesis in apoE4/4 and Tangier macrophages. Also macrophages of a patient with hyperlipidemia and coronary heart disease shows decreased surface expression of Cer and GSLs during E-LDL loading compared with apoE3/3 macrophages. This may allow the conclusion that a defect in lipoprotein metabolism could be associated with a lower expression of GSLs.

ApoE containing lipoproteins are involved in the modulation of amyloid precursor protein (APP) transport and processing by interfering with Kunitz-domain-mediated binding of APP to

the extracellular domain of LRP. Therefore apoE could be regarded as an opsonin for APP binding to LRP receptors (192). Proteolytic cleavage of APP by the action of beta- and gamma secretases leads to amyloid-β (Aβ) peptide which is considered as the hallmark of Alzheimer disease (AD) (194). Recently it has been found that SM levels are predominantly downregulated by Aβ42, due to activation of the SM degrading enzyme neutral SMase. By contrast, Aβ40 downregulates cholesterol de novo synthesis due to inhibition of hydroxymethylglutaryl-CoA reductase (HMGR) activity (408). Considering this regulatory principle apoE could also play a role in modulating SM and cholesterol levels via APP processing.

The decrease of apoE and apoC-I mRNA expression of apoE4/4 compared with apoE3/3 macrophages is associated with decreased secretion of apoE and apoC-I into the culture medium. This could be due to the described lower apoE concentrations and enhanced degradation of apoE because of an additional RXR retention domain in apoE4/4 monocytes compared to apoE3/3 monocytes (256) and is in accordance with a previous publication of our institute of Stöhr et al. (25). Another explanation for the decrease of apoE and apoC-I in the medium could be a redirection of apoE and apoC-I from the secretory to the degradation pathway in apoE4/4 macrophages. Impaired recycling of apoE4 could interfere with intracellular cholesterol transport and contribute to the pathophysiological lipoprotein profile observed in apoE4 homozygotes (254). Macrophage specific expression of human apoE reduces atherosclerosis in hypercholesterolemic apoE null mice, supporting a possible function of macrophage-produced apoE within atherosclerotic plaques in promoting cholesterol efflux. It has been shown that apoE effectively stimulates cholesterol efflux from macrophages (114;250;252). Compared with apoE3, apoE4 is less efficient in promoting cholesterol efflux in fibroblasts and astrocytes (252;253), indicating that apoE isoforms differentially affect the mobilization of cellular cholesterol.

ApoC-I intracellular expression analyzed by flow cytometry revealed a higher level in apoE4/4 macrophages during all states of incubation which could be considered as a genotype specific regulatory effect leading to an atherogenic lipid profile in the apoE4/4 genotype due to the inhibitory effects of apoC-I on lipoprotein lipase.

In ABCA1 deficient (Tangier) macrophages the greatest difference could be observed in the intracellular expression of apoE which shows a lower expression level in Tangier macrophages compared to apoE3/3 macrophages during all states of incubation. This could be associated with the lower levels of HDL in Tangier macrophages and a disturbance in cholesterol metabolism and cholesterol efflux leading to a higher risk factor of atherosclerosis or splenomegaly. Further apoC-I surface expression shows a lower expression during Ox-LDL loading in Tangier macrophages while HDL_3 deloading in Tangier macrophages leads to a strong increase of apoC-I surface expression compared to apoE3/3 macrophages and also

intracellular expression of apoC-I increases strongly during HDL_3 deloading after E-LDL loading compared to apoE3/3 macrophages. These effects might be due to the failure of ABCA1 as a lipid efflux mediator in ABCA1 deficient Tangier macrophages and could result in an atherosclerotic lipid profile in addition to the inhibitory effects of apoC-I on lipoprotein lipase. The expression of CETP fails to illustrate a differential regulation between the apoE3/3, apoE4/4 and tangier macrophages.

Intracellular expression of adipophilin, a sensitive marker of lipid accumulation, increases stronger during E-LDL loading in apoE3/3 than in apoE4/4 macrophages and decreases during HDL_3 deloading in both genotypes. Tangier macrophages show a higher increase of adipophilin during E-LDL loading and a further increase of adipophilin expression during HDL_3 deloading. Possibly, differences in lipid sensitivity, cellular lipid distribution or lipid droplet structure account for this observation. Further the ABCA1 defect in Tangier macrophages lead to a defect in lipid efflux with the consequence that probably the lipid marker protein adipophilin further increases during HDL_3 deloading compared with the apoE3/3 macrophages which show a decrease of adipophilin expression during HDL_3 deloading.

However, despite the importance of apoE4 as a risk factor of atherosclerosis and Alzheimer´s disease (255), the cellular mechanisms, which are responsible for the differences between apoE3 and apoE4, are yet unclear.

Opsonization of lipoproteins, especially of E-LDL with β-Amyloid 42 (Aβ42), a protein involved in the pathogenesis of Alzheimer disease (AD), lead to increased surface expression of Cer, LacCer, Gb_3Cer and GM1 ganglioside compared to non-opsonized E-LDL. Probably the phagocytosis-related pathways which are responsible for E-LDL uptake were facilitated by opsonizing agents such as Aβ42 and lead to increased E-LDL uptake with the result of increased surface expression of Cer and GSLs. Recently it could be demonstrated that Aβ42 leads to a downregulation of SM levels due to the activation of neutral SMase which degrades SM to Cer (408). Therefore the incubation with E-LDL Aβ42 complex could result in an increased amount of Cer and Cer derived GSLs indicative for abnormal processing of GSLs in the pathogenesis of Alzheimer´s disease. Additionally the complex of E-LDL and Aβ42 bind more efficiently to the monocyte subpopulation MNP2 (CD14 high; CD16 high) which have high capacity for phagocytosis. This binding affinity to MNP2 has also been shown for E-LDL alone (149).

PPARγ agonists as drugs important for atherosclerosis associated with the metabolic syndrome and especially insulin resistance are key components of lipid uptake by inducing the SR-B CD36 that mediates Ox-LDL uptake in macrophages. This effect may be compensated by increased expression of ABCA1 and apoE in macrophages (244). The increase of ABCA1 and apoE could further induce cholesterol efflux and attenuate

atherosclerosis which may allow the conclusion that PPARγ agonists have protective effects preventing atherosclerosis by regulating apoE expression in macrophages. Analyzing different glitazones as agonists for PPARγ by flow cytometry an induction of SR-B CD36 surface expression and also of apoE surface and intracellular expression could be detected which is in accordance to the functions of PPARγ. The influence of the PPARγ agonist rosiglitazone as well as the RXR agonists beta carotene, 9-cis retinoic acid (9-cis RA) and all trans retinoic acid (ATRA) have been analyzed on receptors of the monocyte innate immunity receptor cluster. The PPARγ agonist rosiglitazone increases cell surface expression of SR-B CD36. However the RXR/RAR agonists beta carotene, 9-cis RA and ATRA decrease SR-B CD36 surface expression compared to control while a RAR-mediated induction of SR-B CD36 transcription has been shown in THP-1 cells (418). The Fcγ-receptors CD16, CD32 as well as CD11b/CD18 (complement receptor 3) are decreased with beta carotene, 9-cis RA and ATRA indicating reduced phagocytic acitivity with retinoids resulting in reduced uptake of atherogenic lipoproteins with reduced foam cell formation capacity and positive effects for atherosclerotic processes. The glycosylphosphatidylinositol-anchored receptor CD14 which plays a major role in the inflammatory response of monocytes to lipopolysasschariде is decreased during incubation with retinoic acids. Thus the generation of potentially proinflammatory signalling mechanisms could be elicited by retinoids in monocytes.

In addition to the differential expression of receptors involved in lipid uptake and processing the upregulation of genes important for lipid uptake, namely ABCA1, ABCG1, CYP27A1 and LXRα by 9-cis RA and ATRA could be demonstrated by microarray and Taqman RT-PCR analysis (249). Previous reports have shown that ABCA1 and LXRα can be induced at the mRNA and protein level by incubation of murine macrophages and THP-1 cells with ATRA (419;420) confirming these results. Although Wagsater et al. (419) reported that the amount of ABCG1 mRNA was not changed by treatment with ATRA, these results clearly demonstrate that 9-cis RA and ATRA are potent inducers of ABCG1 transcription in primary human monocytes. The CYP27A1 gene, which is critically important for the mitochondrial conversion of cholesterol to 27-hydroxycholesterol in monocytes and macrophages, is highly induced by all analyzed retinoids including β-carotene. Since LXRα is also upregulated by retinoids this could imply that indirect oxysterol-dependent activation of these genes via LXRα and 27-hydroxycholesterol as newly synthesized ligand could be elicited by retinoids. However, recent data suggest that at least for the ABCA1 gene, direct binding of RAR/RXR heterodimers to the DR4 element in the promoter is the most important signaling pathway predominating over LXR-dependent mechanisms (420).

A major side effect of retinoids including ATRA, which is used as therapeutic agent for the treatment of several forms of cancer (421) is the development of hypertriglyceridemia. In our results we could observe a common induction of fatty acid metabolism genes (fatty acid

synthase, fatty acid desaturase 2, monoglyceride lipase), apolipoprotein genes (apoC-I, apoC-II, ApoC-IV, and apoE) and the master regulator of fatty acid gene transcription sterol regulatory element binding protein 1c (SREBP1c), which is in agreement with previous results, demonstrating that hepatic apoC-III transcription is mediated via the RXR-specific agonist LG1069 (422). In this line, Costet et al. (420) have also noticed a slight increase in SREBP1c transcription in mouse macrophages stimulated with ATRA. Furthermore, upregulation of Acyl-coenzyme A: cholesterol acyltransferase 1 (ACAT1) by ATRA in THP-1 cells may cause storage of cholesteryl esters in lipid droplets (423). These findings collectively have encouraged the hypothesis that retinoids and RAR/RXR-mediated gene induction may promote foam cell formation and inflammation and thereby favour the development of atherosclerosis. However, the findings that genes important for lipid efflux such as ABCA1, ABCG1, CYP27A1, LXRα, and apoE are very effectively upregulated by retinoids point out that the net effect of stimulation with these compounds may not result in an augmented uptake and storage of lipids in monocytes and macrophages. This is also supported by cellular lipid efflux. Macrophages incubated in the presence of 9-cis RA and ATRA showed a strong induction of both phospholipid and cholesterol efflux to apoA-I as an acceptor counterbalancing potential esterification and storage mechanisms.

In conclusion, retinoids are potent inducers of genes related to human lipid metabolism and especially of genes involved in reverse cholesterol transport associated with increased macrophage lipid efflux. Based on these findings, the development of selective retinoic receptor agonists promoting the upregulation of antiatherogenic genes without influencing the levels of genes involved in triglyeride metabolism may be a useful tool for the treatment or prevention of atherosclerosis.

VI. Summary

A hallmark in atherosclerosis is the generation of lipid loaded macrophage foam cells. In this thesis the effects of the different atherogenic lipoproteins, enzymatically modified LDL (E-LDL) and mildly oxidized LDL (Ox-LDL) on cellular cholesterol, sphingolipid and glycosphingolipid (GSL) metabolism, raft microdomain generation and cell surface receptor expression during in vitro foam cell formation and HDL_3 dependent deloading of human monocyte-derived macrophages (MDM) were analyzed. Total cell analysis of lipid loaded and deloaded MDM, using lipidomics, genomics and proteomics based on mass spectrometry, Affymetrix microarray analysis, Taqman RT-PCR, flow cytometry, image microscopy and western blot analysis, was applied to unravel key mechanisms underlying the regulation of cellular lipid influx, raft formation, lipid efflux and storage as well as surface expression of receptors involved in lipid uptake and processing.

In the first part of this thesis apoE3/3 homozygous MDM were analyzed. Using mass spectrometry it could be demonstrated that E-LDL loading predominantly increased cellular cholesterol content, while Ox-LDL loading preferentially increased cellular ceramide (Cer) content. This may be due to a stronger upregulation of acid and neutral sphingomyelinase (SMPD1, SMPD2), neutral sphingomyelinase activation associated factor (NSMAF) as well as upregulation of glucosylceramidase during Ox-LDL loading compared with E-LDL loading and not by differences in ceramide synthesis as found by quantitative TaqMan RT-PCR. Ox-LDL in comparison to E-LDL also led to a higher cell surface expression of Cer and the Cer derived GSLs lactosylceramide (LacCer, CDw17), dodecasaccharideceramide (CD65s), globotriaosylceramide (Gb_3Cer, CD77) as well as GM1-ganglioside as determined by flow cytometry. ApoE with its high affinity for Cer in contrast to apoA-I was mainly bound and internalized by Cer enriched Ox-LDL loaded cells. Ox-LDL preferentially induced cholesterol/Cer rich-membrane microdomains while E-LDL loading induced cholesterol/sphingomyelin microdomains as confirmed in situ by confocal microscopy and by mass spectrometry of isolated detergent resistant membranes.

Microarray and flow cytometry analysis of the monocyte innate immunity receptor cluster revealed an induction of the complement system and of Fcγ-receptors with E-LDL but not with Ox-LDL loading. This indicates that E-LDL in contrast to Ox-LDL, which preferentially upregulate CD36, induces type-I and type-II phagocytosis. Further Ox-LDL induced mRNA and protein expression of ABCA1 to a higher extent than E-LDL. ApoE protein expression and expression analyzed by flow cytometry was higher during E-LDL loading while apoC-I expression was higher during Ox-LDL loading compared to MCSF differentiation.

It is concluded that core-depleted E-LDL and surface oxidized Ox-LDL particles originating from the same LDL pool exert differential effects on cholesterol and sphingolipid metabolism as well as on cell surface receptor expression associated with the formation of different raft

microdomains and thereby may trigger different macrophage effector functions during atherogenesis.

In the second part of the thesis apoE3/3 homozygous MDM were compared with MDM of the apoE4/4 genotype and ABCA1 deficient (Tangier) macrophages using the same incubation protocol with E-LDL and Ox-LDL loading and HDL_3 deloading, to search for genotype specific differences in lipid and GSL metabolism. Mass spectrometry revealed a lower phosphatidylserine (PS) but higher phosphatidylcholine (PC) content in apoE4/4 macrophages during lipid loading compared to apoE3/3 macrophages. This could be explained by downregulation of phosphatidylserine synthase gene expression and upregulation of phosphatidylethanolamine-methyltransferase gene expression respectively during lipid loading in apoE4/4 macrophages as found by microarray analysis. GSL surface expression during Ox-LDL loading was higher in apoE3/3 compared with apoE4/4 and ABCA1 deficient macrophages. Quantitative TaqMan-RT-PCR during Ox-LDL loading demonstrated no upregulation of acid SMase and a higher upregulation of acid ceramidase in apoE4/4 compared to apoE3/3 macrophages which could be the reason for the lower GSL surface expression of apoE4/4 macrophages associated with impaired lipid trafficking to the plasma membrane. E-LDL loaded apoE3/3 macrophages demonstrated also a higher GSL surface expression compared with macrophages of a patient with hyperlipidemia and coronary heart disease. The apolipoproteins apoE, apoC-I and CETP which are involved in cholesterol and lipid metabolism were also analyzed in apoE3/3, apoE4/4 and ABCA1 deficient macrophages using the same incubation scheme with E-LDL and Ox-LDL loading and HDL_3 deloading. mRNA expression as well as the protein amount of secreted apoE and apoC-I was higher in apoE3/3 than in apoE4/4 macrophages. Additionally surface and intracellular expression of these proteins was different between the two different genotypes and ABCA1 deficient macrophages. The differences between the two genotypes apoE3 and apoE4 could be due to a third Arg-x-Arg (RXR) endoplasmatic reticulum (ER) retention domain in the apoE4 genotype leading to enhanced degradation of apoE4 in the ER associated with impaired ER to Golgi trafficking and translocation to the plasma membrane. The effect of lipoprotein opsonisation with amyloidβ_{42} a protein involved in the pathogenesis of Alzheimer´s disease on the surface expression of GSLs was also analyzed. It could be shown that opsonisation of E-LDL lead to an enhanced surface expression of Cer and GSLs in apoE3/3 macrophages indicative for abnormal processing of GSLs in the pathogenesis of Alzheimer´s disease. In summary total cell analysis using lipidomics, genomics and proteomics based on mass spectrometry, Affymetrix microarray analysis, Taqman RT-PCR, flow cytometry, image microscopy and western blot analysis is a valuable and reasonable tool to unravel key mechanisms underlying the regulation of cellular lipid influx, raft formation, lipid efflux and storage as well as surface expression of specific receptors and sphingolipids.

VII. References

Reference List

(1) Libby P. Changing concepts of atherogenesis. *J Intern Med* 2000;**247**(3):349-58.

(2) Ross R. Atherosclerosis--an inflammatory disease. *N Engl J Med* 1999;**340**(2):115-26.

(3) Glass CK, Witztum JL. Atherosclerosis. the road ahead. *Cell* 2001;**104**(4):503-16.

(4) Creemers EE, Cleutjens JP, Smits JF *et al*. Matrix metalloproteinase inhibition after myocardial infarction: a new approach to prevent heart failure? *Circ Res* 2001;**89**(3):201-10.

(5) Plutzky J. The vascular biology of atherosclerosis. *Am J Med* 2003;**115 Suppl 8A**:55S-61S.

(6) Williams KJ, Tabas I. The response-to-retention hypothesis of early atherogenesis. *Arterioscler Thromb Vasc Biol* 1995;**15**(5):551-61.

(7) Hurt-Camejo E, Olsson U, Wiklund O *et al*. Cellular consequences of the association of apoB lipoproteins with proteoglycans. Potential contribution to atherogenesis. *Arterioscler Thromb Vasc Biol* 1997;**17**(6):1011-7.

(8) Gustafsson M, Flood C, Jirholt P *et al*. Retention of atherogenic lipoproteins in atherogenesis. *Cell Mol Life Sci* 2004;**61**(1):4-9.

(9) Li H, Forstermann U. Nitric oxide in the pathogenesis of vascular disease. *J Pathol* 2000;**190**(3):244-54.

(10) Orford JL, Selwyn AP, Ganz P *et al*. The comparative pathobiology of atherosclerosis and restenosis. *Am J Cardiol* 2000;**86**(4B):6H-11H.

(11) Kim S, Iwao H. Molecular and cellular mechanisms of angiotensin II-mediated cardiovascular and renal diseases. *Pharmacol Rev* 2000;**52**(1):11-34.

(12) Luster AD. Chemokines--chemotactic cytokines that mediate inflammation. *N Engl J Med* 1998;**338**(7):436-45.

(13) Kume N, Cybulsky MI, Gimbrone MA, Jr. Lysophosphatidylcholine, a component of atherogenic lipoproteins, induces mononuclear leukocyte adhesion molecules in cultured human and rabbit arterial endothelial cells. *J Clin Invest* 1992;**90**(3):1138-44.

(14) Dong ZM, Chapman SM, Brown AA *et al*. The combined role of P- and E-selectins in atherosclerosis. *J Clin Invest* 1998;**102**(1):145-52.

(15) Collins RG, Velji R, Guevara NV *et al*. P-Selectin or intercellular adhesion molecule (ICAM)-1 deficiency substantially protects against atherosclerosis in apolipoprotein E-deficient mice. *J Exp Med* 2000;**191**(1):189-94.

(16) Nie Q, Fan J, Haraoka S *et al*. Inhibition of mononuclear cell recruitment in aortic intima by treatment with anti-ICAM-1 and anti-LFA-1 monoclonal antibodies in hypercholesterolemic rats: implications of the ICAM-1 and LFA-1 pathway in atherogenesis. *Lab Invest* 1997;**77**(5):469-82.

(17) Cybulsky MI, Gimbrone MA, Jr. Endothelial expression of a mononuclear leukocyte adhesion molecule during atherogenesis. *Science* 1991;**251**(4995):788-91.

(18) Nakashima Y, Raines EW, Plump AS *et al*. Upregulation of VCAM-1 and ICAM-1 at atherosclerosis-prone sites on the endothelium in the ApoE-deficient mouse. *Arterioscler Thromb Vasc Biol* 1998;**18**(5):842-51.

(19) Springer TA. Traffic signals for lymphocyte recirculation and leukocyte emigration: the multistep paradigm. *Cell* 1994;**76**(2):301-14.

(20) McMurray HF, Parthasarathy S, Steinberg D. Oxidatively modified low density lipoprotein is a chemoattractant for human T lymphocytes. *J Clin Invest* 1993;**92**(2):1004-8.

(21) Reape TJ, Groot PH. Chemokines and atherosclerosis. *Atherosclerosis* 1999;**147**(2):213-25.

(22) Fan J, Watanabe T. Inflammatory reactions in the pathogenesis of atherosclerosis. *J Atheroscler Thromb* 2003;**10**(2):63-71.

(23) Takahashi K, Takeya M, Sakashita N. Multifunctional roles of macrophages in the development and progression of atherosclerosis in humans and experimental animals. *Med Electron Microsc* 2002;**35**(4):179-203.

(24) Rothe G, Gabriel H, Kovacs E *et al*. Peripheral blood mononuclear phagocyte subpopulations as cellular markers in hypercholesterolemia. *Arterioscler Thromb Vasc Biol* 1996;**16**(12):1437-47.

(25) Stohr J, Schindler G, Rothe G *et al*. Enhanced upregulation of the Fc gamma receptor IIIa (CD16a) during in vitro differentiation of ApoE4/4 monocytes. *Arterioscler Thromb Vasc Biol* 1998;**18**(9):1424-32.

(26) Rothe G, Herr AS, Stohr J *et al*. A more mature phenotype of blood mononuclear phagocytes is induced by fluvastatin treatment in hypercholesterolemic patients with coronary heart disease. *Atherosclerosis* 1999;**144**(1):251-61.

(27) Schmitz, G. and Torzewski, M. Atherosclerosis: an inflammatory disease. [Inflammatory and Infectious Basis of Atherosclerosis]. 2001.
Ref Type: Generic

(28) Fingerle G, Pforte A, Passlick B *et al*. The novel subset of CD14+/CD16+ blood monocytes is expanded in sepsis patients. *Blood* 1993;**82**(10):3170-6.

(29) Hubacek JA, Rothe G, Pit'ha J *et al*. C(-260)-->T polymorphism in the promoter of the CD14 monocyte receptor gene as a risk factor for myocardial infarction. *Circulation* 1999;**99**(25):3218-20.

(30) Pfeiffer A, Bottcher A, Orso E *et al*. Lipopolysaccharide and ceramide docking to CD14 provokes ligand-specific receptor clustering in rafts. *Eur J Immunol* 2001;**31**(11):3153-64.

(31) Schmitz G, Orso E. CD14 signalling in lipid rafts: new ligands and co-receptors. *Curr Opin Lipidol* 2002;**13**(5):513-21.

(32) Weinstein DB, Carew TE, Steinberg D. Uptake and degradation of low density lipoprotein by swine arterial smoot muscle cells with inhibition of cholesterol biosynthesis. *Biochim Biophys Acta* 1976;**424**(3):404-21.

(33) Goldstein JL, Ho YK, Basu SK *et al*. Binding site on macrophages that mediates uptake and degradation of acetylated low density lipoprotein, producing massive cholesterol deposition. *Proc Natl Acad Sci U S A* 1979;**76**(1):333-7.

(34) Traber MG, Kayden HJ. Low density lipoprotein receptor activity in human monocyte-derived macrophages and its relation to atheromatous lesions. *Proc Natl Acad Sci U S A* 1980;**77**(9):5466-70.

(35) Steinbrecher UP, Lougheed M, Kwan WC *et al*. Recognition of oxidized low density lipoprotein by the scavenger receptor of macrophages results from derivatization of apolipoprotein B by products of fatty acid peroxidation. *J Biol Chem* 1989;**264**(26):15216-23.

(36) Febbraio M, Hajjar DP, Silverstein RL. CD36: a class B scavenger receptor involved in angiogenesis, atherosclerosis, inflammation, and lipid metabolism. *J Clin Invest* 2001;**108**(6):785-91.

(37) Steinberg D, Parthasarathy S, Carew TE *et al*. Beyond cholesterol. Modifications of low-density lipoprotein that increase its atherogenicity. *N Engl J Med* 1989;**320**(14):915-24.

(38) Tabas I. Cholesterol and phospholipid metabolism in macrophages. *Biochim Biophys Acta* 2000;**1529**(1-3):164-74.

(39) Bottalico LA, Kendrick NC, Keller A *et al*. Cholesteryl ester loading of mouse peritoneal macrophages is associated with changes in the expression or modification of specific cellular proteins, including increase in an alpha-enolase isoform. *Arterioscler Thromb* 1993;**13**(2):264-75.

(40) Kirchhoff C, Osterhoff C, Young L. Molecular cloning and characterization of HE1, a major secretory protein of the human epididymis. *Biol Reprod* 1996;**54**(4):847-56.

(41) Hara H, Yokoyama S. Interaction of free apolipoproteins with macrophages. Formation of high density lipoprotein-like lipoproteins and reduction of cellular cholesterol. *J Biol Chem* 1991;**266**(5):3080-6.

(42) Diederich W, Orso E, Drobnik W *et al*. Apolipoprotein AI and HDL(3) inhibit spreading of primary human monocytes through a mechanism that involves cholesterol depletion and regulation of CDC42. *Atherosclerosis* 2001;**159**(2):313-24.

(43) Tsukamoto K, Hirano K, Tsujii K *et al*. ATP-binding cassette transporter-1 induces rearrangement of actin cytoskeletons possibly through Cdc42/N-WASP. *Biochem Biophys Res Commun* 2001;**287**(3):757-65.

(44) Schmitz G, Buechler C. ABCA1: regulation, trafficking and association with heteromeric proteins. *Ann Med* 2002;**34**(5):334-47.

(45) Drobnik W, Borsukova H, Bottcher A *et al*. Apo AI/ABCA1-dependent and HDL3-mediated lipid efflux from compositionally distinct cholesterol-based microdomains. *Traffic* 2002;**3**(4):268-78.

(46) Brooks-Wilson A, Marcil M, Clee SM *et al*. Mutations in ABC1 in Tangier disease and familial high-density lipoprotein deficiency. *Nat Genet* 1999;**22**(4):336-45.

(47) Ioannou YA. Multidrug permeases and subcellular cholesterol transport. *Nat Rev Mol Cell Biol* 2001;**2**(9):657-68.

(48) Pentchev PG, Blanchette-Mackie EJ, Dawidowicz EA. The NP-C gene: a key to pathways of intracellular cholesterol transport. *Trends Cell Biol* 1994;**4**(10):365-9.

(49) Vanier MT, Pentchev P, Rodriguez-Lafrasse C *et al*. Niemann-Pick disease type C: an update. *J Inherit Metab Dis* 1991;**14**(4):580-95.

(50) Sillence DJ, Platt FM. Storage diseases: new insights into sphingolipid functions. *Trends Cell Biol* 2003;**13**(4):195-203.

(51) Hevonoja T, Pentikainen MO, Hyvonen MT *et al*. Structure of low density lipoprotein (LDL) particles: basis for understanding molecular changes in modified LDL. *Biochim Biophys Acta* 2000;**1488**(3):189-210.

(52) Acton S, Rigotti A, Landschulz KT *et al*. Identification of scavenger receptor SR-BI as a high density lipoprotein receptor. *Science* 1996;**271**(5248):518-20.

(53) Navab M, Berliner JA, Subbanagounder G *et al*. HDL and the inflammatory response induced by LDL-derived oxidized phospholipids. *Arterioscler Thromb Vasc Biol* 2001;**21**(4):481-8.

(54) Groenendijk M, Cantor RM, de Bruin TW *et al*. The apoAI-CIII-AIV gene cluster. *Atherosclerosis* 2001;**157**(1):1-11.

(55) Soutar AK, Garner CW, Baker HN *et al*. Effect of the human plasma apolipoproteins and phosphatidylcholine acyl donor on the activity of lecithin: cholesterol acyltransferase. *Biochemistry* 1975;**14**(14):3057-64.

(56) Steyrer E, Kostner GM. Activation of lecithin-cholesterol acyltransferase by apolipoprotein D: comparison of proteoliposomes containing apolipoprotein D, A-I or C-I. *Biochim Biophys Acta* 1988;**958**(3):484-91.

(57) Fielding CJ, Shore VG, Fielding PE. A protein cofactor of lecithin:cholesterol acyltransferase. *Biochem Biophys Res Commun* 1972;**46**(4):1493-8.

(58) Johnson WJ, Mahlberg FH, Rothblat GH *et al*. Cholesterol transport between cells and high-density lipoproteins. *Biochim Biophys Acta* 1991;**1085**(3):273-98.

(59) Brinton EA, Eisenberg S, Breslow JL. A low-fat diet decreases high density lipoprotein (HDL) cholesterol levels by decreasing HDL apolipoprotein transport rates. *J Clin Invest* 1990;**85**(1):144-51.

(60) Walsh A, Ito Y, Breslow JL. High levels of human apolipoprotein A-I in transgenic mice result in increased plasma levels of small high density lipoprotein (HDL) particles comparable to human HDL3. *J Biol Chem* 1989;**264**(11):6488-94.

(61) Rubin EM, Krauss RM, Spangler EA *et al*. Inhibition of early atherogenesis in transgenic mice by human apolipoprotein AI. *Nature* 1991;**353**(6341):265-7.

(62) Gordon JI, Sims HF, Lentz SR *et al*. Proteolytic processing of human preproapolipoprotein A-I. A proposed defect in the conversion of pro A-I to A-I in Tangier's disease. *J Biol Chem* 1983;**258**(6):4037-44.

(63) Schaefer EJ, Kay LL, Zech LA *et al*. Tangier disease. High density lipoprotein deficiency due to defective metabolism of an abnormal apolipoprotein A-i (ApoA-ITangier). *J Clin Invest* 1982;**70**(5):934-45.

(64) Kay LL, Ronan R, Schaefer EJ *et al*. Tangier disease: a structural defect in apolipoprotein A-I (apoA-I Tangier). *Proc Natl Acad Sci U S A* 1982;**79**(8):2485-9.

(65) Zannis VI, Lees AM, Lees RS *et al*. Abnormal apoprotein A-I isoprotein composition in patients with Tangier disease. *J Biol Chem* 1982;**257**(9):4978-86.

(66) Jong MC, Hofker MH, Havekes LM. Role of ApoCs in lipoprotein metabolism: functional differences between ApoC1, ApoC2, and ApoC3. *Arterioscler Thromb Vasc Biol* 1999;**19**(3):472-84.

(67) Mahley RW, Innerarity TL, Rall SC, Jr. *et al*. Plasma lipoproteins: apolipoprotein structure and function. *J Lipid Res* 1984;**25**(12):1277-94.

(68) Simonet WS, Bucay N, Pitas RE *et al*. Multiple tissue-specific elements control the apolipoprotein E/C-I gene locus in transgenic mice. *J Biol Chem* 1991;**266**(14):8651-4.

(69) Dang Q, Taylor J. In vivo footprinting analysis of the hepatic control region of the human apolipoprotein E/C-I/C-IV/C-II gene locus. *J Biol Chem* 1996;**271**(45):28667-76.

(70) Weisgraber KH, Mahley RW, Kowal RC *et al*. Apolipoprotein C-I modulates the interaction of apolipoprotein E with beta-migrating very low density lipoproteins (beta-VLDL) and inhibits binding of beta-VLDL to low density lipoprotein receptor-related protein. *J Biol Chem* 1990;**265**(36):22453-9.

(71) Sehayek E, Eisenberg S. Mechanisms of inhibition by apolipoprotein C of apolipoprotein E-dependent cellular metabolism of human triglyceride-rich lipoproteins through the low density lipoprotein receptor pathway. *J Biol Chem* 1991;**266**(27):18259-67.

(72) Swaney JB, Weisgraber KH. Effect of apolipoprotein C-I peptides on the apolipoprotein E content and receptor-binding properties of beta-migrating very low density lipoproteins. *J Lipid Res* 1994;**35**(1):134-42.

(73) Kowal RC, Herz J, Weisgraber KH *et al*. Opposing effects of apolipoproteins E and C on lipoprotein binding to low density lipoprotein receptor-related protein. *J Biol Chem* 1990;**265**(18):10771-9.

(74) Jong MC, Dahlmans VE, van Gorp PJ *et al*. In the absence of the low density lipoprotein receptor, human apolipoprotein C1 overexpression in transgenic mice inhibits the hepatic uptake of very low density lipoproteins via a receptor-associated protein-sensitive pathway. *J Clin Invest* 1996;**98**(10):2259-67.

(75) Soutar AK, Sigler GF, Smith LC *et al*. Lecithin:cholesterol acyltransferase activation and lipid binding by synthetic fragments of apolipoprotein C-I. *Scand J Clin Lab Invest Suppl* 1978;**150**:53-8.

(76) Subbaiah PV, Albers JJ, Chen CH *et al*. Low density lipoprotein-activated lysolecithin acylation by human plasma lecithin-cholesterol acyltransferase. Identity of lysolecithin acyltransferase and lecithin-cholesterol acyltransferase. *J Biol Chem* 1980;**255**(19):9275-80.

(77) Liu M, Subbaiah PV. Activation of plasma lysolecithin acyltransferase reaction by apolipoproteins A-I, C-I and E. *Biochim Biophys Acta* 1993;**1168**(2):144-52.

(78) Brown WV, Baginsky ML. Inhibition of lipoprotein lipase by an apoprotein of human very low density lipoprotein. *Biochem Biophys Res Commun* 1972;**46**(2):375-82.

(79) Poensgen J. Apolipoprotein C-1 inhibits the hydrolysis by phospholipase A2 of phospholipids in liposomes and cell membranes. *Biochim Biophys Acta* 1990;**1042**(2):188-92.

(80) Webb NR. Secretory phospholipase A2 enzymes in atherogenesis. *Curr Opin Lipidol* 2005;**16**(3):341-4.

(81) Kushwaha RS, Hasan SQ, McGill HC, Jr. *et al*. Characterization of cholesteryl ester transfer protein inhibitor from plasma of baboons (Papio sp.). *J Lipid Res* 1993;**34**(8):1285-97.

(82) Gautier T, Masson D, de Barros JP *et al*. Human apolipoprotein C-I accounts for the ability of plasma high density lipoproteins to inhibit the cholesteryl ester transfer protein activity. *J Biol Chem* 2000;**275**(48):37504-9.

(83) Shachter NS, Ebara T, Ramakrishnan R *et al*. Combined hyperlipidemia in transgenic mice overexpressing human apolipoprotein Cl. *J Clin Invest* 1996;**98**(3):846-55.

(84) van Ree JH, Hofker MH, van den Broek WJ *et al*. Increased response to cholesterol feeding in apolipoprotein C1-deficient mice. *Biochem J* 1995;**305 (Pt 3)**:905-11.

(85) Jong MC, van Ree JH, Dahlmans VE *et al*. Reduced very-low-density lipoprotein fractional catabolic rate in apolipoprotein C1-deficient mice. *Biochem J* 1997;**321 (Pt 2)**:445-50.

(86) Weisgraber KH. Apolipoprotein E: structure-function relationships. *Adv Protein Chem* 1994;**45**:249-302.

(87) Weisgraber KH, Rall SC, Jr., Mahley RW *et al*. Human apolipoprotein E. Determination of the heparin binding sites of apolipoprotein E3. *J Biol Chem* 1986;**261**(5):2068-76.

(88) Lalazar A, Weisgraber KH, Rall SC, Jr. *et al*. Site-specific mutagenesis of human apolipoprotein E. Receptor binding activity of variants with single amino acid substitutions. *J Biol Chem* 1988;**263**(8):3542-5.

(89) Weisgraber KH, Innerarity TL, Harder KJ *et al*. The receptor-binding domain of human apolipoprotein E. Monoclonal antibody inhibition of binding. *J Biol Chem* 1983;**258**(20):12348-54.

(90) Innerarity TL, Friedlander EJ, Rall SC, Jr. *et al*. The receptor-binding domain of human apolipoprotein E. Binding of apolipoprotein E fragments. *J Biol Chem* 1983;**258**(20):12341-7.

(91) Rosenfeld ME, Butler S, Ord VA *et al*. Abundant expression of apoprotein E by macrophages in human and rabbit atherosclerotic lesions. *Arterioscler Thromb* 1993;**13**(9):1382-9.

(92) Ji ZS, Fazio S, Lee YL *et al*. Secretion-capture role for apolipoprotein E in remnant lipoprotein metabolism involving cell surface heparan sulfate proteoglycans. *J Biol Chem* 1994;**269**(4):2764-72.

(93) Ji ZS, Brecht WJ, Miranda RD *et al*. Role of heparan sulfate proteoglycans in the binding and uptake of apolipoprotein E-enriched remnant lipoproteins by cultured cells. *J Biol Chem* 1993;**268**(14):10160-7.

(94) Al Haideri M, Goldberg IJ, Galeano NF *et al*. Heparan sulfate proteoglycan-mediated uptake of apolipoprotein E-triglyceride-rich lipoprotein particles: a major pathway at physiological particle concentrations. *Biochemistry* 1997;**36**(42):12766-72.

(95) Futamura M, Dhanasekaran P, Handa T *et al*. Two-step mechanism of binding of apolipoprotein E to heparin: implications for the kinetics of apolipoprotein E-heparan sulfate proteoglycan complex formation on cell surfaces. *J Biol Chem* 2005;**280**(7):5414-22.

(96) Rumsey SC, Obunike JC, Arad Y *et al*. Lipoprotein lipase-mediated uptake and degradation of low density lipoproteins by fibroblasts and macrophages. *J Clin Invest* 1992;**90**(4):1504-12.

(97) Holtzman DM, Pitas RE, Kilbridge J *et al*. Low density lipoprotein receptor-related protein mediates apolipoprotein E-dependent neurite outgrowth in a central nervous system-derived neuronal cell line. *Proc Natl Acad Sci U S A* 1995;**92**(21):9480-4.

(98) Lucas M, Mazzone T. Cell surface proteoglycans modulate net synthesis and secretion of macrophage apolipoprotein E. *J Biol Chem* 1996;**271**(23):13454-60.

(99) Swertfeger DK, Hui DY. Apolipoprotein E: a cholesterol transport protein with lipid transport-independent cell signaling properties. *Front Biosci* 2001;**6**:D526-D535.

(100) Zhu Y, Hui DY. Apolipoprotein E binding to low density lipoprotein receptor-related protein-1 inhibits cell migration via activation of cAMP-dependent protein kinase A. *J Biol Chem* 2003;**278**(38):36257-63.

(101) Bazin HG, Marques MA, Owens AP, III *et al*. Inhibition of apolipoprotein E-related neurotoxicity by glycosaminoglycans and their oligosaccharides. *Biochemistry* 2002;**41**(25):8203-11.

(102) Zhang SH, Reddick RL, Piedrahita JA *et al*. Spontaneous hypercholesterolemia and arterial lesions in mice lacking apolipoprotein E. *Science* 1992;**258**(5081):468-71.

(103) Hussain MM, Maxfield FR, Mas-Oliva J *et al*. Clearance of chylomicron remnants by the low density lipoprotein receptor-related protein/alpha 2-macroglobulin receptor. *J Biol Chem* 1991;**266**(21):13936-40.

(104) Cabezon E, Runswick MJ, Leslie AG *et al*. The structure of bovine IF(1), the regulatory subunit of mitochondrial F-ATPase. *EMBO J* 2001;**20**(24):6990-6.

(105) Martinez LO, Jacquet S, Esteve JP *et al*. Ectopic beta-chain of ATP synthase is an apolipoprotein A-I receptor in hepatic HDL endocytosis. *Nature* 2003;**421**(6918):75-9.

(106) Beisiegel U, Weber W, Havinga JR *et al*. Apolipoprotein E-binding proteins isolated from dog and human liver. *Arteriosclerosis* 1988;**8**(3):288-97.

(107) Mahley RW, Hui DY, Innerarity TL *et al*. Chylomicron remnant metabolism. Role of hepatic lipoprotein receptors in mediating uptake. *Arteriosclerosis* 1989;**9**(1 Suppl):I14-I18.

(108) Das B, Mondragon MO, Sadeghian M *et al*. A novel ligand in lymphocyte-mediated cytotoxicity: expression of the beta subunit of H+ transporting ATP synthase on the surface of tumor cell lines. *J Exp Med* 1994;**180**(1):273-81.

(109) Moser TL, Kenan DJ, Ashley TA *et al*. Endothelial cell surface F1-F0 ATP synthase is active in ATP synthesis and is inhibited by angiostatin. *Proc Natl Acad Sci U S A* 2001;**98**(12):6656-61.

(110) Morita SY, Nakano M, Sakurai A *et al*. Formation of ceramide-enriched domains in lipid particles enhances the binding of apolipoprotein E. *FEBS Lett* 2005;**579**(7):1759-64.

(111) Morita SY, Okuhira K, Tsuchimoto N *et al*. Effects of sphingomyelin on apolipoprotein E- and lipoprotein lipase-mediated cell uptake of lipid particles. *Biochim Biophys Acta* 2003;**1631**(2):169-76.

(112) Morita SY, Kawabe M, Sakurai A *et al*. Ceramide in lipid particles enhances heparan sulfate proteoglycan and low density lipoprotein receptor-related protein-mediated uptake by macrophages. *J Biol Chem* 2004;**279**(23):24355-61.

(113) Huang ZH, Lin CY, Oram JF *et al*. Sterol efflux mediated by endogenous macrophage ApoE expression is independent of ABCA1. *Arterioscler Thromb Vasc Biol* 2001;**21**(12):2019-25.

(114) Lin CY, Duan H, Mazzone T. Apolipoprotein E-dependent cholesterol efflux from macrophages: kinetic study and divergent mechanisms for endogenous versus exogenous apolipoprotein E. *J Lipid Res* 1999;**40**(9):1618-27.

(115) Huang ZH, Mazzone T. ApoE-dependent sterol efflux from macrophages is modulated by scavenger receptor class B type I expression. *J Lipid Res* 2002;**43**(3):375-82.

(116) Mahley RW. Apolipoprotein E: cholesterol transport protein with expanding role in cell biology. *Science* 1988;**240**(4852):622-30.

(117) van den EP, Garg S, Leon L *et al*. Apolipoprotein-mediated pathways of lipid antigen presentation. *Nature* 2005;**437**(7060):906-10.

(118) Brigl M, Brenner MB. CD1: antigen presentation and T cell function. *Annu Rev Immunol* 2004;**22**:817-90.

(119) Sugita M, Cernadas M, Brenner MB. New insights into pathways for CD1-mediated antigen presentation. *Curr Opin Immunol* 2004;**16**(1):90-5.

(120) von Eckardstein A, Langer C, Engel T *et al*. ATP binding cassette transporter ABCA1 modulates the secretion of apolipoprotein E from human monocyte-derived macrophages. *FASEB J* 2001;**15**(9):1555-61.

(121) Heeren J, Beisiegel U. Intracellular metabolism of triglyceride-rich lipoproteins. *Curr Opin Lipidol* 2001;**12**(3):255-60.

(122) Rees D, Sloane T, Jessup W *et al*. Apolipoprotein A-I stimulates secretion of apolipoprotein E by foam cell macrophages. *J Biol Chem* 1999;**274**(39):27925-33.

(123) Basu SK, Ho YK, Brown MS *et al*. Biochemical and genetic studies of the apoprotein E secreted by mouse macrophages and human monocytes. *J Biol Chem* 1982;**257**(16):9788-95.

(124) Herscovitz H, Gantz D, Tercyak AM *et al*. Expression of human apolipoprotein E but not that of apolipoprotein A-I by mouse C127 cells is associated with increased secretion of lipids in the form of vesicles and discs. *J Lipid Res* 1992;**33**(6):791-803.

(125) Wenner C, Lorkowski S, Engel T *et al*. Apolipoprotein E in macrophages and hepatocytes is eegraded via the proteasomal pathway. *Biochem Biophys Res Commun* 2001;**282**(2):608-14.

(126) Schmitt M, Grand-Perret T. Regulated turnover of a cell surface-associated pool of newly synthesized apolipoprotein E in HepG2 cells. *J Lipid Res* 1999;**40**(1):39-49.

(127) Williams KJ, Brocia RW, Fisher EA. The unstirred water layer as a site of control of apolipoprotein B secretion. *J Biol Chem* 1990;**265**(28):16741-4.

(128) Fisher EA, Pan M, Chen X *et al*. The triple threat to nascent apolipoprotein B. Evidence for multiple, distinct degradative pathways. *J Biol Chem* 2001;**276**(30):27855-63.

(129) Pan M, Cederbaum AI, Zhang YL *et al*. Lipid peroxidation and oxidant stress regulate hepatic apolipoprotein B degradation and VLDL production. *J Clin Invest* 2004;**113**(9):1277-87.

(130) Yamashita S, Hirano K, Sakai N *et al*. Molecular biology and pathophysiological aspects of plasma cholesteryl ester transfer protein. *Biochim Biophys Acta* 2000;**1529**(1-3):257-75.

(131) Tall AR, Jiang X, Luo Y *et al*. 1999 George Lyman Duff memorial lecture: lipid transfer proteins, HDL metabolism, and atherogenesis. *Arterioscler Thromb Vasc Biol* 2000;**20**(5):1185-8.

(132) Zhang Z, Yamashita S, Hirano K *et al*. Expression of cholesteryl ester transfer protein in human atherosclerotic lesions and its implication in reverse cholesterol transport. *Atherosclerosis* 2001;**159**(1):67-75.

(133) Faust RA, Tollefson JH, Chait A *et al*. Regulation of LTP-I secretion from human monocyte-derived macrophages by differentiation and cholesterol accumulation in vitro. *Biochim Biophys Acta* 1990;**1042**(3):404-9.

(134) Rye KA, Hime NJ, Barter PJ. The influence of cholesteryl ester transfer protein on the composition, size, and structure of spherical, reconstituted high density lipoproteins. *J Biol Chem* 1995;**270**(1):189-96.

(135) Rye KA, Hime NJ, Barter PJ. Evidence that cholesteryl ester transfer protein-mediated reductions in reconstituted high density lipoprotein size involve particle fusion. *J Biol Chem* 1997;**272**(7):3953-60.

(136) Tall AR, Forester LR, Bongiovanni GL. Facilitation of phosphatidylcholine transfer into high density lipoproteins by an apolipoprotein in the density 1.20-1.26 g/ml fraction of plasma. *J Lipid Res* 1983;**24**(3):277-89.

(137) Desrumaux CM, Mak PA, Boisvert WA *et al*. Phospholipid transfer protein is present in human atherosclerotic lesions and is expressed by macrophages and foam cells. *J Lipid Res* 2003;**44**(8):1453-61.

(138) Tu AY, Nishida HI, Nishida T. High density lipoprotein conversion mediated by human plasma phospholipid transfer protein. *J Biol Chem* 1993;**268**(31):23098-105.

(139) Jauhiainen M, Metso J, Pahlman R *et al*. Human plasma phospholipid transfer protein causes high density lipoprotein conversion. *J Biol Chem* 1993;**268**(6):4032-6.

(140) Lagrost L, Athias A, Herbeth B *et al*. Opposite effects of cholesteryl ester transfer protein and phospholipid transfer protein on the size distribution of plasma high density lipoproteins. Physiological relevance in alcoholic patients. *J Biol Chem* 1996;**271**(32):19058-65.

(141) von Eckardstein A, Jauhiainen M, Huang Y *et al*. Phospholipid transfer protein mediated conversion of high density lipoproteins generates pre beta 1-HDL. *Biochim Biophys Acta* 1996;**1301**(3):255-62.

(142) Jiang XC, Bruce C, Mar J *et al*. Targeted mutation of plasma phospholipid transfer protein gene markedly reduces high-density lipoprotein levels. *J Clin Invest* 1999;**103**(6):907-14.

(143) Cao G, Beyer TP, Yang XP *et al*. Phospholipid transfer protein is regulated by liver X receptors in vivo. *J Biol Chem* 2002;**277**(42):39561-5.

(144) Kostner GM, Oettl K, Jauhiainen M *et al*. Human plasma phospholipid transfer protein accelerates exchange/transfer of alpha-tocopherol between lipoproteins and cells. *Biochem J* 1995;**305 (Pt 2)**:659-67.

(145) Hailman E, Albers JJ, Wolfbauer G *et al*. Neutralization and transfer of lipopolysaccharide by phospholipid transfer protein. *J Biol Chem* 1996;**271**(21):12172-8.

(146) Nishida HI, Nishida T. Phospholipid transfer protein mediates transfer of not only phosphatidylcholine but also cholesterol from phosphatidylcholine-cholesterol vesicles to high density lipoproteins. *J Biol Chem* 1997;**272**(11):6959-64.

(147) Chao FF, Blanchette-Mackie EJ, Tertov VV *et al*. Hydrolysis of cholesteryl ester in low density lipoprotein converts this lipoprotein to a liposome. *J Biol Chem* 1992;**267**(7):4992-8.

(148) Bhakdi S, Dorweiler B, Kirchmann R *et al*. On the pathogenesis of atherosclerosis: enzymatic transformation of human low density lipoprotein to an atherogenic moiety. *J Exp Med* 1995;**182**(6):1959-71.

(149) Kapinsky M, Torzewski M, Buchler C *et al*. Enzymatically degraded LDL preferentially binds to CD14(high) CD16(+) monocytes and induces foam cell formation mediated only in part by the class B scavenger-receptor CD36. *Arterioscler Thromb Vasc Biol* 2001;**21**(6):1004-10.

(150) Bhakdi S, Torzewski M, Klouche M *et al*. Complement and atherogenesis: binding of CRP to degraded, nonoxidized LDL enhances complement activation. *Arterioscler Thromb Vasc Biol* 1999;**19**(10):2348-54.

(151) Torzewski M, Rist C, Mortensen RF *et al*. C-reactive protein in the arterial intima: role of C-reactive protein receptor-dependent monocyte recruitment in atherogenesis. *Arterioscler Thromb Vasc Biol* 2000;**20**(9):2094-9.

(152) Torzewski M, Klouche M, Hock J *et al*. Immunohistochemical demonstration of enzymatically modified human LDL and its colocalization with the terminal complement complex in the early atherosclerotic lesion. *Arterioscler Thromb Vasc Biol* 1998;**18**(3):369-78.

(153) Klouche M, May AE, Hemmes M *et al*. Enzymatically modified, nonoxidized LDL induces selective adhesion and transmigration of monocytes and T-lymphocytes through human endothelial cell monolayers. *Arterioscler Thromb Vasc Biol* 1999;**19**(3):784-93.

(154) Klouche M, Gottschling S, Gerl V *et al*. Atherogenic properties of enzymatically degraded LDL: selective induction of MCP-1 and cytotoxic effects on human macrophages. *Arterioscler Thromb Vasc Biol* 1998;**18**(9):1376-85.

(155) Suriyaphol P, Fenske D, Zahringer U *et al*. Enzymatically modified nonoxidized low-density lipoprotein induces interleukin-8 in human endothelial cells: role of free fatty acids. *Circulation* 2002;**106**(20):2581-7.

(156) Witztum JL, Steinberg D. Role of oxidized low density lipoprotein in atherogenesis. *J Clin Invest* 1991;**88**(6):1785-92.

(157) Stocker R. Lipoprotein oxidation: mechanistic aspects, methodological approaches and clinical relevance. *Curr Opin Lipidol* 1994;**5**(6):422-33.

(158) Berliner JA, Heinecke JW. The role of oxidized lipoproteins in atherogenesis. *Free Radic Biol Med* 1996;**20**(5):707-27.

(159) Kritharides L, Jessup W, Gifford J *et al*. A method for defining the stages of low-density lipoprotein oxidation by the separation of cholesterol- and cholesteryl ester-oxidation products using HPLC. *Anal Biochem* 1993;**213**(1):79-89.

(160) Endemann G, Stanton LW, Madden KS *et al*. CD36 is a receptor for oxidized low density lipoprotein. *J Biol Chem* 1993;**268**(16):11811-6.

(161) Jessup W, Wilson P, Gaus K *et al*. Oxidized lipoproteins and macrophages. *Vascul Pharmacol* 2002;**38**(4):239-48.

(162) Brown AJ, Mander EL, Gelissen IC *et al*. Cholesterol and oxysterol metabolism and subcellular distribution in macrophage foam cells. Accumulation of oxidized esters in lysosomes. *J Lipid Res* 2000;**41**(2):226-37.

(163) Jessup W, Kritharides L. Metabolism of oxidized LDL by macrophages. *Curr Opin Lipidol* 2000;**11**(5):473-81.

(164) Jerome WG, Cash C, Webber R *et al*. Lysosomal lipid accumulation from oxidized low density lipoprotein is correlated with hypertrophy of the Golgi apparatus and trans-Golgi network. *J Lipid Res* 1998;**39**(7):1362-71.

(165) Clare K, Hardwick SJ, Carpenter KL *et al*. Toxicity of oxysterols to human monocyte-macrophages. *Atherosclerosis* 1995;**118**(1):67-75.

(166) Quinn MT, Parthasarathy S, Fong LG *et al*. Oxidatively modified low density lipoproteins: a potential role in recruitment and retention of monocyte/macrophages during atherogenesis. *Proc Natl Acad Sci U S A* 1987;**84**(9):2995-8.

(167) Hessler JR, Morel DW, Lewis LJ *et al*. Lipoprotein oxidation and lipoprotein-induced cytotoxicity. *Arteriosclerosis* 1983;**3**(3):215-22.

(168) Krieger M, Herz J. Structures and functions of multiligand lipoprotein receptors: macrophage scavenger receptors and LDL receptor-related protein (LRP). *Annu Rev Biochem* 1994;**63**:601-37.

(169) Kodama T, Doi T, Suzuki H *et al*. Collagenous macrophage scavenger receptors. *Curr Opin Lipidol* 1996;**7**(5):287-91.

(170) Geng Y, Kodama T, Hansson GK. Differential expression of scavenger receptor isoforms during monocyte-macrophage differentiation and foam cell formation. *Arterioscler Thromb* 1994;**14**(5):798-806.

(171) Suzuki H, Kurihara Y, Takeya M *et al*. A role for macrophage scavenger receptors in atherosclerosis and susceptibility to infection. *Nature* 1997;**386**(6622):292-6.

(172) Gough PJ, Greaves DR, Gordon S. A naturally occurring isoform of the human macrophage scavenger receptor (SR-A) gene generated by alternative splicing blocks modified LDL uptake. *J Lipid Res* 1998;**39**(3):531-43.

(173) Mori T, Takahashi K, Naito M *et al*. Endocytic pathway of scavenger receptors via trans-Golgi system in bovine alveolar macrophages. *Lab Invest* 1994;**71**(3):409-16.

(174) Platt N, Gordon S. Is the class A macrophage scavenger receptor (SR-A) multifunctional? - The mouse's tale. *J Clin Invest* 2001;**108**(5):649-54.

(175) Elomaa O, Kangas M, Sahlberg C *et al*. Cloning of a novel bacteria-binding receptor structurally related to scavenger receptors and expressed in a subset of macrophages. *Cell* 1995;**80**(4):603-9.

(176) Abumrad NA, el Maghrabi MR, Amri EZ *et al*. Cloning of a rat adipocyte membrane protein implicated in binding or transport of long-chain fatty acids that is induced during preadipocyte differentiation. Homology with human CD36. *J Biol Chem* 1993;**268**(24):17665-8.

(177) Nakata A, Nakagawa Y, Nishida M *et al*. CD36, a novel receptor for oxidized low-density lipoproteins, is highly expressed on lipid-laden macrophages in human atherosclerotic aorta. *Arterioscler Thromb Vasc Biol* 1999;**19**(5):1333-9.

(178) Rigotti A, Krieger M. Getting a handle on "good" cholesterol with the high-density lipoprotein receptor. *N Engl J Med* 1999;**341**(26):2011-3.

(179) Trigatti B, Rigotti A, Krieger M. The role of the high-density lipoprotein receptor SR-BI in cholesterol metabolism. *Curr Opin Lipidol* 2000;**11**(2):123-31.

(180) Chinetti G, Gbaguidi FG, Griglio S *et al*. CLA-1/SR-BI is expressed in atherosclerotic lesion macrophages and regulated by activators of peroxisome proliferator-activated receptors. *Circulation* 2000;**101**(20):2411-7.

(181) Ramprasad MP, Fischer W, Witztum JL *et al*. The 94- to 97-kDa mouse macrophage membrane protein that recognizes oxidized low density lipoprotein and phosphatidylserine-rich liposomes is identical to macrosialin, the mouse homologue of human CD68. *Proc Natl Acad Sci U S A* 1995;**92**(21):9580-4.

(182) Naito M, Suzuki H, Mori T *et al*. Coexpression of type I and type II human macrophage scavenger receptors in macrophages of various organs and foam cells in atherosclerotic lesions. *Am J Pathol* 1992;**141**(3):591-9.

(183) Ramprasad MP, Terpstra V, Kondratenko N *et al*. Cell surface expression of mouse macrosialin and human CD68 and their role as macrophage receptors for oxidized low density lipoprotein. *Proc Natl Acad Sci U S A* 1996;**93**(25):14833-8.

(184) Sawamura T, Kume N, Aoyama T *et al*. An endothelial receptor for oxidized low-density lipoprotein. *Nature* 1997;**386**(6620):73-7.

(185) Moriwaki H, Kume N, Sawamura T *et al*. Ligand specificity of LOX-1, a novel endothelial receptor for oxidized low density lipoprotein. *Arterioscler Thromb Vasc Biol* 1998;**18**(10):1541-7.

(186) Cominacini L, Pasini AF, Garbin U *et al*. Oxidized low density lipoprotein (ox-LDL) binding to ox-LDL receptor-1 in endothelial cells induces the activation of NF-kappaB through an increased production of intracellular reactive oxygen species. *J Biol Chem* 2000;**275**(17):12633-8.

(187) Li D, Mehta JL. Antisense to LOX-1 inhibits oxidized LDL-mediated upregulation of monocyte chemoattractant protein-1 and monocyte adhesion to human coronary artery endothelial cells. *Circulation* 2000;**101**(25):2889-95.

(188) Oka K, Sawamura T, Kikuta K *et al*. Lectin-like oxidized low-density lipoprotein receptor 1 mediates phagocytosis of aged/apoptotic cells in endothelial cells. *Proc Natl Acad Sci U S A* 1998;**95**(16):9535-40.

(189) Kakutani M, Masaki T, Sawamura T. A platelet-endothelium interaction mediated by lectin-like oxidized low-density lipoprotein receptor-1. *Proc Natl Acad Sci U S A* 2000;**97**(1):360-4.

(190) Shimaoka T, Kume N, Minami M *et al*. LOX-1 supports adhesion of Gram-positive and Gram-negative bacteria. *J Immunol* 2001;**166**(8):5108-14.

(191) Minami M, Kume N, Shimaoka T *et al*. Expression of SR-PSOX, a novel cell-surface scavenger receptor for phosphatidylserine and oxidized LDL in human atherosclerotic lesions. *Arterioscler Thromb Vasc Biol* 2001;**21**(11):1796-800.

(192) Fadok VA, Bratton DL, Rose DM *et al*. A receptor for phosphatidylserine-specific clearance of apoptotic cells. *Nature* 2000;**405**(6782):85-90.

(193) Kounnas MZ, Moir RD, Rebeck GW *et al*. LDL receptor-related protein, a multifunctional ApoE receptor, binds secreted beta-amyloid precursor protein and mediates its degradation. *Cell* 1995;**82**(2):331-40.

(194) Gonias SL, Wu L, Salicioni AM. Low density lipoprotein receptor-related protein: regulation of the plasma membrane proteome. *Thromb Haemost* 2004;**91**(6):1056-64.

(195) Herz J, Beffert U. Apolipoprotein E receptors: linking brain development and Alzheimer's disease. *Nat Rev Neurosci* 2000;**1**(1):51-8.

(196) Trommsdorff M, Borg JP, Margolis B *et al*. Interaction of cytosolic adaptor proteins with neuronal apolipoprotein E receptors and the amyloid precursor protein. *J Biol Chem* 1998;**273**(50):33556-60.

(197) Hardy J, Allsop D. Amyloid deposition as the central event in the aetiology of Alzheimer's disease. *Trends Pharmacol Sci* 1991;**12**(10):383-8.

(198) Frackowiak J, Zoltowska A, Wisniewski HM. Non-fibrillar beta-amyloid protein is associated with smooth muscle cells of vessel walls in Alzheimer disease. *J Neuropathol Exp Neurol* 1994;**53**(6):637-45.

(199) De Meyer GR, De Cleen DM, Cooper S *et al*. Platelet phagocytosis and processing of beta-amyloid precursor protein as a mechanism of macrophage activation in atherosclerosis. *Circ Res* 2002;**90**(11):1197-204.

(200) Younkin SG. Evidence that A beta 42 is the real culprit in Alzheimer's disease. *Ann Neurol* 1995;**37**(3):287-8.

(201) Attems J, Lintner F, Jellinger KA. Amyloid beta peptide 1-42 highly correlates with capillary cerebral amyloid angiopathy and Alzheimer disease pathology. *Acta Neuropathol (Berl)* 2004;**107**(4):283-91.

(202) McLaurin J, Yang D, Yip CM *et al*. Review: modulating factors in amyloid-beta fibril formation. *J Struct Biol* 2000;**130**(2-3):259-70.

(203) Casserly I, Topol E. Convergence of atherosclerosis and Alzheimer's disease: inflammation, cholesterol, and misfolded proteins. *Lancet* 2004;**363**(9415):1139-46.

(204) Stanyer L, Betteridge DJ, Smith CC. Potentiation of beta-amyloid polymerisation by low-density lipoprotein enhances the peptide's vasoactivity. *Biochim Biophys Acta* 2004;**1670**(2):147-55.

(205) Moore KJ, El Khoury J, Medeiros LA *et al*. A CD36-initiated signaling cascade mediates inflammatory effects of beta-amyloid. *J Biol Chem* 2002;**277**(49):47373-9.

(206) El Khoury JB, Moore KJ, Means TK *et al*. CD36 mediates the innate host response to beta-amyloid. *J Exp Med* 2003;**197**(12):1657-66.

(207) Coraci IS, Husemann J, Berman JW *et al*. CD36, a class B scavenger receptor, is expressed on microglia in Alzheimer's disease brains and can mediate production of reactive oxygen species in response to beta-amyloid fibrils. *Am J Pathol* 2002;**160**(1):101-12.

(208) Bamberger ME, Harris ME, McDonald DR *et al*. A cell surface receptor complex for fibrillar beta-amyloid mediates microglial activation. *J Neurosci* 2003;**23**(7):2665-74.

(209) Laporte V, Lombard Y, Levy-Benezra R *et al*. Uptake of Abeta 1-40- and Abeta 1-42-coated yeast by microglial cells: a role for LRP. *J Leukoc Biol* 2004;**76**(2):451-61.

(210) Haverkate F, Thompson SG, Pyke SD *et al*. Production of C-reactive protein and risk of coronary events in stable and unstable angina. European Concerted Action on Thrombosis and Disabilities Angina Pectoris Study Group. *Lancet* 1997;**349**(9050):462-6.

(211) Bhakdi S, Torzewski M, Klouche M *et al*. Complement and atherogenesis: binding of CRP to degraded, nonoxidized LDL enhances complement activation. *Arterioscler Thromb Vasc Biol* 1999;**19**(10):2348-54.

(212) Marnell LL, Mold C, Volzer MA *et al*. C-reactive protein binds to Fc gamma RI in transfected COS cells. *J Immunol* 1995;**155**(4):2185-93.

(213) Bharadwaj D, Stein MP, Volzer M *et al*. The major receptor for C-reactive protein on leukocytes is fcgamma receptor II. *J Exp Med* 1999;**190**(4):585-90.

(214) Shakor AB, Czurylo EA, Sobota A. Lysenin, a unique sphingomyelin-binding protein. *FEBS Lett* 2003;**542**(1-3):1-6.

(215) Bodin S, Viala C, Ragab A *et al*. A critical role of lipid rafts in the organization of a key FcgammaRIIa-mediated signaling pathway in human platelets. *Thromb Haemost* 2003;**89**(2):318-30.

(216) Rollet-Labelle E, Marois S, Barbeau K *et al*. Recruitment of the cross-linked opsonic receptor CD32A (FcgammaRIIA) to high-density detergent-resistant membrane domains in human neutrophils. *Biochem J* 2004;**381**(Pt 3):919-28.

(217) Li XA, Hatanaka K, Ishibashi-Ueda H *et al*. Characterization of serum amyloid P component from human aortic atherosclerotic lesions. *Arterioscler Thromb Vasc Biol* 1995;**15**(2):252-7.

(218) Hicks PS, Saunero-Nava L, Du Clos TW *et al*. Serum amyloid P component binds to histones and activates the classical complement pathway. *J Immunol* 1992;**149**(11):3689-94.

(219) Miida T, Yamada T, Yamadera T *et al*. Serum amyloid A protein generates pre beta 1 high-density lipoprotein from alpha-migrating high-density lipoprotein. *Biochemistry* 1999;**38**(51):16958-62.

(220) Uhlar CM, Whitehead AS. Serum amyloid A, the major vertebrate acute-phase reactant. *Eur J Biochem* 1999;**265**(2):501-23.

(221) Mironova M, Virella G, Lopes-Virella MF. Isolation and characterization of human antioxidized LDL autoantibodies. *Arterioscler Thromb Vasc Biol* 1996;**16**(2):222-9.

(222) Le C, V, Carreno S, Moisand A *et al*. Complement receptor 3 (CD11b/CD18) mediates type I and type II phagocytosis during nonopsonic and opsonic phagocytosis, respectively. *J Immunol* 2002;**169**(4):2003-9.

(223) Daeron M. Fc receptor biology. *Annu Rev Immunol* 1997;**15**:203-34.

(224) Chawla A, Barak Y, Nagy L *et al*. PPAR-gamma dependent and independent effects on macrophage-gene expression in lipid metabolism and inflammation. *Nat Med* 2001;**7**(1):48-52.

(225) Peters JM, Hennuyer N, Staels B *et al*. Alterations in lipoprotein metabolism in peroxisome proliferator-activated receptor alpha-deficient mice. *J Biol Chem* 1997;**272**(43):27307-12.

(226) Kubota N, Terauchi Y, Miki H *et al*. PPAR gamma mediates high-fat diet-induced adipocyte hypertrophy and insulin resistance. *Mol Cell* 1999;**4**(4):597-609.

(227) Michalik L, Desvergne B, Tan NS *et al*. Impaired skin wound healing in peroxisome proliferator-activated receptor (PPAR)alpha and PPARbeta mutant mice. *J Cell Biol* 2001;**154**(4):799-814.

(228) Tan NS, Michalik L, Noy N *et al*. Critical roles of PPAR beta/delta in keratinocyte response to inflammation. *Genes Dev* 2001;**15**(24):3263-77.

(229) Chawla A, Lee CH, Barak Y *et al*. PPARdelta is a very low-density lipoprotein sensor in macrophages. *Proc Natl Acad Sci U S A* 2003;**100**(3):1268-73.

(230) Bishop-Bailey D. Peroxisome proliferator-activated receptors in the cardiovascular system. *Br J Pharmacol* 2000;**129**(5):823-34.

(231) Ricote M, Huang J, Fajas L *et al*. Expression of the peroxisome proliferator-activated receptor gamma (PPARgamma) in human atherosclerosis and regulation in macrophages by colony stimulating factors and oxidized low density lipoprotein. *Proc Natl Acad Sci U S A* 1998;**95**(13):7614-9.

(232) Tontonoz P, Nagy L, Alvarez JG *et al*. PPARgamma promotes monocyte/macrophage differentiation and uptake of oxidized LDL. *Cell* 1998;**93**(2):241-52.

(233) Tontonoz P, Nagy L. Regulation of macrophage gene expression by peroxisome-proliferator-activated receptor gamma: implications for cardiovascular disease. *Curr Opin Lipidol* 1999;**10**(6):485-90.

(234) Nagy L, Tontonoz P, Alvarez JG *et al*. Oxidized LDL regulates macrophage gene expression through ligand activation of PPARgamma. *Cell* 1998;**93**(2):229-40.

(235) Kliewer SA, Lenhard JM, Willson TM *et al*. A prostaglandin J2 metabolite binds peroxisome proliferator-activated receptor gamma and promotes adipocyte differentiation. *Cell* 1995;**83**(5):813-9.

(236) Forman BM, Tontonoz P, Chen J *et al*. 15-Deoxy-delta 12, 14-prostaglandin J2 is a ligand for the adipocyte determination factor PPAR gamma. *Cell* 1995;**83**(5):803-12.

(237) Tontonoz P, Nagy L, Alvarez JG *et al*. PPARgamma promotes monocyte/macrophage differentiation and uptake of oxidized LDL. *Cell* 1998;**93**(2):241-52.

(238) Fu X, Menke JG, Chen Y *et al*. 27-hydroxycholesterol is an endogenous ligand for liver X receptor in cholesterol-loaded cells. *J Biol Chem* 2001;**276**(42):38378-87.

(239) Huang JT, Welch JS, Ricote M *et al*. Interleukin-4-dependent production of PPAR-gamma ligands in macrophages by 12/15-lipoxygenase. *Nature* 1999;**400**(6742):378-82.

(240) Marx N, Sukhova G, Murphy C *et al*. Macrophages in human atheroma contain PPARgamma: differentiation-dependent peroxisomal proliferator-activated receptor gamma(PPARgamma) expression and reduction of MMP-9 activity through PPARgamma activation in mononuclear phagocytes in vitro. *Am J Pathol* 1998;**153**(1):17-23.

(241) Marx N, Schonbeck U, Lazar MA *et al*. Peroxisome proliferator-activated receptor gamma activators inhibit gene expression and migration in human vascular smooth muscle cells. *Circ Res* 1998;**83**(11):1097-103.

(242) Jiang C, Ting AT, Seed B. PPAR-gamma agonists inhibit production of monocyte inflammatory cytokines. *Nature* 1998;**391**(6662):82-6.

(243) Ricote M, Li AC, Willson TM *et al*. The peroxisome proliferator-activated receptor-gamma is a negative regulator of macrophage activation. *Nature* 1998;**391**(6662):79-82.

(244) Chinetti G, Lestavel S, Bocher V *et al*. PPAR-alpha and PPAR-gamma activators induce cholesterol removal from human macrophage foam cells through stimulation of the ABCA1 pathway. *Nat Med* 2001;**7**(1):53-8.

(245) Venkateswaran A, Laffitte BA, Joseph SB *et al*. Control of cellular cholesterol efflux by the nuclear oxysterol receptor LXR alpha. *Proc Natl Acad Sci U S A* 2000;**97**(22):12097-102.

(246) Laffitte BA, Repa JJ, Joseph SB *et al*. LXRs control lipid-inducible expression of the apolipoprotein E gene in macrophages and adipocytes. *Proc Natl Acad Sci U S A* 2001;**98**(2):507-12.

(247) Pasceri V, Wu HD, Willerson JT *et al*. Modulation of vascular inflammation in vitro and in vivo by peroxisome proliferator-activated receptor-gamma activators. *Circulation* 2000;**101**(3):235-8.

(248) Allenby G, Bocquel MT, Saunders M *et al*. Retinoic acid receptors and retinoid X receptors: interactions with endogenous retinoic acids. *Proc Natl Acad Sci U S A* 1993;**90**(1):30-4.

(249) Langmann T, Liebisch G, Moehle C *et al*. Gene expression profiling identifies retinoids as potent inducers of macrophage lipid efflux. *Biochim Biophys Acta* 2005;**1740**(2):155-61.

(250) Cullen P, Cignarella A, Brennhausen B *et al*. Phenotype-dependent differences in apolipoprotein E metabolism and in cholesterol homeostasis in human monocyte-derived macrophages. *J Clin Invest* 1998;**101**(8):1670-7.

(251) Hara M, Matsushima T, Satoh H *et al*. Isoform-dependent cholesterol efflux from macrophages by apolipoprotein E is modulated by cell surface proteoglycans. *Arterioscler Thromb Vasc Biol* 2003;**23**(2):269-74.

(252) Huang Y, von Eckardstein A, Wu S *et al*. Effects of the apolipoprotein E polymorphism on uptake and transfer of cell-derived cholesterol in plasma. *J Clin Invest* 1995;**96**(6):2693-701.

(253) Michikawa M, Fan QW, Isobe I *et al*. Apolipoprotein E exhibits isoform-specific promotion of lipid efflux from astrocytes and neurons in culture. *J Neurochem* 2000;**74**(3):1008-16.

(254) Heeren J, Grewal T, Laatsch A *et al*. Impaired recycling of apolipoprotein E4 is associated with intracellular cholesterol accumulation. *J Biol Chem* 2004;**279**(53):55483-92.

(255) Davignon J, Gregg RE, Sing CF. Apolipoprotein E polymorphism and atherosclerosis. *Arteriosclerosis* 1988;**8**(1):1-21.

(256) Gregg RE, Zech LA, Schaefer EJ *et al*. Abnormal in vivo metabolism of apolipoprotein E4 in humans. *J Clin Invest* 1986;**78**(3):815-21.

(257) Hopkins PC, Huang Y, McGuire JG *et al*. Evidence for differential effects of apoE3 and apoE4 on HDL metabolism. *J Lipid Res* 2002;**43**(11):1881-9.

(258) Miyata M, Smith JD. Apolipoprotein E allele-specific antioxidant activity and effects on cytotoxicity by oxidative insults and beta-amyloid peptides. *Nat Genet* 1996;**14**(1):55-61.

(259) Vitek MP, Snell J, Dawson H *et al*. Modulation of nitric oxide production in human macrophages by apolipoprotein-E and amyloid-beta peptide. *Biochem Biophys Res Commun* 1997;**240**(2):391-4.

(260) Brown CM, Wright E, Colton CA *et al*. Apolipoprotein E isoform mediated regulation of nitric oxide release. *Free Radic Biol Med* 2002;**32**(11):1071-5.

(261) Colton CA, Brown CM, Cook D *et al*. APOE and the regulation of microglial nitric oxide production: a link between genetic risk and oxidative stress. *Neurobiol Aging* 2002;**23**(5):777-85.

(262) Colton CA, Brown CM, Czapiga M *et al*. Apolipoprotein-E allele-specific regulation of nitric oxide production. *Ann N Y Acad Sci* 2002;**962**:212-25.

(263) Bodzioch M, Orso E, Klucken J *et al*. The gene encoding ATP-binding cassette transporter 1 is mutated in Tangier disease. *Nat Genet* 1999;**22**(4):347-51.

(264) Hobbs HH, Rader DJ. ABC1: connecting yellow tonsils, neuropathy, and very low HDL. *J Clin Invest* 1999;**104**(8):1015-7.

(265) Chatterjee S. Sphingolipids in atherosclerosis and vascular biology. *Arterioscler Thromb Vasc Biol* 1998;**18**(10):1523-33.

(266) Levade T, Auge N, Veldman RJ *et al*. Sphingolipid mediators in cardiovascular cell biology and pathology. *Circ Res* 2001;**89**(11):957-68.

(267) English D, Kovala AT, Welch Z *et al*. Induction of endothelial cell chemotaxis by sphingosine 1-phosphate and stabilization of endothelial monolayer barrier function by lysophosphatidic acid, potential mediators of hematopoietic angiogenesis. *J Hematother Stem Cell Res* 1999;**8**(6):627-34.

(268) Merrill AH, Jr., Jones DD. An update of the enzymology and regulation of sphingomyelin metabolism. *Biochim Biophys Acta* 1990;**1044**(1):1-12.

(269) Koval M, Pagano RE. Intracellular transport and metabolism of sphingomyelin. *Biochim Biophys Acta* 1991;**1082**(2):113-25.

(270) van Blitterswijk WJ, van der Luit AH, Caan W *et al*. Sphingolipids related to apoptosis from the point of view of membrane structure and topology. *Biochem Soc Trans* 2001;**29**(Pt 6):819-24.

(271) Diringer H, Marggraf WD, Koch MA *et al*. Evidence for a new biosynthetic pathway of sphingomyelin in SV 40 transformed mouse cells. *Biochem Biophys Res Commun* 1972;**47**(6):1345-52.

(272) Ullman MD, Radin NS. The enzymatic formation of sphingomyelin from ceramide and lecithin in mouse liver. *J Biol Chem* 1974;**249**(5):1506-12.

(273) Marggraf WD, Anderer FA, Kanfer JN. The formation of sphingomyelin from phosphatidylcholine in plasma membrane preparations from mouse fibroblasts. *Biochim Biophys Acta* 1981;**664**(1):61-73.

(274) Huitema K, van den DJ, Brouwers JF *et al*. Identification of a family of animal sphingomyelin synthases. *EMBO J* 2004;**23**(1):33-44.

(275) Liu B, Andrieu-Abadie N, Levade T *et al*. Glutathione regulation of neutral sphingomyelinase in tumor necrosis factor-alpha-induced cell death. *J Biol Chem* 1998;**273**(18):11313-20.

(276) Tepper CG, Jayadev S, Liu B *et al*. Role for ceramide as an endogenous mediator of Fas-induced cytotoxicity. *Proc Natl Acad Sci U S A* 1995;**92**(18):8443-7.

(277) Levade T, Jaffrezou JP. Signalling sphingomyelinases: which, where, how and why? *Biochim Biophys Acta* 1999;**1438**(1):1-17.

(278) Schissel SL, Keesler GA, Schuchman EH *et al*. The cellular trafficking and zinc dependence of secretory and lysosomal sphingomyelinase, two products of the acid sphingomyelinase gene. *J Biol Chem* 1998;**273**(29):18250-9.

(279) Yamaji A, Sekizawa Y, Emoto K *et al*. Lysenin, a novel sphingomyelin-specific binding protein. *J Biol Chem* 1998;**273**(9):5300-6.

(280) Nakai Y, Sakurai Y, Yamaji A *et al*. Lysenin-sphingomyelin binding at the surface of oligodendrocyte lineage cells increases during differentiation in vitro. *J Neurosci Res* 2000;**62**(4):521-9.

(281) Hanada K. Serine palmitoyltransferase, a key enzyme of sphingolipid metabolism. *Biochim Biophys Acta* 2003;**1632**(1-3):16-30.

(282) Hanada K, Hara T, Nishijima M. Purification of the serine palmitoyltransferase complex responsible for sphingoid base synthesis by using affinity peptide chromatography techniques. *J Biol Chem* 2000;**275**(12):8409-15.

(283) Perry DK, Carton J, Shah AK *et al*. Serine palmitoyltransferase regulates de novo ceramide generation during etoposide-induced apoptosis. *J Biol Chem* 2000;**275**(12):9078-84.

(284) Yasuda S, Kitagawa H, Ueno M *et al*. A novel inhibitor of ceramide trafficking from the endoplasmic reticulum to the site of sphingomyelin synthesis. *J Biol Chem* 2001;**276**(47):43994-4002.

(285) Fukasawa M, Nishijima M, Hanada K. Genetic evidence for ATP-dependent endoplasmic reticulum-to-Golgi apparatus trafficking of ceramide for sphingomyelin synthesis in Chinese hamster ovary cells. *J Cell Biol* 1999;**144**(4):673-85.

(286) Hanada K, Kumagai K, Yasuda S *et al*. Molecular machinery for non-vesicular trafficking of ceramide. *Nature* 2003;**426**(6968):803-9.

(287) Loewen CJ, Roy A, Levine TP. A conserved ER targeting motif in three families of lipid binding proteins and in Opi1p binds VAP. *EMBO J* 2003;**22**(9):2025-35.

(288) Tsujishita Y, Hurley JH. Structure and lipid transport mechanism of a StAR-related domain. *Nat Struct Biol* 2000;**7**(5):408-14.

(289) Zhang M, Liu P, Dwyer NK *et al*. MLN64 mediates mobilization of lysosomal cholesterol to steroidogenic mitochondria. *J Biol Chem* 2002;**277**(36):33300-10.

(290) de Brouwer AP, Bouma B, van Tiel CM *et al*. The binding of phosphatidylcholine to the phosphatidylcholine transfer protein: affinity and role in folding. *Chem Phys Lipids* 2001;**112**(2):109-19.

(291) Memon RA, Holleran WM, Moser AH *et al*. Endotoxin and cytokines increase hepatic sphingolipid biosynthesis and produce lipoproteins enriched in ceramides and sphingomyelin. *Arterioscler Thromb Vasc Biol* 1998;**18**(8):1257-65.

(292) Farrell AM, Uchida Y, Nagiec MM *et al*. UVB irradiation up-regulates serine palmitoyltransferase in cultured human keratinocytes. *J Lipid Res* 1998;**39**(10):2031-8.

(293) van Meer G, Holthuis JC. Sphingolipid transport in eukaryotic cells. *Biochim Biophys Acta* 2000;**1486**(1):145-70.

(294) Hannun YA, Bell RM. Functions of sphingolipids and sphingolipid breakdown products in cellular regulation. *Science* 1989;**243**(4890):500-7.

(295) Geilen CC, Bektas M, Wieder T *et al*. The vitamin D3 analogue, calcipotriol, induces sphingomyelin hydrolysis in human keratinocytes. *FEBS Lett* 1996;**378**(1):88-92.

(296) Kolesnick RN, Kronke M. Regulation of ceramide production and apoptosis. *Annu Rev Physiol* 1998;**60**:643-65.

(297) Pettus BJ, Chalfant CE, Hannun YA. Ceramide in apoptosis: an overview and current perspectives. *Biochim Biophys Acta* 2002;**1585**(2-3):114-25.

(298) Sugita M, Dulaney JT, Moser HW. Ceramidase deficiency in Farber's disease (lipogranulomatosis). *Science* 1972;**178**(65):1100-2.

(299) Xu CB, Hansen-Schwartz J, Edvinsson L. Sphingosine signaling and atherogenesis. *Acta Pharmacol Sin* 2004;**25**(7):849-54.

(300) Gulbins E, Kolesnick R. Raft ceramide in molecular medicine. *Oncogene* 2003;**22**(45):7070-7.

(301) Gulbins E, Grassme H. Ceramide and cell death receptor clustering. *Biochim Biophys Acta* 2002;**1585**(2-3):139-45.

(302) Abdel Shakor AB, Kwiatkowska K, Sobota A. Cell surface ceramide generation precedes and controls FcgammaRII clustering and phosphorylation in rafts. *J Biol Chem* 2004;**279**(35):36778-87.

(303) Sweet MJ, Hume DA. Endotoxin signal transduction in macrophages. *J Leukoc Biol* 1996;**60**(1):8-26.

(304) Wright SD, Kolesnick RN. Does endotoxin stimulate cells by mimicking ceramide? *Immunol Today* 1995;**16**(6):297-302.

(305) Triantafilou M, Triantafilou K. Lipopolysaccharide recognition: CD14, TLRs and the LPS-activation cluster. *Trends Immunol* 2002;**23**(6):301-4.

(306) Spiegel S. Sphingosine 1-phosphate: a prototype of a new class of second messengers. *J Leukoc Biol* 1999;**65**(3):341-4.

(307) Sugiyama A, Yatomi Y, Ozaki Y *et al*. Sphingosine 1-phosphate induces sinus tachycardia and coronary vasoconstriction in the canine heart. *Cardiovasc Res* 2000;**46**(1):119-25.

(308) Ohmori T, Yatomi Y, Osada M *et al*. Sphingosine 1-phosphate induces contraction of coronary artery smooth muscle cells via S1P2. *Cardiovasc Res* 2003;**58**(1):170-7.

(309) Karliner JS. Lysophospholipids and the cardiovascular system. *Biochim Biophys Acta* 2002;**1582**(1-3):216-21.

(310) Garcia JG, Liu F, Verin AD *et al*. Sphingosine 1-phosphate promotes endothelial cell barrier integrity by Edg-dependent cytoskeletal rearrangement. *J Clin Invest* 2001;**108**(5):689-701.

(311) Rosen H, Sanna G, Alfonso C. Egress: a receptor-regulated step in lymphocyte trafficking. *Immunol Rev* 2003;**195**:160-77.

(312) Meyer zu HD, Lass H, Kuchar I *et al*. Stimulation of intracellular sphingosine-1-phosphate production by G-protein-coupled sphingosine-1-phosphate receptors. *Eur J Pharmacol* 2001;**414**(2-3):145-54.

(313) Chun J, Goetzl EJ, Hla T *et al*. International Union of Pharmacology. XXXIV. Lysophospholipid receptor nomenclature. *Pharmacol Rev* 2002;**54**(2):265-9.

(314) Lee OH, Kim YM, Lee YM *et al*. Sphingosine 1-phosphate induces angiogenesis: its angiogenic action and signaling mechanism in human umbilical vein endothelial cells. *Biochem Biophys Res Commun* 1999;**264**(3):743-50.

(315) Kimura T, Watanabe T, Sato K *et al*. Sphingosine 1-phosphate stimulates proliferation and migration of human endothelial cells possibly through the lipid receptors, Edg-1 and Edg-3. *Biochem J* 2000;**348 Pt 1**:71-6.

(316) Okazaki T, Kondo T, Kitano T *et al*. Diversity and complexity of ceramide signalling in apoptosis. *Cell Signal* 1998;**10**(10):685-92.

(317) Spiegel S, Milstien S. Sphingosine-1-phosphate: an enigmatic signalling lipid. *Nat Rev Mol Cell Biol* 2003;**4**(5):397-407.

(318) Igarashi Y. [Current studies on a novel lipid mediator, sphingosine 1-phosphate, and its receptors]. *Tanpakushitsu Kakusan Koso* 2002;**47**(4 Suppl):476-9.

(319) Cuvillier O, Pirianov G, Kleuser B *et al*. Suppression of ceramide-mediated programmed cell death by sphingosine-1-phosphate. *Nature* 1996;**381**(6585):800-3.

(320) Kondo T, Kitano T, Iwai K *et al*. Control of ceramide-induced apoptosis by IGF-1: involvement of PI-3 kinase, caspase-3 and catalase. *Cell Death Differ* 2002;**9**(6):682-92.

(321) Perry DK, Kolesnick RN. Ceramide and sphingosine 1-phosphate in anti-cancer therapies. *Cancer Treat Res* 2003;**115**:345-54.

(322) Jacobson K, Dietrich C. Looking at lipid rafts? *Trends Cell Biol* 1999;**9**(3):87-91.

(323) Harder T, Scheiffele P, Verkade P *et al*. Lipid domain structure of the plasma membrane revealed by patching of membrane components. *J Cell Biol* 1998;**141**(4):929-42.

(324) Friedrichson T, Kurzchalia TV. Microdomains of GPI-anchored proteins in living cells revealed by crosslinking. *Nature* 1998;**394**(6695):802-5.

(325) Mayor S, Maxfield FR. Insolubility and redistribution of GPI-anchored proteins at the cell surface after detergent treatment. *Mol Biol Cell* 1995;**6**(7):929-44.

(326) Waheed AA, Shimada Y, Heijnen HF *et al*. Selective binding of perfringolysin O derivative to cholesterol-rich membrane microdomains (rafts). *Proc Natl Acad Sci U S A* 2001;**98**(9):4926-31.

(327) Fujimoto T, Hayashi M, Iwamoto M *et al*. Crosslinked plasmalemmal cholesterol is sequestered to caveolae: analysis with a new cytochemical probe. *J Histochem Cytochem* 1997;**45**(9):1197-205.

(328) Hagiwara H, Kogure SY, Nakamura M *et al*. Cross-linking of plasmalemmal cholesterol in lymphocytes induces capping, membrane shedding, and endocytosis through coated pits. *Biochem Biophys Res Commun* 1999;**260**(2):516-21.

(329) Schutz GJ, Kada G, Pastushenko VP *et al*. Properties of lipid microdomains in a muscle cell membrane visualized by single molecule microscopy. *EMBO J* 2000;**19**(5):892-901.

(330) Bi K, Tanaka Y, Coudronniere N *et al*. Antigen-induced translocation of PKC-theta to membrane rafts is required for T cell activation. *Nat Immunol* 2001;**2**(6):556-63.

(331) Simons K, Ikonen E. Functional rafts in cell membranes. *Nature* 1997;**387**(6633):569-72.

(332) Brown DA, London E. Structure and origin of ordered lipid domains in biological membranes. *J Membr Biol* 1998;**164**(2):103-14.

(333) Paul P, Kamisaka Y, Marks DL *et al*. Purification and characterization of UDP-glucose:ceramide glucosyltransferase from rat liver Golgi membranes. *J Biol Chem* 1996;**271**(4):2287-93.

(334) Ichikawa S, Sakiyama H, Suzuki G *et al*. Expression cloning of a cDNA for human ceramide glucosyltransferase that catalyzes the first glycosylation step of glycosphingolipid synthesis. *Proc Natl Acad Sci U S A* 1996;**93**(22):12654.

(335) Sasaki T. Glycolipid transfer protein and intracellular traffic of glucosylceramide. *Experientia* 1990;**46**(6):611-6.

(336) Huwiler A, Kolter T, Pfeilschifter J *et al*. Physiology and pathophysiology of sphingolipid metabolism and signaling. *Biochim Biophys Acta* 2000;**1485**(2-3):63-99.

(337) Kolter T, Proia RL, Sandhoff K. Combinatorial ganglioside biosynthesis. *J Biol Chem* 2002;**277**(29):25859-62.

(338) Chatterjee, S. Regulation of synthesis of lactosylceramide and long chain bases in normal and familial hypercholesterolemic cultured proximal tubular cells. 13017-13022. 1988.
Ref Type: Generic

(339) Chatterjee SB, Dey S, Shi WY *et al*. Accumulation of glycosphingolipids in human atherosclerotic plaque and unaffected aorta tissues. *Glycobiology* 1997;**7**(1):57-65.

(340) Mukhin DN, Chao FF, Kruth HS. Glycosphingolipid accumulation in the aortic wall is another feature of human atherosclerosis. *Arterioscler Thromb Vasc Biol* 1995;**15**(10):1607-15.

(341) Bhunia AK, Han H, Snowden A *et al*. Lactosylceramide stimulates Ras-GTP loading, kinases (MEK, Raf), p44 mitogen-activated protein kinase, and c-fos expression in human aortic smooth muscle cells. *J Biol Chem* 1996;**271**(18):10660-6.

(342) Bhunia AK, Han H, Snowden A *et al*. Redox-regulated signaling by lactosylceramide in the proliferation of human aortic smooth muscle cells. *J Biol Chem* 1997;**272**(25):15642-9.

(343) Chatterjee, S. B. and Gosh, N. Oxidized low density lipoprotein stimulates aortic smooth muscle cell proliferation. 303-311. 1996.
Ref Type: Generic

(344) Arai T, Bhunia AK, Chatterjee S *et al*. Lactosylceramide stimulates human neutrophils to upregulate Mac-1, adhere to endothelium, and generate reactive oxygen metabolites in vitro. *Circ Res* 1998;**82**(5):540-7.

(345) Zimmermann J.W. A novel carbohydrate-glycosphingolipid interaction between a beta-(1-3)-glucan immunomodulator, PGG-glucan, and lactosylceramide of human leukocytes. Lindermuth J. 22014-22020. 1998.
Ref Type: Generic

(346) Chatterjee S, Ghosh N, Castiglione E *et al*. Regulation of glycosphingolipid glycosyltransferase by low density lipoprotein receptors in cultured human proximal tubular cells. *J Biol Chem* 1988;**263**(26):13017-22.

(347) Griffin JH, Fernandez JA, Deguchi H. Plasma lipoproteins, hemostasis and thrombosis. *Thromb Haemost* 2001;**86**(1):386-94.

(348) Mangeney M, Lingwood CA, Taga S *et al*. Apoptosis induced in Burkitt's lymphoma cells via Gb3/CD77, a glycolipid antigen. *Cancer Res* 1993;**53**(21):5314-9.

(349) Postigo AA, Marazuela M, Sanchez-Madrid F *et al*. B lymphocyte binding to E- and P-selectins is mediated through the de novo expression of carbohydrates on in vitro and in vivo activated human B cells. *J Clin Invest* 1994;**94**(4):1585-96.

(350) Wagers AJ, Stoolman LM, Kannagi R *et al*. Expression of leukocyte fucosyltransferases regulates binding to E-selectin: relationship to previously implicated carbohydrate epitopes. *J Immunol* 1997;**159**(4):1917-29.

(351) Lund-Johansen F, Olweus J, Horejsi V *et al*. Activation of human phagocytes through carbohydrate antigens (CD15, sialyl-CD15, CDw17, and CDw65). *J Immunol* 1992;**148**(10):3221-9.

(352) Inokuchi J, Radin NS. Preparation of the active isomer of 1-phenyl-2-decanoylamino-3-morpholino-1-propanol, inhibitor of murine glucocerebroside synthetase. *J Lipid Res* 1987;**28**(5):565-71.

(353) Inokuchi J, Mizutani A, Jimbo M *et al*. Up-regulation of ganglioside biosynthesis, functional synapse formation, and memory retention by a synthetic ceramide analog (L-PDMP). *Biochem Biophys Res Commun* 1997;**237**(3):595-600.

(354) van Meer G, Sillence D, Sprong H *et al*. Transport of (glyco)sphingolipids in and between cellular membranes; multidrug transporters and lateral domains. *Biosci Rep* 1999;**19**(4):327-33.

(355) Miller-Podraza H, Bradley RM, Fishman PH. Biosynthesis and localization of gangliosides in cultured cells. *Biochemistry* 1982;**21**(14):3260-5.

(356) Lindberg AA, Brown JE, Stromberg N *et al*. Identification of the carbohydrate receptor for Shiga toxin produced by Shigella dysenteriae type 1. *J Biol Chem* 1987;**262**(4):1779-85.

(357) Mallard F, Antony C, Tenza D *et al*. Direct pathway from early/recycling endosomes to the Golgi apparatus revealed through the study of shiga toxin B-fragment transport. *J Cell Biol* 1998;**143**(4):973-90.

(358) Orlandi PA, Curran PK, Fishman PH. Brefeldin A blocks the response of cultured cells to cholera toxin. Implications for intracellular trafficking in toxin action. *J Biol Chem* 1993;**268**(16):12010-6.

(359) Sandhoff K, Kolter T. Topology of glycosphingolipid degradation. *Trends Cell Biol* 1996;**6**(3):98-103.

(360) Hiraiwa M, O'Brien JS, Kishimoto Y *et al*. Isolation, characterization, and proteolysis of human prosaposin, the precursor of saposins (sphingolipid activator proteins). *Arch Biochem Biophys* 1993;**304**(1):110-6.

(361) Schuette CG, Pierstorff B, Huettler S *et al*. Sphingolipid activator proteins: proteins with complex functions in lipid degradation and skin biogenesis. *Glycobiology* 2001;**11**(6):81R-90R.

(362) Kishimoto Y, Hiraiwa M, O'Brien JS. Saposins: structure, function, distribution, and molecular genetics. *J Lipid Res* 1992;**33**(9):1255-67.

(363) Schnabel D, Schroder M, Sandhoff K. Mutation in the sphingolipid activator protein 2 in a patient with a variant of Gaucher disease. *FEBS Lett* 1991;**284**(1):57-9.

(364) Prigozy TI, Naidenko O, Qasba P *et al*. Glycolipid antigen processing for presentation by CD1d molecules. *Science* 2001;**291**(5504):664-7.

(365) Sacks FM, Krukonis GP. The influence of apolipoprotein E on the interactions between normal human very low density lipoproteins and U937 human macrophages: heterogeneity among persons. *Vasc Med* 1996;**1**(1):9-18.

(366) Matsunaga I, Bhatt A, Young DC *et al*. Mycobacterium tuberculosis pks12 produces a novel polyketide presented by CD1c to T cells. *J Exp Med* 2004;**200**(12):1559-69.

(367) Muller G, Kerkhoff C, Hankowitz J *et al*. Effects of purinergic agents on human mononuclear phagocytes are differentiation dependent. Implications for atherogenesis. *Arterioscler Thromb* 1993;**13**(9):1317-26.

(368) Lindgren FT, Adamson GL, Jenson LC *et al*. Lipid and lipoprotein measurements in a normal adult American population. *Lipids* 1975;**10**(12):750-6.

(369) Pitas RE, Innerarity TL, Weinstein JN *et al*. Acetoacetylated lipoproteins used to distinguish fibroblasts from macrophages in vitro by fluorescence microscopy. *Arteriosclerosis* 1981;**1**(3):177-85.

(370) BLIGH EG, DYER WJ. A rapid method of total lipid extraction and purification. *Can J Biochem Physiol* 1959;**37**(8):911-7.

(371) Liebisch G, Drobnik W, Reil M *et al*. Quantitative measurement of different ceramide species from crude cellular extracts by electrospray ionization tandem mass spectrometry (ESI-MS/MS). *J Lipid Res* 1999;**40**(8):1539-46.

(372) Brugger B, Erben G, Sandhoff R *et al*. Quantitative analysis of biological membrane lipids at the low picomole level by nano-electrospray ionization tandem mass spectrometry. *Proc Natl Acad Sci U S A* 1997;**94**(6):2339-44.

(373) Vermes I, Haanen C, Steffens-Nakken H *et al*. A novel assay for apoptosis. Flow cytometric detection of phosphatidylserine expression on early apoptotic cells using fluorescein labelled Annexin V. *J Immunol Methods* 1995;**184**(1):39-51.

(374) Shimada Y, Maruya M, Iwashita S *et al*. The C-terminal domain of perfringolysin O is an essential cholesterol-binding unit targeting to cholesterol-rich microdomains. *Eur J Biochem* 2002;**269**(24):6195-203.

(375) Mujumdar RB, Ernst LA, Mujumdar SR *et al*. Cyanine dye labeling reagents: sulfoindocyanine succinimidyl esters. *Bioconjug Chem* 1993;**4**(2):105-11.

(376) Tew DG, Southan C, Rice SQ *et al*. Purification, properties, sequencing, and cloning of a lipoprotein-associated, serine-dependent phospholipase involved in the oxidative modification of low-density lipoproteins. *Arterioscler Thromb Vasc Biol* 1996;**16**(4):591-9.

(377) Macphee CH, Moores KE, Boyd HF *et al*. Lipoprotein-associated phospholipase A2, platelet-activating factor acetylhydrolase, generates two bioactive products during the oxidation of low-density lipoprotein: use of a novel inhibitor. *Biochem J* 1999;**338 (Pt 2)**:479-87.

(378) Steinbrecher UP, Pritchard PH. Hydrolysis of phosphatidylcholine during LDL oxidation is mediated by platelet-activating factor acetylhydrolase. *J Lipid Res* 1989;**30**(3):305-15.

(379) Dennis EA. The growing phospholipase A2 superfamily of signal transduction enzymes. *Trends Biochem Sci* 1997;**22**(1):1-2.

(380) Li N, Mak A, Richards DP *et al*. Monocyte lipid rafts contain proteins implicated in vesicular trafficking and phagosome formation. *Proteomics* 2003;**3**(4):536-48.

(381) Li N, Shaw AR, Zhang N *et al*. Lipid raft proteomics: analysis of in-solution digest of sodium dodecyl sulfate-solubilized lipid raft proteins by liquid chromatography-matrix-assisted laser desorption/ionization tandem mass spectrometry. *Proteomics* 2004;**4**(10):3156-66.

(382) Bae TJ, Kim MS, Kim JW *et al*. Lipid raft proteome reveals ATP synthase complex in the cell surface. *Proteomics* 2004;**4**(11):3536-48.

(383) Foster LJ, De Hoog CL, Mann M. Unbiased quantitative proteomics of lipid rafts reveals high specificity for signaling factors. *Proc Natl Acad Sci U S A* 2003;**100**(10):5813-8.

(384) Blonder J, Hale ML, Lucas DA *et al*. Proteomic analysis of detergent-resistant membrane rafts. *Electrophoresis* 2004;**25**(9):1307-18.

(385) Desjardins M. ER-mediated phagocytosis: a new membrane for new functions. *Nat Rev Immunol* 2003;**3**(4):280-91.

(386) Harding CV, Geuze HJ. Class II MHC molecules are present in macrophage lysosomes and phagolysosomes that function in the phagocytic processing of Listeria monocytogenes for presentation to T cells. *J Cell Biol* 1992;**119**(3):531-42.

(387) Schmitz G, Langmann T, Heimerl S. Role of ABCG1 and other ABCG family members in lipid metabolism. *J Lipid Res* 2001;**42**(10):1513-20.

(388) Huuskonen J, Jauhiainen M, Ehnholm C *et al*. Biosynthesis and secretion of human plasma phospholipid transfer protein. *J Lipid Res* 1998;**39**(10):2021-30.

(389) Fossel ET, Zanella CL, Fletcher JG *et al*. Cell death induced by peroxidized low-density lipoprotein: endopepsis. *Cancer Res* 1994;**54**(5):1240-8.

(390) Simionescu N, Vasile E, Lupu F *et al*. Prelesional events in atherogenesis. Accumulation of extracellular cholesterol-rich liposomes in the arterial intima and cardiac valves of the hyperlipidemic rabbit. *Am J Pathol* 1986;**123**(1):109-25.

(391) Seifert PS, Hugo F, Tranum-Jensen J *et al*. Isolation and characterization of a complement-activating lipid extracted from human atherosclerotic lesions. *J Exp Med* 1990;**172**(2):547-57.

(392) Maor I, Mandel H, Aviram M. Macrophage uptake of oxidized LDL inhibits lysosomal sphingomyelinase, thus causing the accumulation of unesterified cholesterol-sphingomyelin-rich particles in the lysosomes. A possible role for 7-Ketocholesterol. *Arterioscler Thromb Vasc Biol* 1995;**15**(9):1378-87.

(393) Kinscherf R, Claus R, Deigner HP *et al*. Modified low density lipoprotein delivers substrate for ceramide formation and stimulates the sphingomyelin-ceramide pathway in human macrophages. *FEBS Lett* 1997;**405**(1):55-9.

(394) Deigner HP, Claus R, Bonaterra GA *et al*. Ceramide induces aSMase expression: implications for oxLDL-induced apoptosis. *FASEB J* 2001;**15**(3):807-14.

(395) Hundal RS, Gomez-Munoz A, Kong JY *et al*. Oxidized low density lipoprotein inhibits macrophage apoptosis by blocking ceramide generation, thereby maintaining protein kinase B activation and Bcl-XL levels. *J Biol Chem* 2003;**278**(27):24399-408.

(396) Ridgway ND, Lagace TA, Cook HW *et al*. Differential effects of sphingomyelin hydrolysis and cholesterol transport on oxysterol-binding protein phosphorylation and Golgi localization. *J Biol Chem* 1998;**273**(47):31621-8.

(397) Chatterjee S. Neutral sphingomyelinase action stimulates signal transduction of tumor necrosis factor-alpha in the synthesis of cholesteryl esters in human fibroblasts. *J Biol Chem* 1994;**269**(2):879-82.

(398) Langmann T, Buechler C, Ries S *et al*. Transcription factors Sp1 and AP-2 mediate induction of acid sphingomyelinase during monocytic differentiation. *J Lipid Res* 1999;**40**(5):870-80.

(399) Gulbins E. Regulation of death receptor signaling and apoptosis by ceramide. *Pharmacol Res* 2003;**47**(5):393-9.

(400) Grassme H, Jendrossek V, Riehle A *et al*. Host defense against Pseudomonas aeruginosa requires ceramide-rich membrane rafts. *Nat Med* 2003;**9**(3):322-30.

(401) Grassme H, Jekle A, Riehle A *et al*. CD95 signaling via ceramide-rich membrane rafts. *J Biol Chem* 2001;**276**(23):20589-96.

(402) Ruvolo PP. Intracellular signal transduction pathways activated by ceramide and its metabolites. *Pharmacol Res* 2003;**47**(5):383-92.

(403) Slotte JP, Hedstrom G, Rannstrom S *et al*. Effects of sphingomyelin degradation on cell cholesterol oxidizability and steady-state distribution between the cell surface and the cell interior. *Biochim Biophys Acta* 1989;**985**(1):90-6.

(404) Cremesti AE, Goni FM, Kolesnick R. Role of sphingomyelinase and ceramide in modulating rafts: do biophysical properties determine biologic outcome? *FEBS Lett* 2002;**531**(1):47-53.

(405) Wang TY, Silvius JR. Sphingolipid partitioning into ordered domains in cholesterol-free and cholesterol-containing lipid bilayers. *Biophys J* 2003;**84**(1):367-78.

(406) Xu X, Bittman R, Duportail G *et al*. Effect of the structure of natural sterols and sphingolipids on the formation of ordered sphingolipid/sterol domains (rafts).

Comparison of cholesterol to plant, fungal, and disease-associated sterols and comparison of sphingomyelin, cerebrosides, and ceramide. *J Biol Chem* 2001;**276**(36):33540-6.

(407) London M, London E. Ceramide selectively displaces cholesterol from ordered lipid domains (rafts): implications for lipid raft structure and function. *J Biol Chem* 2004;**279**(11):9997-10004.

(408) Grimm MO, Grimm HS, Patzold AJ *et al*. Regulation of cholesterol and sphingomyelin metabolism by amyloid-beta and presenilin. *Nat Cell Biol* 2005.

(409) Floto RA, Clatworthy MR, Heilbronn KR *et al*. Loss of function of a lupus-associated FcgammaRIIb polymorphism through exclusion from lipid rafts. *Nat Med* 2005;**11**(10):1056-8.

(410) Buechler C, Ritter M, Orso E *et al*. Regulation of scavenger receptor CD163 expression in human monocytes and macrophages by pro- and antiinflammatory stimuli. *J Leukoc Biol* 2000;**67**(1):97-103.

(411) Wieland E, Dorweiler B, Bonitz U *et al*. Complement activation by oxidatively modified low-density lipoproteins. *Eur J Clin Invest* 1999;**29**(10):835-41.

(412) Suchard SJ, Hinkovska-Galcheva V, Mansfield PJ *et al*. Ceramide inhibits IgG-dependent phagocytosis in human polymorphonuclear leukocytes. *Blood* 1997;**89**(6):2139-47.

(413) Hinkovska-Galcheva V, Boxer L, Mansfield PJ *et al*. Enhanced phagocytosis through inhibition of de novo ceramide synthesis. *J Biol Chem* 2003;**278**(2):974-82.

(414) Ehlers MR. CR3: a general purpose adhesion-recognition receptor essential for innate immunity. *Microbes Infect* 2000;**2**(3):289-94.

(415) Miller YI, Chang MK, Binder CJ *et al*. Oxidized low density lipoprotein and innate immune receptors. *Curr Opin Lipidol* 2003;**14**(5):437-45.

(416) Witting SR, Maiorano JN, Davidson WS. Ceramide enhances cholesterol efflux to apolipoprotein A-I by increasing the cell surface presence of ATP-binding cassette transporter A1. *J Biol Chem* 2003;**278**(41):40121-7.

(417) Tsutsumi K. Lipoprotein lipase and atherosclerosis. *Curr Vasc Pharmacol* 2003;**1**(1):11-7.

(418) Wuttge DM, Romert A, Eriksson U *et al*. Induction of CD36 by all-trans retinoic acid: retinoic acid receptor signaling in the pathogenesis of atherosclerosis. *FASEB J* 2001;**15**(7):1221-3.

(419) Wagsater D, Dimberg J, Sirsjo A. Induction of ATP-binding cassette A1 by all-trans retinoic acid: possible role of liver X receptor-alpha. *Int J Mol Med* 2003;**11**(4):419-23.

(420) Costet P, Lalanne F, Gerbod-Giannone MC *et al*. Retinoic acid receptor-mediated induction of ABCA1 in macrophages. *Mol Cell Biol* 2003;**23**(21):7756-66.

(421) Soprano DR, Qin P, Soprano KJ. Retinoic acid receptors and cancers. *Annu Rev Nutr* 2004;**24**:201-21.

(422) Vu-Dac N, Gervois P, Torra IP *et al*. Retinoids increase human apo C-III expression at the transcriptional level via the retinoid X receptor. Contribution to the hypertriglyceridemic action of retinoids. *J Clin Invest* 1998;**102**(3):625-32.

(423) Yang JB, Duan ZJ, Yao W *et al*. Synergistic transcriptional activation of human Acyl-coenzyme A: cholesterol acyltransterase-1 gene by interferon-gamma and all-trans-retinoic acid THP-1 cells. *J Biol Chem* 2001;**276**(24):20989-98.

Eidesstattliche Erklärung

Ich erkläre hiermit an Eides statt, daß ich die vorliegende Arbeit ohne unzulässige Hilfe Dritter und ohne Benutzung anderer als der angegebenen Hilfsmittel angefertigt habe; die aus anderen Quellen direkt oder indirekt übernommenen Daten und Konzepte sind unter Angabe des Literaturzitats gekennzeichnet.

Bei der Auswahl und Auswertung folgenden Materials haben mir die nachstehend aufgeführten Personen in der jeweils beschriebenen Weise entgeltlich/unentgeltlich geholfen:

1. .....

2. .....

3. .....

Weitere Personen waren an der inhaltlich-materiellen Herstellung der vorliegenden Arbeit nicht beteiligt. Insbesondere habe ich hierfür nicht die entgeltliche Hilfe eines Promotionsberaters oder anderer Personen in Anspruch genommen. Niemand hat von mir weder unmittelbar noch mittelbar geldwerte Leistungen für Arbeiten erhalten, die im Zusammenhang mit dem Inhalt der vorgelegten Dissertation stehen.

Die Arbeit wurde bisher weder im In- noch im Ausland in gleicher oder ähnlicher Form einer anderen Prüfungsbehörde vorgelegt.

Regensburg, den 18.12.2005 _____

Margot Grandl

Dank

Hiermit möchte ich allen Kollegen danken, welche die Erstellung dieser Arbeit durch ihre Unterstützung ermöglicht haben. Vor allem gilt mein Dank Herrn Prof. Dr. Gerd Schmitz für die Betreuung dieser Arbeit mit vielen interessanten fachlichen Gesprächen und die daraus hervorgegangenen Anregungen für neue experimentielle Ansätze.

Bei Herrn Prof. Dr. A. Buschauer möchte ich mich für die fakultätsinterne Betreuung bedanken und für die Aufnahme als assoziiertes Mitglied in das Graduiertenkolleg „Medizinische Chemie: Molekulare Erkennung-Ligand-Rezeptor-Wechselwirkungen“.

Mein herzlicher Dank gilt natürlich allen Mitarbeitern des Institutes, vor allem dem Team des Flow-Labors, welches immer sehr hilfsbereit und zuvorkommend war. Insbesondere Ella schaffte es mit ihrem freundlichen Wesen mich immer wieder aufzuheitern. Auch dem Elu-Team und der Zellkulturbesetzung Conny, Otti und Astrid sei für die große Hilfsbereitschaft gedankt. Für die Unterstützung bei der Mikrosopie möchte ich mich auch bei Tobias und Wolfgang bedanken.

Ein großes Dankeschön auch an alle anderen Doktoranden Rainer, Guido, Zsuzsa, Alex, Marion, Christoph, Sascha sowie meinen Bürokollegen Gerhard und Alfred.

Und ganz besonders möchte ich mich bei meinen Eltern für die großartige Unterstützung bedanken.